L

D

The General Electric Company, King of Prussia, Pennsylvania; Evendale, Ohio; and Pittsburgh, Pennsylvania	Harry Straub Vincent DiNenna David Hetzel
Gougeon Brothers, Inc., Bay City, Michigan	William D. Bertelsen Ronald C. Forrest Robert H. Kunesh, Consultant

DOE/NASA/20320--76

DE91 000529

Structural Properties of Laminated Douglas Fir/ Epoxy Composite Material

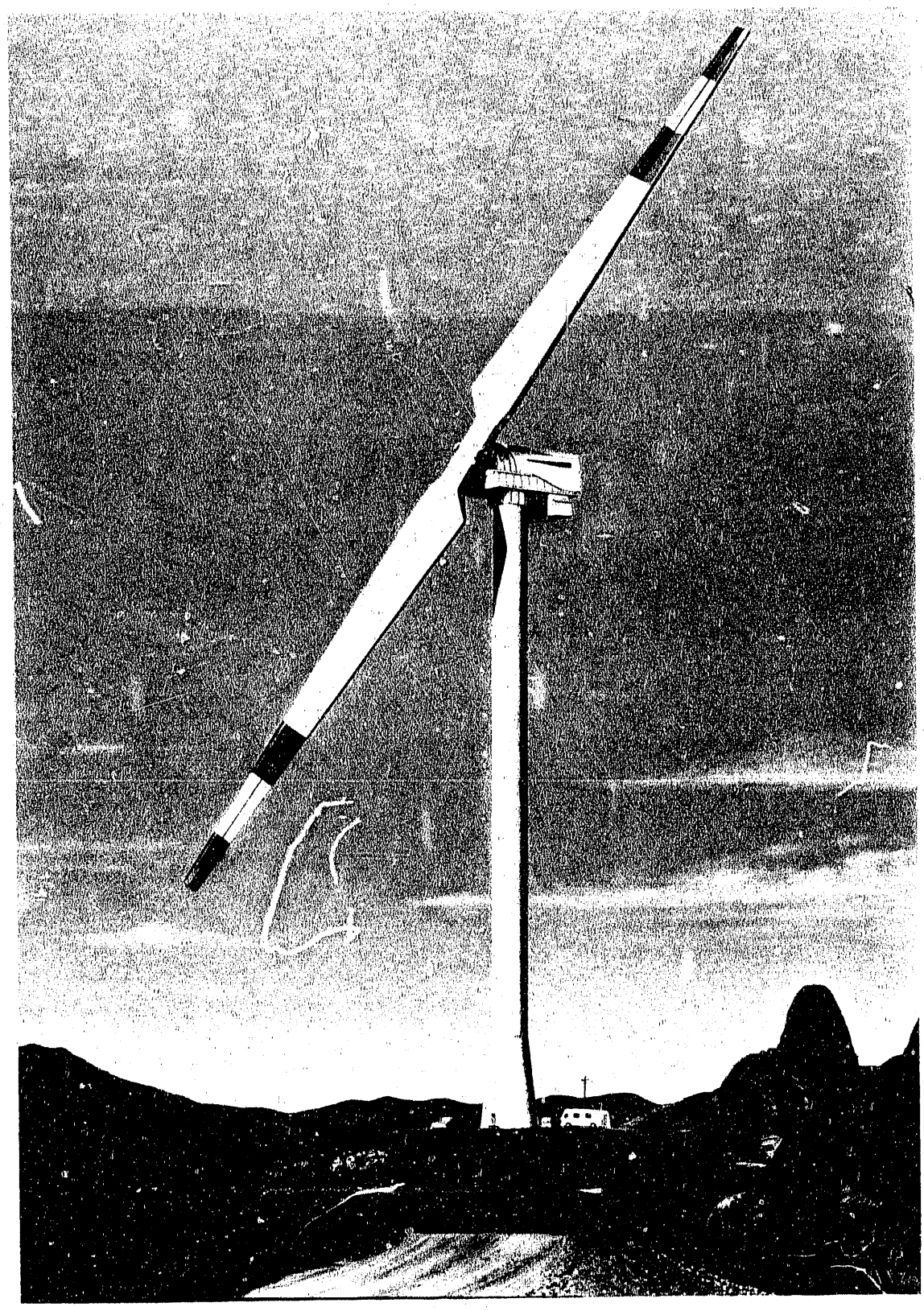

Conceptual drawing of the Mod-5A 7.3-MW wind turbine generator designed by the General Electric Company for NASA and the U.S. Department of Energy. The proposed rotor is 400 ft long, from tip to tip, and is constructed almost entirely from laminated Douglas fir/epoxy material.

NASA Reference Publication 1236

DOE/NASA/ 20320-76

1990

Structural Properties of Laminated Douglas Fir/ Epoxy Composite Material

David A. Spera
Lewis Research Center
Cleveland, Ohio

Jack B. Esgar
Sverdrup Technology, Inc.
Lewis Research Center Group
Cleveland, Ohio

Meade Gougeon and Michael D. Zuteck
Gougeon Brothers, Inc.
Bay City, Michigan

Work performed for
U.S. Department of Energy
Conservation and Renewable Energy
Wind/Ocean Technology Division
Washington, D.C. 20545
Under Interagency Agreement DE-AI01-76ET20320

NASA
National Aeronautics and Space Administration
Office of Management
Scientific and Technical Information Division

DISCLAIMER

Printed in the United States of America

Available from
National Technical Information Service
U.S. Department of Commerce
5285 Port Royal Road
Springfield, VA 22161

NTIS price codes[1]
Printed copy:
Microfiche copy: A01

[1]Codes are used for pricing all publications. The code is determined by the number of pages in the publication. Information pertaining to the pricing codes can be found in the current issues of the following publications, which are generally available in most libraries: *Energy Research Abstracts (ERA); Government Reports Announcements* and Index (*GRA* and I); *Scientific and Technical Abstract Reports (STAR);* and publication, NTIS-PR-360 available from NTIS at the above address.

Preface

This publication contains a compilation of static and fatigue strength data for laminated-wood material made from Douglas fir and epoxy. Results of tests conducted by several organizations are correlated to provide insight into the effects of variables such as moisture, size, lamina-to-lamina joint design, wood veneer grade, and the ratio of cyclic stress to steady stress during fatigue testing. These test data were originally obtained during development of wood rotor blades for large-scale wind turbines of the horizontal-axis (propeller) configuration. Most of the strength property data in this compilation are not found in the published literature. Test sections ranged from round cylinders 2.25 in. in diameter to rectangular slabs 6 in. by 24 in. in cross section and approximately 30 ft long. All specimens were made from Douglas fir veneers 0.10 in. thick, bonded together with the WEST epoxy system developed for fabrication and repair of wood boats. Loading was usually parallel to the grain. Size effects (reduction in strength with increase in test volume) are observed in some of the test data, and a simple mathematical model is presented that includes the probability of failure. General characteristics of the wood/epoxy laminate are discussed, including features that make it useful for a wide variety of applications.

Contents

Table

Chapter I
Introduction

The NASA Lewis Research Center began a series of projects in 1977 to develop low-cost rotor blades for megawatt-scale wind turbines. This work was sponsored by the U.S. Department of Energy as part of its renewable energy technology programs. One concept that was explored for constructing wind turbine blades was to fabricate them from laminated wood, using methods developed for building the hulls of high-performance boats. This work was very successful, leading to the production of blades up to 70 ft in length. Many thousands of smaller blades have been fabricated from laminated wood for commercial wind power stations.

The purpose of this publication is to provide an integrated collection of static and fatigue data on one of the most promising wood laminate materials: Douglas fir bonded with epoxy. Early in the wood blade project, it became evident that there was a serious lack of design data on wood laminated from thin veneers joined with modern adhesives. This was particularly true for fatigue data, which are critical to the design of dynamic structures. Several laboratories were given NASA subcontracts to test specimens of Douglas fir/epoxy material in a wide variety of shapes and sizes and under a variety of loading conditions. Results were documented in internal reports, but most of these data have been unpublished until now.

The properties of Douglas fir/epoxy laminates represent a balanced combination of static and fatigue strength, stiffness, density, resistance to moisture and decay, availability, ease of fabrication, and cost. Therefore, the data reported here should be useful to the designers of a wide range of wood structures, not just wind turbine blades.

The principal sources of the data in this publication were internal reports of the General Electric Company, supporting the design of an all-wood rotor for the Mod-5A 7.3-MW wind turbine (frontispiece and ref. 1), a rotor measuring 400 ft from tip to tip. Although the Mod-5A project was limited to the preparation of a wind turbine design, considerable experience was obtained in the manufacture and testing of laminated-wood specimens, some with volumes in excess of 7000 cubic inches.

A second source of data was Gougeon Brothers, Inc., the manufacturer of all of the Douglas fir/epoxy material tested. Some of the GBI work in wind turbine blade development is described in reference 2. Reference 3 provides comparative data on clear, solid (unlaminated) wood and basic equations with which to correct test data for moisture and temperature effects. Reference 4 contains clear-wood property data similar to that in reference 3. No data are available in references 3 and 4 on laminated-wood products.

The data reported in this publication are for test specimens with a minimum of nine laminas. More frequently there are 15 or more laminas, with some specimens having as many as 60. Materials with only a few laminas (three to five) exhibited significantly lower fatigue strength and a great deal of scatter (ref. 5).

Background information on laminated wood as a high-performance structural material is given in chapter II, together with descriptions of applications and manufacturing methods. Chapter III summarizes the most useful test data and presents mathematical models for predicting the effects of size and moisture content on mechanical properties. Chapter III will probably satisfy most data needs.

Chapter IV presents detailed test data in tabular and graphical form, providing a data base suitable for further analysis and updating. In addition, chapter IV contains discussions of the test data as well as descriptions of test specimens, testing procedures, and test equipment. Uncorrected test results are also listed in the data tables to permit users of the data to make different moisture corrections or data interpretations. Because of the size and complexity of the data set in chaper IV, numerically indexed headings are used to organize the information.

Listed below are the organizations responsible for the data contained in this publication and some of the important contributors from these organizations.

The General Electric Company, King of Prussia, Pennsylvania; Evendale, Ohio; and Pittsburgh, Pennsylvania	Harry Straub Vincent DiNenna David Hetzel
Gougeon Brothers, Inc., Bay City, Michigan	William D. Bertelsen Ronald C. Forrest Robert H. Kunesh, Consultant Michael D. Zuteck, Consultant
University of Illinois, Urbana, Illinois	Darrell F. Socie
University of Dayton Research Institute, Dayton, Ohio	Paul E. Johnson
Washington State University, Pullman, Washington	Roy Pellerin
ITT Research Institute, Chicago, Illinois	S.A. Bortz Gregory Skaper
Lehigh University, Bethlehem, Pennsylvania	Roger Slutter
NASA Lewis Research Center, Cleveland, Ohio	James R. Faddoul Raymond F. Lark

References

1. MOD-5-A Wind Turbine Generator Program Design Report. Volume II—Conceptual and Preliminary Design. Books 1 and 2. NASA CR-174735-VOL2-BK1 and NASA CR-174735-VOL2-BK2, 1984.
2. Stroebel, T.; Dechow, C.; and Zuteck, M.: Design of Advanced Wood Composite Rotor and Development of Wood Composite Blade Technology. (GBI-ER-11, Gougeon Brothers, Inc.; NASA Contract DEN3-260) NASA CR-174713, 1984.
3. Wood Handbook: Wood as an Engineering Material. Forest Service Agriculture Handbook No. 72, U.S. Forest Products Laboratory, Madison, WI, 1974.
4. Summitt, R.; and Sliker, A.: CRC Handbook of Materials Science. Vol. IV: Wood. CRC Press, Inc., Boca Raton, FL, 1982.
5. Johnson, P.E.: Design of Test Specimens and Procedures for Generating Material Properties of Douglas Fir/Epoxy Laminated Wood Composite Material. (UDR-TR-85-45, University of Dayton Research Institute; NASA Contract DEN3-286) NASA CR-174910, 1985.

Chapter II

Laminated Wood/Epoxy Composites in High-Performance Structures

Meade Gougeon and Michael D. Zuteck**

For most of recorded history wood has been the primary structural material used for large structures subjected to dynamic loads. In recent times wood has been largely replaced by steel, aluminum, and fiberglass composites. This transition has been due mostly to problems associated with moisture control and joining efficiency, rather than to a lack of attractive material properties of the wood itself. The systematic application of modern synthetic resins and joining techniques has now overcome most of the historical problems that limited the efficient use of wood. In many large-scale dynamic applications wood can now provide both structural and economic advantages over competing materials. This chapter summarizes the historical uses and problems of wood, the modern approach to solving these problems, and the potential economics of the resulting wood/epoxy technology. It also gives a brief perspective on the nature of wood as an engineering material, and the significance of the data base contained in chapters III and IV in this compendium of test results for wood/epoxy laminates.

Historical Development of Wood Technology

The most extensive efforts at optimizing the use of wood in large dynamic structures have been in building ships. Two thousand years of evolutionary shipbuilding technology reached its zenith in the 16th century with ships capable of supporting the great voyages of exploration. The fundamentals of shipbuilding technology of this era were sound enough that only small improvements were made over the next 300 to 400 years. Essentially the same materials and construction methods were still used in the great clipper ships of the 19th century.

Up to this point the long evolution of wood technology had focused upon "the weak link"—the capability of the joint between individual wood pieces. Wooden ships were built of thousands of wood parts that all needed to be joined together with the manufacturing capability then available. The evolution of shipbuilding essentially relied upon improvements in joint technology, which allowed larger and larger ships to be built. However, these ships were far heavier than they needed to be because only a small fraction of the true structural potential of wood could be used with the existing types of joints.

A shore-bound relative of wooden shipbuilding success was the Dutch windmill (fig. 1), a superb technical achievement. Recent wind turbine experience has given us a proper appreciation of what was accomplished with wooden wind machines over 400 years ago.

With the arrival of manned flight lightweight structural capability became paramount for the success of aviation. At this point the true limitations of past wood technologies were addressed. For the first 30 years of the development of the airplane, wood was the primary structural material. Pressures to develop safe, reliable, lightweight structures fueled research and development efforts that, for the first time, began to scientifically characterize wood properties. Aircraft engineers quickly realized that even the best mechanically fastened wood joints could transfer only a little over 30 percent of downstream wood material capability. Thus, the full *material* capability of wood had rarely been utilized in any of the dynamic wood structures of the past.

Because of the limitations of early adhesives, bonded wood joint technology did not become fully viable until the mid-1930's, when more advanced adhesives became available. This late development, combined with a lack of uniform, consistent wood physical properties that could be relied upon in a quality control effort, limited the use of wood in the then rapidly developing aircraft industry.

Metals quickly gained favor as a safer material for most larger and faster aircraft. Metals not only possessed more

*Gougeon Brothers, Inc., Bay City, Michigan

Figure 1.—Eighteenth century windmill still in use in the Netherlands.

consistent properties but could be fabricated with a high degree of reliability by a semiskilled work force. In comparison, woodworking required a high degree of skill that took a long apprenticeship to acquire.

Some efforts to keep aviation-oriented wood technology alive persisted in both the United States and Great Britain. With the coming of World War II and the ensuing shortages of all metal materials, the substitution of wood in aircraft and other highly sophisticated structures became crucial to the war effort. For the first time a serious effort was begun to perform the necessary testing so that an engineering data base could be established for wood materials.

The De Havilland Aircraft Company of Great Britain developed a unique stressed-skin monocoque shell design that was the culmination of 23 years of experience in wooden aircraft. The chief structural feature of this design was a wood composite sandwich of birch veneers over a unidirectional balsa core. The design for De Havilland's *Mosquito* bomber using this advanced structural concept was conceived in 1939 (ref. 1). This extremely successful airplane was in full-scale production in 1941 and saw much service in World War II. Figure 2(a) shows the overall configuration of the plane, figure 2(b) illustrates some of the details of the wood sandwich construction, and figure 2(c) is a photograph of a *Mosquito* bomber that is still flying. This two-man-crew wooden bomber, one of the most advanced aircraft of its day, had a

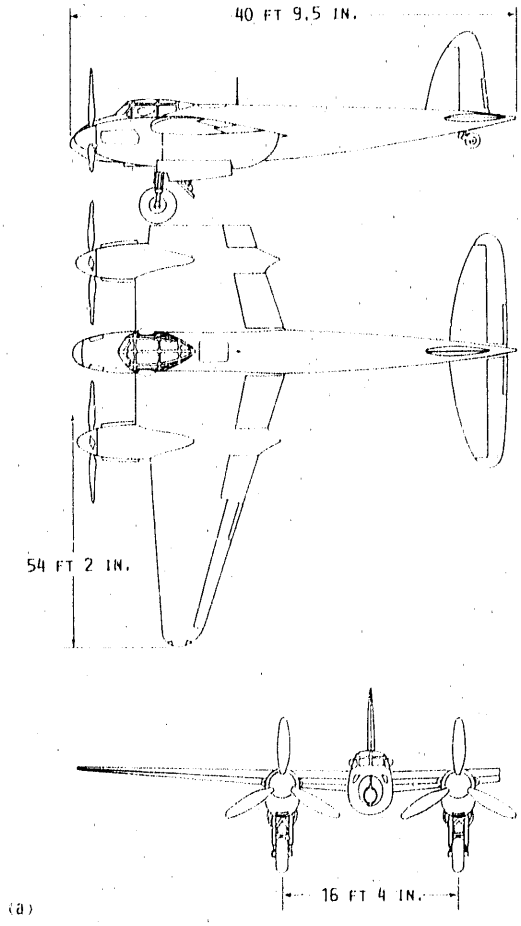

(a) Overall configuration.

Figure 2.—Laminated-wood *Mosquito* bomber built in early 1940's by De Havilland Aircraft Co.

level flight speed of over 400 mph and was capable of carrying a 3000-lb bomb load. Operating at fighter speed without armament, it had a 1500-mile range.

In the United States an effort to build the world's largest aircraft, the Hughes flying boat, nicknamed the *Spruce Goose*, was a controversial wartime project that relied on the most advanced aircraft engineering and wood technology then available. The completed aircraft, shown in figure 3(a) at takeoff for its only flight, is still the largest totally bonded, all-wood structure ever built. The authors had the opportunity to inspect the internal structure of this airplane in 1979. At a constructed weight of 400 000 lb, it is an engineering marvel for its unparalleled combination of fine structural detail, bonded construction, and immense size. Figure 3(b) shows an example of the internal construction of the *Spruce Goose*.

Major pioneering efforts in wood technology ended at the close of World War II. One reason was that aluminum alloy technology evolved quickly in response to the needs of modern aircraft. This was compounded by wood's past image, traditions, limitations, and folklore. However, the main reason

L

D

The General Electric Company, King of Prussia, Pennsylvania; Evendale, Ohio; and Pittsburgh, Pennsylvania	Harry Straub Vincent DiNenna David Hetzel
Gougeon Brothers, Inc., Bay City, Michigan	William D. Bertelsen Ronald C. Forrest Robert H. Kunesh, Consultant

DOE/NASA/20320--76

DE91 000529

Structural Properties of Laminated Douglas Fir/ Epoxy Composite Material

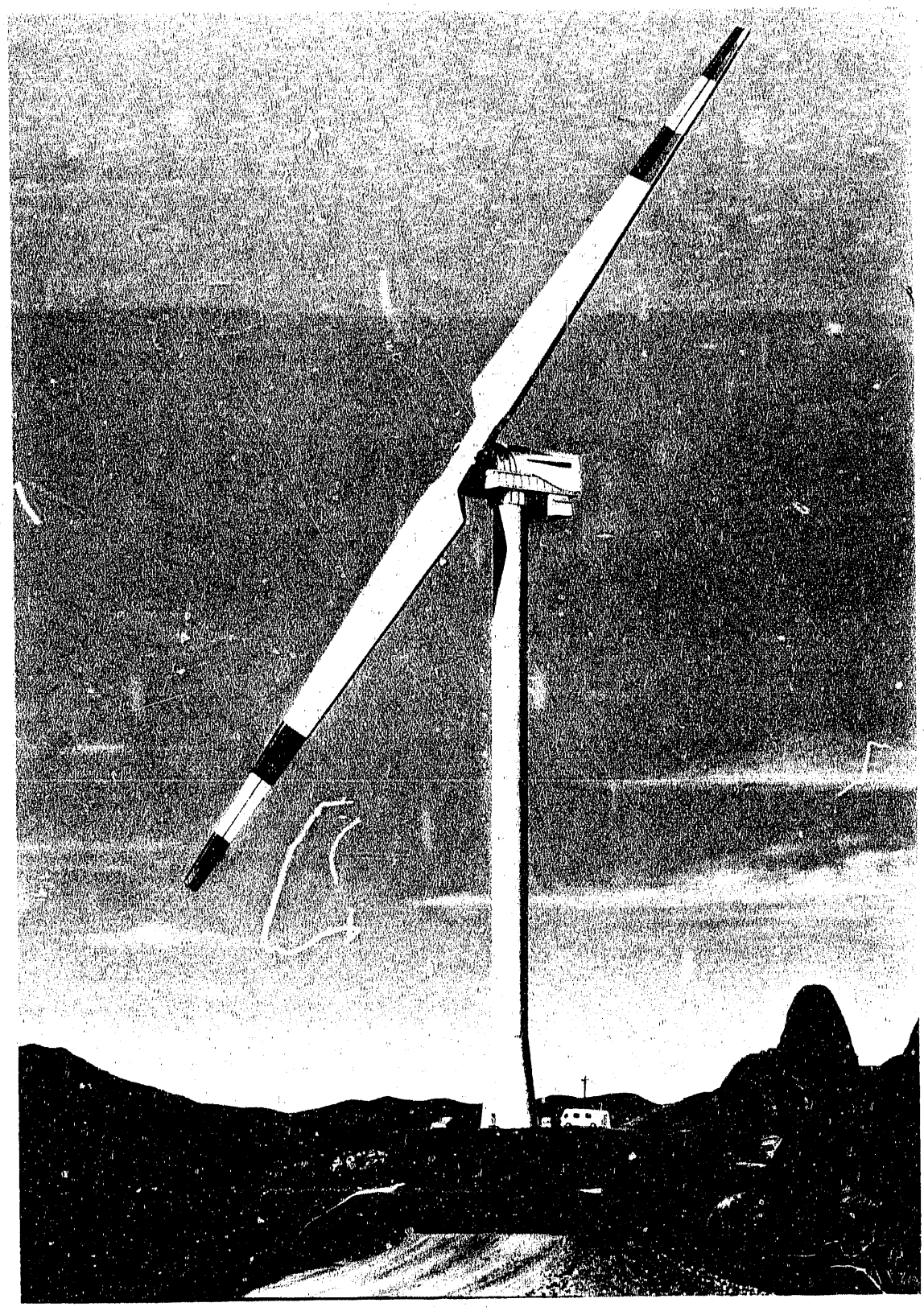

Conceptual drawing of the Mod-5A 7.3-MW wind turbine generator designed by the General Electric Company for NASA and the U.S. Department of Energy. The proposed rotor is 400 ft long, from tip to tip, and is constructed almost entirely from laminated Douglas fir/epoxy material.

NASA Reference Publication 1236

DOE/NASA/ 20320-76

1990

Structural Properties of Laminated Douglas Fir/ Epoxy Composite Material

David A. Spera
Lewis Research Center
Cleveland, Ohio

Jack B. Esgar
Sverdrup Technology, Inc.
Lewis Research Center Group
Cleveland, Ohio

Meade Gougeon and Michael D. Zuteck
Gougeon Brothers, Inc.
Bay City, Michigan

Work performed for
U.S. Department of Energy
Conservation and Renewable Energy
Wind/Ocean Technology Division
Washington, D.C. 20545
Under Interagency Agreement DE-AI01-76ET20320

NASA
National Aeronautics and Space Administration
Office of Management
Scientific and Technical Information Division

DISCLAIMER

Printed in the United States of America

Available from
National Technical Information Service
U.S. Department of Commerce
5285 Port Royal Road
Springfield, VA 22161

NTIS price codes[1]
Printed copy:
Microfiche copy: A01

[1]Codes are used for pricing all publications. The code is determined by the number of pages in the publication. Information pertaining to the pricing codes can be found in the current issues of the following publications, which are generally available in most libraries: *Energy Research Abstracts (ERA); Government Reports Announcements* and Index (*GRA* and I); *Scientific and Technical Abstract Reports (STAR);* and publication, NTIS-PR-360 available from NTIS at the above address.

Preface

This publication contains a compilation of static and fatigue strength data for laminated-wood material made from Douglas fir and epoxy. Results of tests conducted by several organizations are correlated to provide insight into the effects of variables such as moisture, size, lamina-to-lamina joint design, wood veneer grade, and the ratio of cyclic stress to steady stress during fatigue testing. These test data were originally obtained during development of wood rotor blades for large-scale wind turbines of the horizontal-axis (propeller) configuration. Most of the strength property data in this compilation are not found in the published literature. Test sections ranged from round cylinders 2.25 in. in diameter to rectangular slabs 6 in. by 24 in. in cross section and approximately 30 ft long. All specimens were made from Douglas fir veneers 0.10 in. thick, bonded together with the WEST epoxy system developed for fabrication and repair of wood boats. Loading was usually parallel to the grain. Size effects (reduction in strength with increase in test volume) are observed in some of the test data, and a simple mathematical model is presented that includes the probability of failure. General characteristics of the wood/epoxy laminate are discussed, including features that make it useful for a wide variety of applications.

Contents

Table

Chapter I
Introduction

The NASA Lewis Research Center began a series of projects in 1977 to develop low-cost rotor blades for megawatt-scale wind turbines. This work was sponsored by the U.S. Department of Energy as part of its renewable energy technology programs. One concept that was explored for constructing wind turbine blades was to fabricate them from laminated wood, using methods developed for building the hulls of high-performance boats. This work was very successful, leading to the production of blades up to 70 ft in length. Many thousands of smaller blades have been fabricated from laminated wood for commercial wind power stations.

The purpose of this publication is to provide an integrated collection of static and fatigue data on one of the most promising wood laminate materials: Douglas fir bonded with epoxy. Early in the wood blade project, it became evident that there was a serious lack of design data on wood laminated from thin veneers joined with modern adhesives. This was particularly true for fatigue data, which are critical to the design of dynamic structures. Several laboratories were given NASA subcontracts to test specimens of Douglas fir/epoxy material in a wide variety of shapes and sizes and under a variety of loading conditions. Results were documented in internal reports, but most of these data have been unpublished until now.

The properties of Douglas fir/epoxy laminates represent a balanced combination of static and fatigue strength, stiffness, density, resistance to moisture and decay, availability, ease of fabrication, and cost. Therefore, the data reported here should be useful to the designers of a wide range of wood structures, not just wind turbine blades.

The principal sources of the data in this publication were internal reports of the General Electric Company, supporting the design of an all-wood rotor for the Mod-5A 7.3-MW wind turbine (frontispiece and ref. 1), a rotor measuring 400 ft from tip to tip. Although the Mod-5A project was limited to the preparation of a wind turbine design, considerable experience was obtained in the manufacture and testing of laminated-wood specimens, some with volumes in excess of 7000 cubic inches.

A second source of data was Gougeon Brothers, Inc., the manufacturer of all of the Douglas fir/epoxy material tested. Some of the GBI work in wind turbine blade development is described in reference 2. Reference 3 provides comparative data on clear, solid (unlaminated) wood and basic equations with which to correct test data for moisture and temperature effects. Reference 4 contains clear-wood property data similar to that in reference 3. No data are available in references 3 and 4 on laminated-wood products.

The data reported in this publication are for test specimens with a minimum of nine laminas. More frequently there are 15 or more laminas, with some specimens having as many as 60. Materials with only a few laminas (three to five) exhibited significantly lower fatigue strength and a great deal of scatter (ref. 5).

Background information on laminated wood as a high-performance structural material is given in chapter II, together with descriptions of applications and manufacturing methods. Chapter III summarizes the most useful test data and presents mathematical models for predicting the effects of size and moisture content on mechanical properties. Chapter III will probably satisfy most data needs.

Chapter IV presents detailed test data in tabular and graphical form, providing a data base suitable for further analysis and updating. In addition, chapter IV contains discussions of the test data as well as descriptions of test specimens, testing procedures, and test equipment. Uncorrected test results are also listed in the data tables to permit users of the data to make different moisture corrections or data interpretations. Because of the size and complexity of the data set in chaper IV, numerically indexed headings are used to organize the information.

Listed below are the organizations responsible for the data contained in this publication and some of the important contributors from these organizations.

The General Electric Company, King of Prussia, Pennsylvania; Evendale, Ohio; and Pittsburgh, Pennsylvania	Harry Straub Vincent DiNenna David Hetzel
Gougeon Brothers, Inc., Bay City, Michigan	William D. Bertelsen Ronald C. Forrest Robert H. Kunesh, Consultant Michael D. Zuteck, Consultant
University of Illinois, Urbana, Illinois	Darrell F. Socie
University of Dayton Research Institute, Dayton, Ohio	Paul E. Johnson
Washington State University, Pullman, Washington	Roy Pellerin
ITT Research Institute, Chicago, Illinois	S.A. Bortz Gregory Skaper
Lehigh University, Bethlehem, Pennsylvania	Roger Slutter
NASA Lewis Research Center, Cleveland, Ohio	James R. Faddoul Raymond F. Lark

References

1. MOD-5-A Wind Turbine Generator Program Design Report. Volume II—Conceptual and Preliminary Design. Books 1 and 2. NASA CR-174735-VOL2-BK1 and NASA CR-174735-VOL2-BK2, 1984.
2. Stroebel, T.; Dechow, C.; and Zuteck, M.: Design of Advanced Wood Composite Rotor and Development of Wood Composite Blade Technology. (GBI-ER-11, Gougeon Brothers, Inc.; NASA Contract DEN3-260) NASA CR-174713, 1984.
3. Wood Handbook: Wood as an Engineering Material. Forest Service Agriculture Handbook No. 72, U.S. Forest Products Laboratory, Madison, WI, 1974.
4. Summitt, R.; and Sliker, A.: CRC Handbook of Materials Science. Vol. IV: Wood. CRC Press, Inc., Boca Raton, FL, 1982.
5. Johnson, P.E.: Design of Test Specimens and Procedures for Generating Material Properties of Douglas Fir/Epoxy Laminated Wood Composite Material. (UDR-TR-85-45, University of Dayton Research Institute; NASA Contract DEN3-286) NASA CR-174910, 1985.

Chapter II

Laminated Wood/Epoxy Composites in High-Performance Structures

Meade Gougeon and Michael D. Zuteck**

For most of recorded history wood has been the primary structural material used for large structures subjected to dynamic loads. In recent times wood has been largely replaced by steel, aluminum, and fiberglass composites. This transition has been due mostly to problems associated with moisture control and joining efficiency, rather than to a lack of attractive material properties of the wood itself. The systematic application of modern synthetic resins and joining techniques has now overcome most of the historical problems that limited the efficient use of wood. In many large-scale dynamic applications wood can now provide both structural and economic advantages over competing materials. This chapter summarizes the historical uses and problems of wood, the modern approach to solving these problems, and the potential economics of the resulting wood/epoxy technology. It also gives a brief perspective on the nature of wood as an engineering material, and the significance of the data base contained in chapters III and IV in this compendium of test results for wood/epoxy laminates.

Historical Development of Wood Technology

The most extensive efforts at optimizing the use of wood in large dynamic structures have been in building ships. Two thousand years of evolutionary shipbuilding technology reached its zenith in the 16th century with ships capable of supporting the great voyages of exploration. The fundamentals of shipbuilding technology of this era were sound enough that only small improvements were made over the next 300 to 400 years. Essentially the same materials and construction methods were still used in the great clipper ships of the 19th century.

Up to this point the long evolution of wood technology had focused upon "the weak link"—the capability of the joint between individual wood pieces. Wooden ships were built of thousands of wood parts that all needed to be joined together with the manufacturing capability then available. The evolution of shipbuilding essentially relied upon improvements in joint technology, which allowed larger and larger ships to be built. However, these ships were far heavier than they needed to be because only a small fraction of the true structural potential of wood could be used with the existing types of joints.

A shore-bound relative of wooden shipbuilding success was the Dutch windmill (fig. 1), a superb technical achievement. Recent wind turbine experience has given us a proper appreciation of what was accomplished with wooden wind machines over 400 years ago.

With the arrival of manned flight lightweight structural capability became paramount for the success of aviation. At this point the true limitations of past wood technologies were addressed. For the first 30 years of the development of the airplane, wood was the primary structural material. Pressures to develop safe, reliable, lightweight structures fueled research and development efforts that, for the first time, began to scientifically characterize wood properties. Aircraft engineers quickly realized that even the best mechanically fastened wood joints could transfer only a little over 30 percent of downstream wood material capability. Thus, the full *material* capability of wood had rarely been utilized in any of the dynamic wood structures of the past.

Because of the limitations of early adhesives, bonded wood joint technology did not become fully viable until the mid-1930's, when more advanced adhesives became available. This late development, combined with a lack of uniform, consistent wood physical properties that could be relied upon in a quality control effort, limited the use of wood in the then rapidly developing aircraft industry.

Metals quickly gained favor as a safer material for most larger and faster aircraft. Metals not only possessed more

*Gougeon Brothers, Inc., Bay City, Michigan

Figure 1.—Eighteenth century windmill still in use in the Netherlands.

consistent properties but could be fabricated with a high degree of reliability by a semiskilled work force. In comparison, woodworking required a high degree of skill that took a long apprenticeship to acquire.

Some efforts to keep aviation-oriented wood technology alive persisted in both the United States and Great Britain. With the coming of World War II and the ensuing shortages of all metal materials, the substitution of wood in aircraft and other highly sophisticated structures became crucial to the war effort. For the first time a serious effort was begun to perform the necessary testing so that an engineering data base could be established for wood materials.

The De Havilland Aircraft Company of Great Britain developed a unique stressed-skin monocoque shell design that was the culmination of 23 years of experience in wooden aircraft. The chief structural feature of this design was a wood composite sandwich of birch veneers over a unidirectional balsa core. The design for De Havilland's *Mosquito* bomber using this advanced structural concept was conceived in 1939 (ref. 1). This extremely successful airplane was in full-scale production in 1941 and saw much service in World War II. Figure 2(a) shows the overall configuration of the plane, figure 2(b) illustrates some of the details of the wood sandwich construction, and figure 2(c) is a photograph of a *Mosquito* bomber that is still flying. This two-man-crew wooden bomber, one of the most advanced aircraft of its day, had a

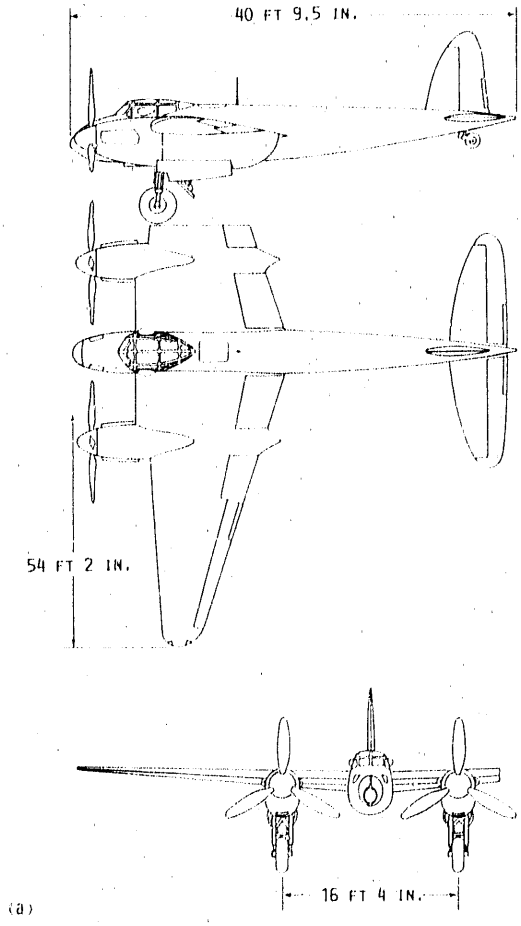

(a) Overall configuration.

Figure 2.—Laminated-wood *Mosquito* bomber built in early 1940's by De Havilland Aircraft Co.

level flight speed of over 400 mph and was capable of carrying a 3000-lb bomb load. Operating at fighter speed without armament, it had a 1500-mile range.

In the United States an effort to build the world's largest aircraft, the Hughes flying boat, nicknamed the *Spruce Goose*, was a controversial wartime project that relied on the most advanced aircraft engineering and wood technology then available. The completed aircraft, shown in figure 3(a) at takeoff for its only flight, is still the largest totally bonded, all-wood structure ever built. The authors had the opportunity to inspect the internal structure of this airplane in 1979. At a constructed weight of 400 000 lb, it is an engineering marvel for its unparalleled combination of fine structural detail, bonded construction, and immense size. Figure 3(b) shows an example of the internal construction of the *Spruce Goose*.

Major pioneering efforts in wood technology ended at the close of World War II. One reason was that aluminum alloy technology evolved quickly in response to the needs of modern aircraft. This was compounded by wood's past image, traditions, limitations, and folklore. However, the main reason

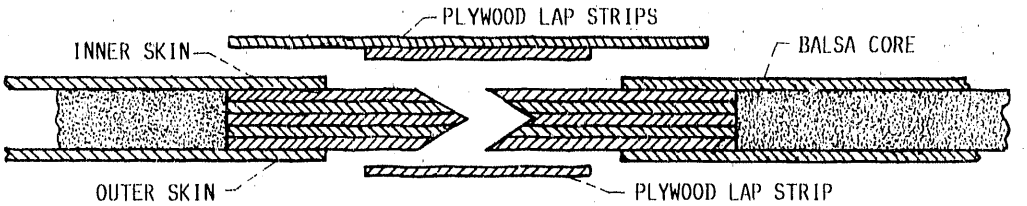

DETAILS OF SKIN JOINT WHERE FUSELAGE HALVES ARE MATED;
PLYWOOD LAP STRIPS ARE GLUED AND SCREWED INTO SHELL MEMBERS

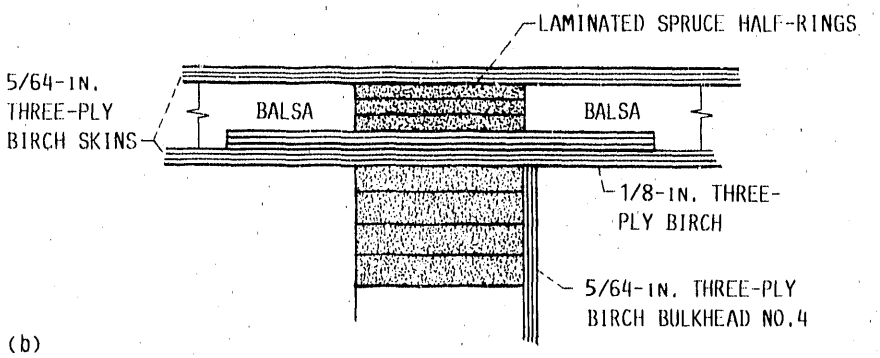

METHOD OF REINFORCING MONOCOQUE WALLS AT BULKHEADS

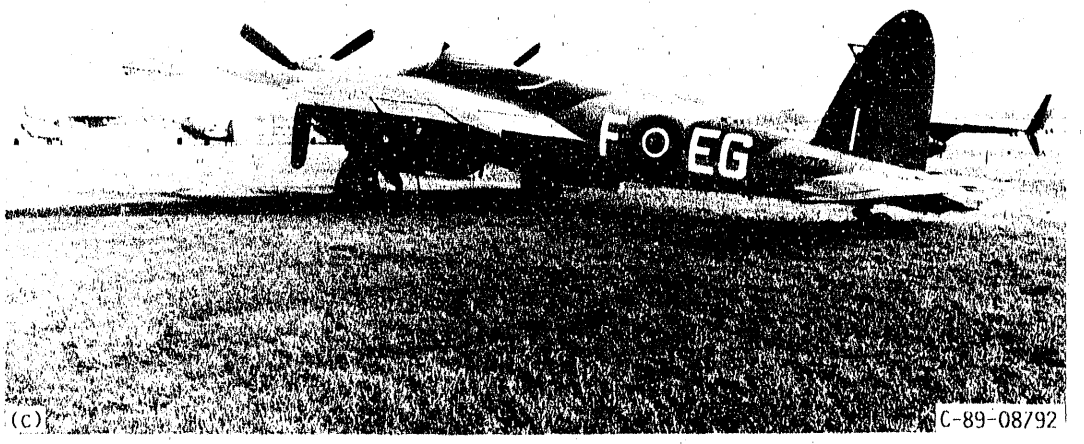

(b) Some details of wood structure and joints.
(c) Restored *Mosquito* bomber at 1989 Experimental Aircraft Association Convention and Exhibition in Oshkosh, Wisconsin.

Figure 2.—Concluded.

wood lost favor was related to maintenance. Lack of a viable moisture protection system for a completed structure was at the heart of the problem. All wooden structures need some reasonable moisture stability to prevent internal stressing and fungus attack. The old wood technology of ships had evolved to the point where it could successfully deal with large changes in wood moisture content, but the rot problem was never solved. Although the development of all-bonded joints solved the major structural limitation of wood construction, moisture-related problems persisted. By 1945, moisture problems were perceived by the aircraft engineering community as a fundamental unresolved dilemma that severely limited wood as a viable engineering material for high-performance dynamic structures. Another major drawback was the lack of adequate quality controls that could be implemented in large-scale manufacturing efforts with mass production.

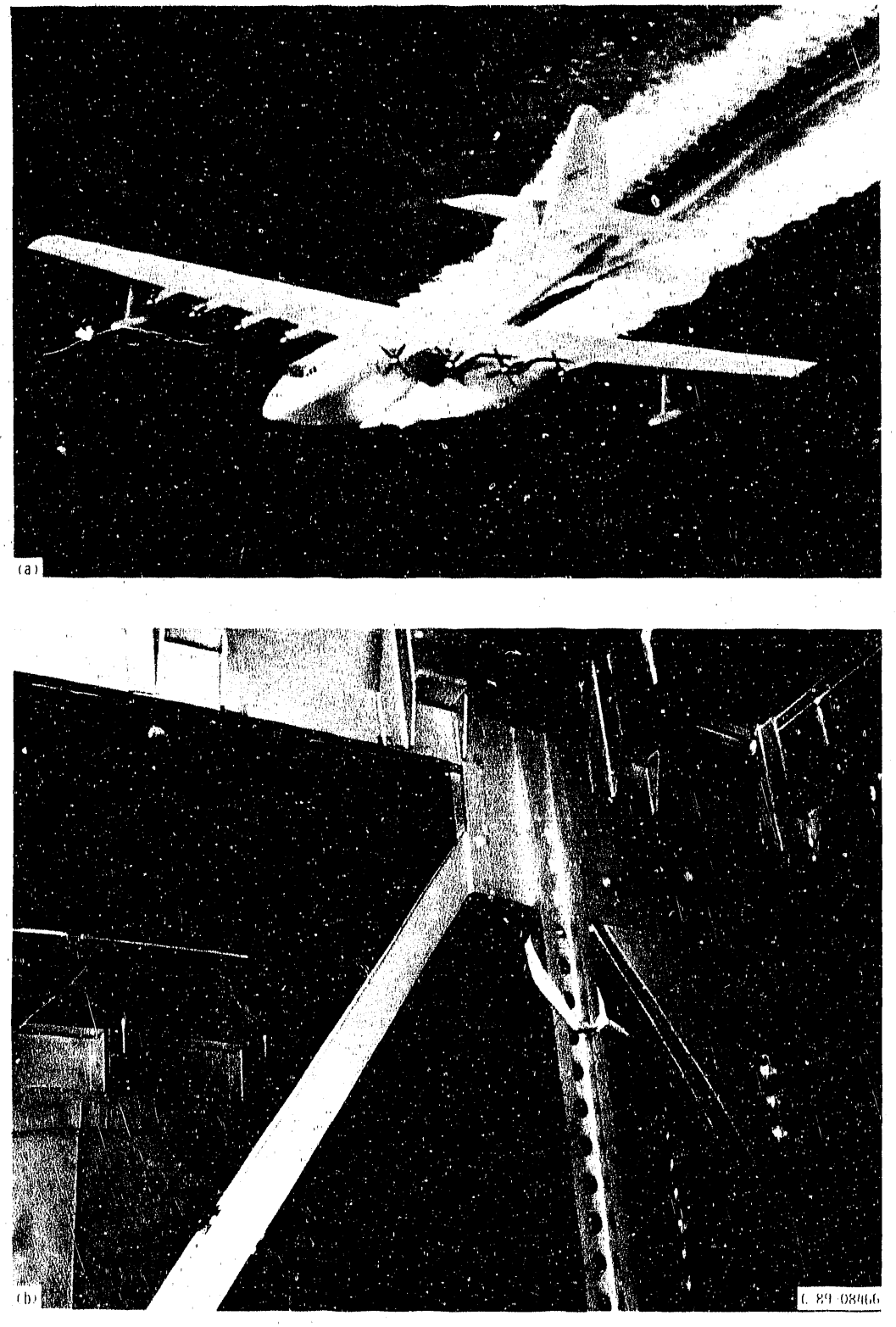

(a) General view.
(b) Typical internal structure.

Figure 3.—Hughes all-wood flying boat, nicknamed the *Spruce Goose*, on its one and only test flight. Designed and built for the U.S. Navy, it is the largest aircraft ever constructed of wood (320-ft wing span; 219-ft-long fuselage; 400 000-lb gross weight). Photo courtesy of Wrather Port Properties, Ltd., Long Beach, CA.

Moisture and Dry Rot

Moisture is the major ingredient of all woods, usually being more than 80 percent on a weight basis in the living tree. Even wood that is properly dried or cured will have a significant percentage of its weight in moisture. This will typically range from 6 to 15 percent of the oven dry weight of the wood, depending upon the surrounding atmospheric conditions. Figure 4 shows the long-term moisture content of wood when subjected to various relative humidities at a temperature of 70 °F. The subject is somewhat more complicated than the graph portrays because the moisture content in air at 50 percent relative humidity is much different at 40 °F than at 70 °F. (Warm air holds more moisture than cold air.) However, every geographical area has an average year-round moisture and temperature that will determine the local average wood moisture content. In the Great Lakes area wood seems to equalize at about a 10 to 12 percent long-term moisture content when dried in a sheltered but unheated area.

Wood as a living organism remains at a relatively constant moisture level during its entire lifetime until it is harvested. The real problem with wood begins after it is cut, when its moisture level is rather quickly influenced by short-term changes in local weather conditions. Unprotected wood may undergo many moisture changes in a short time, and the repeated expansion and contraction of the wood under these conditions is thought to be the leading cause of premature wood aging. Wood over 3000 years old has been taken out of the tombs of Egypt. Because of the constant temperature and humidity in which it was stored, the wood was found to have lost none of the physical properties typical of its species.

This sponge-like capacity to take on and give off moisture at the whim of the surrounding environment is the root cause of nearly all of the problems with wood. Specifically, varying moisture levels in wood are responsible for dimensional instability, internal stressing that can lead to checking and cracking, potential loss of strength and stiffness, and decay due to dry rot.

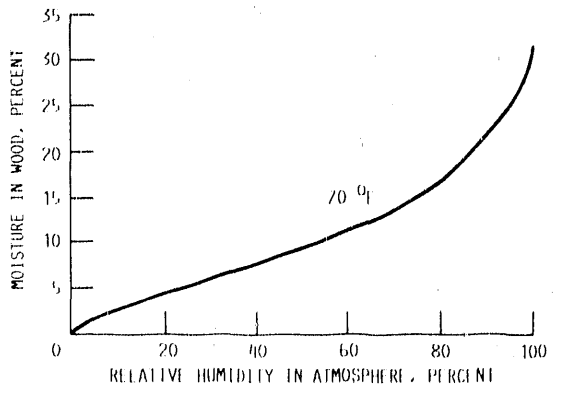

Figure 4.—Equilibrium moisture content of wood as a function of ambient humidity.

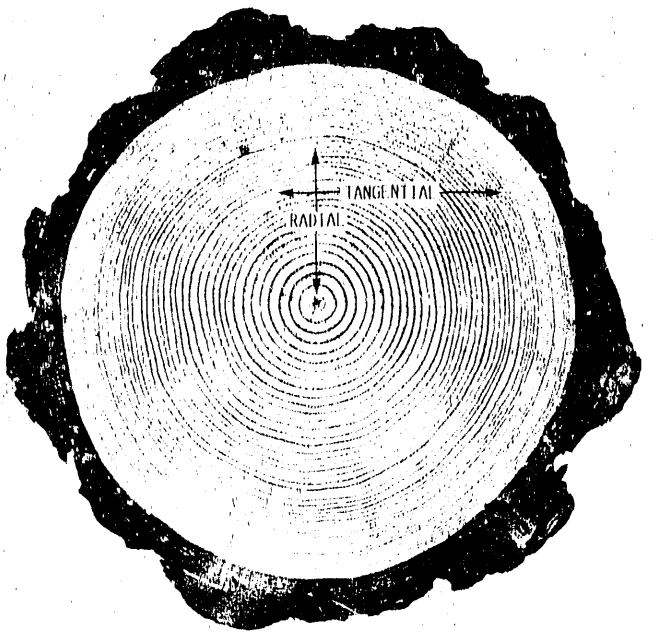

Figure 5.—Cross section of a typical log from which veneers are cut, showing principal directions (longitudinal direction is lengthwise).

Dimensional instability has always been a factor limiting the use of wood in many engineering applications where reasonable tolerances on size must be maintained. To complicate matters, the dimensional instability of wood has never been constant. It varies widely between species of wood and depends strongly on how the wood is cut from the tree. Referring to figure 5, radial-grain wood (cut perpendicular to annual rings) in most species is more stable than is tangential-grain wood (cut parallel to annual rings). The dimensional change of wood due to moisture changes always occurs on outer surfaces first, caused by differing moisture levels within the same piece of wood. This can lead to internal stressing that often causes surface checking and cracking.

Of all the problems of wood, dry rot decay is the most known and feared. Dry rot is a misleading term, since dry wood does not rot. In fact, four rather specific conditions must be met for dry rot spore activity to occur:

(1) The moisture content of the wood must be at or near the fiber saturation point of 30 percent (rot is unknown in wood with a moisture content of less than 20 percent).

(2) An adequate supply of oxygen must be available to the rot spore fungi (i.e., the wood must not get too wet).

(3) The temperature must be warm (76 to 80 °F is ideal, although fungi have been known to be active at temperatures as low as 50 °F).

(4) The spores must have the proper kind of food (some woods, such as western red cedar, are resistant to rot because of the tannic acid in their cellular makeup).

Although many types of rot fungi worldwide can destroy wood, in North America two species of the brown rot family are dominant. These fungi are extremely hardy and seem to survive the worst temperature extremes in a dormant state,

waiting only for the right conditions to become active. Efforts to control brown rot in solid (unlaminated) wood have had only limited success and generally center around poisoning the food supply with various commercial wood preservatives. The approach to solving this problem in laminated wood is quite different, as will be explained later.

Wood Technology Today

The demise of wood as a serious engineering material was both unfortunate and premature. With the help of modern technology most of the problems with wood can be solved in a practical manner. For nearly two decades the authors have successfully used wood as a composite with plastic resins to build high-performance ice boats (fig. 6), multihull racing sailboats (fig. 7), and blades for modern wind turbines. An experimental 200-kW wind turbine on Oahu in the Hawaiian Islands (fig. 8) has a 125-ft-diameter turbine rotor constructed

Figure 6.– A GBI iceboat traveling at a speed of 60 mph. Hull and outriggers are constructed of laminated fir/epoxy.

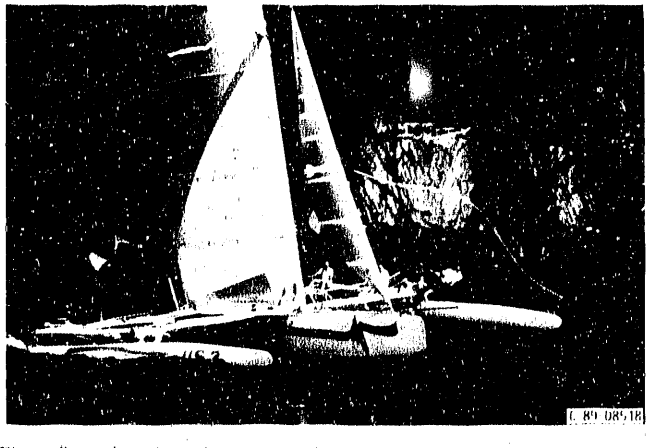

Figure 7.—*Adrenalin*, a 40-ft racing trimaran with laminated wood/epoxy hulls.

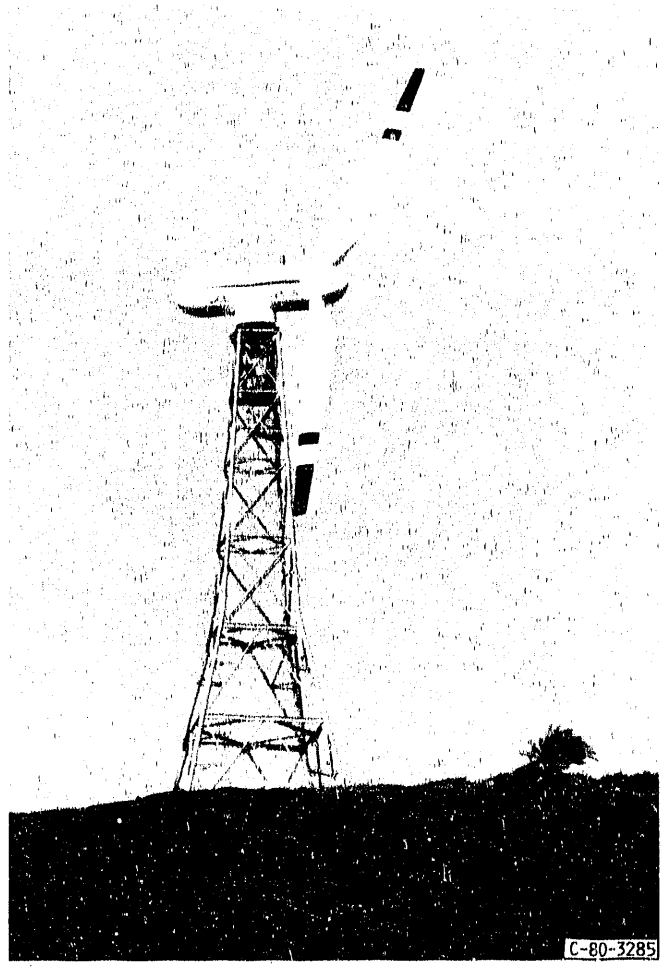

Figure 8.—DOE/NASA 200-kW Mod-0A experimental wind turbine near Kahuku Village, Oahu, Hawaii. Laminated Douglas fir/epoxy blades form the 125-ft-diameter rotor.

of Douglas fir/epoxy laminate. The boats and turbine blades were built by Gougeon Brothers, Inc. (GBI). These dynamic structures must be built with high strength to weight ratios to be successful. These examples have been successful, in part, because wood itself is an excellent engineering material and in some applications has capabilities that are unavailable with any other material. The ability to solve both woods' moisture and joining problems, however, is the key to its use as a practical and competitive engineering material.

At a time when fiberglass was dominating the boatbuilding industry, a unique wood technology was developed at GBI that relied on a new plastic ingredient: epoxy resin. For the first time the industry possessed a key ingredient that could be used to both bond and seal wood structures, permitting high strength to weight ratios that efficiently utilized wood's excellent physical properties. This upgrading of an old material with a new technology has evolved considerably during the past two decades and is the basis for a revolution taking place in wood technology.

Wood as an Engineering Material

In considering using wood as an engineering material, it is pertinent to note that wood is not a single material with one fixed set of mechanical properties. Wood includes many species with a wide range of properties, depending upon both the species and the density selected. The range of properties is considerably wider than that generally available with most other materials. In a given metal, for example, some variation of properties can be attained by alloying or tempering, but little variation of material density is possible. The density of wood, on the other hand, can be selected over more than a full order of magnitude, from 6 lb/ft^3 (or even less) for selected grades of balsa to over 60 lb/ft^3 for certain species of hardwood. Designers using other materials can perhaps best appreciate what this means by imagining that a factor of 10 in density variation were somehow readily available for steel, aluminum, or composite materials.

The basic mechanical properties of wood such as strength and modulus are roughly proportional to its density. This is true regardless of species, since the basic organic material is the same in all species. Thus, changing density is rather like compressing or expanding the net strength and elastic stiffness into different cross-sectional areas, with little net variation of total properties per unit of weight.

The design flexibility this can provide is obvious. Low-density species can be selected for efficient use as sandwich panel core materials and for panels or beams where stiffness or buckling resistance per unit of weight is of primary importance. High-density species can be selected where there is a need for high strength or stiffness per unit of volume, such as panel skins or structural members that must occupy constrained geometric volumes. The full range of intermediate densities provides a match for requirements anywhere between these extremes. For example, for a given buckling load and weight per unit length, approximately a factor of 10 in unsupported panel length and a factor of 3 in unsupported column length are readily available to the designer of wooden structures.

Granted that the density variation of wood can be of advantage to designers of wooden structures, one must also inquire how good are its net properties per unit of weight relative to other structural materials. After all, other light, variable-density materials, such as expanded foams, are available. For modern structures where weight is an important issue, designers often select materials on the basis of specific strength, or strength divided by density. For example, a fir/epoxy laminate with a tension strength of 12 000 psi and a density of 0.023 $lb/in.^3$ is competitive on a specific strength basis with steels as strong as 156 000 psi and aluminum alloys with tension strengths to 52 000 psi.

In addition to specific strength advantages, the lower density of wood materials permits greater wall thicknesses in wooden structures with the same overall weight as structures made of other materials. This feature provides the designer with significant advantages in solving problems involving stiffness, elastic compressive buckling, and deflection.

This strength comparison considered the properties of wood along its grain direction. However, the same piece of fir that displays 12 000-psi tension strength along its grain will have something like 300-psi maximum tension strength across its grain. That is a 40-to-1 variation in tension strength with load direction. The other physical properties of wood are also distinctly anisotropic, although not to as great a degree as tension strength. What this means is that the designer of wooden structures may have to take explicit measures to deal with cross-grain and shearing forces, unlike the designer who uses conventional materials with isotropic properties. It also means that in cases where large loads flow in more than one direction, wood grain will have to be arranged to align with all of these loads. For cases where the large loads are confined to a single plane, laminated veneer or plywood can meet the requirements. Where loads exist in all three axes, the designer must use more sophisticated approaches tailored to the loads and the geometry. All these factors are the other side of the wooden structure's "coin," and dealing with them is the price the designer pays in order to gain the advantages of this easily fabricated, high-performance, low-density structural material.

Fatigue Resistance

Another factor that must be considered when evaluating wood is its performance in fatigue. By its nature as a fibrous material, wood is not given to the kind of fatigue crack propagation that is familiar in metals. The literature of the fatigue properties of wood is not as well developed as that of some other materials, but in round numbers, one can expect essentially infinite fatigue life (more than 10^8 cycles of loading) for wood with maximum stresses to 30 percent of static tension strength. For some kinds of loading even higher percentages are acceptable. Figure 9 illustrates how the fatigue resistance of laminated wood (Gougeon engineered laminate,

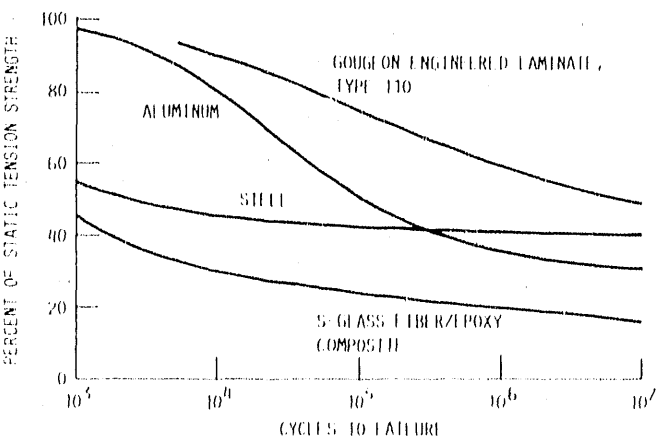

Figure 9.—Tension-tension fatigue strength of various structural materials.

type 110) compares favorably with that of other structural materials.

Because a large structure will be composed of a great deal more material than a small one, it will include a much larger number of built-in defects. Statistics dictate that the worst defect (which sets the strength level for a whole piece or structure) will be more severe in a large structure than in a small one and that a lower level of practical working strength will therefore result for the large structure. Although ductile yield can somewhat mask this effect for one-time or low-cycle loading in some materials, long-term fatigue inevitably seeks out these strength-limiting defects. The size effect must therefore be accounted for to properly design large fatigue-driven structures.

The wealth of experimental data in chapters III and IV provides a modern basis for assessing the fatigue performance of fir/epoxy laminates that goes well beyond what was previously available. Work continues on a volume of wood/epoxy test data that addresses two other central issues for large, fatigue-driven structures; namely, what is the effect of size upon the strength and fatigue performance of a material, and what role do defects play in setting these overall strength levels?

The Sequoias of the western United States are colossal trees that must withstand nature's fatigue loads for centuries and must do so in the presence of defects from boring insects, physical damage, and disease. Because the survival of any tree dictates that the weakening effects of size, defects, and fatigue are successfully dealt with, the utility of wood for large fatigue-driven structures should come as no surprise.

Wood/Resin Composite

The basic principle of laminating wood has been used effectively for many years. The major difference between a standard wood laminate (such as plywood) and the new wood-resin composite developed by GBI is that as much as 20 to 25 percent of this new material is resin. The main reason for this change in approach is to provide the wood fiber with maximum protection against moisture. A second reason is to provide sufficient resin to fill the inevitable voids and gaps that can occur with low-pressure bonding and thus reduce the number of defects that might act as nuclei for failures.

A schematic view of a typical laminate (fig. 10) shows its directional geometry. Two types of laminate joints are illustrated here, namely, scarf and butt joints. Both have been used successfully at GBI.

As already discussed, most of the problems with wood are moisture related. The basic approach at GBI is to seal all wood surfaces with a properly formulated resin system. A typical laminate using 1/10-in.-thick veneers will have nine glue lines per inch of thickness, and each glue line must be penetrated by water vapor to either increase or decrease the moisture content of the entire laminate. All subsequent joints in the

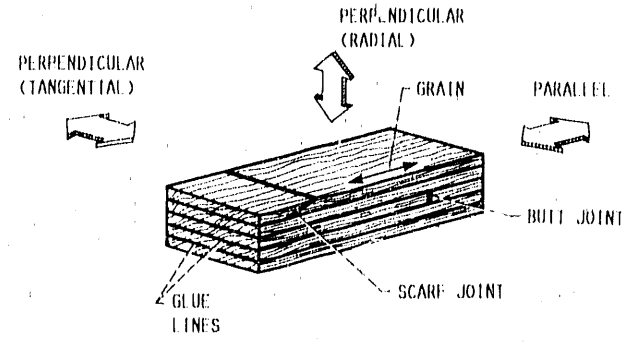

Figure 10.—Grain orientation in a typical laminate and illustration of types of laminate joints.

wood/resin composite structure must also be sealed at the same time a proper bond is being made.

The basic success of the wood/resin composite depends on the ability of the resin system to both effect an adequate bond and resist the passage of moisture. An epoxy-based resin system has evolved over the past 20 years that has been proven effective through actual usage in a wide range of environments with both marine and wind turbine blade applications. At present no known resin system can form a perfect moisture barrier. However, the present level of capability is sufficient to slow the passage of moisture to such an extent that actual moisture change within the wood is kept to a minimum. In the presence of the short-term fluctuations in atmospheric conditions that are so damaging to wood stability, the wood inside the resin glue lines remains at a virtually constant moisture level that is in equilibrium with the average annual humidity. The more violent short-term and seasonal moisture fluctuations are easily resisted.

With proper sealing, dry rot has been eliminated by keeping the moisture content below that required for dry rot activity and also by sealing the wood from any oxygen source. This removes two of the necessary ingredients for the rot spore to function.

A third benefit of using a high resin ratio in a wood composite is utilization of the excellent physical properties available with modern resin systems. Some of these unique properties can be used to enhance the capabilities of many wood species, especially in the secondary properties of cross-grain compression, tension, and shear.

Early in the GBI wood composite development, the Douglas fir species was chosen as the best available to fulfill all long-term needs. The reason for this decision was primarily economic, but it was also recognized that the Douglas fir species possesses excellent specific physical properties, better than those of many other readily available wood species. Of particular interest was Douglas fir's ideal density for use in many types of high-performance structures. Its density is high enough to give needed strength, yet low enough to provide efficient buckling stability.

Douglas fir, widely traded as a commodity in a veneer form, supports a large plywood industry. An active reforestation effort with this species has meant that a significant portion of the market is in second-growth trees that range from 20 to 30 in. in diameter. These trees, cut into 8-ft lengths called peeler logs, are efficiently turned into veneers with a minimum of waste. At historic growth rates the present reforestation efforts should ensure an ample supply of this species through the next century.

Economical Fabrication of Wood/Epoxy Composite Structures

The price of ideal 1/10-in.-thick premium-grade (AB) Douglas fir veneers has averaged approximately $55 per thousand square feet from 1975 to 1985. More recent prices in 1989 have been as high as $86 per thousand square feet, an increase that is still well below the inflation rate since 1975. Our experience has been that this basic veneer price increases by 60 percent after drying, grading, spoilage, and shipping costs are taken into account. But even at 14 cents per square foot, the 1989 per-pound cost of Douglas fir veneer only amounts to about 40 cents, which is about half the price of unwoven synthetic fiberglass materials. The wood industry has made significant strides to improve overall efficiency in past years, and it appears that a low-cost supply of the Douglas fir species will be available for many years to come.

Laminating pressures of 100 psi or above are typically necessary to make effective bonds with traditional wood adhesives. Achieving these high pressures can be expensive, and this limits the size of the laminated parts that can be made. With special epoxy-based adhesives excellent bonds can now be made at low pressures under room-temperature conditions. Lowering the pressure needed for laminating has the positive effect of lowering the cost of wood bonding. Pressures to 12 psi are easily and cheaply produced with a vacuum-bag system that has been used at GBI to manufacture laminated parts for wood/epoxy wind turbine blades as long as 68 ft.

The ability to join veneer subassemblies into a useful structure with low bonding pressures at room temperatures relies upon a high-strength, gap-filling adhesive. Test data suggest that gaps of 0.250 in. in longitudinal joints can be successfully bridged with a thickened WEST SYSTEM epoxy adhesive, without measurable reduction in long-term fatigue resistance.

Costly quality problems due to low or uneven bonding pressures that produce gaps are significantly reduced. A high-strength adhesive with bridging capacity can provide a wide safety margin by successfully spanning significant voids in a laminate. The physical properties of specially formulated epoxy-based resins can be considerably higher than the static cross-grain strength or shear properties of most woods. The ability to make highly reliable joints with only contact pressure has thus been important to the economical fabrication of large, lightweight wooden structures.

The fact that wood is a defect-laden material has led to the development of two separate procedures for minimizing the effect of defects on the laminate. The first is a randomization of defects by systematically arranging veneers to scatter defects as evenly as possible through the laminate. Statistically, this procedure reduces the severity of defect-initiated failure, but it does not eliminate the problem. The second, and far more effective procedure, is to ultrasonically inspect all veneers. This 100-percent-inspection process can be performed by a machine in what is a high-speed, in-line process at minimal cost. About 30 percent of the veneers typically do not pass inspection, and these are sold back to the plywood market. Depending on volume, the total grading costs can be as low as $10 per thousand square feet of veneer. This new and effective method of quality control provides a more homogeneous wood laminate material that consistently meets high physical property standards.

The base material costs for producing wood composite materials are a function of the relative amounts of the two principal ingredients: wood veneer and bonding/sealing resin. Although the relationship will vary, 80 percent wood veneer and 20 percent resin (by weight) is typical of a standard laminate. The base raw material cost can be figured on this veneer/resin ratio as follows (assuming 100 lb of laminate):

1/10-in.-thick Douglas fir veneer at $0.40/lb × 80 lb	= $32.00
Gougeon WEST SYSTEM resin at $2.57/lb × 20 lb	= $51.40
	$83.40
	$83.40/100 = $0.834/lb

Wastage and handling costs must be added to this base cost. According to GBI experience, this increases the total raw material cost to almost $1.00 per pound.

The total cost of a wood/epoxy laminate is obviously sensitive to resin costs, and there is far greater need to reduce this cost element than to reduce wood costs. It is important to understand that any attempt to reduce the percentage of resin in the laminate will adversely affect both moisture resistance and proper bonding. Wood/epoxy ratios will vary depending on a number of factors, but the resin content cannot usually drop much below 20 percent of laminate weight without performance losses.

From GBI's experience a high-volume, mature manufacturing plant is generally capable of producing ordinary structures at roughly double the base material cost. This suggests that a production cost of $2.00 per lb (in 1989 dollars) could be attained under the right circumstances for a fully mature, high-volume product constructed of wood and epoxy.

Development of Wood/Epoxy Wind Turbine Blades

The successful development of wood/epoxy composite blades for modern wind turbines (fig. 8) serves to illustrate the large potential for many other high-performance structures designed and fabricated using the same basic technology.

Wind turbine blades may well be one of the most difficult performance applications for any material. Blades built of steel, aluminum, and fiberglass have all suffered from fatigue failures. One reason is that peak blade loads and their cyclic components have turned out to be more severe than anyone anticipated. Long-term performance (more than 20 years of life) has not yet been demonstrated by any material for this difficult application, but a wood/epoxy composite has demonstrated excellent potential for achieving this life span.

Personnel from the NASA Lewis Research Center in Cleveland, Ohio, who were involved in developing large, horizontal-axis wind turbines for the Department of Energy, contacted GBI in 1977 while searching for ways to reduce the high cost of blades. Efforts to develop aluminum, fiberglass, and steel blades were already under way, and GBI was asked to perform a wood-blade feasibility study. Early results of the study were encouraging, and a 20-ft-long, full-size test section that represented the inboard one-third of a 60-ft blade was constructed.

NASA's experience had shown that the inboard ends of turbine blades were the most susceptible to fatigue failure. The hub end of the 20-ft sample contained a ring of 24 studs bonded into the 3-in.-thick blade walls with epoxy. GBI designed this somewhat unusual but simple method for attaching the wood blades to the rotor hub. A typical stud, 18 in. long, is shown in figure 11. Other stud configurations are discussed in references 2 and 3. NASA tests confirmed that individual studs had sufficient static and fatigue strength in the bonds, but testing of the complete blade-to-hub joint was necessary before this novel method could be accepted for use on a wind turbine.

The completed 20-ft blade section was delivered to NASA in July 1978 for evaluation. After rigorous testing with both static and fatigue loads, the wood/epoxy portion of the sample was undamaged, confirming the potential application of wood/epoxy laminates as a structural material for wind turbine blades. The steel studs, however, failed in fatigue outside the blade as a result of flexibility in the support plate to which they were attached. This led to a recognition of the importance of stiffness in the hub attachment flanges, and modifications were made to prevent this type of failure in the future.

Subsequently, several contracts were awarded for the design and manufacture of blades for four 200-kW Mod-0A wind turbines with rotors 125 ft in diameter. The first pair of blades was built on an accelerated schedule that allowed only 5 months for design, tooling, and fabrication. The blades were delivered on time and on budget and performed satisfactorily for 7844 hours before a corrosion-fatigue failure occurred in one steel stud as a result of misalignment during assembly. As a precautionary measure the blades were removed from service. Follow-on blades saw satisfactory service on all four of the Mod-0A experimental turbines, confirming the success of the wood/epoxy composite blade approach.

The success of these early blades was made possible by a combination of good luck and conservatism in the design and engineering effort. Many years of working with wood composite materials in the marine industry helped significantly by providing a practical working knowledge of the material. A major problem was the lack of specific material data upon which to base a set of design stress allowables for a 30-year life (4×10^8 major load cycles). A secondary and still prevalent problem in the wind power industry was a lack of knowledge of the real loads that wind turbine blades had to withstand, particularly in extreme operating conditions.

The issue of material performance capability was more seriously addressed in late 1980 when GBI began a subcontract with the General Electric Company to develop a 400-ft-diameter wind turbine rotor for their 7.3-MW Mod-5A wind turbine, a project managed by NASA and sponsored by DOE. The need for considerably better material understanding than that resulting from the earlier Mod-0A effort became a major obstacle. This need resulted in funding of the most comprehensive fatigue testing program ever undertaken on a wood material.

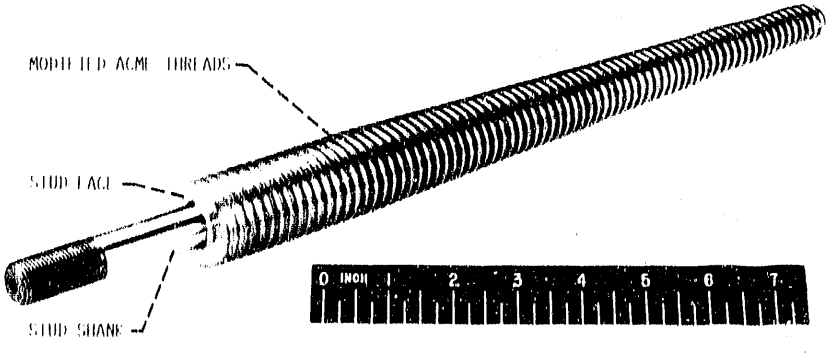

C-82-4953

Figure 11.—Steel stud typical of type bonded into end of 60 ft wind turbine blade for attachment to rotor hub.

Unfortunately, the entire Mod-5A program was then operating on an accelerated schedule, and the blade design effort was always waiting for material test results. Because of the time pressure the cyclic fatigue testing was concentrated on those basic laminate properties most relevant to stress conditions driving the blade design. Minimum numbers of test samples sometimes provided data that were not conclusive, requiring careful interpretation to develop meaningful design parameters. This was a particularly difficult problem in the area of secondary properties.

The test program was completed in June 1984 after the Mod-5A project was terminated at the end of the design phase. Although a wood/epoxy rotor 400 ft in diameter was not built, a qualified design was completed, together with a manufacturing plan.

Since the demise of the Mod-5A project, both DOE-funded and GBI-funded testing programs have added significantly to the data base. However, many design-allowable issues are still not completely resolved, such as size effects and cross-grain tension strength. Until these issues are better defined, conservative use of certain design allowables must prevail.

Production of Commercial Wind Turbine Blades

GBI made a decision to enter the commercial wind turbine blade business in 1981. Over the next 2 years, four different blades ranging from 10 ft to 38 ft in length were designed and put into production. Altogether, over 4300 of these blades were built and sold by late 1985 for use in generating power. To date, none of these blades has failed in normal service, with some of them achieving well over 20 000 service hours.

In November 1983, GBI was contacted by Westinghouse Electric Corporation to design and develop blades for a 142-ft-diameter rotor for its 600-kW utility-oriented wind energy system. Production tooling was completed by April 1985, and 36 blades were built and delivered by November 1986. These blades, one of which is shown in figure 12, have performed satisfactorily on a Westinghouse-constructed wind power station located on the Hawaiian island of Oahu. These 600-kW turbines are the largest commercial units yet to be built in a series production and are thought to be an ideal size for commercialization with utilities in the near future.

A vital factor in determining the ideal wind turbine machine size for economical operation is rotor cost. Both wood/epoxy and fiberglass blades were considered for the Westinghouse wind turbines. The GBI wood/epoxy blades cost less and were considerably lighter than the fiberglass option. A lighter blade allowed significant weight-associated savings in other components of the machine, which meant that an extra premium price could be justified because of the low rotating mass.

Manufacturing High-Performance Laminated Wooden Structures

The basic approach to manufacturing wood/epoxy laminate structures has not changed since the first Mod-0A blades were built in 1980. The steps in the manufacturing process are illustrated in figure 13 and described in more detail in references 2, 4, and 5.

Figure 13(a) shows the female mold for one-half of the blade airfoil. A layer of fiberglass cloth and a layer of aluminum screening installed for lightning protection form the external surface of the blade. Figure 13(b) shows precut and fitted

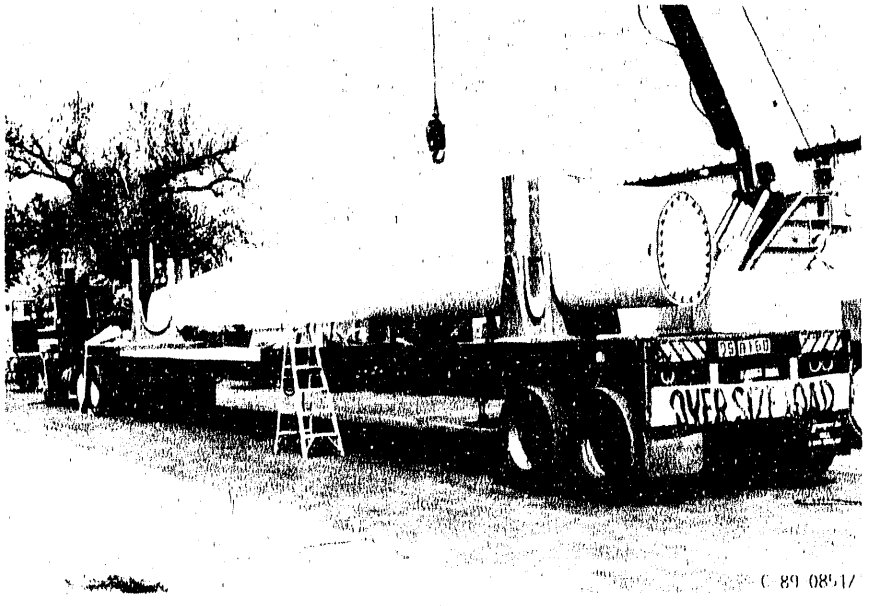

C-89-08517

Figure 12.—Laminated fir/epoxy blade for 142-ft-diameter Westinghouse 600-kW commercial wind turbine.

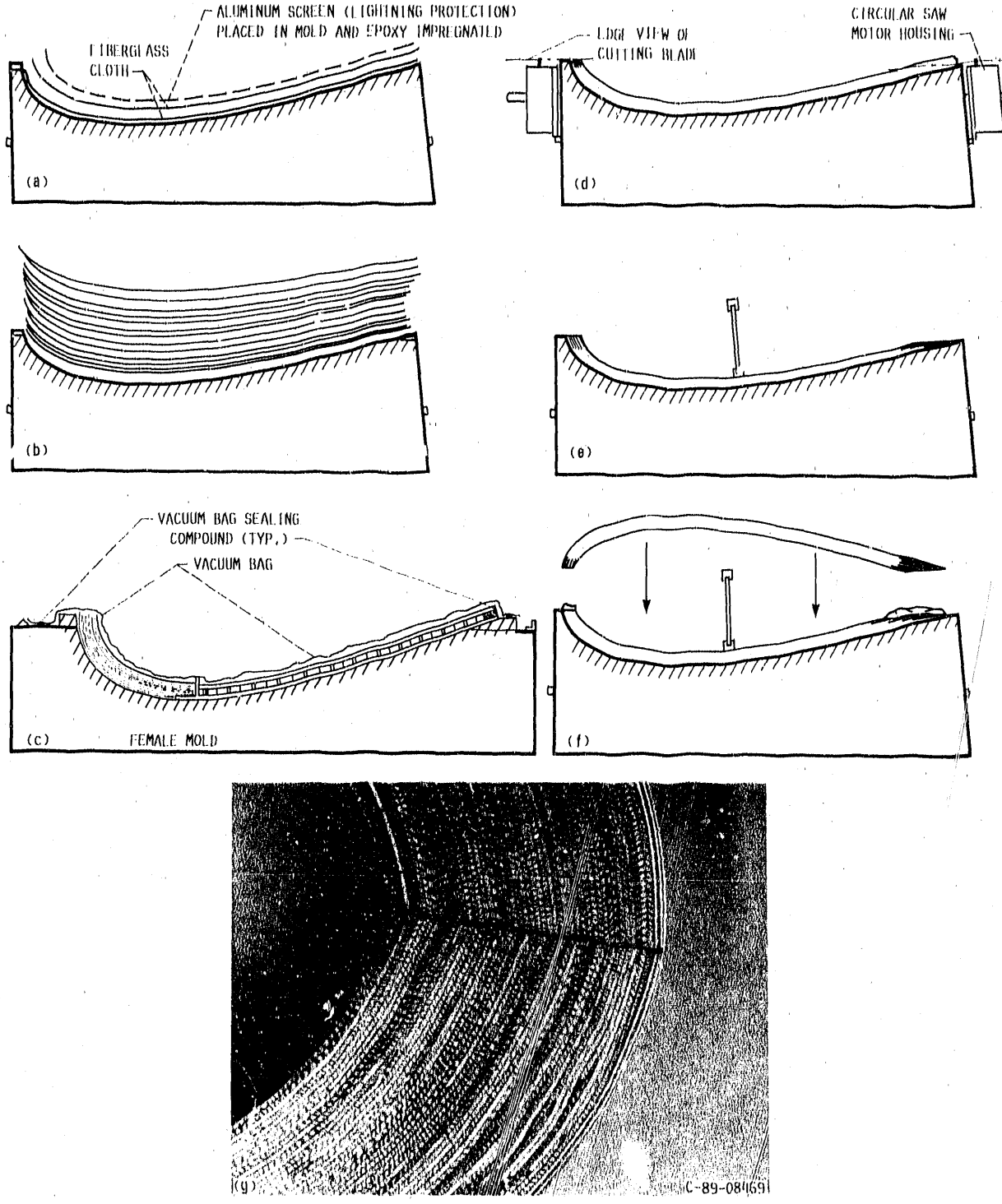

(a) Installation of materials for blade external surface in female mold.
(b) Stacking of epoxy-coated wood veneers that form blade shell.
(c) Vacuum bagging used to apply atmospheric pressure to veneers during epoxy cure cycle.
(d) Trimming leading and trailing edges prior to mating of shell halves.
(e) Installation of shear web into blade half-shell.
(f) Mating and bonding of shell halves.
(g) Closeup of leading-edge bonded joint.

Figure 13.—Manufacturing steps for Douglas fir/epoxy wind turbine blades.

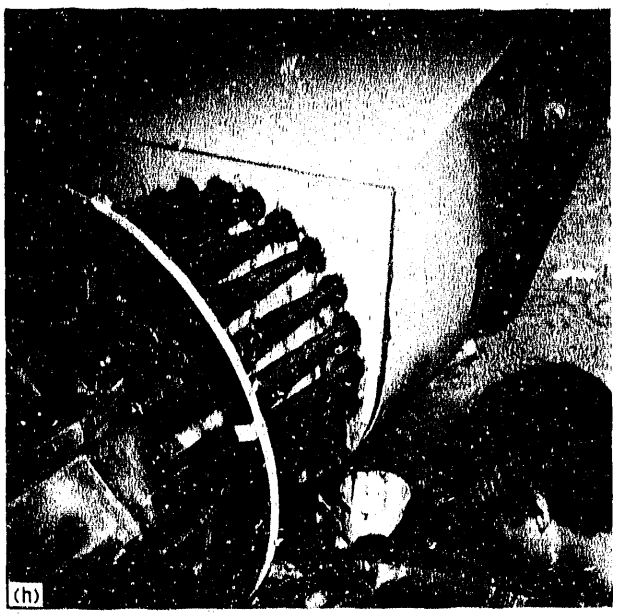

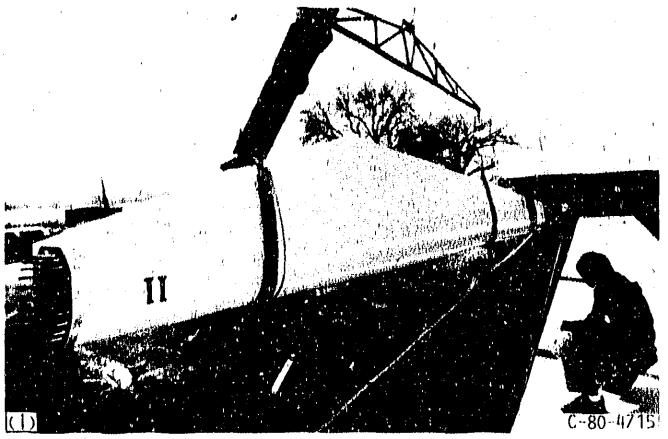

(h) Inserting adhesive-coated studs into blade root end.
(i) Completed blade being prepared for shipment.

Figure 13.—Concluded.

epoxy-coated fir veneers stacked in the mold. During this operation veneers are stapled in a number of locations to ensure proper stacking. Figure 13(c) shows the installation of a vacuum bag over the half-shell for the purpose of applying light, uniform pressure to the veneers during the epoxy cure. Figure 13(d) shows the cutting operation that trims the leading and trailing edges of the half-shell so that it will mate properly with the other half-shell. Figure 13(e) shows placement of the shear web, and figures 13(f) and (g) illustrate mating and bonding of the two half-shells. Steel studs of the type shown in figure 11 are held in a fixture, coated with a thickened epoxy, and inserted as a set into the blade root as shown in figure 13(h). The finished blade is shown in figure 13(i) being loaded for shipment in a protective carrier.

Beginning blade manufacturing efforts were limited to prototype development and small-volume production. Typical costs ranged from $20 to $30 per pound (1981 dollars) for these early blades, reflecting high labor costs. Serious production efforts begun in late 1982 started a natural evolution in improving efficiencies in the basic manufacturing procedure. By late 1985, prices for blades had dropped to the $7 to $10 per pound range depending on blade size, complexity, and volume. These prices are still dominated by high hourly labor costs, but modest capital expenditures have made large reductions in labor hours.

With labor costs being a high percentage of the total cost, there is considerable room to reduce future costs through mechanization of the work effort. Many labor-saving improvements have been identified and are awaiting proper business levels to justify the capital expenditures needed for implementation. It is believed that a sales price of under $5 per pound can be achieved for a completed wind turbine blade. This prediction assumes leveled production in a mature plant, with moderate capital expenditures for machinery and equipment. It should be recognized that wind turbine blade manufacturing needs strict quality control procedures, and this is a significant cost element that is not likely to decrease much with increased volume.

Concluding Remarks

The success of boat and wind turbine blade applications would indicate that this new laminated wood/epoxy technology is both a viable and an advantageous approach for many types of high-performance structures. Its inherent low density provides adequate buckling strength through the use of thicker wall sections at the same weight. Both its natural fibrous composition and its ability to be readily bonded into a virtually monolithic structure contribute to long fatigue life. Its excellent physical properties for its weight, together with high specific stiffness make extremely lightweight structures that are still strong and stiff enough to meet tough dynamic operating conditions. In addition, the basic material is reasonably priced, domestically available, ecologically sound, and most importantly, easily fabricated.

Numerous other potential commercial applications for this technology have been identified. Many of these potentials will be fully developed in the years to come. There has already been a direct spinoff in the marine industry with an improvement in the design and manufacturing approach to boat construction.

References

1. Ricker, C.S.: De Havilland "Mosquito", Aviation, Part I—May 1944, pp. 127-140; Part II—June 1944, pp. 123-137.
2. Strobel, T.; Dechow, C.; and Zuteck, M.: Design of an Advanced Wood Composite Rotor and Development of Wood Composite Blade Technology, DOE/NASA/0260-1, NASA CR-174713, Dec. 1984.
3. Faddoul, J.R.: Improved Stud Configurations for Attaching Laminated Wood Wind Turbine Blades. DOE/NASA/20320/66, NASA TM-87109, 1985.
4. Lark, R.F.; Gougeon, M.; Thomas, G.; and Zuteck, M.: Fabrication of Low-Cost Mod-0A Wood Composite Wind Turbine Blades. DOE/NASA/20320-45, NASA TM-83323, 1983.
5. Lieblein, S.; Gougeon, M.; Thomas, G.; and Zuteck, M.: Design and Evaluation of Low-Cost Laminated Wood Composite Blades for Intermediate-Size Wind Turbines: Blade Design, Fabrication Concept, and Cost Analysis. DOE/NASA/0101-1, NASA CR-165463, 1982.

Chapter III
Data Summary and Analysis

David A. Spera and Jack B. Esgar***

This chapter of the report summarizes the static and fatigue tests conducted on laminated Douglas fir/epoxy. In addition, information is provided on the fatigue strength of various joining methods, including glued joints between wood members and the use of metal studs for attaching laminated-wood structures to metal components of the overall structure. Analyses are developed for correcting strength values for wood moisture content and, based on the data available, for more generalized strength models. Approaches used for statistical analysis are described in both this chapter and chapter IV.

Chapter IV, which follows, contains tables of all the data presented in chapter III, some further analysis, and additional data on shear strength, modulus of elasticity, strength in other directions relative to grain direction, and damping characteristics.

Correction for Moisture Content

The moisture content of wood affects its strength. Higher moisture content results in reduced strength. Wood generally stabilizes at a moisture content that is dependent upon its environment. This moisture content may be different from the value at which experimental tests were conducted, and indeed the moisture content may vary between specimens during experimental testing. It is therefore necessary to have a means of correcting strength data for moisture.

Reference 1 presents an analytical method for correcting the static strength of clear wood specimens for moisture content, but information is not presented for laminated specimens. Experimental evidence presented in reference 2, particularly for tension parallel to the grain, indicates that the approach of reference 1 is not necessarily valid for wood moisture contents below about 8 to 10 percent. Unfortunately most data obtained on laminated Douglas fir/epoxy were at moisture contents below 8 percent. Lacking a better analytical approach than reference 1, however, we used the reference 1 method herein. Reference 1 presents the following equation to calculate a clear wood property P for any moisture content (in percent) M.

$$P = P_{12}\left(\frac{P_{12}}{P_g}\right)^{-[(M-12)/(M_p-12)]} \tag{1}$$

where

P_{12} property at 12 percent wood moisture content
P_g property (in green condition) for all wood moisture contents greater than M_p
M_p wood moisture content at which changes in property due to drying are first observed (M_p = 24 percent for Douglas fir)

Since P_{12} and P_g do not vary

$$\frac{P_{12}}{P_g} = K \tag{2}$$

where K is a constant for a given wood property. Values of K are discussed later.

In laminate testing, the moisture content of the test specimens was determined by weighing the test specimen, or a portion thereof, after mechanical property testing and both before and after oven drying. Specimens were oven dried at approximately 220 °F for at least 12 hr until their weight stabilized. Then

$$M_L = \frac{W_B - W_D}{W_D} \times 100 \tag{3}$$

*NASA Lewis Research Center.
**Sverdrup Technology, Inc., Lewis Research Center Group.

where

M_L moisture content of laminated specimen
W_B weight of moisture-content specimen as tested and before drying
W_D weight of moisture-content specimen after oven drying

For the laminates reported herein the epoxy weight was approximately 22 percent of the wood weight. The epoxy absorbed little moisture; therefore

$$M_W = 1.22\ M_L \tag{4}$$

where M_W is the moisture content of the wood. Combining equations (1) and (4) and letting P_B be the mechanical property as tested gives

$$P_{12} = P_B K^{(1.22M_L - 12)/12} \tag{5}$$

Combining equations (1) and (5) yields

$$P_X = P_B K^{(M_L - M_X)/9.84} \tag{6}$$

where P_X is the corrected mechanical property of the laminate at a specified laminate moisture content M_X.

In the data reported herein there was some variation in the moisture content of the specimens as tested. The midrange of most test conditions was at a laminate moisture content of 6 percent. The physical property data of the specimens were therefore arbitrarily corrected to 6 percent laminate moisture content as a standardized condition. At this condition equation (6) becomes

$$P_6 = P_B K^{(M_L - 6)/9.84} \tag{7}$$

Equation (7) was the basis of moisture-content correction for all data in this report. Values of K used in the equation for laminated Douglas fir/epoxy were obtained empirically where possible. Where data were insufficient for an empirical determination, values were taken from reference 1 for clear Douglas fir.

To correct the data to any other level of laminate moisture content M_X, combine equations (6) and (7) to yield

$$P_X = P_6 K^{(6 - M_X)/9.84} \tag{8}$$

To correct the data to a specified level of *wood* moisture content M_{XW}, combine equations (4) and (8) to give

$$P_X = P_6 K^{(7.32 - M_{XW})/12} \tag{9}$$

Correlation Coefficient

Values of the constant K were determined empirically for fatigue tests by finding the value of K that resulted in the highest correlation coefficient. The correlation coefficient r is a measure of the scatter of data about a linear regression line for log-log plots of cyclic fatigue data. The following equation defines r:

$$r = m \left[\frac{\dfrac{\sum_{i=1}^{n} X_i^2}{n} - \bar{X}^2}{\dfrac{\sum_{i=1}^{n} Y_i^2}{n} - \bar{Y}^2} \right]^{1/2} \tag{10}$$

where

m slope of least-squares regression line
X log S (S = maximum cyclic stress)
Y log N (N = cycles to failure)
$\bar{X}$ mean value of X_i
$\bar{Y}$ mean value of Y_i

The value of r will lie between 1 and -1 with the least scatter when $r \to 1$ or $r \to -1$.

Evaluation of K

Evaluating K empirically was considerably more successful for fatigue than for static data. As stated above, the constant K was determined for fatigue data that resulted in a maximum value of the correlation coefficient r for the regression line calculated for all data points. Figure 1 shows how correcting compression fatigue data for moisture content moves the data points in a vertical direction and how it can improve r. A range of K was chosen by a trial-and-error process to find the value resulting in a maximum r. In the case shown, the regression line is not appreciably affected by the moisture correction, even though r is improved. The reason the regression line was only slightly affected was that the moisture contents of the specimens as tested were about equally split above and below the arbitrary reference value of 6 percent. If the bulk of the specimens had a moisture content either higher or lower than 6 percent, the regression line would have shifted.

Attempts were made to find static strength data at different moisture contents and then to establish an empirical value of K that would correlate the data. In most cases the data scatter was far greater than the variation in strength due to moisture content, and empirical evaluation of K was not possible. Evaluation of K is discussed further in chapter IV.

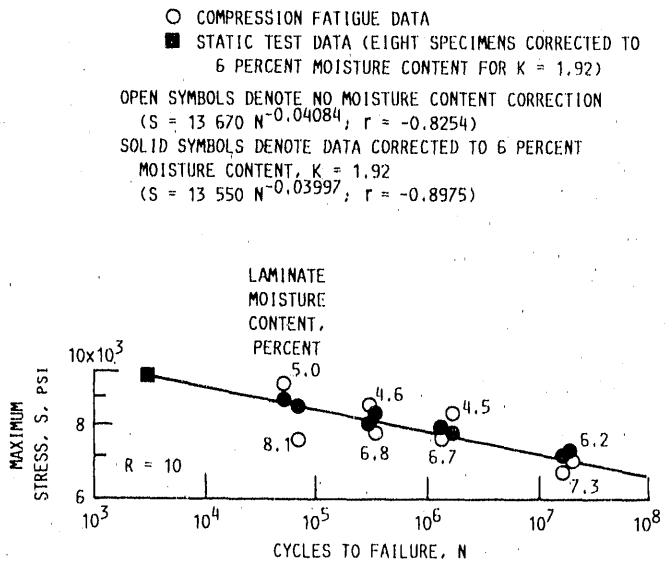

Figure 1.—Moisture correction of data for compression fatigue ($R = 10$) parallel to grain in laminated Douglas fir/epoxy specimens. Veneer grade, A+. Data from figure 4.2-1 of chapter IV.

The following table lists K values taken from reference 1 for clear Douglas fir and the values used for laminated Douglas fir/epoxy. The values for laminated Douglas fir/epoxy shown enclosed in brackets [ ] were taken from reference 1 because empirical determination was not considered possible or was probably inaccurate.

Property	Clear Douglas fir (ref. 1)	Laminated Douglas fir/epoxy
	K values used for moisture-content correction	
Static tension parallel to grain	1.21	[1.21]
Static tension perpendicular to grain	1.13	[1.13]
Static compression parallel to grain	1.92	[1.92]
Static compression perpendicular to grain	----	1.50
Static shear parallel to grain	1.26	1.07
Modulus of elasticity parallel to grain	1.25	1.05
Tension-tension fatigue parallel to grain	----	1.21
Compression-compression fatigue parallel to grain	----	1.92
Tension-compression fatigue parallel to grain	----	1.57

Note that the empirical values of K that could be determined from static tests of laminated specimens were lower than the K values from reference 1 for clear specimens but that the empirical values for fatigue of laminated specimens were equal to static tension and compression values from reference 1 for clear specimens. Further, the tension-compression fatigue tests of laminated specimens yielded a K value that was the average for static tension and static compression for clear specimens as obtained from reference 1.

Additional Statistical Analysis Methods for Mechanical Property Data

Standard Deviation

Standard deviation σ is a measure of the variability of data that have been averaged to obtain a mean value. The equation for standard deviation is available from many sources, such as reference 3.

$$\sigma = \left[\frac{\Sigma(P - \bar{P})^2}{n}\right]^{1/2} \qquad (11)$$

$$\sigma = \left[\frac{n\Sigma P^2 - (\Sigma P)^2}{n^2}\right]^{1/2}$$

where

P individual value of property measured
$\bar{P}$ mean value of n measurements of P

These two equations are equal and the choice of equation may depend on the chosen calculation procedure.

The t Test

The t test is discussed in reference 3. In this investigation the t test was used for two purposes: (1) to estimate the precision of the mean value of individual measurements P for a specified confidence level, normally 95 percent (at this confidence level there would be one chance in 20 that the true mean lies outside of the specified range), and (2) to test whether the means of two different groups could have come from the same population or from populations with the same means for a specified confidence level, such as 95 percent.

The precision limits, usually called precision, can be specified by the symbol ℓ. Again for a confidence level of 95 percent

$$\ell_{0.95} = \pm t_{0.05,f}\sigma \qquad (12)$$

where $t_{0.05,f}$ is read from a t table available in statistics books such as reference 3 or in books of mathematics tables, 0.05 is the probability of observing a larger absolute value of t, and f is the degrees of freedom and is equal to $n - 1$, where n is the number of specimens tested. Note that a confidence level of 0.95 requires using 0.05 in the t tables. Different values of confidence level can, of course, be substituted for a specific application.

Then for a confidence level of 95 percent the minimum value of a property that could be expected would be

$$P_{\min} = P - |t_{0.95}| \tag{13}$$

In testing whether the means of two different groups could be from the same population the following equation is used:

$$t = \frac{|P_1 - P_2|}{\sigma\left(\frac{1}{n_1} + \frac{1}{n_2}\right)^{1/2}} \tag{14}$$

The subscripts 1 and 2 refer to the two different groups, and

$$\sigma = \frac{\sum_{i=1}^{n_1} P_1^2 + \sum_{i=1}^{n_2} P_2^2 - n_1 P_1^2 - n_2 P_2^2}{n_1 + n_2 - 2} \tag{15}$$

where σ is a pooled estimate of the standard deviation for the two groups.

The value of t calculated from equation (14) is compared with a value of t read from the t table for the degrees of freedom equal to $n_1 + n_2 - 2$ and a preselected probability α. If the calculated t is larger than the tabulated t (from the t table), then we conclude that the population mean estimated by P_1 is significantly different from the population estimated by P_2, with the chance α of being wrong. Conversely, matching the calculated t as closely as possible with a t from the table for the corresponding degrees of freedom can be used to determine the value of α, that is, the probability that the two means are *not* from the same population.

For example, to interpret the significance of a calculated value of $t = 2.53$ for 20 degrees of freedom (22 data points in the combined samples), we can look at a t table and determine the values of α that closely correspond to this value of t. The t table shows that for 20 degrees of freedom t values for α of 0.05 and 0.02 are 2.086 and 2.528, respectively. Therefore there is about a 2 percent probability (1 chance in 50) of being wrong by saying that the two population means being compared by equation (15) are significantly different. In other words the higher the value of t, the smaller the probability that you will be wrong in assuming that the means are from different populations.

Static Strength Data

Static tension and compression data with load applied parallel to the grain are available to investigate the effects of specimen size, or volume, on failure strength. Information on the effects of joints in the laminations is also available. Mean values of strength, corrected to 6 percent laminate moisture content, and standard deviations are plotted in figure 2 for specimens with no joints, butt joints, and scarf joints in the laminations. The number of specimens tested for each data point is indicated. The abscissa is a logarithmic scale to cover the wide range of specimen volumes.

Structures or specimens fabricated from laminated wood that are longer than approximately 8 ft and wider than approximately 4 ft require joints or discontinuities in the laminations. A few of the smaller specimens represented in figure 2 had no joints in the laminations. The remaining specimens contained either butt joints, where the two adjacent veneers were trimmed and butted against each other, or scarf joints, where the veneers were scarfed at a slope of 12:1 and the scarfs overlapped so that more tension load could be carried through the glue line of the joint.

Figure 2 shows primarily the scope of the tests and also shows a general trend of decreasing mean strength with increasing specimen volume for the static tension case. This

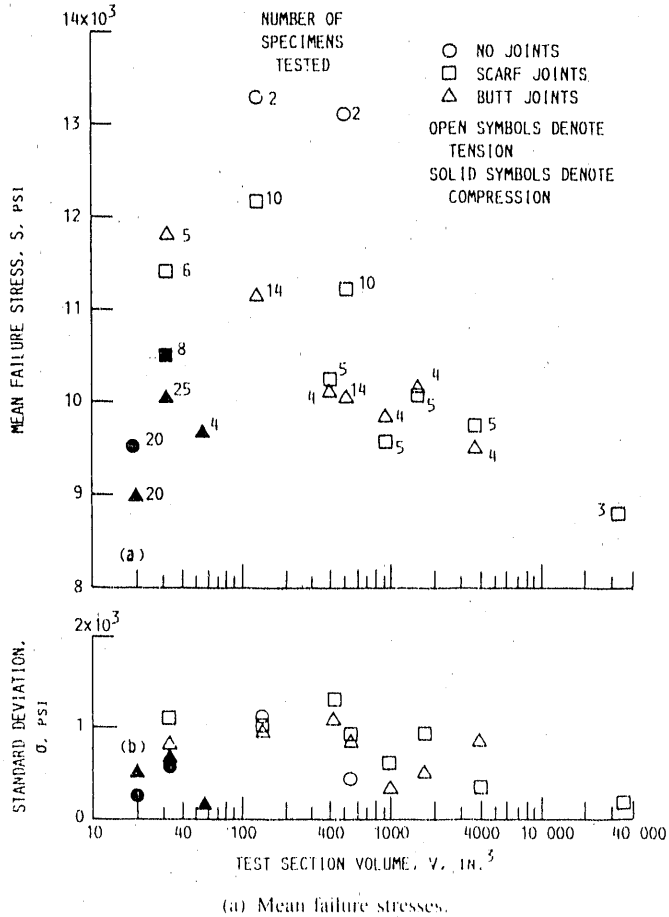

(a) Mean failure stresses.
(b) Standard deviations.

Figure 2.- Compilation of mean values of static tension and compression failure stresses (parallel to grain) in laminated Douglas fir/epoxy specimens for range of specimen volumes. Data corrected to 6 percent laminate moisture content ($K = 1.21$ for tension and $K = 1.92$ for compression). Veneer grade, A-4.

trend can be expected owing to the probability of a larger number of defects, or stress raisers, in large specimens. The figure also shows decreasing values of standard deviation with increasing specimen volume.

The static tension tests were conducted on 88 Douglas fir/epoxy specimens 1.5 in. thick (15 laminations) with widths varying from 2 in. to 8 in. and lengths of 7.5 to 30 ft. The test section volumes varied between 132 and 3768 in.^{3}. All specimens were cut from large panels. Veneer grade and fabrication procedures were closely controlled in an attempt to eliminate extraneous factors in specimen strength. In addition to these specimens, three tests were conducted on specimens with a test volume of 32 832 in.^{3} (specimen size, 6 in. thick by 24 in. wide by 28 ft long). Most specimens contained butt or scarf joints in the laminations perpendicular to the load direction.

Standard deviations for the tension specimens with test volumes of 3768 in.^{3} or less ranged from a minimum of 307 psi to a maximum of 1297 psi with mean strengths for groups of specimens at each specimen volume ranging from 9497 to 13 289 psi. The three largest specimens with test volumes of 32 832 in.^{3} had a standard deviation of 160 psi and a mean tensile strength of 8187 psi.

The compression strength data for 77 specimens are limited to a much smaller range of specimen volumes. Further, the compression specimens were fabricated at a different time and from different panels than the tension specimens. The compression specimens ranged from 1.5 to 3 in. thick and had three different aspect ratios (ratio of length to thickness), 2.667, 3.560, and 4.333.

Strength Models for Static Tension and Compression

A strength model to condense the data of figure 2 into what could be a basis for designing structures of a size different from the specimens tested would be quite useful. One such model with variations for tension and compression is presented herein.

Strength Model for Static Tension

It seems obvious that a strength model for static tension must show a decreased tension strength with increasing volume, but the model cannot be a straight-line variation on linear, logarithmic, or semilogarithmic plots because such plots would result in essentially zero strength at very large volumes. It is more reasonable that an asymptotic value of strength be reached at high volumes. It would appear therefore that a reasonable model might take the form

$$S = AV^{-B} + C \tag{16}$$

where

S	mean failure stress
V	volume
A,B,C	empirical constants

Because of variations in test failure strengths for replicate tests, this variability should also be considered in the model. Standard deviation is a reasonable basis for this variability consideration. Therefore in a manner similar to that for stress, the standard deviation σ can be modeled by an equation in the form

$$\sigma = DV^{-B} \tag{17}$$

which has another empirical constant, D.

The curves of figure 3, along with their equations, were developed from the static tension strength data in figure 2 for scarf-jointed specimens from 132 to 32 822 in.^{3} in volume. These equations were developed by iteration to obtain the constants A, B, C, and D in which the sum of the deviations of the mean strength from the model approaches zero, with the further stipulation that the model agree with the mean strength at the largest volume.

Figure 3 also shows four lines of strength minus N times the standard deviation. The value of $N = 2.837$ was obtained from the ratio D/A (18 300/6450) in the two preceding equations. For $N = 2.837$, $S - N\sigma$ is equal to the constant C for all volumes. The constant C is the asymptotic strength at

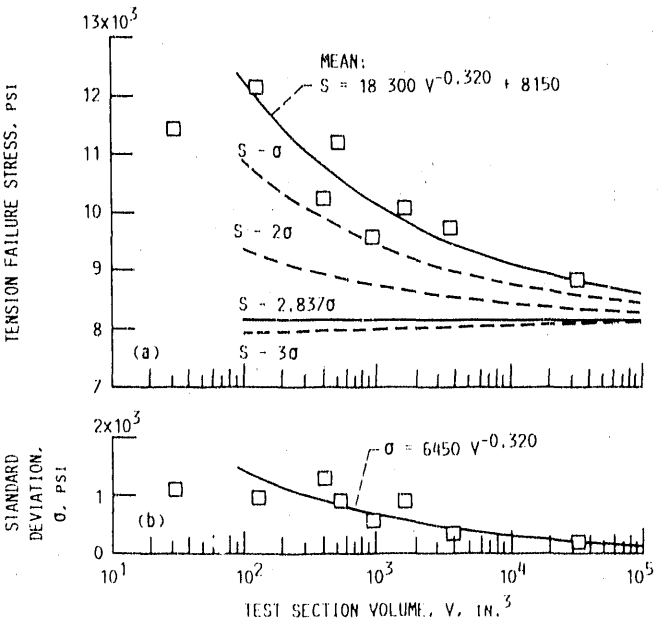

(a) Strength model.
(b) Standard deviation model.

Figure 3.—Strength and standard deviation models for static tension in laminated Douglas fir/epoxy specimens with scarf joints in laminations. Data corrected to 6 percent laminate moisture content ($K = 1.21$). Veneer grade, A+.

large volumes. A statistical t table shows that for a normal distribution of data 99.5 percent of all data points will have a value greater than $S - 2.837\sigma$. The model shown in figure 3 is therefore very convenient for extrapolating strength data to predict minimum failure tension stress with a confidence level of approximately 0.995 for specimens or structures much larger than those for which test data are available.

Note, however, that the equations presented in figure 3 should not be considered as a design basis for all scarf-jointed Douglas fir/epoxy structures. On the basis of various investigations compiled in this volume there can be significant variations in strength data from specimens fabricated at various times. It is believed, however, that the model shown in figure 3 can be a basis for other batches of specimens. Equations for butt-jointed specimens in static tension and for both scarf- and butt-jointed specimens in static compression follow.

Figure 4 shows the model equations for static tension with butt joints in the laminations, along with standard deviations, mean strengths, and $S - 2.837\sigma$. The resulting equations are

$$S = E(AV^{-B} + C) \tag{18}$$

and

$$\sigma = E(DV^{-B}) \tag{19}$$

where the constants A, B, C, and D are the same as for the scarf-jointed specimens and the value of E is determined by iteration to result in the summation of the deviations between the mean stresses and the model approaching zero. Figure 4 shows butt-jointed specimens in static tension to be 96.5 percent as strong as scarf-jointed specimens.

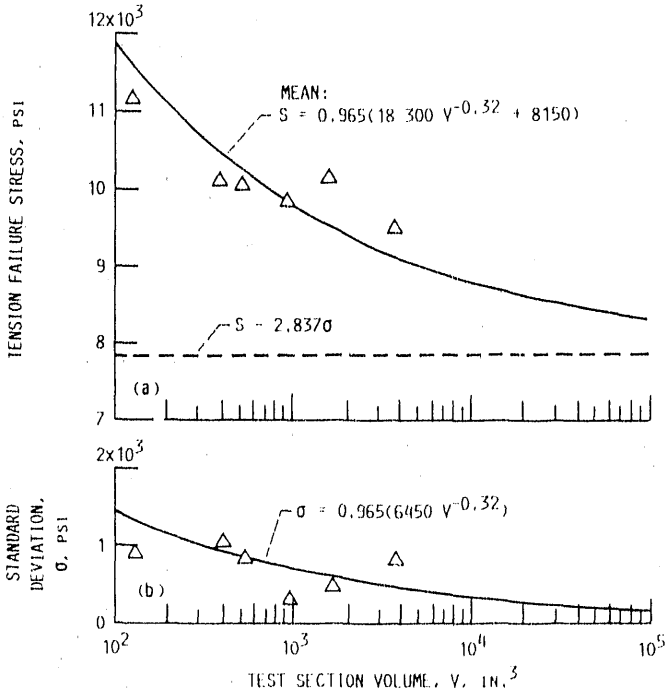

(a) Strength model.
(b) Standard deviation model.

Figure 4.—Strength and standard deviation models for static tension in laminated Douglas fir/epoxy specimens with butt joints in laminations. Data corrected to 6 percent laminate moisture content ($K = 1.21$). Veneer grade, A+.

Strength Model for Static Compression

Figure 5 shows model equations for the static compression strength data shown in figure 2 for both scarf- and butt-jointed specimens. There was an added complication in obtaining these models. The compression tests were conducted on specimens having three different aspect ratios (ratio of length to thickness). Increasing aspect ratio will result in increased buckling in compression; therefore a correction must be made for aspect ratio. In the case shown in figure 5 all specimens were corrected to an aspect ratio of 3.56, the aspect ratio of specimens having a volume of 31.8 in.^{3}. (The development of this correction is discussed later in relation to compression fatigue. The aspect ratio effect for compression fatigue was assumed to be applicable to static compression.) The three groups of mean strengths for butt-jointed static compression specimens were then weight averaged, based on the number of specimens tested at each volume. The resulting weight-averaged strength is shown as the solid triangle in figure 5 for butt-jointed specimens. The standard deviations for the three groups of butt-jointed compression specimens were weight averaged to obtain a mean value of standard deviation. The model equations were then developed by the following procedure:

(1) The value of $D/A = 2.837$ in the model for static tension was assumed for static compression since $S - 2.837\sigma$ encompasses 99.5 percent of normal distribution data. Then the constant A could be calculated from

$$\sigma = \frac{AV^{-0.320}}{2.837} \tag{20}$$

(2) The constant C could then be calculated from the mean value of strength S represented by the solid triangle in figure 5 and the value of the constant A from the equation

$$S = AV^{-0.320} + C \tag{21}$$

For scarf-jointed static compression specimens the equations for S and σ obtained for butt-jointed static compression specimens could be corrected by the value E in the same manner as for static tension specimens. For these static compression specimens, where the strength was available at only one volume, the value of E was taken as equal to the ratio of mean scarf-jointed specimen strength to the weighted value of mean butt-jointed specimen strength at a volume of 31.8 in.^{3}, corresponding to an aspect ratio of 3.56 for both types of specimens.

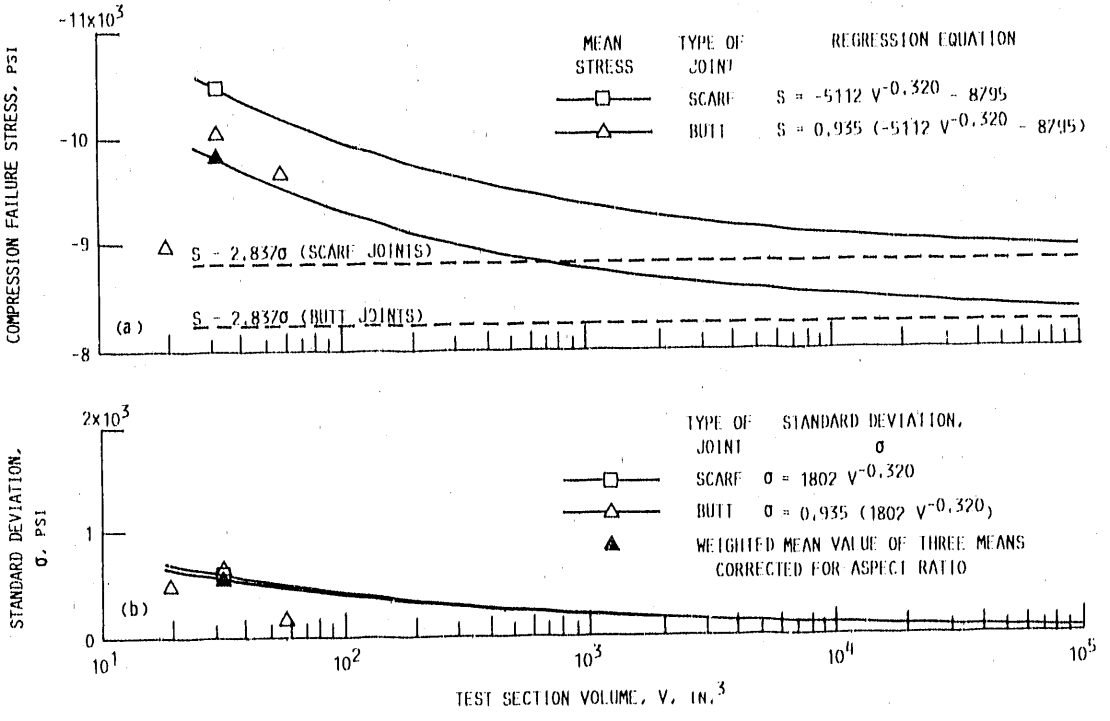

(a) Strength model.
(b) Standard deviation model.

Figure 5.—Strength and standard deviation models for static compression in laminated Douglas fir/epoxy specimens. Data corrected to 6 percent laminate moisture content ($K = 1.21$). Veneer grade, A+.

Figure 6 compares strength models for static tension and for static compression with both scarf and butt joints in the laminations. The asymptotic strengths, represented by $S - 2.837\sigma$, are also shown. From the models shown, the asymptotic strengths for compression are higher than those for tension. In addition, the models for compression show less sensitivity to volume than the models for tension.

Figure 7 compares the stress models' asymptotic strength with the minimum strength measured in replicate tests. A total of 168 tests were conducted in both tension and compression. Except for one compression data point all of the asymptotic strengths were at least 5 percent more conservative than the minimum strengths measured in tests. These results are consistent with the confidence level of 0.995 previously mentioned for all test data having strengths at or above $S - 2.837\sigma$.

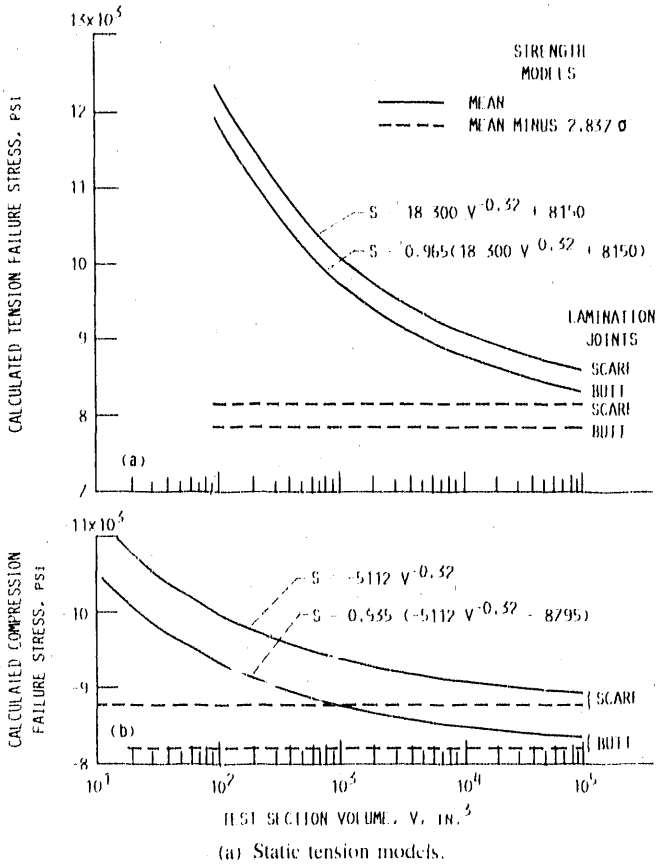

(a) Static tension models.
(b) Static compression models.

Figure 6.—Comparison of strength models for static tension and compression in laminated Douglas fir/epoxy specimens with scarf and butt joints in laminations. Data corrected to 6 percent laminate moisture content ($K = 1.21$). Veneer grade, A+.

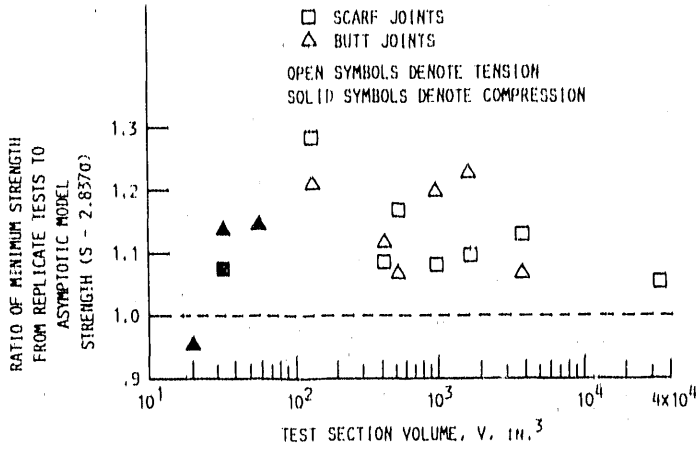

Figure 7.—Ratio of minimum experimental static tension and compression strengths from replicate tests to calculated asymptotic strengths ($S - 2.837\ \sigma$) from strength models for laminated Douglas fir/epoxy specimens with scarf and butt joints in laminations. Data corrected to 6 percent laminate moisture content ($K = 1.21$). Veneer grade, A+.

Fatigue Strength Data

Fatigue tests of laminated Douglas fir/epoxy specimens showed far less scatter in the data than static tests. Typical fatigue test data are shown in figure 8 for tension-tension, compression-compression, and reverse axial tension-compression. Strengths in tension-tension fatigue ($R = 0.1$) and compression-compression fatigue ($R = 10$) are of comparable absolute value. (Note that R is the stress ratio, the ratio of arithmetic minimum load to maximum load during the fatigue test.) The fully reversed axial tension-compression ($R = -1$) fatigue strength is on the order of 60 percent of the tension-tension fatigue or compression-compression fatigue strength.

Joint and Aspect Ratio Effects on Compression-Compression Fatigue

The effect of laminate joint configuration on compression-compression ($R = 10$) fatigue strength is illustrated in figure 9. Data points are not shown in the figure to improve clarity. The actual data points are presented in chapter IV in the compilation of data for laminated wood. Figure 9(a) shows how the slope of the scarf in laminate joints affects compression-compression fatigue life. The longer the joint (flatter slope), the better the fatigue life. Figure 9(b) shows how joint imperfections affect fatigue life for scarfs with a 10:1 slope. Mismatches by overlapping the scarfs or underlapping (which provides gaps in the joints of up to 50

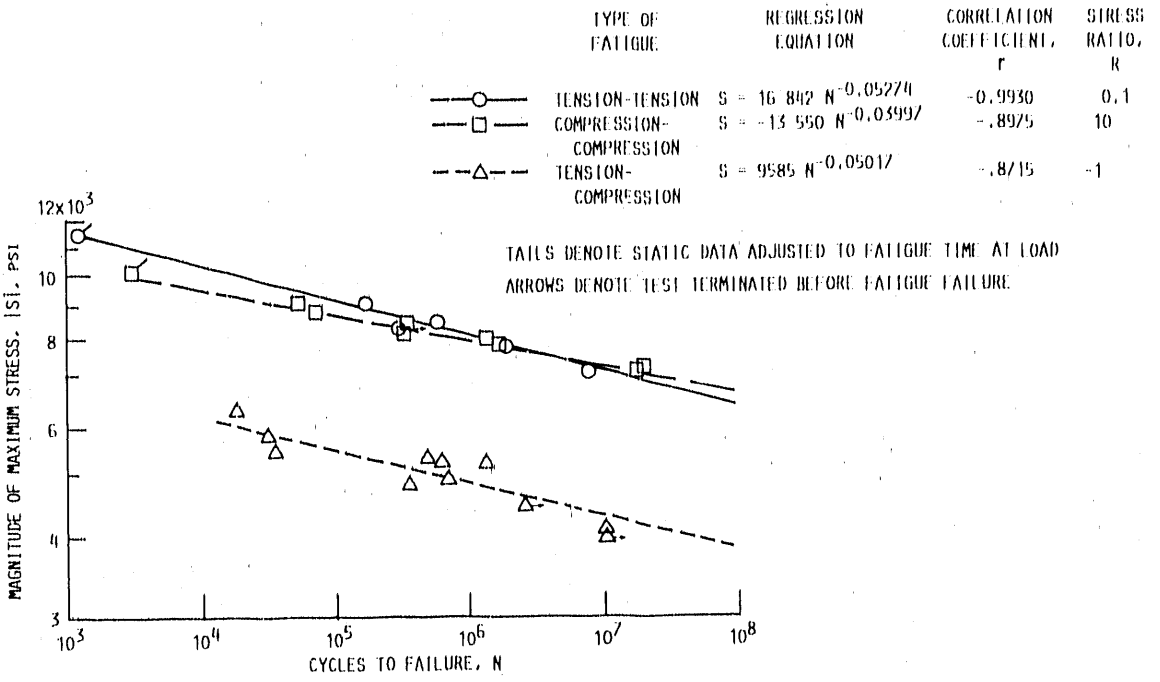

Figure 8.—Examples of fatigue test data for laminated Douglas fir/epoxy dogbone specimens 2.25 in. in diameter and 8 in. in effective test section length (31.8-in.^{3} volume and 3.56 aspect ratio) and 12:1-slope scarf joints in laminations. Data corrected to 6 percent laminate moisture content. Veneer grade, A+; test temperature, 70 °F. Reference figures 4.1-1(b), 4.2-1(b), and 4.3-1(d) of chapter IV.

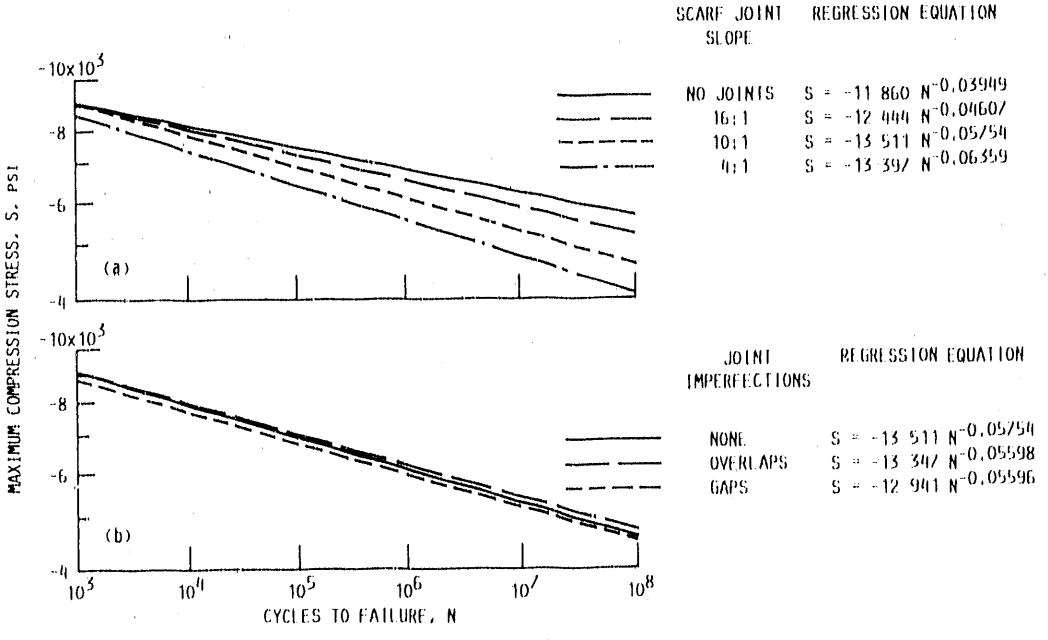

(a) Summary of effects of scarf slope.
(b) Summary of effects of imperfections in 10:1-slope scarf joints.

Figure 9.—Effect of scarf slope and imperfections in lamination joints for compression-compression fatigue (R = 10) parallel to grain in laminated Douglas fir/epoxy specimens. Square-cross-section specimens 2 in. by 2 in. by 12 in. long contained scarf joints staggered 3 in. apart in center three laminations. Data corrected to 6 percent laminate moisture content (K = 1.92). Veneer grade, A+; test temperature, 70 °F. Reference figures 4.2-4(g) and (h) of chapter IV.

percent of the scarf length) had an almost negligible effect on compression-compression fatigue life.

Compression-compression fatigue test data from figure 9(a) and from specimens having a different aspect ratio and with scarf or butt joints in the laminations were used to develop a compression-compression ($R = 10$) fatigue model to provide insight on the effects of these variables. Figure 10 illustrates the model for a life of 10 million cycles. Two specimen configurations were investigated. One was a cylindrical dogbone specimen 2.25 in. in diameter and 8 in. in effective test section length (aspect ratio AR equals 3.56), and the other was a square-cross-section specimen 2 in. by 2 in. by 12 in. long ($AR = 6$). Unfortunately the same joint configurations were not tested in both types of specimens. A model was developed in a somewhat similar manner as the model for effect of volume on static strength. In the present case the model was assumed to have the form

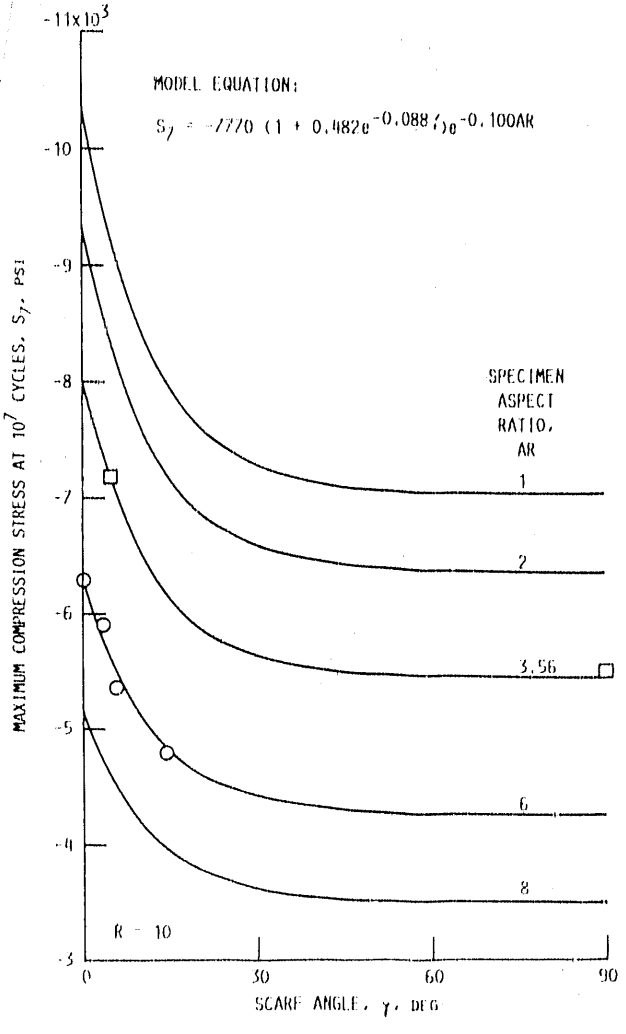

Figure 10.—Strength model that accounts for lamination scarf angle and specimen aspect ratio for compression-compression fatigue at 10 million cycles in laminated Douglas fir/epoxy specimens. Data corrected to 6 percent laminate moisture content ($K = 1.92$). Veneer grade, A+.

$$S_n = B(1 + Ce^{-D\gamma})e^{-E(AR)} \qquad (22)$$

where

S_n	maximum compressive stress at 10 cycles
B, C, D, E	empirical constants
γ	angle of scarf slope, deg
AR	specimen aspect ratio

The four empirical constants were determined by curve fitting the 10-million-cycle life data points shown in figure 10 for two specimen configurations and a variety of joints in the laminations. Square-cross-section specimens ($AR = 6$) consisted of those without joints ($\gamma = 0°$) and those with scarf joints having slopes of 4:1, 10:1, and 16:1. Cylindrical specimens ($AR = 3.56$) consisted of those with scarf joints having a slope of 12:1 and with those butt joints ($\gamma = 90°$). From this model the curves for aspect ratios of 1, 2, and 8 were also calculated. The figure illustrates that the complication of scarfing the edges of the laminates to make a small-angle scarf substantially improved fatigue strength.

Stress Ratio and Specimen Size (Volume) Effects on Fatigue

Figure 11 shows compression-compression fatigue curves (without data points) for stress ratios R of 2.5 and 10 for a 12:1 slope scarf and butt joints in the laminations. As expected the loading amplitude, as indicated by the stress ratio, does affect fatigue life; a ratio of 2.5:1 in loads ($R = 2.5$) is less severe than a ratio of 10:1 ($R = 10$) for both butt and scarf joints in the laminations. The effect shown for the type of lamination joint is consistent with the effect shown in figure 10.

Figure 12 shows the effect of lamination joint configuration and specimen size for tension-compression fatigue ($R = -1$). Figure 13 shows similar effects for tension-tension fatigue ($R = 0.1$) plus the effect of veneer quality for butt-jointed specimens. Grade A+ veneers are superior to grade A veneers. Veneer grade is based upon both the visual quality of the veneers and an ultrasonic grading technique. The better veneers provide better fatigue life, as might be expected.

Far less information is available for the effect of specimen size on fatigue than there is for static tension. The results of specimen size are qualitatively the same, however. Larger specimens have shorter fatigue lives than smaller specimens, but available data are insufficient to develop a model for predicting fatigue life as a function of size.

Many of the strength effects discussed in this section can be illustrated by using a Goodman diagram, as shown in figure 14. This figure presents a composite illustration of static and fatigue strengths for laminated Douglas fir/epoxy specimens. The data shown illustrate the effects of both scarf joints (12:1 slope) and butt joints in the laminations and indicate the effect of specimen size. The data points lying on the abscissa are static data. Those lying on the ordinate are tension-compression fatigue data. Points to the left of the ordinate axis and above the abscissa are compression-

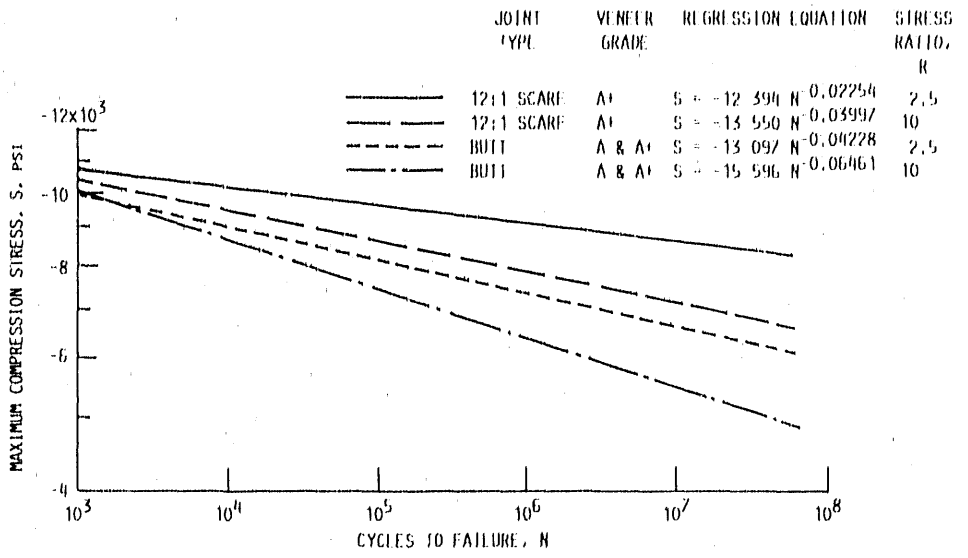

Figure 11.—Effects of joint type and stress ratio on compression-compression fatigue parallel to grain in laminated Douglas fir/epoxy specimens. Cylindrical specimens 2.25 in. in diameter by 8 in. long containing joints staggered 3 in. apart in center three laminations. Data corrected to 6 percent laminate moisture content ($K = 1.92$). Test temperature, 70 °F. Reference figures 4.2-1(b), 4.2-2(b), and 4.2-3(a) of chapter IV.

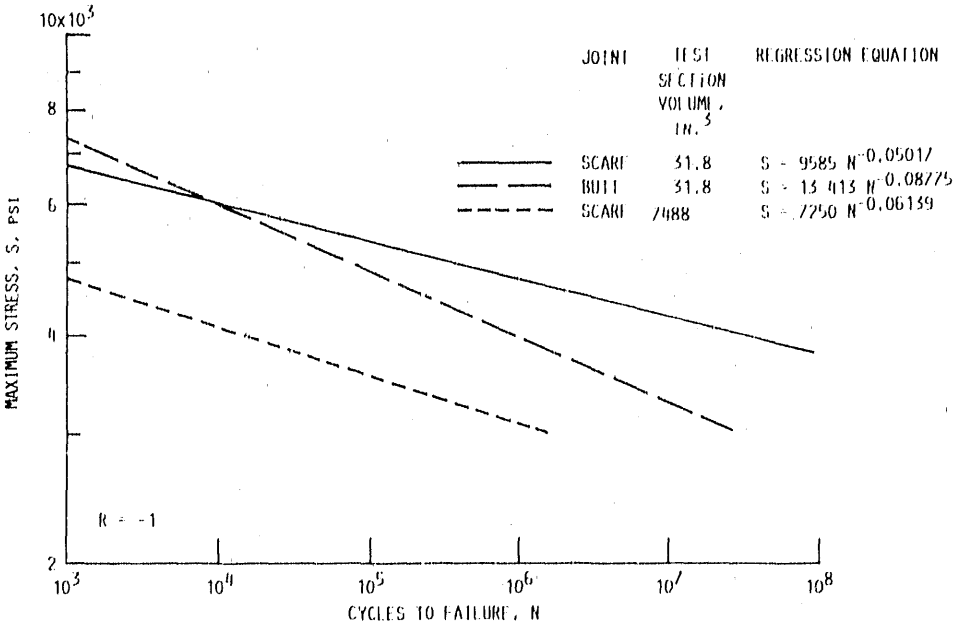

Figure 12.—Effect of specimen size and joint type on reverse axial tension-compression fatigue ($R = -1.0$) parallel to grain for laminated Douglas fir/epoxy specimens. Data corrected to 6 percent laminate moisture content ($K = 1.57$). Veneer grade, A+; test temperature, 70 °F. Reference figure 4.3-2 of chapter IV.

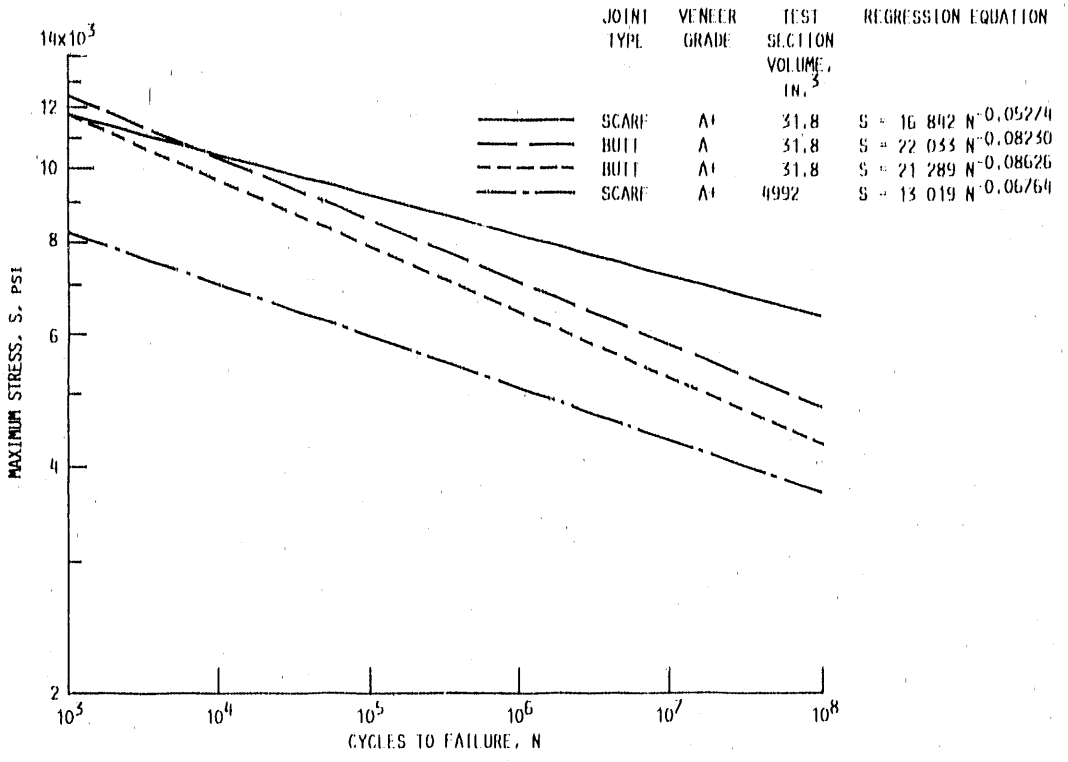

Figure 13.—Effects of joint type, veneer grade, and specimen size on tension-tension fatigue ($R = 0.1$) parallel to grain for laminated Douglas fir/epoxy specimens. Data corrected to 6 percent laminate moisture content ($K = 1.21$). Test temperature, 70 °F. Reference figures 4.1-1(b), 4.1-2, and 4.1-3 of chapter IV.

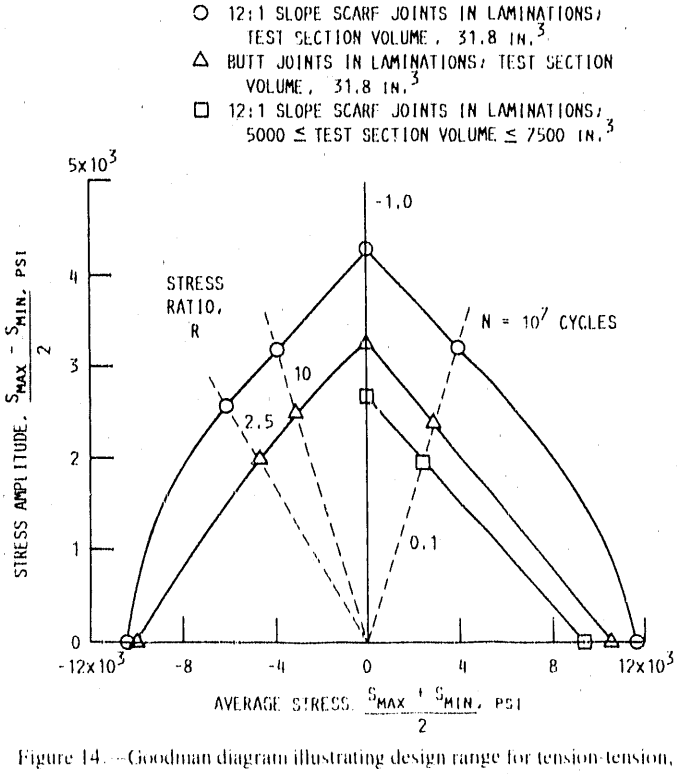

Figure 14.—Goodman diagram illustrating design range for tension-tension, compression-compression, and reverse axial tension-compression fatigue plus static tension and compression for various specimen sizes and joint configurations. Fatigue strengths based on 10 million cycles to failure.

compression fatigue data, and those to the right are tension-tension fatigue data. For illustrative purposes the straight dashed lines connect data points for specific values of R.

The curves connecting the circular data points are for small specimens (31.8-in.^{3} test section) with scarf joints in the laminations. The curves connecting the triangular data points are for small specimens (31.8-in.^{3} test section) with butt joints in the laminations. The line connecting the square data points (tension only) is for larger specimens (5000- to 7500-in.^{3} test section volume) with scarf joints in the laminations. The areas enclosed by the lowest lines and the abscissa indicate a probable safe operating region for cyclic loads up to 10 million cycles.

Effect of Stress Raisers (Cutouts) on Compression-Compression Fatigue

Figure 15 compares compression-compression fatigue ($R = 10$) data for 6-in.-wide, 1.5-in.-thick, and 12-in.-long specimens containing a 2-in.-diameter circular hole with data for 2-in.-wide, 2-in.-thick, and 12-in.-long specimens without a hole. The fatigue strengths of these specimens undoubtedly contain an aspect ratio effect as well as a hole effect, but in general the effect of the hole was no more serious that would be expected in a homogeneous material. The strength reduction from the cutout was approximately 38 percent.

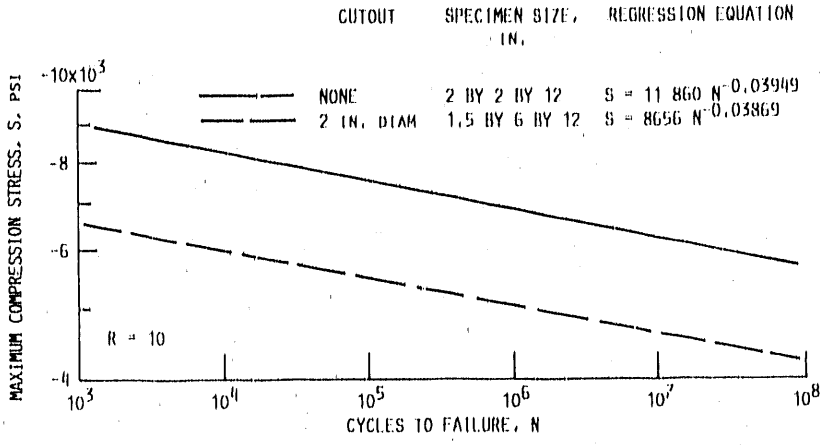

Figure 15.—Effect of 2-in.-diameter circular cutout on compression-compression fatigue ($R = 10$) parallel to grain for laminated Douglas fir/epoxy specimens. Data corrected to 6 percent laminate moisture content ($K = 1.92$). Veneer grade, A+; test temperature, 70 °F. Reference figure 4.2-7(a) of chapter IV.

Joints for Laminated-Wood Structures

Three types of joints may be required for joining laminated-wood substructures. Longitudinal butted joints may be used where the load across the joint is small. Finger joints may be required for carrying large loads between substructures, and metal studs embedded in the wood structure may be used for attachment to a metal structure. Two types of longitudinal joints are illustrated in figure 16. Finger joints and metal studs are illustrated in figure 17.

The longitudinal wedge joint has an assembly advantage over the longitudinal butt joint (fig. 16). A closer fit can be provided by driving the wedge in until the proper glue joint separation is achieved. The butt joint, on the other hand, may fit closely in some places but have a poor fit in others. Figure 18 shows that the butt joint has potential for greater strength in low-cycle fatigue but the wedge joint appears better for high-cycle fatigue. The data shown are for controlled fits in the joint. Under practical applications the wedge joint may provide a better fit and be superior for the complete range of fatigue cycles.

Figure 19 compares the tension-tension fatigue strength of specimens having three different finger joint configurations with the fatigue strength of specimens without finger joints. A joint bond gap of 0.015 in. is considered practical. The figure shows a fatigue strength reduction on the order of 35 to 40 percent, relative to no finger joints, for a joint bond gap of 0.015 in. and an approximately 50 percent strength reduction if the gap was 0.062 in. Part of this strength loss for the larger gap resulted from less bond area because the larger gap was obtained by reducing the finger engagement distance. Reinforcement with glass fibers (Burlington Style 7500 glass fiber fabric) between the veneers in the finger joint area increased fatigue strength about 8.5 percent over that of unreinforced finger joints.

Metal studs of the type illustrated in figure 17 can be used to attach a laminated-wood structure to a metal structure. Metal studs embedded in wooden specimens were tested. These studs have circumferential grooves and are glued with epoxy into oversize, stepped holes in the laminated wood. Several stud configurations were investigated in an attempt to provide a strain distribution along the embedded length that would be compatible with strains in the laminated wood. Fatigue tests in tension-tension, compression-compression, and reverse axial tension-compression were conducted on one of the strongest configurations. The results are shown by the regression curves

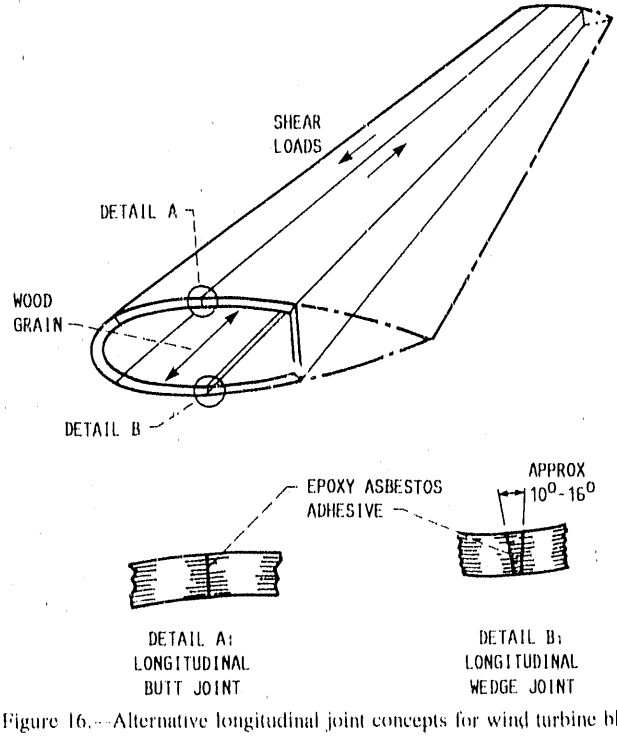

Figure 16.—Alternative longitudinal joint concepts for wind turbine blade.

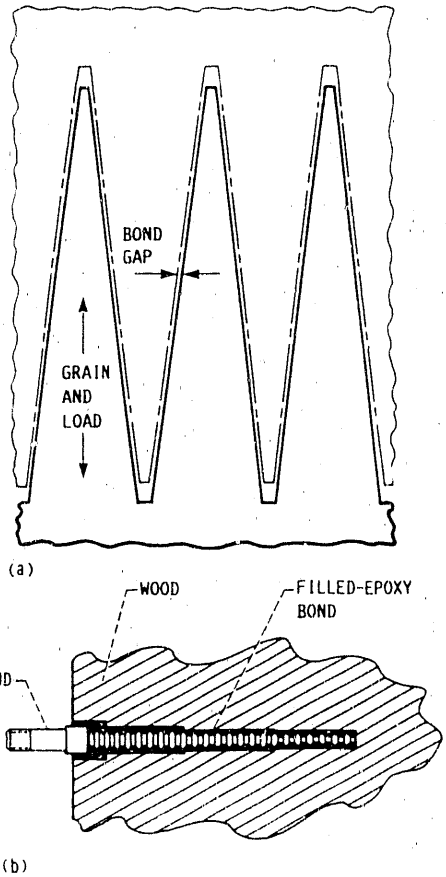

(a) Finger joints for attaching wood subassemblies.
(b) Metal studs for attaching laminated-wood structures to metal structures

Figure 17.—Joint configurations for laminated-wood structures.

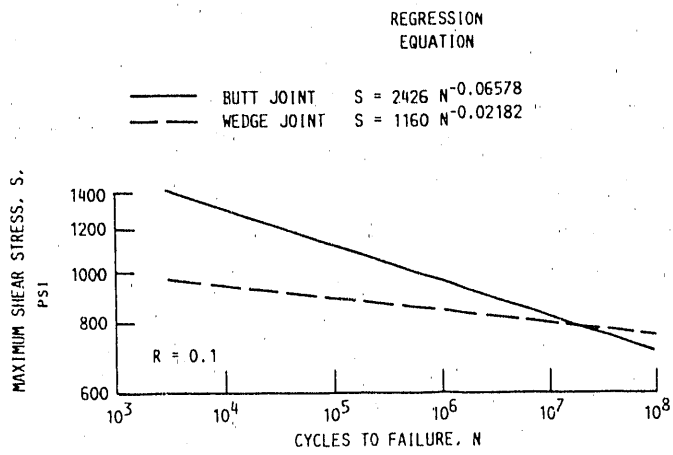

Figure 18.—Three-point-bending fatigue tests ($R = 0.1$) on longitudinal wedge and butt joints. Epoxy-asbestos adhesive in joints 1 in. wide. Data corrected to 6 percent laminate moisture content ($K = 1.26$). Test temperature, 70 °F. Reference figure 6.4-1(c) of chapter IV.

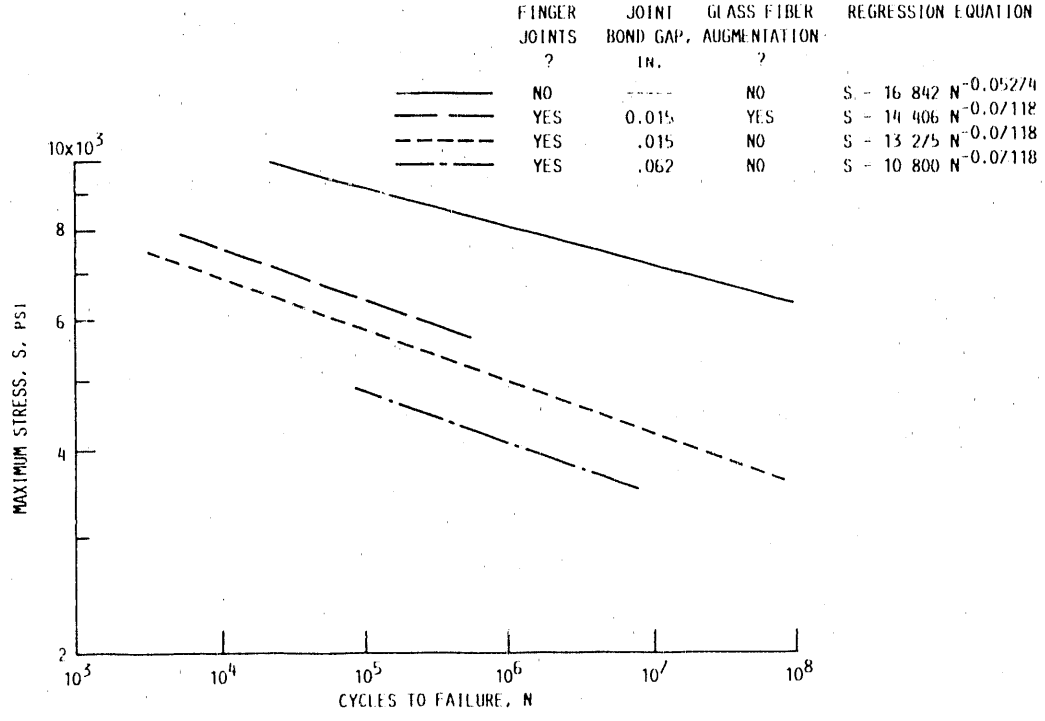

Figure 19.—Effect of finger joints on tension-tension fatigue ($R = 0.1$) parallel to grain for laminated Douglas fir/epoxy dogbone specimens. Finger joints 10 in. long; finger slope, 1:10. Dogbone specimens, 2.25 in. in diameter at test section and 57 in. long. Data corrected to 6 percent laminate moisture content ($K = 1.21$). Veneer grade, A+; test temperature, ~68 °F. Reference figure 6.2-1 of chapter IV.

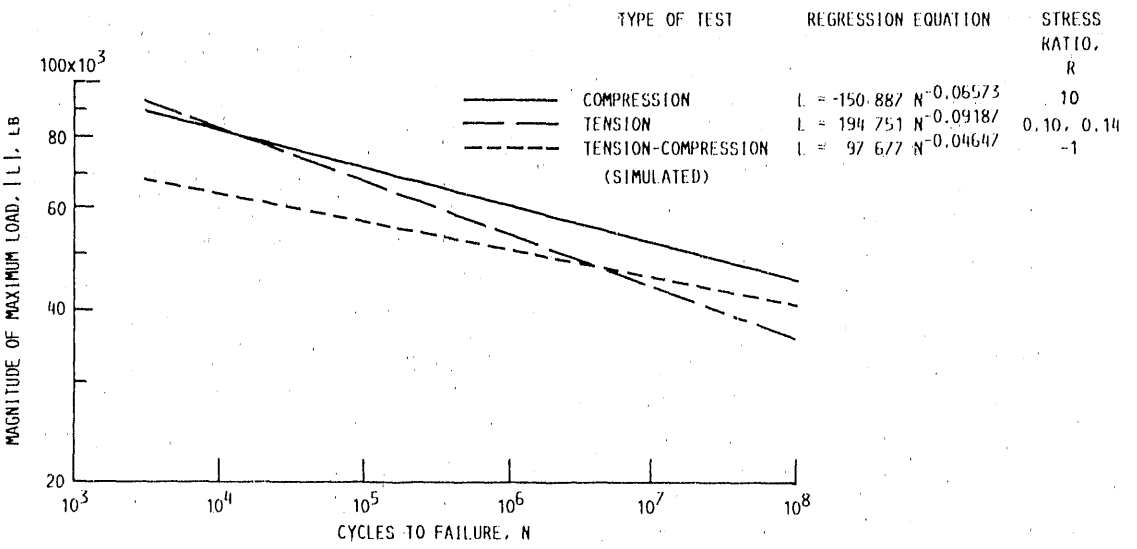

Figure 20.—Fatigue tests of metal studs (design 5) embedded in laminated Douglas fir/epoxy specimens with carbon-fiber-filled epoxy resin. Room-temperature tests. Reference figures 7.2-1(b) and 7.2-2(a) and (b) of chapter IV.

in figure 20. Loads greater than 30 000 lb per stud seem feasible up to 100 million cycles.

Concluding Remarks

This chapter has provided strength models for accounting for specimen size in static tension and compression and for evaluating the effects of lamination joint scarf angle and specimen aspect ratio for compression-compression fatigue. Highlights of other strength investigations of laminated Douglas fir/epoxy were also presented. Chapter IV, which follows, presents tabular data that may be evaluated in a different manner from the curves presented in this report if an investigator so desires. The data have been gathered from a number of sources, and the matrix of test specimens and conditions was generally incomplete. As a result some comparisons are difficult to make directly, and estimates based on simple models are required. The data that have been collected and analyzed are provided for the purpose of assessing the feasibility of using laminated wood for engineering structures. Specifying or recommending design-allowable stresses is beyond the scope of this test data compilation.

References

1. Wood Handbook: Wood as an Engineering Material. Forest Service Agriculture Handbook No. 72, U.S. Forest Products Laboratory, Madison, VA, 1974.
2. Gerhards, C.C.: Effect of Moisture Content and Temperature on the Mechanical Properties of Wood: An Analysis of Immediate Effects. Wood and Fiber, vol. 14, no. 1, Jan. 1982, pp. 4-36.
3. Volk, W.: Applied Statistics for Engineers. McGraw-Hill Book Company, Inc., 1958.

Chapter IV
Compilation of Data for Laminated Wood

*Jack B. Esgar**

This chapter presents tables of all the data, in both raw form and corrected for moisture content, gleaned from references 1 and 2 and from unreferenced engineering reports written by authors from various organizations. Mean or corrected values of the data, or both, are also plotted in figures. The methods of correcting for moisture content and definitions of standard deviation, correlation coefficient, and *t* test are presented in chapter III.

Testing procedures, specimen configurations, and test equipment are described in this chapter. Since uncorrected test data, as well as data corrected for moisture content, are listed in the tables, users of the data may provide their own moisture-content corrections or data interpretations that may differ from those presented herein.

1.0 Description of Douglas Fir/Epoxy Laminate Material

1.1 General

The discussion in this report is limited to applications of formed, laminated-wood composites made of peeled Douglas fir veneers. The composite resembles conventional plywood, but with some major differences. The differences relate to veneer (or ply) thickness, grain orientation between veneers, the glues used, the care used in selecting and grading the veneers, the care used in fitting veneers together, the layup of the veneers in molds prior to curing, and the pressure application during curing.

Laminated composite veneer material is different in character, composition, and variability from solid wood, and they are therefore not directly comparable. Properly assembled veneer composites are more uniform in composition and less subject to strength losses from defects such as cracks and knots than solid wood. Further, defects are less likely to propagate in a composite structure such as laminated veneers.

*Sverdrup Technology, Inc., Lewis Research Center Group.

1.2 Wood Investigated

1.2.1 Veneer.—In conventional plywood the veneers can be made of hardwood or softwood. The terms "hardwood" and "softwood" have no reference to the hardness of the wood. Softwood can be harder than hardwood, and vice versa. Hardwoods refer to the botanical groups of trees that have broad leaves, in contrast to the conifers, which have needlelike or scalelike leaves and are classified as softwoods (ref. 3). The data in this report are for the softwood Douglas fir glued with an epoxy to form a laminate, hence the term "Douglas fir/epoxy" used throughout this document. Douglas fir is the most widely used wood in the plywood industry.

Veneers for fabricating laminated composite structures can be formed by two main methods: (1) rotary peeling of right-circular cylindrical logs, and (2) slicing of logs of rectangular cross section. The first method is the one most commonly used in the plywood industry. It provides the greatest yield and the lowest cost. In this method, a log is positioned in a lathe type of machine and spun against a knife that slowly moves in toward the center, peeling off a given thickness of veneer with each revolution of the log. Limitations to this method of producing veneer are veneer length, which is limited to a little over 8 ft, and that the veneer produced is somewhat wavy from cutting tangentially along the growth rings. These limitations can be overcome by straight slicing the veneer from logs that have been sawn into sections. This process is more expensive, but it produces veneers in lengths up to 17 ft, and slicing across the growth rings results in a flatter veneer, which improves the conformity of the veneers when they are placed in a mold for lamination. Sliced veneers have the disadvantage of generally being in narrower widths than the peeled veneers.

Data presented in this document are limited to peeled Douglas fir veneers with a thickness of 0.1 in. This thickness was about the maximum considered feasible for molding into contoured shapes for fabrication of wind turbine blades.

1.2.2 Grade, modulus, and defects.—Veneers can be graded both visually and mechanically. Grade, defects, and the modulus of elasticity of the veneer are related. Visual grading is based upon observed defects; mechanical grading is based upon sonic velocity in the veneer as measured by ultrasonic pulse transit times in microseconds for a 92-in. gage length. This ultrasonic pulse transit time can be used to calculate the modulus of elasticity. Some veneer grade definitions are given in the following tables:

Visual grade for wood veneers	Description
A	Up to 18 neat repairs in a 4-ft by 8-ft sheet
B	Solid surface with repair plugs and tight knots to 1 in. in diameter
C	Tight knots to 1.5 in. in diameter and knot holes to 1 in. in diameter; plugged 1/8-in.-wide splits and some broken grain permitted
D	Knots and knot holes to 2.5 in. in diameter; limited splits allowed

Douglas fir veneer grade based upon modulus of elasticity	Visual grade	Ultrasonic pulse time, μsec	Average modulus of elasticity, psi
A+	A or B	< 406	2 450 000 greater
A	A or B	406 to 438	2 100 000 to 2 450 000
C	C or D	< 438	2 100 000 or greater

Note that on the basis of ultrasonic pulse time, veneer grade C is as good as veneer grade A and can be as good as veneer grade A+. Veneer grade C consists of veneers having visual grades C or D; veneer grades A+ and A consist of veneers having visual grades A or B. Veneer with pulse times greater than 438 μsec were not used in the program.

For all materials the modulus of elasticity and the sonic velocity in the material are related. The square of the sonic velocity is proportional to the modulus of elasticity divided by the density with a correction for Poisson's ratio. On the basis of this relationship an ultrasonic grader was developed by the Trus Joist Corporation Micro-Lam plant in Eugene, Oregon. This grader measures the time for a mechanically induced pulse to be transmitted through a 92-in. gage length of the veneer. The process is nondestructive and can be done rapidly. Transducer wheels contacting each end of the veneer sheet transmit and receive ultrasonic signals, but they are actually measuring sonic transmission time in the veneer sheet. The veneer sheets are placed on a conveyer belt that moves at speeds of over 100 ft/min. The transducer wheels roll over the ends of the veneer sheets. A pulse of ultrasonic energy is transmitted along the grain by the transducer wheel at one end of the veneer sheet in the test zone, and an electronic timer is started. When the leading edge of the ultrasonic pulse is detected by the receiving transducer at the other end of the veneer sheet, the timer is stopped and the propagation time averaged with other samples similarly taken on the veneer sheet. Photosensors detect a sheet of veneer in the test zone and activate grade determination and marking equipment when the veneer leaves the test zone. The entire grading procedure takes about 1 sec per sheet. The operation is automatic. Veneer is graded, grade marks sprayed on the veneer, and a tally kept of the number of pieces of veneer falling in each grade. At a line speed of 100 ft/min, a 25-in.-wide sheet of veneer will have at least 10 and as many as 80 samples of propagation time averaged to determine the average propagation time or sheet stiffness. Grade breakpoints are set on precision potentiometers that are user adjustable. References 4 and 5 describe a somewhat similar process for grading veneers.

1.3 Glue

The test data in this report are based upon the laminations being glued with an epoxy of proprietary formulation. This epoxy glue is WEST SYSTEM 105 epoxy resin and 206 hardener supplied by Gougeon Brothers, Inc., Bay City, Michigan. For applications where it was necessary to fill voids, such as installing metal studs into laminated-wood structures or where finger joints were used to join structural sections, a filler such as asbestos or carbon had to be added to the epoxy adhesive. Filled epoxies investigated included the following three proprietary epoxy systems:

(1) WEST SYSTEM asbestos-filled thixotropic epoxy 206–ASB
(2) WEST SYSTEM carbon-filled thixotropic epoxy 206–CFX
(3) WEST SYSTEM modified thixotropic epoxy X-216–CFW

1.3.1 Spread rate.—Most tests were conducted on specimens that had glue spread rates of 60 pounds per thousand square feet of double glue line, abbreviated as 60 lb/MDGL, but block shear tests were conducted over a range of spread rates from 45 to 65 lb/MDGL to determine optimum spread rate.

1.3.2 Reinforcement.—Three types of reinforcement between veneers were investigated:

(1) The addition of 10-oz/yd^2 glass fiber fabric, Burlington Style 7500 or Burlington Style 7781, with fibers at 45° to the wood grain direction

(2) The addition of unidirectional ORCOWEB graphite (4.75 oz/yd^2 and 0.010-in. dry thickness) with fibers parallel to grain direction

(3) Unidirectional FIBERITE Style W-1705 (5.86 oz/yd^2 and 0.015-in. dry thickness) with graphite fibers parallel to the grain direction and held in place with crosswise fiberglass fill yarns

1.4 Lamination Process

The lamination process described herein is of a generalized nature.

1.4.1 Veneer preparation.—Ultrasonically graded sheets of veneer were selected to provide uniformity. These graded sheets were kept in a controlled environment in order to control moisture content prior to fabricating the veneers into billets, specimens, or structures. Moisture content was measured by weighing a sample of the wood before and after moisture was driven from the wood by heating the sample in an oven at approximately 220 °F for at least 12 hr, until the weight of the specimen stabilized.

The ends of the veneers were trimmed, either square to provide butt joints or scarfed to provide longitudinal load transfer in scarf joints. These end joints are necessary when the laminated piece is longer than the veneers.

1.4.2 Layup and glue application.—The trimmed veneers were assembled, on a layout table, with staggered longitudinal and transverse joints. One edge of this layout pile was then trimmed to provide a pilot surface. Each veneer was run through a glue machine that applied glue of a predetermined thickness to rollers. This thickness determined the weight of glue per thousand square feet that was to be applied. The veneer traveled between two rollers and glue was applied to both sides of each veneer.

The veneers were then placed in the mold in the same order as they were on the layout table. The mold could be either contoured (usually a female mold) or flat, depending upon the application. The veneers could be stapled to eliminate shifting during the pressure application that followed.

1.4.3 Vacuum bagging and curing.—For large laminated structures of a contoured shape it is not practical to apply mechanical pressure during the curing process. The method used for applying pressure was to enclose the uncured laminated component in a vacuum bag. Air was removed from the bag by suction to provide a curing pressure of 20 to 25 in. of mercury. This vacuum was held until curing was complete. The laminated component was then removed, trimmed, and machined as required.

1.5 Selected Physical and Mechanical Properties

Nominal values of some physical and mechanical properties of Douglas fir from reference 3 are listed in the following table. The properties are for 12 percent wood moisture content. Because wood is very anisotropic, the properties differ in the longitudinal, radial, and transverse directions. These directions are illustrated in figure 10 of chapter II.

Modulus of elasticity, psi:	
Longitudinal (parallel to grain), E_L	1.95×10^6
Radial (perpendicular to growth rings and to grain), E_R	0.133×10^6
Tangential (parallel to growth rings and perpendicular to grain), E_T	0.098×10^6
Modulus of rigidity in TR plane, G_{TR}, psi	0.014×10^6
Thermal conductivity, Btu/hr ft °F:	
Longitudinal, k_L	0.172
Radial, k_R	0.075
Tangential, k_T	0.068
Coefficient of thermal expansion, °F^{-1}:	
Longitudinal, α_L	2.10×10^{-6}
Radial, α_R	25.90×10^{-6}
Tangential, α_T	34.90×10^{-6}
Poisson's ratio:[a]	
μ_{LR}	0.292
μ_{LT}	0.449
μ_{RT}	0.390
μ_{RL}	0.020
μ_{TR}	0.287
μ_{TL}	0.022
Density, ρ, lb/ft^3	34.9

[a]The first letter of the subscript refers to the direction of applied stress and the second letter refers to the direction of lateral deformation. Note that reference 3 has the values of μ_{TR} and μ_{RL} inadvertently reversed; they are correct here.

2.0 Testing Procedures

2.1 ASTM Standards

Wherever it was feasible, ASTM standards (refs. 6 and 7) were used for testing. The standards used are listed in the following table. Specimens are shown in figures 2.2-1 to 2.2-15.

Test	ASTM standard	Title	Loading rate	Specimen shown in figure 2.2-
Static tension parallel to grain	D 198	Standard Methods of Static Tests of Timbers in Structural Sizes	5 min to failure	1 to 4
Static tension perpendicular to grain	D 1037	Standard Methods of Evaluating the Properties of Wood-Base Fiber and Particle Panel Materials	0.15 in./min	5, 6
Static compression parallel to grain	D 198	Standard Methods of Static Tests of Timbers in Structural Sizes	0.01 in./min	7, 9, 10
Static compression perpendicular to grain	D 143	Standard Methods of Testing Small Clear Specimens of Timber	------	8
Static shear	D 905	Standard Method for Test for Strength Properties of Adhesive Bonds in Shear by Compression Loading	0.015 in./min	11
Tension fatigue	(a)	----------	------	4, 13, 14
Compression fatigue	(a)			15
Damping coefficient	(a)	----------	------	1
Reverse fatigue	(a)	----------	------	13
Wood moisture content	D 2016	Standard Test Methods for Moisture Content of Wood	------	------

[a]There are no ASTM standards for fatigue testing or determining the damping coefficient of wood specimens.

2.2 Specimen Configurations

Specimens used in the investigations are described in this section. Specimen drawings are not to scale.

2.2.1 Static tension specimens.—The following table lists the figures describing each of the types of specimens tested:

Specimen	Figure	Comment
Parallel to grain	2.2-1	----------
Parallel to grain; transverse scarf joints	2.2-2	Three laminations with joints in each specimen
Parallel to grain; transverse butt joints	2.2-3	Three laminations with joints in each specimen
Parallel to grain; size effect	2.2-1 2.2-3 2.2-4	Same proportion of lamination butt joints per unit volume in each specimen
Perpendicular to grain; radial direction	2.2-5	Radial direction perpendicular to growth rings
Perpendicular to grain; tangential direction	2.2-6	Tangential direction perpendicular to grain and radial directions

2.2.2 Static compression specimens.—The following table lists the specimens tested:

Specimen	Figure	Comment
Parallel to grain	2.2-7 2.2-10	Scarf joint effects
Perpendicular to grain; radial direction	2.2-8	Specimen dimensions the same for each grain direction
Perpendicular to grain; tangential direction	2.2-8	Specimen dimensions the same for each grain direction
Parallel to grain; circular hole	2.2-9	Augmented specimens (10 oz/yd^2 of glass cloth between each lamination)

2.2.3 Static shear and bending strength specimens.—The following table lists the specimens tested:

Specimen	Figure
Block shear	2.2-11
Bending	2.2-12

2.2.4 Tension fatigue specimens.—The following table lists the specimens tested:

Specimen	Figure	Comment
Parallel to grain	2.2-13	.....
Parallel to grain; size effect	2.2-14	.....
Parallel to grain; transverse butt joints	2.2-13	Three transverse butt joints in center veneers—3-in. spacing

2.2.5 Compression fatigue specimens.—The following table lists the specimens tested:

Specimen	Figure	Comment
Parallel to grain; transverse scarf joints	2.2-15	Specimen configuration the same; three joints in each specimen
Parallel to grain; transverse butt joints	2.2-15	Specimen configuration the same; three joints in each specimen

2.2.6 Reverse axial tension-compression fatigue specimens.—Specimens were tested parallel to the grain (fig. 2.2-13).

2.2.7 Damping ratio specimens.—Specimens were tested parallel to the grain (fig. 2.2-1). Specimen lengths varied from 166 to 235.6 in.

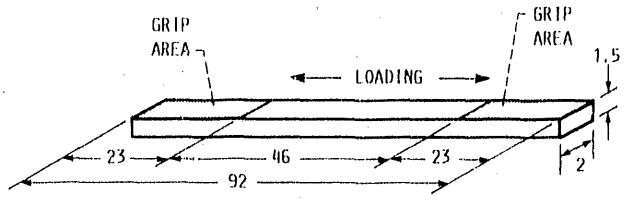

Figure 2.2-1.—Test specimen for tension parallel to grain. (Dimensions are in inches.)

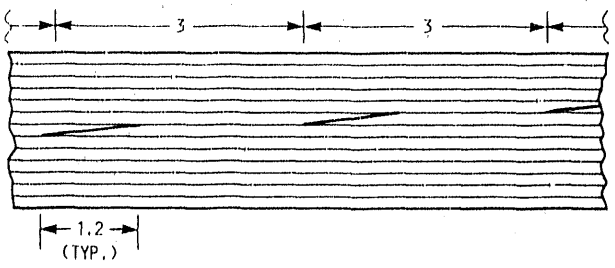

Figure 2.2-2.—Details of veneer scarf joints for tension, compression, and fatigue specimens. (Dimensions are in inches.)

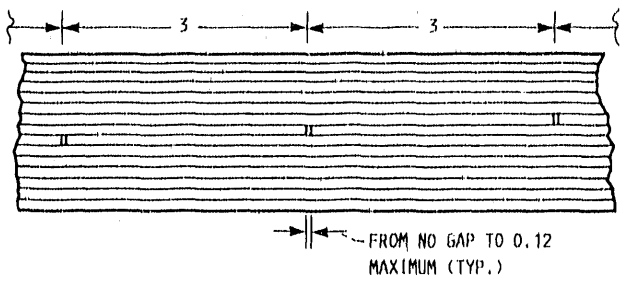

Figure 2.2-3.—Details of veneer butt joints for tension, compression, and fatigue specimens. (Dimensions are in inches.)

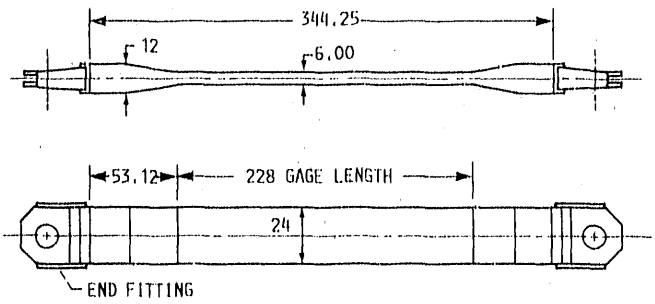

Figure 2.2-4.—Test specimen for size effect on tension. (Dimensions are in inches.)

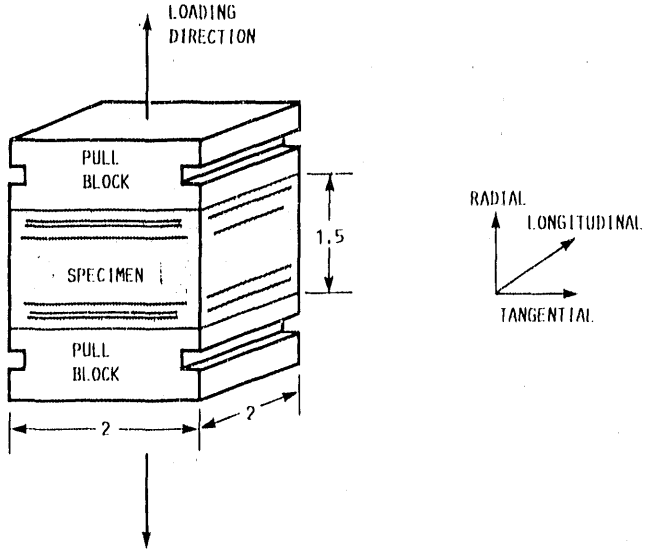

Figure 2.2-5.—Test specimen for tension perpendicular to grain (radial direction). (Dimensions are in inches.)

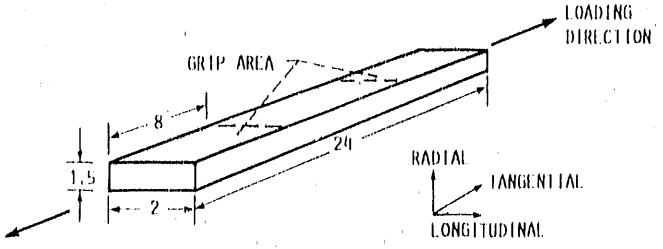

Figure 2.2–6.—Test specimen for tension perpendicular to grain (tangential direction). (Dimensions are in inches.)

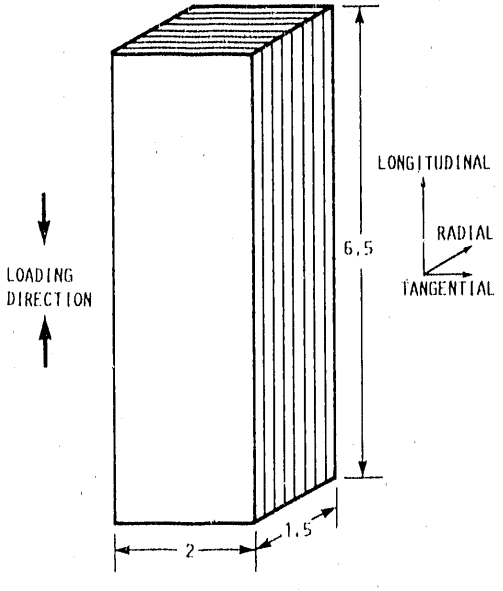

Figure 2.2–7.—Test specimen for compression parallel to grain. (Dimensions are in inches.)

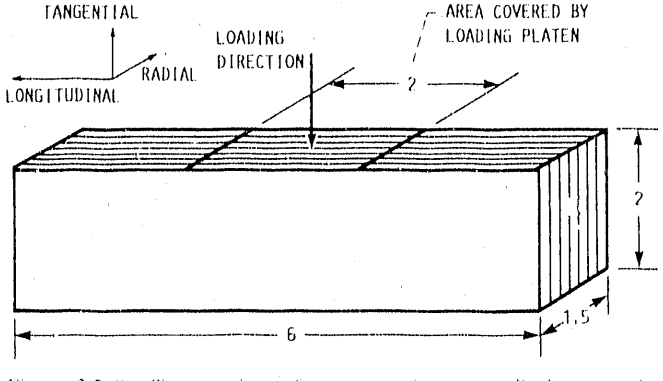

Figure 2.2–8.—Test specimen for compression perpendicular to grain. (Dimensions are in inches.)

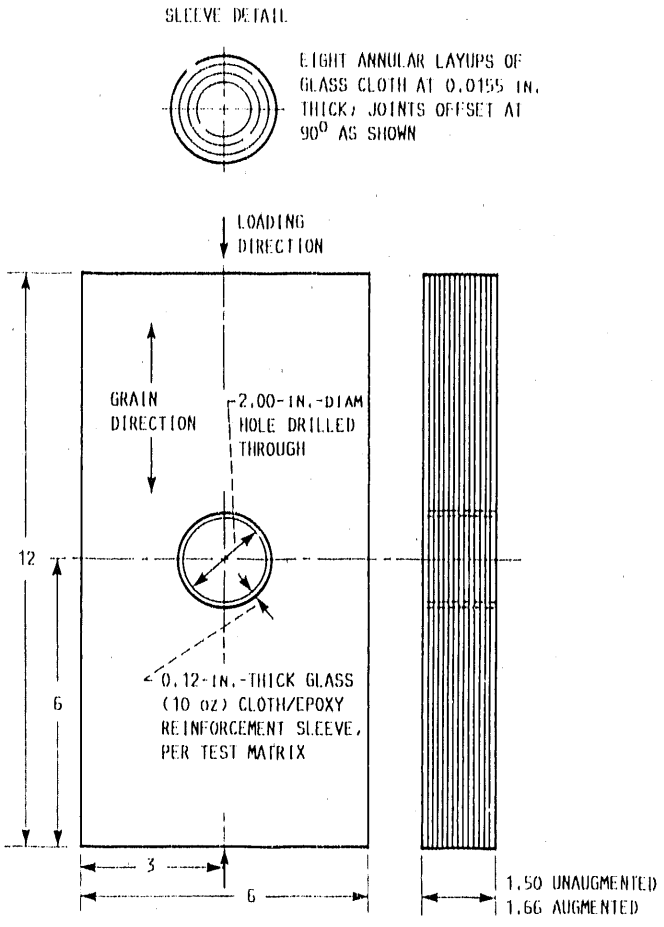

Figure 2.2–9.—Specimen for testing effects of unreinforced and glass-fiber-fabric-reinforced central hole. (Dimensions are in inches.)

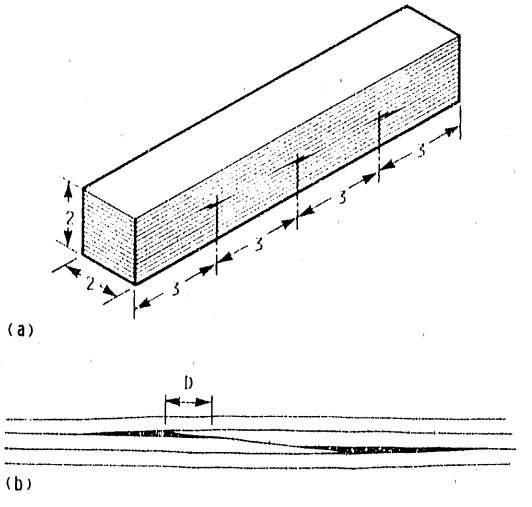

(a) Staggered scarf joint test sample configuration. (Control specimens have same overall dimensions but contain no scarf joints.)
(b) Overlap joint: 50 percent overlap, D = 0.50 in.; 25 percent overlap, D = 0.25 in. (Overlap joints tend to distort somewhat within the laminate.)

Figure 2.2–10.—Static compression and compression compression fatigue specimen for investigations of scarf joint configuration strength.

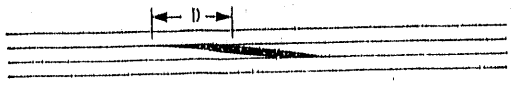

(c) Gap joint: 50 percent gap, $D = 0.50$ in.; 25 percent gap, $D = 0.25$ in.

Figure 2.2-10.—Concluded.

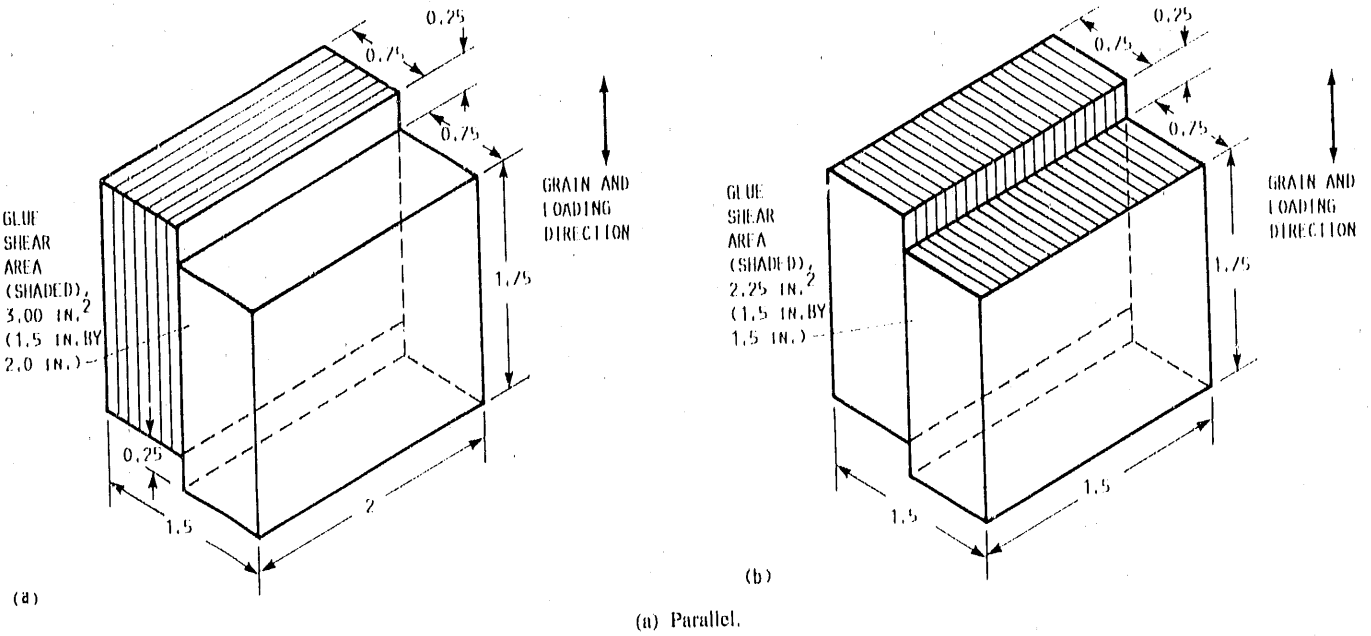

(a) Parallel.
(b) Perpendicular.

Figure 2.2-11.—Block shear specimens parallel and perpendicular to laminations. (Dimensions are in inches.)

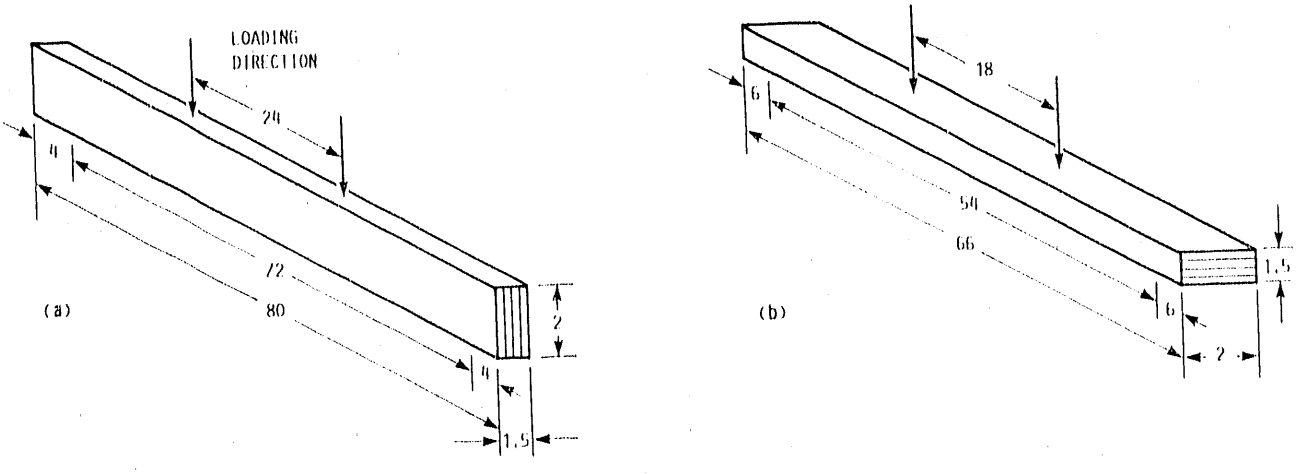

(a) Vertical laminations.
(b) Horizontal laminations.

Figure 2.2-12.—Specimens for bending with vertical and horizontal laminations. (Dimensions are in inches.)

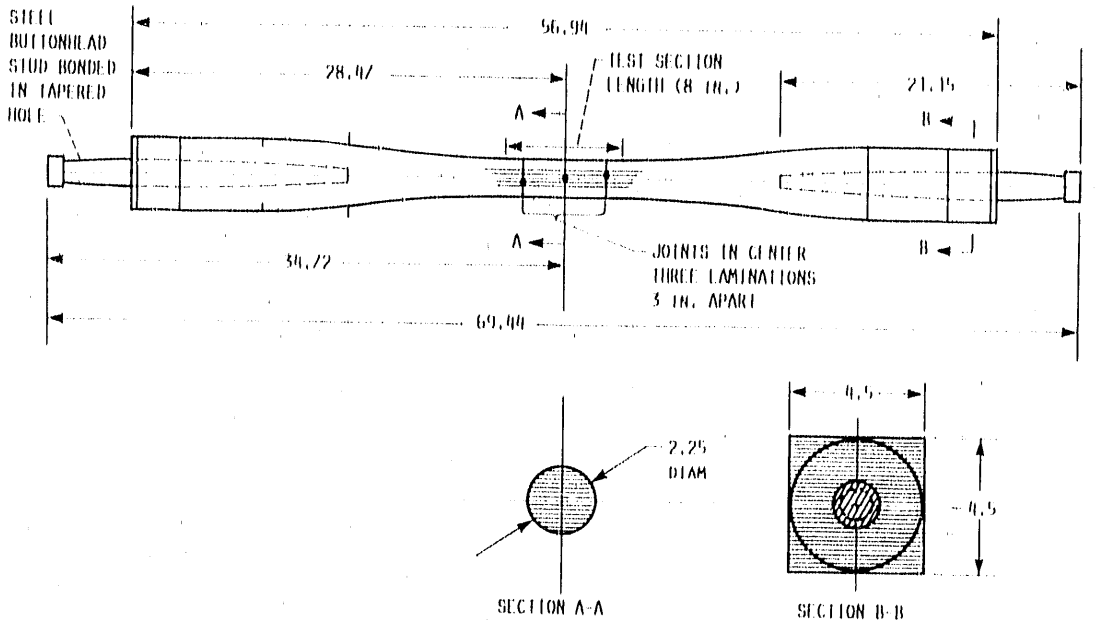

Figure 2.2–13.—Dogbone test specimen for fatigue testing. (Dimensions are in inches.)

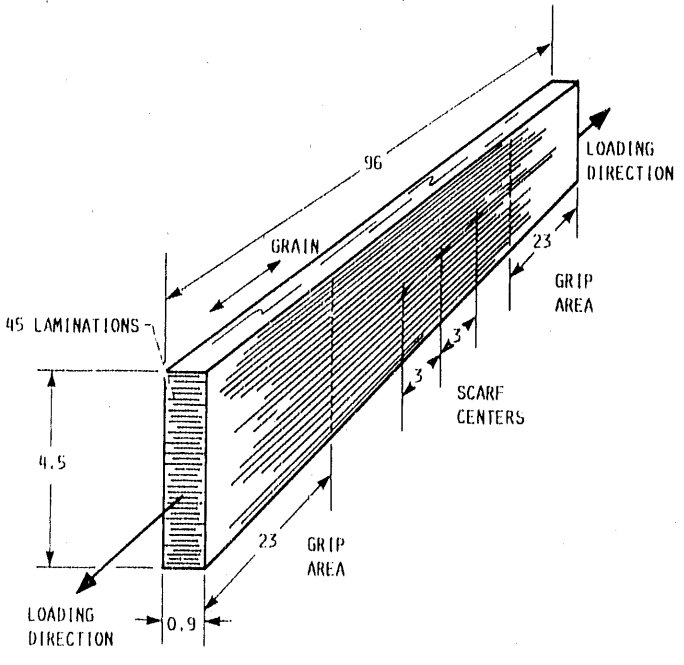

Figure 2.2–14.—"Plank" style static tension test specimen. (Dimensions are in inches.)

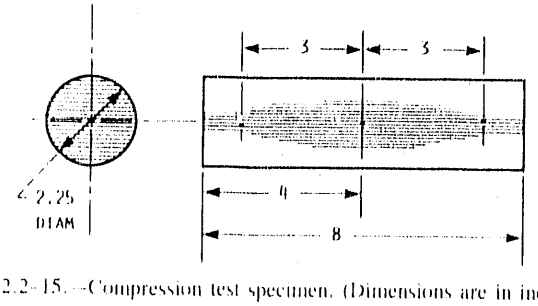

Figure 2.2–15.—Compression test specimen. (Dimensions are in inches.)

2.3 Specimens With Structural Joints

In large structures it may be necessary to use joints to join subassemblies together, as illustrated in figure 2.3–1 for transverse joints in a wind turbine blade. This section of the report describes specimens that were tested to determine the strength of such joints.

2.3.1 Finger joints.—Figure 2.3–2 illustrates the general geometry of finger joints, and figure 2.3–3 provides some details on how the specimens were cut from laminated billets, machined, and joined. The following table lists the figures (2.3–4 to 2.3–9) describing each of the types of finger joint specimens tested:

Specimen	Figure	Comments
Six-in. finger length, various slopes	2.3–4	
Three-in. finger length	2.3–5	Static tension tests
Aging effects	2.3–6	
Augmentation	2.3–7	Glass fiber or Kevlar between veneers; static tension tests
Dogbone	2.3–8 2.3–9	Tension and compression fatigue tests

2.3.2 Longitudinal bonded joints.—Some structural joints may not have to carry the tension load that would make finger joints necessary. Simpler longitudinal joints for a wind turbine blade are illustrated in figures 2.3–10 and 2.3–11 and in figure 16 in chapter III. Bending test specimens for longitudinal butt and wedge joints are shown in figure 2.3–12.

2.3.3 Stud joints.—Wooden structures can be attached to metal components by using metal studs bonded into the laminated wood. A specimen for investigating such joints in shown in figure 2.3-13.

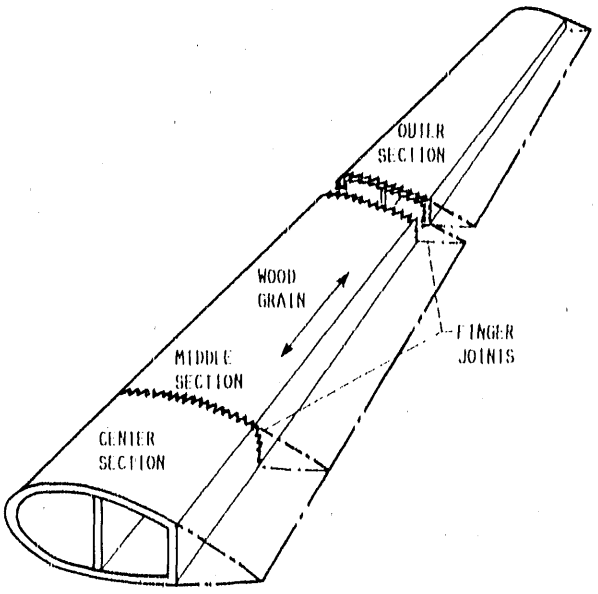

Figure 2.3-1.—Field splice finger joint concept for wind turbine blade.

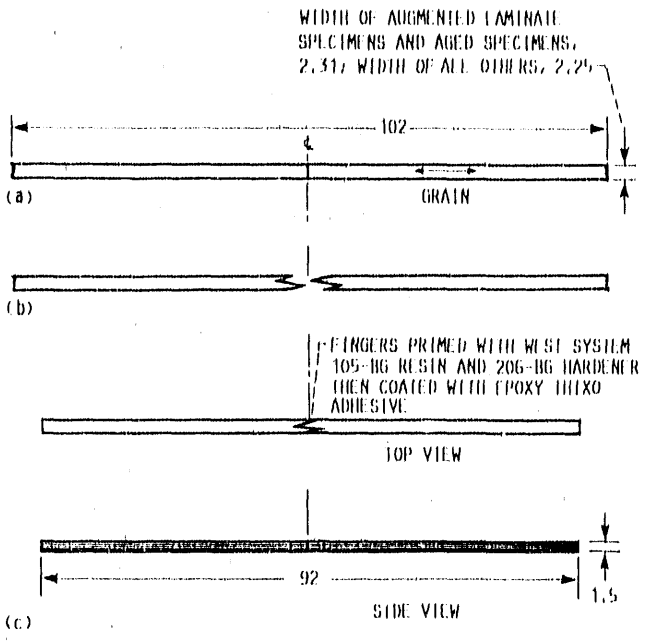

(a) Saw-cut billet.
(b) Bandsaw-cut fingers.
(c) Bonded fingers cut to finished length.

Figure 2.3-3.—Fabrication of finger joint tensile test specimens. (Dimensions are in inches.)

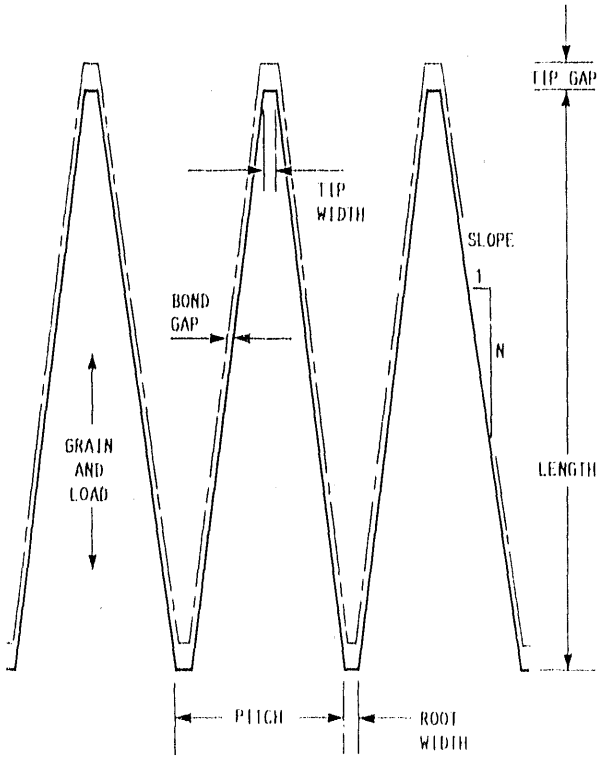

Figure 2.3-2.—Finger joint design geometry.

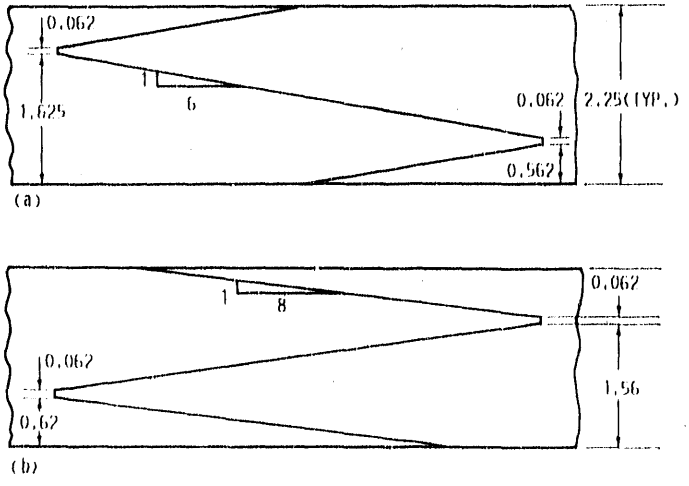

(a) 1:6 Slope. Pitch, 2.125 in.
(b) 1:8 Slope. Pitch, 1.625 in.

Figure 2.3-4.—Tensile test specimens showing details of machined fingers with slopes of 1:6, 1:8, 1:10, and 1:14. (Dimensions are in inches.)

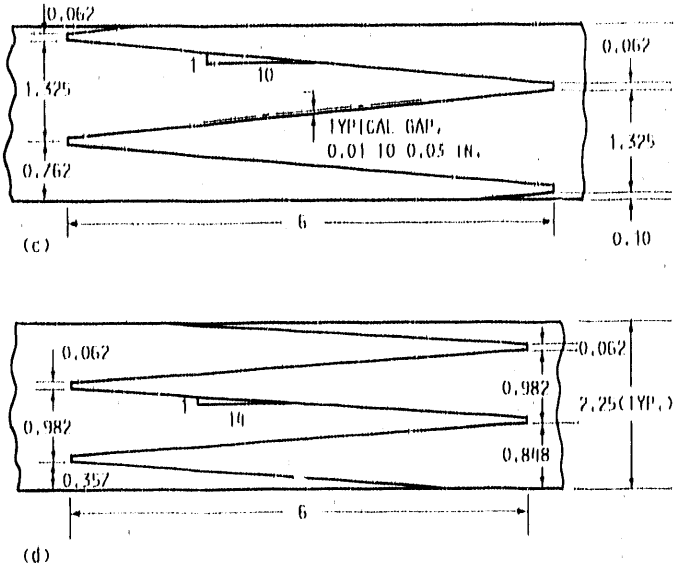

(c) 1:10 Slope.
(d) 1:14 Slope.

Figure 2.3-4.—Concluded.

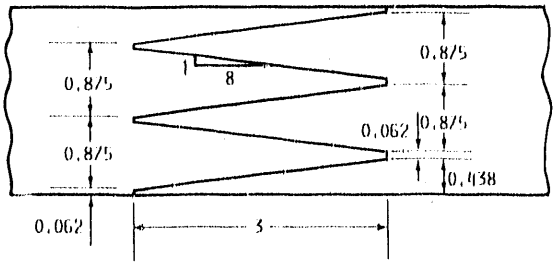

Figure 2.3-5.—Details of tensile test specimens with machined fingers 3 in. long and having a slope of 1:8. (Dimensions are in inches.)

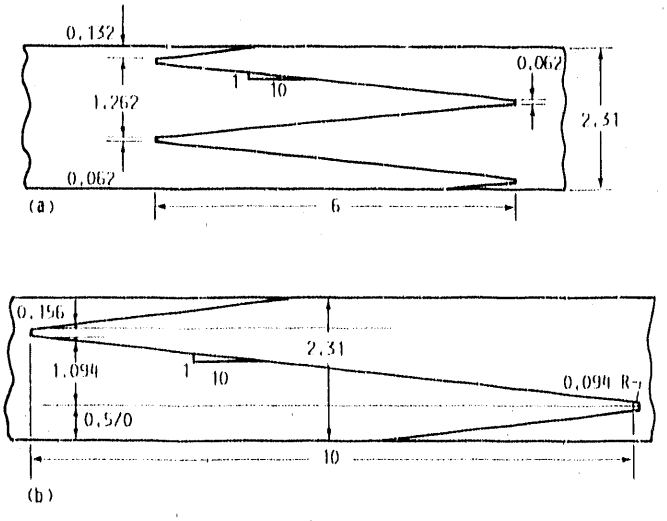

(a) 6-in. fingers.
(b) 10-in. fingers. Pitch, 2.344 in.

Figure 2.3-6.—Detail of machined fingers in aged tension test specimens. (Dimensions are in inches.)

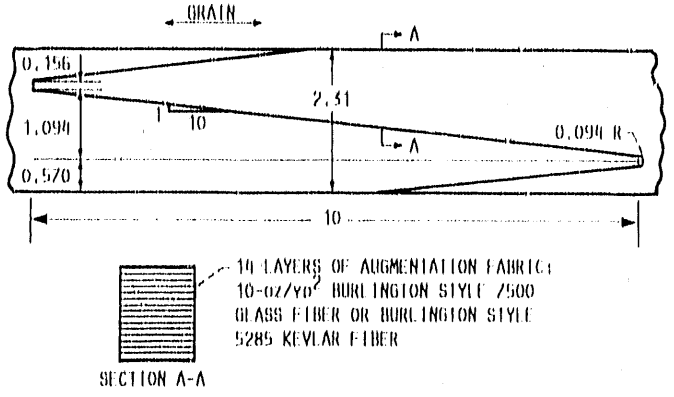

Figure 2.3-7.—Detail of machined fingers in augmented specimens for tensile tests. Pitch, 2.344 in. (Dimensions are in inches.)

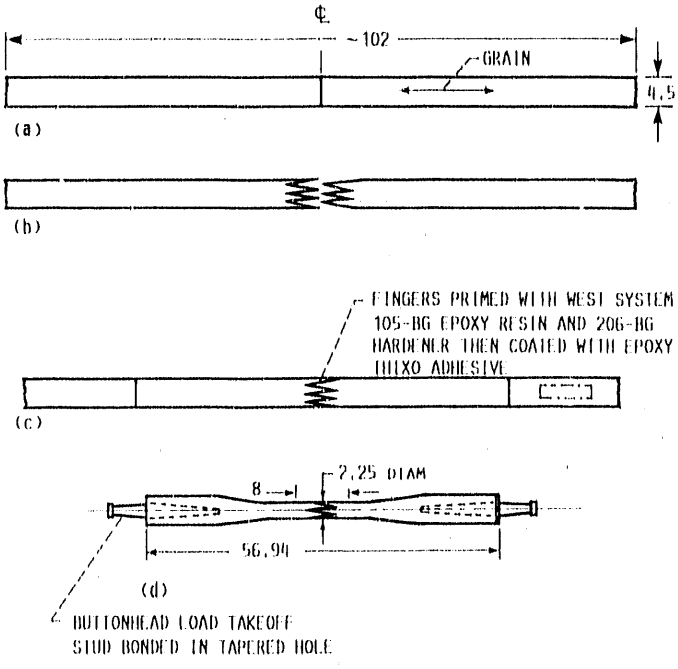

(a) Saw-cut billet.
(b) Bandsaw-cut fingers.
(c) Bonded fingers and ends cut off for compression test blocks.
(d) Machined and finished dogbone with studs installed.

Figure 2.3-8.—Fabrication of finger joints in dogbone specimens for fatigue tests. (Dimensions are in inches.)

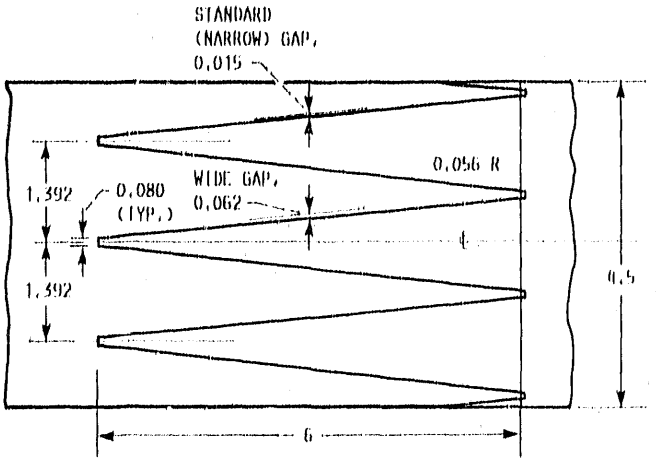

Figure 2.3-9.—Detail of machined fingers in dogbone specimens for fatigue tests. (Dimensions are in inches.)

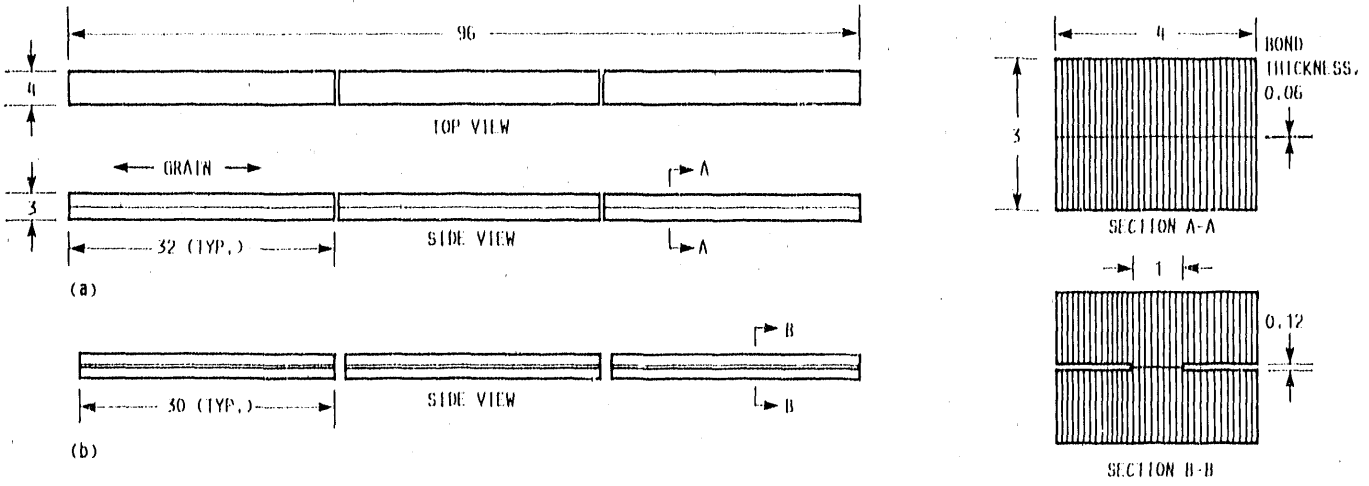

(a) Saw cut 96-in.-long strips into 32-in.-long pieces; bond two pieces at centerline with epoxy asbestos adhesive.
(b) Saw cut 0.12-in.-thick slots; saw cut to 30 in. long; epoxy coat cut edges. (See section B-B.)

Figure 2.3-10.—Fabricating longitudinal butt joint test specimens. (Dimensions are in inches.)

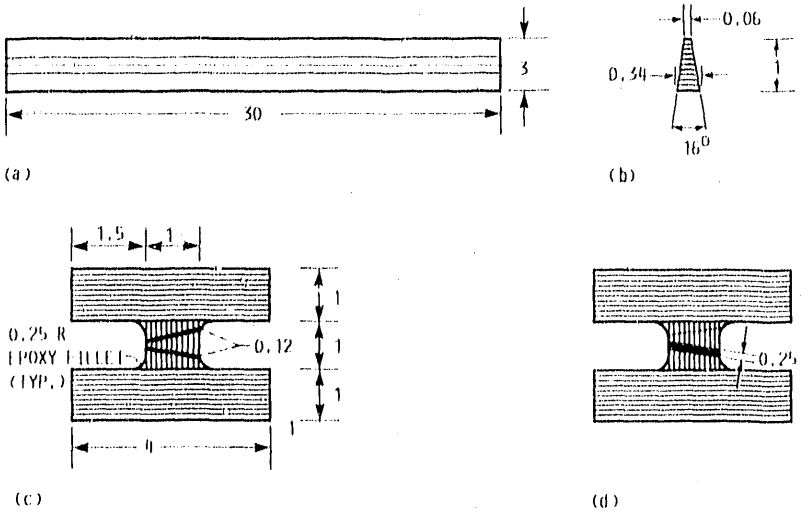

(a) Side view. (b) Wedge detail. (c) Centered wedge. (d) Shifted wedge.

Figure 2.3-11.—Longitudinal wedge joint test specimens. (Dimensions are in inches.)

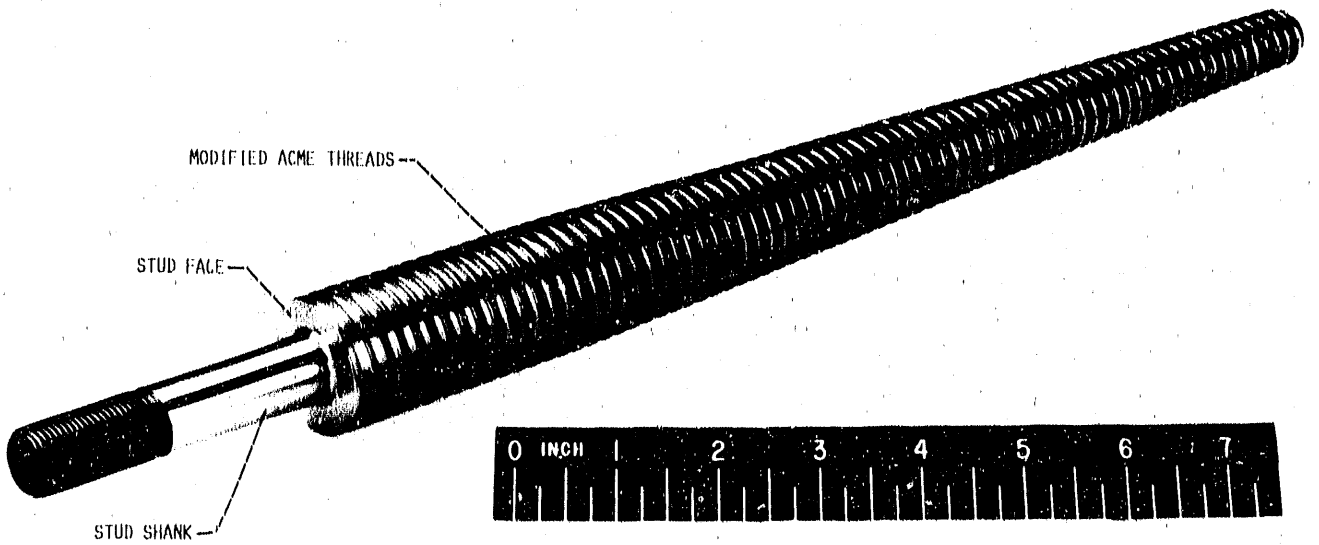

(a)

C-82-4953

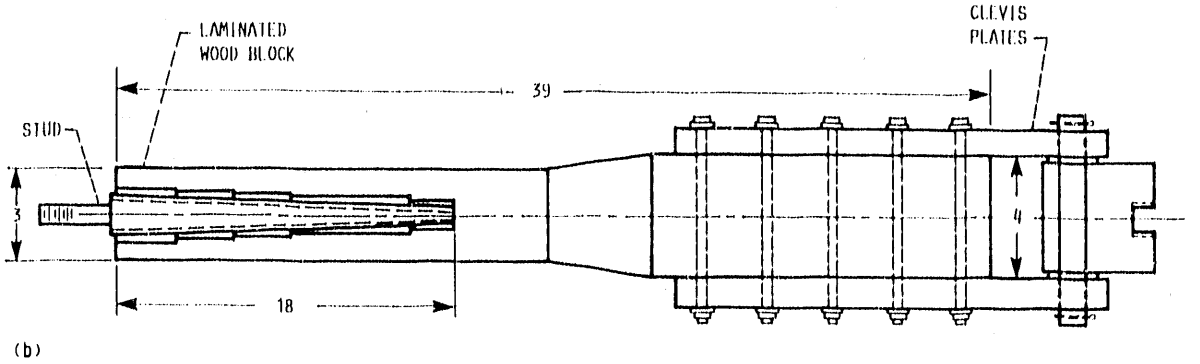

(b)

(a) Typical steel stud.
(b) Stud bonded into wood block.

Figure 2.3-12.—Stud test specimen configuration. (Dimensions are in inches.)

2.4 Test Equipment

Tests on laminated-wood specimens were conducted at a number of different organizations. In most cases standard testing machines were used, but in some instances special machines were designed or existing machines were modified for the tests. The apparatus and a specimen used for measuring damping characteristics during transverse vibration are shown in figure 2.4–1. The equipment used is listed in the following table:

Equipment description	Test organization	Types of tests
MTS model 810.14-2 two-column material test machine. Test opening, 30 in. wide by 81 in. high; capacity, 110 000 lb. MTS 643.67 buttonhead grips	Gougeon Brothers, Inc., Bay City, Michigan	Static tension and compression; fatigue
MTS 200 000-lb hydraulic universal test machine with 77 000-lb actuator for high-cycle fatigue	University of Dayton Research Institute, Dayton, Ohio	Static tension and compression; high-cycle fatigue
MTS 110 000-lb load frame with 50 000-lb hydraulic actuators and 50 000-lb fatigue-rated load cell. MTS 643.67 buttonhead grips	University of Dayton Research Institute, Dayton, Ohio	Fatigue
MTS model 308.01 four-column material test machine. Capacity, 20 000 lb	Illinois Institute of Technology Research Institute, Chicago, Illinois	Static tension and fatigue
Baldwin 5-million-lb screw-driven universal test machine	Lehigh University, Bethlehem Pennsylvania	Static tension
Metriguard 186 000-lb-tension, 200 000-lb-compression horizontal hydraulic test machine. Specimen lengths up to 312 in.	Washington State University, Pullman, Washington	Static tension and compression fatigue
Specially designed 300 000-lb tensile test machine	Oregon State University, Corvallis, Oregon	Static tension
Tinius Olsen test machine. Capacity, 60 000 lb.	Oregon State University, Corvallis, Oregon	Static tension
Nicolet Instruments model 206, Explorer III, digital storage oscilloscope Metriguard model 3300 transverse vibration E-computer Hewlett-Packard model 7034A X–Y recorder	Metriguard, Inc., Pullman, Washington	Damping
Modulus grader (see subsection 1.2.2)	Trus Joist Corporation, Eugene, Oregon	Laminate modulus of elasticity

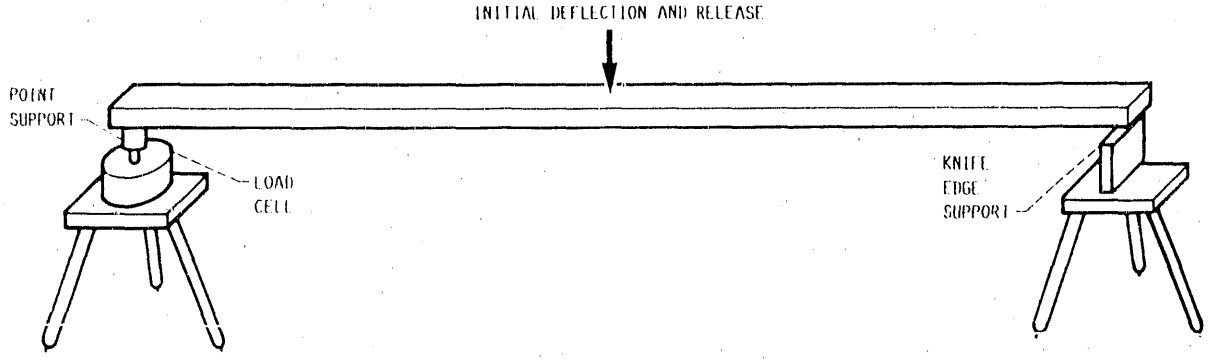

Figure 2.4–1.—Apparatus and specimen for measuring damping characteristics.

3.0 Static Strength of Laminated Composite Specimens

Considerable data are available on the static tension, compression, and shear strength of Douglas fir/epoxy laminates. Among the variables investigated were (1) direction of force relative to grain direction (parallel, perpendicular in a direction radial from the tree centerline, and perpendicular in a direction tangential to the peeling surface of the log, see fig. 10 in chapter II), (2) specimen size, (3) specimen temperature, (4) moisture content, (5) laminate or veneer grade, (6) butt joints or scarf joints in laminates with the joint transverse to the direction of force, (7) glue spread rate, (8) effect of circular holes in the specimen, and (9) graphite fiber augmentation between laminates. Note that more significant figures are presented in the tables of this report than are warranted by the precision of the data. All numbers are based upon computer calculation without rounding. Rounding to the nearest 100 psi is probably warranted in most cases, based on a load cell accuracy of 0.5 percent of full-scale reading.

3.1 Static Tension Strength

3.1.1 Parallel to grain.—In order to achieve the greatest strength in laminated wood, the load direction should be parallel to the grain, but there are many variables that can affect the strength. The larger the specimen or structure, the more defects are apt to be present and the lower the strength. If the structure is larger than the length of log peeled to make the veneers, there will be joints in the individual veneers that can reduce strength. Temperature, moisture content, and veneer grade also affect strength. The effects of these variables are shown in the following subsections.

3.1.1.1 Effect of moisture content on tension strength: The effect of moisture content is predicted analytically in reference 3 by means of equation (1) in chapter III of this report. This equation can be manipulated to predict strength or modulus of elasticity for any wood moisture content less than the fiber saturation value of about 24 percent from any other known values of strength or modulus and the moisture content at which those values were determined. Figure 3.1-1 shows how the properties parallel to the grain of Douglas fir laminates are predicted to vary with moisture content, according to equation (8) in chapter III and its accompanying table of K values.

Table 3.1-I presents experimental data for two specimen configurations of Douglas fir/epoxy laminates tested at laminate moisture contents from 4.6 to 9.2 percent. The specimens were of the type shown in figures 2.2-1 and 2.2-12. Other data over a smaller range of moisture contents are presented in tables 3.1-II to 3.1-IV. The data from these tables for specimen volumes of 402 in.^{3} or less are shown in figure 3.1-2 along with an analytical curve of the type in figure 3.1-1. It is obvious that the data shown do not verify the effect of moisture on tension strength predicted by the method of reference 3.

Since the experimental static tension data available for Douglas fir/epoxy laminates did not satisfactorily determine an experimental correlation of moisture effects, we used the method of reference 3 to correct the data obtained at laminate moisture contents different from 6 percent. In general the corrections were small, but the static tension data were tabulated for two cases: (1) without a moisture correction and (2) corrected to 6 percent laminate moisture content by using the methods described in the subsection "Correction of Moisture Content" in chapter III and a value of $K = 1.21$ from reference 3.

Limited additional information on how moisture content

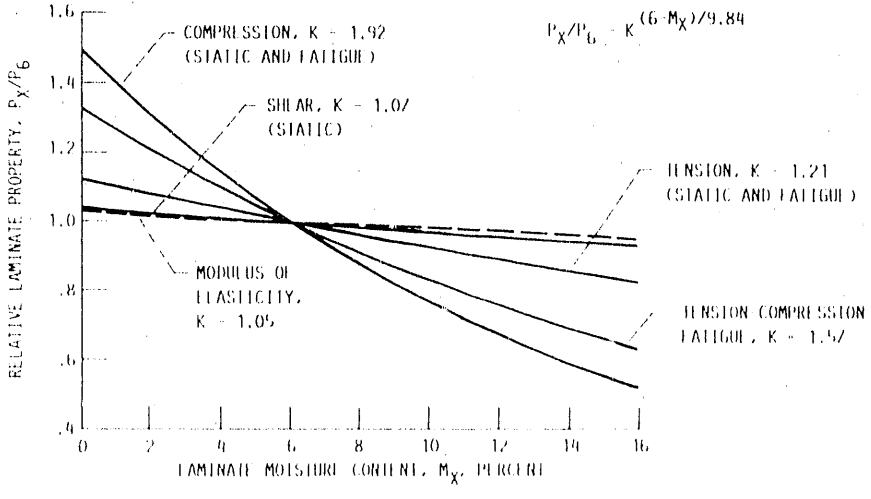

Figure 3.1-1.—Predicted variation with moisture content of mechanical properties of Douglas fir wood laminates parallel to grain (see eq. (8), chapter III).

TABLE 3.1-1.—EFFECT OF MOISTURE CONTENT ON STATIC TENSION STRENGTH PARALLEL TO GRAIN

[Laminated Douglas fir/epoxy specimens; veneer grade, A+; test temperature, 70 °F; 5-min ramp to failure.]

Specimen description	Veneer grade	Laminate moisture content, percent	Failure stress, psi	Failure stress corrected to 6 percent laminate moisture content, psi
2.25-in.-diameter dogbone shape with three transverse butt joints in center veneers with 3-in. spacing between joints (fig. 2.2-14)	A+	5.5	10 841	10 736
		5.8	11 287	11 243
		6.0	12 363	12 362
		8.9	11 267	11 918
		9.2	12 195	12 974
		Mean	11 591	11 847
		Standard deviation	587	792
2.25-in.-diameter dogbone shape with three transverse butt joints in center veneers with 3-in. spacing between joints (fig. 2.2-14)	A	7.4	10 028	10 303
	A	8.7	13 187	13 894
		Mean	11 608	12 099
		Standard deviation	1580	1796
0.9- by 4.5- by 96-in. specimens with 45 laminations; three transverse 12:1-slope scarf joints in center veneers with 3-in. spacing between joints (similar to fig. 2.2-1)	A+	4.6	10 130	9 859
		5.0	11 971	11 741
		5.8	10 990	10 947
		6.5	10 438	10 539
		7.1	12 937	13 215
		9.0	11 512	12 200
		Mean	11 330	11 417
		Standard deviation	947	1108

TABLE 3.1-II.—EFFECT OF TEST SECTION VOLUME ON STATIC TENSION STRENGTH FOR BUTT-JOINTED SPECIMENS—PANELS 1 AND 2

[Laminated Douglas fir/epoxy specimens 1.5 in. thick with 15 laminations. Butt joints spaced 3 in. apart in adjacent laminations. Veneer grade, A+.]

Panel	Specimen width, in.	Total specimen length, ft	Test section volume, in.	Stress area, in.	Total weight, lb	Number of butts		Number of face sheet scarf joints	Number of edge defects	Laminate moisture content, percent	Gage length, in.	Failure load, lb	Failure stress, psi	Failure strain, in./in.	Modulus, psi	Corrected to 6 percent laminate moisture content	
						Between jaws	In failure									Failure stress ($K = 1.21$), psi	Modulus ($K = 1.05$), psi
1	2	7.5	132	3.02	6.25	7	--	0	0	7.2	36.0	29 400	9 727	0.00355	2.73×10^6	9 955	2.81×10^6
↓	↓	↓	↓	3.03	6.18	13	13	1	1	7.1	↓	37 040	12 197	.00473	2.57	12 459	2.64
↓	↓	↓	↓	3.01	6.32	13	10	0	1	6.7	↓	33 920	11 259	.00422	2.66	11 412	2.71
↓	↓	↓	↓	3.02	6.27	8	5	2	0	7.0	↓	30 920	10 220	.00391	2.61	10 419	2.67
2	↓	↓	↓	2.99	6.25	5	1	0	2	7.0	↓	33 440	11 172	.00416	2.68	11 390	2.74
↓	↓	↓	↓	3.02	5.85	0	--	1	1	7.3	↓	42 480	14 049	.00616	2.27	14 407	2.34
↓	↓	↓	↓	3.01	5.97	0	--	2	2	7.1	↓	35 920	11 915	.00480	2.48	12 171	2.54
↓	↓	↓	↓	3.01	5.91	5	5	2	1	7.0	↓	35 160	11 645	.00493	2.63	11 872	2.69
1	8	↓	528	12.02	24.68	7	4	0	0	7.2	↓	134 600	11 196	.00422	2.65	11 431	2.72
↓	↓	↓	↓	12.02	24.45	12	10	0	↓	7.1	↓	119 200	9 912	.00387	2.56	10 125	2.62
↓	↓	↓	↓	12.03	24.95	13	13	1	↓	6.7	↓	99 800	8 296	.00302	2.74	8 409	2.78
↓	↓	↓	↓	12.02	24.98	7	2	2	↓	7.1	↓	103 200	8 504	.00326	2.63	8 687	2.69
2	↓	↓	↓	12.01	25.03	8	4	0	1	7.2	↓	124 200	10 340	.00386	2.67	10 583	2.74
↓	↓	↓	↓	11.99	23.30	0	--	1	0	7.2	↓	149 000	12 418	.00513	2.41	12 709	2.48
↓	↓	↓	↓	11.98	23.80	0	--	2	1	7.4	↓	157 800	13 169	.00543	2.42	13 530	2.50
↓	↓	↓	↓	11.94	23.40	5	5	2	2	7.0	↓	123 200	10 312	.00423	2.43	10 513	2.49
↓	2	15	402	3.02	11.92	13	0	2	2	6.7	120.0	33 600	11 092	.00461	2.40	11 243	2.44
↓	↓	↓	↓	3.00	11.88	14	9	4	1	7.0	↓	32 520	10 818	.00440	2.45	11 029	2.51
1	↓	↓	↓	3.04	12.77	21	13	2	3	7.0	↓	27 680	9 098	.00358	2.53	9 276	2.59
↓	↓	↓	↓	3.04	12.72	22	10	2	2	7.1	↓	26 160	8 622	.00321	2.68	8 807	2.74
↓	8	15	1608	12.01	50.09	21	12	2	1	7.2	↓	114 000	9 489	.00375	2.53	9 712	2.60
↓	↓	↓	↓	12.02	49.80	22	10	2	1	7.1	↓	124 000	10 313	.00393	2.62	10 535	2.68
2	↓	↓	↓	12.00	47.10	14	13	2	1	6.8	↓	113 400	9 448	.00400	2.36	9 636	2.40
↓	↓	↓	↓	12.01	46.90	14	13	4	0	7.2	↓	125 600	10 453	.00436	2.39	10 698	2.46
↓	2	30	942	3.01	-----	39	9	6	0	6.7	↓	29 120	9 661	.00416	2.31	9 792	2.35
↓	↓	↓	↓	3.01	-----	39	12	↓	2	7.0	↓	30 440	10 093	.00431	2.33	10 290	2.39
1	↓	↓	↓	3.03	-----	45	11	↓	4	7.0	↓	29 400	9 672	.00366	2.63	9 861	2.69
↓	↓	↓	↓	3.03	-----	46	5	↓	1	7.2	↓	27 920	9 210	.00346	2.65	9 426	2.72
↓	8	30	3768	12.02	-----	46	6	↓	4	7.2	↓	112 600	9 365	.00373	2.50	9 585	2.57
↓	↓	↓	↓	12.02	-----	46	7	↓	1	7.4	↓	98 200	8 164	.00315	2.59	8 388	2.67
2	↓	↓	↓	12.01	-----	39	13	↓	2	7.6	↓	108 400	9 022	.00371	2.42	9 306	2.51
2	↓	↓	↓	12.00	-----	39	9	9	8	7.2	↓	125 200	10 426	.00451	2.30	10 708	2.37

TABLE 3.1-III.—EFFECT OF TEST SECTION VOLUME ON STATIC TENSION STRENGTH FOR BUTT- AND SCARF-JOINTED SPECIMENS—PANEL 3

[Laminated Douglas fir/epoxy specimens 1.5 in. thick with 15 laminations. Butt or scarf joints spaced 3 in. apart in adjacent laminations. Veneer grade, A+; total specimen length, 7.5 ft; gage length, 36.0 in.]

Specimen width, in.	Test volume, $in.^3$	Stress area, $in.^2$	Weight, lb	Density, $lb/in.^3$	Number of joints		Laminate moisture content, percent	Failure load, lb	Failure stress, psi	Failure strain, in./in.	Modulus, psi	Corrected to 6 percent laminate moisture content	
					Butt	Scarf						Failure stress ($K = 1.21$), psi	Modulus ($K = 1.05$), psi
8	528	12.01	25.97	0.0240	13	--	6.9	110 000	9 158	0.00338	2.70×10^6	9 319	2.75×10^6
		12.00	25.63	.0237	--	13	7.1	122 000	10 163	.00406	2.50	10 381	2.56
		12.00	26.30	.0243	13	--	7.2	107 600	8 961	.00352	2.54	9 171	2.61
		12.01	25.90	.0239	--	13	7.3	136 000	11 318	.00436	2.59	11 606	2.67
		11.99	25.71	.0238	13	--	6.5	124 000	10 337	.00409	2.52	10 437	2.55
		12.01	25.40	.0235	--	13	7.3	125 000	10 406	.00416	2.49	10 671	2.57
		11.99	25.46	.0236	13	--	6.0	120 000	10 007	.00411	2.43	10 007	2.43
		12.01	25.97	.0240	--	13	8.8	126 000	10 490	.00472	2.22	11 074	2.36
		12.00	26.15	.0242	13	--	7.1	132 000	10 993	.00406	2.70	11 229	2.77
		12.00	26.11	.0249	--	13	6.7	132 000	10 993	.00433	2.53	11 143	2.57
		12.01	26.12	.0241	13	--	6.2	120 000	9 990	.00370	2.69	10 028	2.70
		12.00	25.95	.0240	--	13	6.8	138 000	11 492	.00433	2.65	11 671	2.70
		12.01	25.65	.0237	13	--	6.6	122 000	10 157	.00423	2.39	10 275	2.43
		12.01	25.92	.0239	--	13	6.7	128 000	10 656	.00388	2.74	10 801	2.78
		12.00	25.90	.0240	13	--	6.7	123 000	10 250	.00372	2.75	10 389	2.79
		12.00	26.65	.0246	--	13	7.4	150 200	12 517	.00403	2.75	12 861	2.84
2	132	3.02	6.58	.0242	13	--	7.0	34 600	11 457	.00413	2.76	11 681	2.83
		3.02	6.53	.0240	--	13	6.7	40 806	13 512	.00512	2.63	13 696	2.68
		3.02	6.56	.0241	13	--	6.3	32 680	10 821	.00391	2.76	10 884	2.78
		3.01	6.50	.0239	--	13	6.7	31 160	10 332	.00395	2.61	10 473	2.65
		3.01	6.48	.0239	13	--	6.6	37 520	12 449	.00452	2.74	12 594	2.78
		3.01	6.46	.0238	--	13	7.1	32 000	10 610	.00405	2.61	10 838	2.68
		3.01	6.45	.0237	13	--	7.5	30 000	9 937	.00392	2.53	10 230	2.61
		3.03	6.60	.0242	--	13	7.3	36 400	11 993	.00456	2.66	12 298	2.74
		3.02	6.51	.0239	13	--	6.8	33 600	11 104	.00417	2.66	11 277	2.71
		3.02	6.45	.0237	--	13	7.1	36 000	11 913	.00467	2.55	12 169	2.61
		3.01	6.57	.0242	13	--	6.4	28 440	9 430	.00386	2.59	9 503	2.61
		3.02	6.46	.0238	--	13	6.5	36 800	12 185	.00494	2.46	12 303	2.49
		3.02	6.52	.0240	13	--	6.9	36 240	11 968	.00467	2.55	12 178	2.61
		3.02	6.48	.0238	--	13	6.9	33 600	11 107	.00440	2.52	11 302	2.57
		3.02	6.43	.0236	13	--	6.9	30 080	9 957	.00369	2.69	10 132	2.75
		3.03	6.60	.0242	--	13	7.0	36 400	12 005	.00440	2.72	12 239	2.79

TABLE 3.1-IV.—EFFECT OF TEST SECTION VOLUME ON STATIC TENSION STRENGTH FOR SCARF-JOINTED SPECIMENS—PANELS 4 AND 5

[Laminated Douglas fir/epoxy specimens 1.5 in. thick with 15 laminations. Scarf joints spaced 3 in. apart in adjacent laminations unless otherwise noted. Veneer grade, A+.]

Panel	Specimen width, in.	Total specimen length, ft	Test volume, $in.^3$	Stress area, $in.^2$	Total weight, lb	Density, lb/in.	Laminate moisture content, percent	Gage length, in.	Failure load, lb	Failure stress, psi	Failure strain, in./in.	Modulus, psi	Corrected to 6 percent laminate moisture content	
													Failure stress ($K = 1.21$), psi	Modulus ($K = 1.05$), psi
4	2	7.5	132	3.07	6.69	0.0248	6.3	36.0	41 160	13 407	0.00503	2.66×10^6	13 485	2.68×10^6
	2		132	3.04	6.44	.0239	4.4		39 920	13 093	.00502	2.61	12 693	2.51
	8		528	12.08	26.5	.0245	7.2		145 800	12 067	.00437	2.76	12 350	2.83
	8		528	11.83	25.63	.0237	4.5		116 200	9 820	.00388	2.52	9 538	2.44
	2	15.0	402	3.00	12.75	.0236	6.2	120.0	35 960	11 971	.00465	2.57	12 017	2.58
5	2			3.03	12.5	.0231	4.5		27 560	9 093	.00365	2.49	8 832	2.40
	2			3.02	12.5	.0231	4.9		36 440	12 042	.00513	2.34	11 788	2.28
	[a]2			3.02	12.5	.0231	5.2		26 400	8 724	.0036	2.42	8 589	2.37
	[a]2			2.99	12.0	.0222	5.1		32 400	10 804	.00473	2.28	10 617	2.23
4	8		1608	12.04	51.25	.0237	6.1		139 600	11 589	.00465	2.49	11 611	2.49
5	8			12.1	51.0	.0236	4.4		119 000	9 835	.00378	2.60	9 534	2.50
	8			12.01	50.38	.0233	4.9		109 800	9 138	.00355	2.57	8 945	2.51
	[a]8			12.01	51.0	.0236	5.0		130 000	10 819	.00417	2.59	10 611	2.53
	[a]8			11.95	51.0	.0236	5.0		119 200	9 972	.00383	2.60	9 780	2.54
4	2	30.0	942	3.04	26.0	.0241	5.6		32 520	10 690	.00422	2.53	10 607	2.51
4				3.01	25.88	.0240	6.2		26 480	8 777	.00337	2.60	8 811	2.61
5				2.98	25.38	.0235	6.3		27 680	9 279	.00345	2.69	9 333	2.70
5				3.03	25.0	.0231	4.6		29 880	9 855	.00387	2.54	9 591	2.46
5	[a]2			3.03	25.0	.0231	5.1		29 200	9 637	.00383	2.51	9 470	2.46
4	8		3768	12.15	104.56	.0242	5.9		121 200	9 975	.00383	2.60	9 955	2.59
4				12.05	105.0	.0243	5.9		120 000	9 956	.00383	2.59	9 936	2.59
4				11.91	102.88	.0238	6.6		119 000	9 987	.00370	2.69	10 103	2.73
5				12.03	100.5	.0233	4.5		114 000	9 474	.00383	2.47	9 202	2.39
5	[a]8			11.99	101.5	.0235	4.6		116 200	9 687	.00393	2.46	9 427	2.38

[a]Scarf joints spaced 6 in. apart in adjacent laminations.

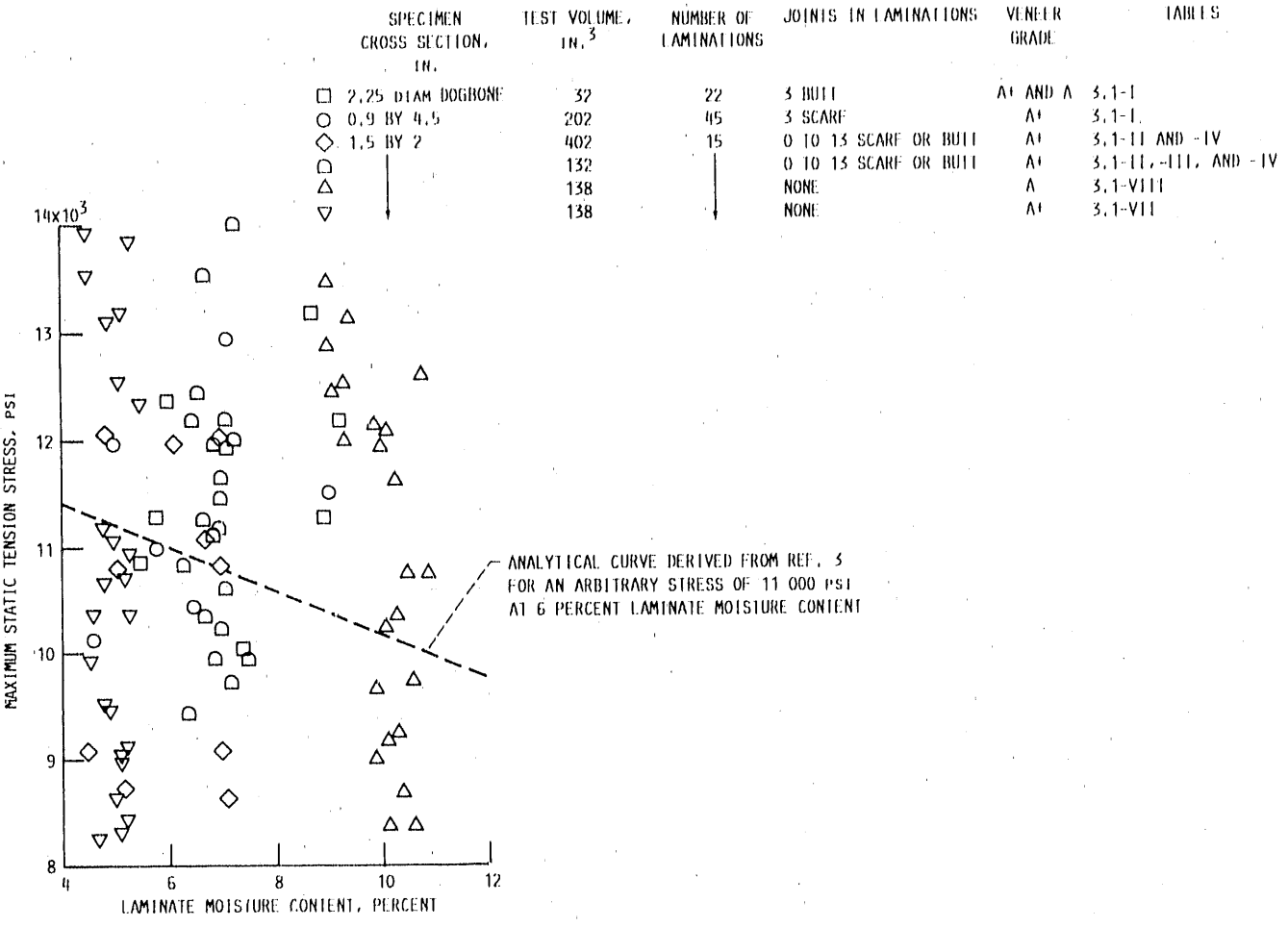

Figure 3.1-2.—Maximum static tension strength for laminated Douglas fir/epoxy specimens over a range of laminate moisture contents.

affects static tension strength is given in subsection 3.1.1.5. Subsections 3.2.1.2 and 3.2.2.1 also provide information on the effect of moisture content on Douglas fir/epoxy compressive strength.

3.1.1.2 Effect of laminate joint configuration on tension strength: Tables 3.1-II to 3.1-IV tabulate experimental data for Douglas fir/epoxy specimens containing butt or scarf joints in the laminates. The test specimens were cut from five different panels. These panels were approximately 60 ft long, 20 in. wide, and 1.5 in. thick. The panel numbers are listed in the tables. The test specimen configurations were similar to those shown in figures 2.2-1 to 2.2-3. All specimens contained 15 laminations. Specimen widths were 2 or 8 in. Overall lengths varied from 7.5 to 30 ft and the corresponding specimen test section volumes varied from 132 to 3768 $in.^3$. The veneer grade was A+ for all specimens. (See subsection 1.2.2 on veneer grade.) All tests were run with a 5-min load ramp to expected failure. All specimens failed in the gage length without any indication of significant involvement of the grips.

Table 3.1-V presents the mean values of tension strength and modulus of elasticity and their standard deviations σ for specimens cut from panels 4 and 5. The specimens had scarf joints in the laminations spaced at either 3 or 6 in. in adjacent laminations. The mean values were calculated from the data points listed in table 3.1-IV. The two joint spacings are compared for (1) same-size specimens, (2) same-width specimens (but varying length), and (3) same-length specimens (but varying width). Although the total number of specimens was small, only 13 cut from panel 5, there was no consistent trend in the effect that spacing between scarf joints had on mean tension strength. The table also shows mean strength for specimens with 3-in. spacing between scarf joints and cut from two different panels. In all cases the mean strengths were higher for specimens from both panels 4 and 5 than for specimens from panel 5 alone. This consistent trend showed panel 4 specimens to be stronger. It was therefore concluded that panel-to-panel variations, where the panels were manufactured by the same process and with the same grade of veneers, were greater than the scarf joint spacing variations.

All the data from tables 3.1-II, -III, and -IV are compiled in figure 3.1-3. Mean values of replicate tests and standard deviations σ for specimens with butt and scarf joints in the

TABLE 3.1-V.—EFFECT OF SCARF JOINT SPACING ON MEAN FAILURE STRESSES, MEAN MODULI OF ELASTICITY, AND STANDARD DEVIATIONS—PANELS 4 AND 5

[Two scarf joint spacings in adjacent laminations of Douglas fir/epoxy specimens. All specimens 1.5 in. thick with 15 laminations. Veneer grade, A-4. Data corrected to 6 percent laminate moisture content, and based on table 3.1-IV.]

Specimen size	Panel								
	5			5			4 and 5		
	Spacing between scarfs, in.								
	6			3			3		
	Number of specimens in group	Mean failure stress[a] ($K = 1.21$), psi	Mean modulus of elasticity[a] ($K = 1.05$), psi	Number of specimens in group	Mean failure stress[a] ($K = 1.21$), psi	Mean modulus of elasticity[a] ($K = 1.05$), psi	Number of specimens in group	Mean failure stress[a] ($K = 1.21$), psi	Mean modulus of elasticity[a] ($K = 1.05$), psi
All 2 in. by 7.5 ft	---	----- -----	----- -----	---	----- -----	----- -----	2	13 089 [396]	2.600×10^6 [0.083×10^6]
All 8 in. by 7.5 ft	---	----- -----	----- -----	---	----- -----	----- -----	2	10 944 [1406]	2.641 [.196]
All 2 in. by 15 ft	2	9 603 [1014]	2.309×10^6 [0.070×10^6]	2	10 310 [1478]	2.349×10^6 [0.060×10^6]	3	10 879 [1450]	2.428 [.122]
All 8 in. by 15 ft	2	10 196 [415]	2.541 [.005]	2	9 240 [.294]	2.510 [.000]	3	10 030 [1143]	2.506 [.005]
All 2 in. by 30 ft	1	9 470 [-----]	2.465 [-----]	2	9 462 [129]	2.588 [.120]	4	9 586 [653]	2.575 [.094]
All 8 in. by 30 ft	1	9 427 [-----]	2.388 [-----]	1	9 202 [-----]	2.391 [-----]	4	9 799 [351]	2.580 [.123]
All 2 in. wide	3	9 558 [830]	2.361 [.094]	4	9 886 [1132]	2.468 [.153]	9	10 795 [1658]	2.531 [.126]
All 8 in. wide	3	9 939 [496]	2.490 [.072]	3	9 227 [241]	2.470 [.056]	9	10 130 [1063]	2.568 [.134]
All 7.5 ft long	---	----- -----	----- -----	---	----- -----	----- -----	4	12 017 [1489]	2.620 [.152]
All 15 ft long	4	9 899 [830]	2.425 [.126]	4	9 775 [1193]	2.429 [.091]	6	10 455 [1373]	2.467 [.095]
All 30 ft long	2	[9 449] [22]	2.437 [.038]	3	9 375 [161]	2.522 [.135]	8	[9 692] [535]	2.577 [.109]
All specimens	6	9 749 [710]	[2.425] [.105]	7	9 604 [929]	2.469 [.121]	18	10 463 [1431]	2.550 [.131]

[a]Numbers in brackets are the standard deviations of the mean stresses and moduli listed above.

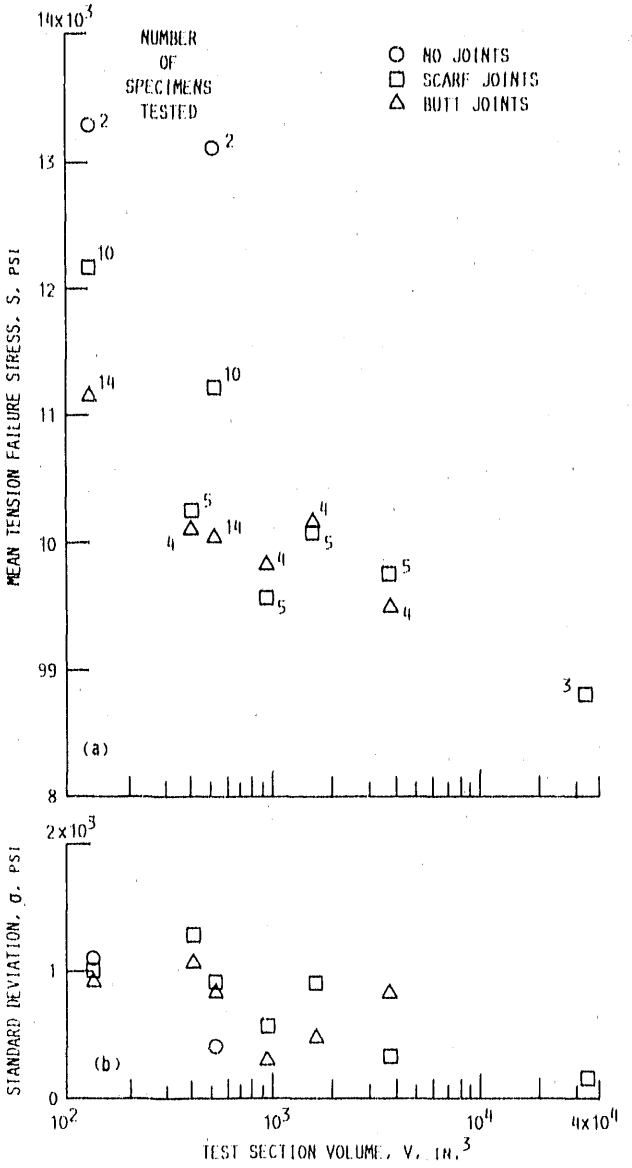

(a) Mean failure stresses.
(b) Standard deviations.

Figure 3.1-3.—Compilation of mean values of static tension failure stresses (parallel to grain) in laminated Douglas fir/epoxy specimens for a range of test section volumes. Data corrected to 6 percent laminate moisture content ($K = 1.21$). Veneer grade, A+.

laminations are shown, as well as limited data for specimens without joints in the laminations. As might have been expected, the mean strength values were consistently higher for specimens without joints than for specimens with either butt or scarf joints. In most, but not all, cases scarf-jointed specimens were stronger than butt-jointed specimens. As the specimen size increased, the effect of joint configuration generally decreased, indicating that with the larger volume there was a greater probability of other defects being present that could affect overall strength. In addition, the data scatter decreased with increasing test section volume as shown by the somewhat smaller standard deviations at larger volumes.

Table 3.1-VI contains the mean values of all data from tables 3.1-II, -III, and -IV for scarf and butt joints with 3-in. spacing of the joints in adjacent laminations. These data are compared in a manner similar to that for table 3.1-V for (1) specimens of the same configuration, (2) specimens having the same length but different widths, (3) specimens having the same width but different lengths, and (4) specimens from different panels. With only two exceptions in the entire table, the scarf-jointed specimens were shown to be stronger than the butt-jointed specimens, and in these two cases the difference in strength was small. These same two exceptions are also shown in figure 3.1-3 for test section volumes of 942 and 1608 in.^{3}.

3.1.1.3 Effect of specimen size on tension strength: The data in tables 3.1-II to 3.1-IV cover a range of tension specimen volumes from 132 to 3768 in.^{3}. Limited tests were also conducted on a specimen shown in figure 2.2-4 that required loads in excess of 1 million lb to fail. The specimen had a test section volume of 32 832 in.^{3} and had scarf joints in the laminations. The following data points were obtained for three specimens:

Failure stress, psi	Failure stress, corrected to 6 percent laminate moisture content, psi
8542	8575
8778	8811
8986	9021

The mean values of these data are also plotted in figure 3.1-3.

Several approaches were use in attempts to find an extrapolation method for the data from tables 3.1-II to 3.1-IV that would predict the failure stress for the 32 832-in.^{3} specimens. Reference 8 used a Weibull statistical strength theory to correlate bending strength data for wood members over a range of sizes. The approach used for the variable stress distribution across the depth of a bending member is not applicable to specimens in pure tension.

Figure 3.1-4 illustrates two approaches investigated that were based on regression lines of log-log plots of strength versus volume. By using data illustrated in figure 3.1-3 and including the scatterband of the data, regression lines can be calculated for (1) the means of all the data at each volume, and (2) the minimums of the scatterbands (excluding data at a volume of 132 in.^{3}). Both types of regression lines showed a reasonable and conservative extrapolation of data obtained in the volume range 132 to 3768 in.^{3} to large-volume (32 832 in.^{3}) specimens. A disadvantage of using straight-line regression curves for extrapolation to very large volumes is the unrealistic conclusion that the strength would approach zero. Other approaches that were investigated included the following:

TABLE 3.1–VI.—EFFECTS OF BUTT AND SCARF JOINTS ON MEAN FAILURE STRESSES, MEAN MODULI OF ELASTICITY, AND STANDARD DEVIATIONS—VARIOUS PANELS

[Laminated Douglas fir/epoxy specimens 1.5 in. thick with 15 laminations containing scarf or butt laminate joints spaced 3 in. apart in adjacent laminations. Veneer grade, A+. Data corrected to 6 percent laminate moisture content and based on tables 3.1–II, III, and IV.]

Specimen size	Panel								
	3			3			1, 2, and 3		
	Type of joint								
	Butt			Scarf			Butt		
	Number of specimens in group	Mean failure stress[a] ($K = 1.21$), psi	Mean modulus of elasticity[a] ($K = 1.05$), psi	Number of specimens in group	Mean failure stress[a] ($K = 1.21$), psi	Mean modulus of elasticity[a] ($K = 1.05$), psi	Number of specimens in group	Mean failure stress[a] ($K = 1.21$), psi	Mean modulus of elasticity[a] ($K = 1.05$), psi
All 2 in by 7.5 ft	8	11 060 [1003]	2.713×10^6 [0.083×10^6]	8	11 914 [952]	2.654×10^6 [0.087×10^6]	14	11 143 [943]	2.712×10^6 [0.072×10^6]
All 8 in. by 7.5 ft	4	9 734 [514]	2.589 [.116]	4	10 933 [460]	2.544 [.111]	10	9 868 [899]	2.643 [.114]
All 2 in. by 15 ft	---	---	---	---	---	---	---	---	---
All 8 in. by 15 ft	---	---	---	---	---	---	---	---	---
All 2 in. by 30 ft	---	---	---	---	---	---	---	---	---
All 8 in. by 30 ft.	---	---	---	---	---	---	---	---	---
All 2 in. wide	8	11 060 [1003]	2.713 [.083]	8	11 914 [952]	2.654 [.087]	22	10 715 [1056]	2.657 [.128]
All 8 in. wide	4	9 734 [514]	2.589 [.116]	4	10 933 [460]	2.544 [.111]	10	9 868 [899]	2.643 [.114]
All 7.5 ft long	12	10 618 [1072]	2.672 [.112]	12	11 587 [942]	2.618 [.109]	24	10 612 [1119]	2.684 [.098]
All 15 ft long	---	---	---	---	---	---	---	---	---
All 30 ft long	---	---	---	---	---	---	---	---	---
All specimens	12	10 618 [1072]	2.672 [.112]	12	11 587 [942]	2.618 [.109]	24	10 612 [1119]	2.684 [.098]

[a]Mean values for a group of specimens may appear in more than one location in the table. Numbers in brackets are the standard deviations of the mean stresses and moduli listed above.

TABLE 3.I VI.– Concluded.

Specimen size	Panel								
	3, 4, and 5			1 and 2			4 and 5		
	Type of joint								
	Scarf			Butt			Scarf		
	Number of specimens in group	Mean failure stress[a] ($K = 1.21$), psi	Mean modulus of elasticity[a] ($K = 1.05$), psi	Number of specimens in group	Mean failure stress[a] ($K = 1.21$), psi	Mean modulus of elasticity[a] ($K = 1.05$), psi	Number of specimens in group	Mean failure stress[a] ($K = 1.21$), psi	Mean modulus of elasticity[a] ($K = 1.05$), psi
All 2 in. by 7.5 ft	10	12 150 [989]	2.643×10^6 [0.098×10^6]	6	11 255 [845]	2.712×10^6 [0.054×10^6]	2	13 089 [0.396]	2.600×10^6 [0.083×10^6]
All 8 in. by 7.5 ft	6	10 936 [894]	2.576 [.152]	6	9 958 [1073]	2.679 [.097]	2	10 944 [1406]	2.641 [.196]
All 2 in by 15 ft	...	...	...	4	10 089 [1063]	2.575 [.114]	3	10 879 [1450]	2.428 [.122]
All 8 in. by 15 ft	...	...	...		10 145 [476]	2.538 [.112]	3	10 030 [1143]	2.506 [.005]
All 2 in. by 30 ft	...	...	...		9 842 [307]	2.543 [.171]	4	9 586 [.653]	2.575 [.094]
All 8 in. by 30 ft	...	...	...		9 497 [828]	2.536 [.110]	4	9 799 [.351]	2.580 [.123]
All 2 in. wide	10	12 150 [989]	2.643 [.089]	14	10 518 [1035]	2.625 [.139]	9	10 795 [1658]	2.531 [.126]
All 8 in. wide	6	10 936 [894]	2.576 [.152]	14	9 880 [905]	2.598 [.127]	9	10 130 [1063]	2.586 [.134]
All 7.5 ft long	16	11 695 [1121]	2.618 [.121]	12	10 606 [1163]	2.696 [.080]	4	12 107 [1489]	2.620 [.152]
All 15 ft long	...	...	...	8	10 117 [824]	2.557 [.114]	6	10 455 [1373]	2.467 [.095]
All 30 ft long	...	...	...	8	9 670 [648]	2.539 [.144]	8	9 692 [.535]	2.577 [.109]
All specimens	16	11 695 [1121]	2.618 [.121]	28	10 199 [1023]	2.611 [.133]	18	10 463 [1431]	2.550 [.131]

[a]Mean values for a group of specimens may appear in more than one location in the table. Numbers in brackets are the standard deviations of the mean stresses and moduli listed above.

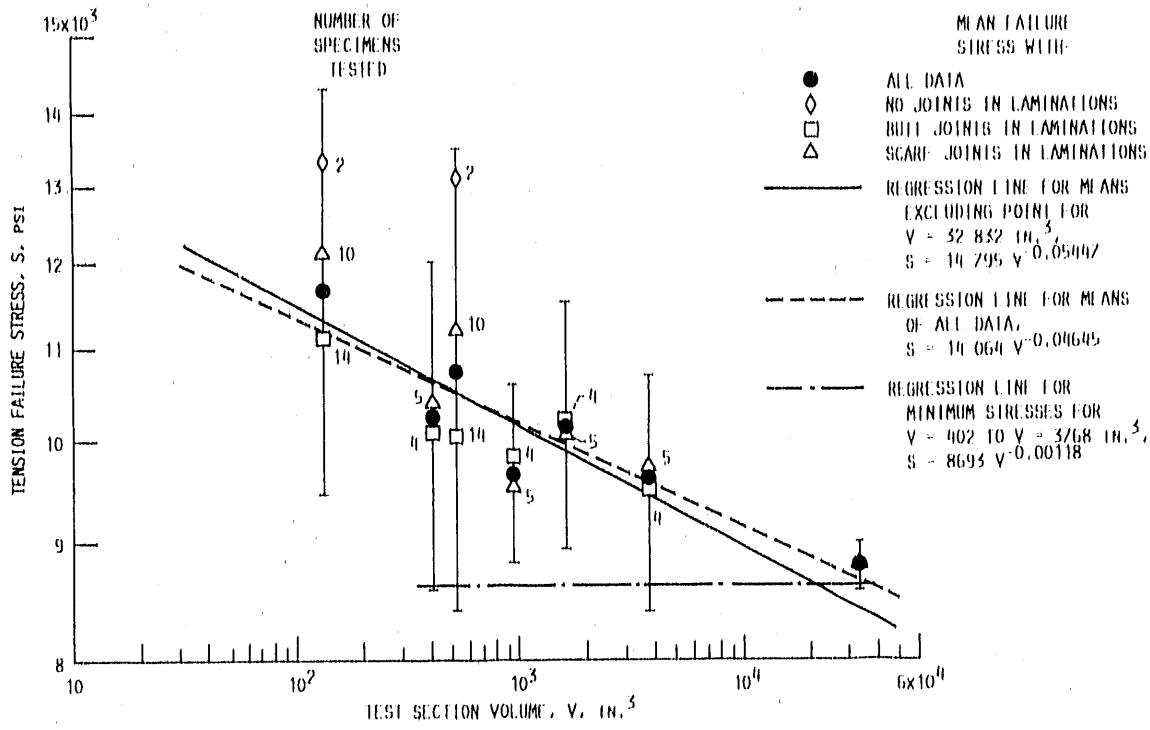

Figure 3.1-4.—Effect of specimen size on static tension failure stress (parallel to grain) for laminated Douglas fir/epoxy specimens. Data corrected to 6 percent laminate moisture content ($K = 1.21$). Veneer grade, A+.

(1) Ordering the replicate data at each volume and summing the volumes in the following manner: The highest strength point was plotted at the volume corresponding to the test section volume, the second highest point at two times that volume, the third highest at three times that volume, and so on until the weakest point was plotted at N times the test section volume, where N is the number of tests at that particular volume. Regression lines for the N-times-volume points were calculated. The scatter was large and extrapolation was doubtful.

(2) A double logarithm of strength was plotted versus the log of volume with no improvement in extrapolation relative to that shown in figure 3.1-4.

(3) A semi-log plot was less satisfactory than the log-log plot of figure 3.1-4.

The most reasonable model for determining the strength that can be expected for volumes larger than test specimen volumes was developed in chapter III and shown in figures 3 and 4 of chapter III for scarf and butt joints, respectively, in the laminations. The pertinent parts of figure 3 from chapter III are reproduced herein as figure 3.1-5. As discussed in chapter III, the significance of the horizontal line represented by $S - 2.837\sigma$ is that it is the asymptotic value of strength (8150 psi in fig. 3.1-5) at large volumes. According to statistics tables for a normal distribution of data, 99.5 percent of all data points will fall at strength values higher than this asymptotic value. It would seem therefore that $S - 2.837\sigma$ represents a conservative approach to predicting the strength of large structures.

Tables 3.1-II to 3.1-IV also show modulus of elasticity values that were measured while investigating the effect of specimen volume on strength. Figure 3.1-6 is a plot of maximum static tension stress versus modulus of elasticity that was made to determine if there is a relation between strength and modulus. In grading the veneers the higher grades were given to the veneers with the generally higher moduli. One might therefore expect higher strength to correlate with higher modulus. Figure 3.1-6 contains too much scatter to develop a correlation, but observation of the data points shows that for a specimen volumes of 132, 402, and 942 in.^{3} there is a rough trend of lower failure stress with higher modulus, which is opposite to what might be expected. This trend was confirmed by least-squares fit of straight lines (not shown in the figure) that showed a negative slope for points for each volume. For the largest specimens shown on the plot, 3768 in.^{3}, no variation of failure stress with modulus was observable.

Note, however, that as the result of ultrasonic testing of the veneers prior to fabrication, the choice of veneers was highly selective. The modulus-of-elasticity range and the relation between measured modulus of elasticity and strength may not be representative where there is less selectivity in choosing the veneers. This factor, as well as the large scatter in the data, makes it questionable to draw conclusions on the relation between tension strength and modulus of elasticty from the data presented.

3.1.1.4 Effect of veneer grade on tension strength: A series of static tension tests were conducted on laminated Douglas

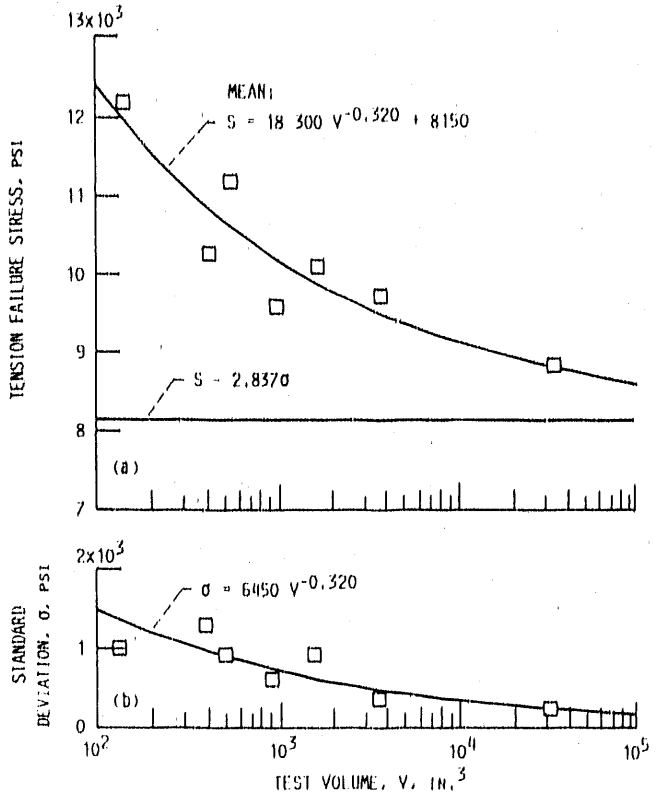

(a) Strength model.
(b) Standard deviation model.

Figure 3.1-5.—Strength and standard deviation models for static tension in laminated Douglas fir/epoxy specimens with scarf joints in laminations. Data corrected to 6 percent laminate moisture content ($K = 1.21$). Veneer grade, A+.

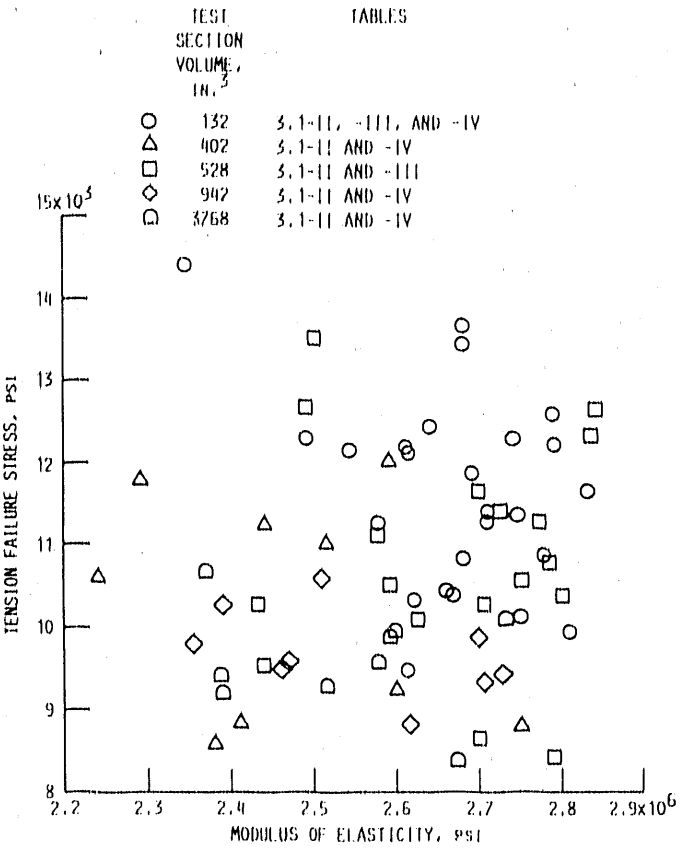

Figure 3.1-6.—Effect of modulus of elasticity on static tension strength of laminated Douglas fir/epoxy specimens with butt and scarf joints in laminations. Data corrected to 6 percent laminate moisture content.

fir/epoxy specimens of the configuration shown in figure 2.2-1, 1.5 in. thick containing 15 laminations, 2 in. wide, and 92 in. long. Six groups of specimens were tested with 25 specimens in each group. The specimens were of three veneer grades: A+, A, and C. Veneer grades are defined in the tables in subsection 1.2.2. For each veneer grade tests were conducted on specimens without joints in the laminations and on specimens with butt joints in each lamination spaced 3 in. apart in adjacent laminations. These joints were transverse to the direction of force on the specimens. The results of these tests are presented in table 3.1-VII. Table 3.1-VIII presents similar results for veneer grade A with no joints but with a higher specimen moisture content and also tested at a higher temperature and humidity. For all tables failure stresses are presented as tested and as corrected to a standard laminate moisture content of 6 percent for $K = 1.21$. Mean failure stresses, minimum failure stresses, and standard deviations σ for all of these tests are summarized in table 3.1-IX.

The following conclusions can be drawn from table 3.1-IX:

(1) The standard deviations σ for all specimens except those having a high laminate moisture content were higher for the better veneer grades but not necessarily higher for higher mean corrected stresses. An explanation of this behavior would be only speculation.

(2) Generally for a given veneer grade the minimum corrected failure stress in each group of specimens was somewhat higher than the mean minus 2σ. The only exception was for veneer grade C specimens with no joints in the laminations. For a normal distribution there is a 95 percent probability that observations of any group will lie within 2σ of the sample mean and a 99.8 percent probability that all observations will lie within 3σ of the mean.

(3) Generally the mean, minimum, or mean minus 2σ or 3σ corrected failure stresses were lower for specimens containing butt joints in the laminations than for specimens without joints. Such behavior would be expected. For these tests there was an exception, however; the specimens of veneer grade A+ showed higher failure stresses for butt-jointed laminations than for specimens without joints. The investigator in these tests suggests that this anomaly may have arisen from stress risers resulting from small changes in grain angle in some of the laminations of the A+ specimens without joints. Tension strength parallel to the grain is 30 to 40 times that perpendicular to the grain so that small variations can result in significant strength differences.

(4) Although there was a trend of reduced strength for lower veneer grades when comparing either specimens without joints or specimens with butt joints in the laminations, there were

TABLE 3.1-VII.—EFFECTS OF VENEER GRADE AND JOINT TYPE ON STATIC TENSION STRENGTH PARALLEL TO GRAIN

[Laminated Douglas fir/epoxy specimens 1.5 in. thick with 15 laminations, 2 in. wide, and 92 in. long. Test temperature, 71 °F. Data corrected to 6 percent laminate moisture content ($K = 1.21$).]

(a) Veneer grade, A+; no joints in laminations

Stress area, $in.^2$	Laminate moisture content, percent	Failure load, lb	Failure stress, psi	Corrected failure stress, psi
3.02	4.7	24 900	8 245	8 040
3.03	4.9	28 720	9 479	9 279
3.02	4.5	29 960	9 921	9 637
3.02	4.8	28 700	9 503	9 285
3.02	5.1	27 040	8 954	8 799
2.98	4.5	40 300	13 523	13 136
3.08	5.1	27 770	8 994	8 839
3.03	5.2	27 770	9 142	9 001
3.07	5.1	27 770	9 023	8 867
3.02	5.0	33 500	11 093	10 880
3.07	5.2	25 860	8 423	8 293
3.02	5.1	39 860	13 199	12 971
3.01	5.2	32 220	10 704	10 539
3.02	4.9	39 600	13 113	12 836
2.96	5.3	41 040	13 865	13 678
3.01	4.5	41 960	13 940	13 541
3.03	5.5	37 400	12 343	12 224
3.03	5.3	33 140	10 937	10 790
3.00	5.0	25 920	8 640	8 474
2.91	4.8	31 050	10 674	10 429
3.01	5.3	31 180	10 359	10 219
3.04	4.8	34 020	11 191	10 934
3.05	5.1	38 280	12 551	12 334
3.02	5.1	25 080	8 305	8 161
3.05	4.6	31 680	10 387	10 109
		Mean	10 660	10 452
		Standard deviation, σ	1862	1784

(b) Veneer grade, A+; butt joints spaced 3 in. apart in adjacent laminations

3.00	4.5	38 520	12 840	12 472
3.02	4.7	37 520	12 424	12 115
3.04	5.2	40 080	13 184	12 981
3.06	5.3	36 060	11 784	11 625
3.05	4.8	40 020	13 121	12 819
3.03	5.0	41 560	13 716	13 453
3.07	4.9	39 960	13 016	12 742
3.01	5.2	36 520	12 133	11 946
3.03	5.1	43 000	14 194	13 949
3.03	5.0	42 860	14 145	13 874
3.02	4.9	41 420	13 715	13 426
3.04	5.4	27 360	9 000	8 896
3.05	5.2	25 760	8 446	8 316
3.01	4.8	29 500	9 801	9 576
3.01	4.5	25 640	8 518	8 274
2.94	5.3	27 120	9 224	9 100
2.95	5.0	27 560	9 342	9 163
2.97	4.9	29 420	9 906	9 697
2.98	4.6	29 060	9 752	9 491
2.92	4.8	28 580	9 788	9 563
2.95	4.9	28 500	9 661	9 457
2.96	5.2	30 440	10 284	10 126
2.94	4.9	31 120	10 585	10 362
2.98	5.0	33 380	11 201	10 986
3.00	5.1	29 380	9 793	9 624
		Mean	11 183	10 961
		Standard deviation, σ	1903	1826

(c) Veneer grade, A; no joints in laminations

Stress area, $in.^2$	Laminate moisture content, percent	Failure load, lb	Failure stress, psi	Corrected failure stress, psi
3.13	4.7	39 700	12 684	12 368
3.18	4.6	38 060	11 969	11 649
3.11	4.2	38 220	12 289	11 868
3.04	4.3	35 680	11 737	11 357
3.02	4.8	35 240	11 669	11 401
3.05	4.9	33 600	11 016	10 784
3.03	5.0	30 740	10 145	9 950
3.05	4.6	31 180	10 223	9 949
3.04	4.4	28 300	9 309	9 025
3.01	4.5	34 380	11 422	11 095
3.12	4.9	28 540	9 147	8 954
3.12	4.4	33 160	10 628	10 304
3.14	4.9	28 480	9 070	8 879
3.07	5.5	30 180	9 831	9 736
3.04	4.7	33 140	10 901	10 630
3.03	↓	35 120	11 591	11 303
3.02	↓	33 100	10 960	10 687
2.99	↓	31 320	10 475	10 214
2.99	4.9	37 100	12 408	12 146
2.96	5.2	35 460	11 980	11 796
3.02	4.8	32 000	10 596	10 352
3.10	4.9	34 620	11 168	10 932
3.06	5.1	31 200	10 196	10 020
3.03	5.2	36 760	12 132	11 945
3.01	6.0	37 100	12 326	12 326
		Mean	11 035	10 787
		Standard deviation, σ	1058	1021

(d) Veneer grade, A; butt joints spaced 3 in. apart in adjacent laminations

3.05	5.1	27 760	9 102	8 945
3.04	5.3	30 340	9 980	9 846
3.04	5.3	31 140	10 243	10 105
3.03	5.4	27 820	9 182	9 076
3.02	5.1	30 080	9 960	9 788
2.99	5.6	29 880	9 993	9 916
3.02	5.5	32 920	10 901	10 796
3.00	5.8	30 100	10 033	9 994
3.06	5.6	33 300	10 882	10 798
3.06	5.6	30 900	10 098	10 020
3.09	5.6	34 720	11 236	11 149
3.07	5.4	26 420	8 606	8 507
3.03	5.5	28 220	9 314	9 224
3.08	5.6	31 580	10 253	10 174
3.07	4.5	23 880	7 779	7 556
3.03	4.4	26 920	8 884	8 613
3.02	4.6	25 220	8 351	8 127
3.01	4.8	23 100	7 674	7 498
2.97	5.1	25 560	8 606	8 457
3.15	4.6	28 060	8 908	8 670
3.12	4.5	24 600	7 885	7 659
3.10	4.7	25 140	8 110	7 908
3.12	4.8	28 260	9 058	8 850
3.07	5.5	27 700	9 023	8 936
3.06	5.1	29 080	9 503	9 339
		Mean	9343	9198
		Standard deviation, σ	998	1020

TABLE 3.1-VII.—Concluded.

[Laminated Douglas fir/epoxy specimens 1.5 in. thick with 15 laminations, 2 in. wide, and 92 in. long. Test temperature, 71 °F. Data corrected to 6 percent laminate moisture content ($K = 1.21$).]

(e) Veneer grade, C; no joints in laminations

Stress area, $in.^2$	Laminate moisture content, percent	Failure load, lb	Failure stress, psi	Corrected failure stress, psi
3.04	6.0	28 920	9 513	9 513
3.04	5.9	28 920	9 513	9 495
3.03	5.9	27 540	9 089	9 071
3.08	6.0	29 460	9 565	9 565
3.05	6.1	31 580	10 354	10 374
3.09	6.2	32 160	10 510	10 551
3.06	3.8	24 560	8 026	7 691
3.07	3.2	31 920	10 397	9 848
3.09	2.7	29 680	9 605	9 010
3.09	2.5	30 400	9 838	9 193
3.07	2.8	33 640	10 958	10 299
3.06	2.9	29 420	9 614	9 053
3.01	3.6	29 140	9 681	9 241
2.94	3.8	31 700	10 782	10 332
2.95	3.5	32 940	11 166	10 638
2.94	2.7	31 100	10 578	9 923
2.92	2.5	31 080	10 644	9 946
3.00	2.2	34 400	11 467	10 653
2.98	2.4	35 260	11 832	11 035
2.95	3.8	33 400	11 322	10 849
2.93	3.4	27 360	9 338	8 879
2.96	3.0	32 100	10 845	10 232
2.94	3.1	27 440	9 333	8 823
2.98	3.4	27 320	9 168	8 718
2.97	3.7	27 120	9 131	8 733
		Mean	10 091	9667
		Standard deviation, σ	915	811

(f) Veneer grade, C; butt joints spaced 3 in. apart in adjacent laminations

Stress area, $in.^2$	Laminate moisture content, percent	Failure load, lb	Failure stress, psi	Corrected failure stress, psi
3.07	3.5	24 720	8 052	7 671
3.08	2.9	30 460	9 890	9 313
3.05	4.0	27 300	8 951	8 611
3.07	3.2	23 520	7 661	7 256
3.07	3.0	22 880	7 453	7 032
3.02	4.6	22 720	7 523	7 322
3.00	2.7	26 860	8 953	8 398
3.11	2.9	22 980	7 389	6 958
3.11	2.7	27 060	8 701	8 162
3.08	2.7	22 340	7 253	6 804
3.06	2.6	22 080	7 216	6 756
2.96	4.8	28 760	9 716	9 493
2.99	4.0	25 200	8 428	8 108
2.97	3.4	28 120	9 468	9 003
2.99	2.7	27 620	9 237	8 665
2.99	2.6	27 320	9 137	8 554
2.97	3.0	22 060	7 428	7 008
2.90	4.7	26 080	8 993	8 769
2.95	3.6	26 600	9 017	8 607
2.96	3.5	24 000	8 108	7 725
2.97	3.2	26 120	8 795	8 330
2.98	2.6	25 480	8 671	8 118
2.99	2.6	23 740	7 940	7 434
3.02	2.9	21 640	7 166	6 748
2.98	2.8	26 920	9 034	8 491
		Mean	8407	7973
		Standard deviation, σ	847	816

again exceptions. The effect of small variations in grain angle as described previously may be the explanation.

(5) The failure stress differences between veneer grades A+ and A did not appear to be significant, particularly when comparing minimum corrected failure stresses or mean corrected failure stresses minus 2σ or 3σ. As a result the more stringent specifications for A+ veneers may not be warranted.

(6) *t*-Tests were conducted on all of the groups of specimens listed in table 3.1-IX to determine if they came from the same population as the veneer grade A+ specimens without joints. These tests revealed that at the 95 percent confidence level all of the groups of specimens except the butt-jointed specimens of veneer grades A and C were from the same populations as the A+ specimens without joints. Therefore veneer grade level probably did not significantly affect strength, and butt joints in veneer grade A+ specimens are not a significant factor.

3.1.1.5 Effect of temperature on tension strength: Information presented in reference 3 shows the mechanical properties of wood to be inversely proportional to temperature in an approximately linear relation below 400 °F. As wood moisture content increases, the effect is more pronounced. For example, reference 3 shows that reducing test temperature from room temperature to −20 °F increases strength about 12 percent at zero wood moisture content and about double that amount at 12 percent wood moisture content.

The data available from reference 1 relating to temperature are extremely sparse, incomplete, and inconclusive. Tests were conducted at −20 °F on three tension specimens of the configuration shown in figure 2.2-1 for laminated Douglas fir/epoxy with the following results:

Specimen	Failure stress, psi	Modulus of elasticity, psi
1	10 600	2 270 000
2	8 800	2 566 000
3	8 440	2 461 000
Mean	9 280	2 432 000

TABLE 3.1-VIII.—STATIC TENSION STRENGTH PARALLEL TO GRAIN AT HIGH MOISTURE CONTENT

[Laminated Douglas fir/epoxy specimens 1.5 in. thick with 15 laminations, 2 in. wide, and 92 in. long. No joints in laminations; veneer grade, A; test temperature, 90 °F at 90 percent relative humidity. Data corrected to 6 percent laminate moisture content (K = 1.21).]

Stress area, in.^{2}	Laminate moisture content, percent	Failure load, lb	Failure stress, psi	Corrected failure stress, psi
3.14	9.3	37 540	11 955	12 745
3.11	9.0	41 940	13 486	14 293
3.15	9.0	40 620	12 895	13 667
3.05	9.4	40 040	13 128	14 022
3.07	9.1	38 240	12 456	13 227
3.02	9.3	37 860	12 536	13 364
3.07	10.5	33 080	10 775	11 757
3.07	10.6	25 700	8 371	9 152
3.08	9.6	22 620	7 344	7 875
3.06	10.1	25 560	8 353	9 044
3.00	9.9	27 000	9 000	9 707
3.03	10.0	36 140	11 927	12 888
3.05	9.9	37 040	12 144	13 098
3.04	9.9	29 380	9 664	10 423
3.07	10.3	28 340	9 231	10 033
3.05	10.6	29 620	9 711	10 617
3.05	10.4	26 400	8 656	9 427
3.03	10.5	23 020	7 597	8 289
3.08	10.9	33 100	10 747	11 818
3.06	10.1	37 020	12 098	13 099
3.08	10.1	31 520	10 234	11 080
3.09	10.1	28 340	9 172	9 931
3.08	10.3	31 980	10 383	11 285
3.08	10.3	35 980	11 644	12 656
3.12	10.8	39 300	12 596	13 824
		Mean	10 644	11 493
		Standard deviation, σ	1851	1898

Information is lacking on laminate moisture content and whether laminate joints were present.

Comparing these low-temperature test results to room-temperature tests presented in table 3.1-VI for 2-in. by 7.5-ft specimens with scarf or butt joints in the laminations shows the low-temperature test data to have significantly lower tension strength and modulus of elasticity. The mean low-temperature values fall at approximately the lower boundary of the 1-σ and 2-σ bands of the room-temperature data for modulus of elasticity and tension strength, respectively. The trend is opposite to that shown in reference 3. Because of the limited number of specimens tested, these results are questionable. Until more reliable data are obtained, it seems prudent to use the trends of reference 3 to determine the estimated effect of temperature on mechanical properties of laminated-wood products. Subsection 3.2.1.1 shows a temperature effect more consistent with reference 3 for Douglas fir/epoxy in compression.

Some inference on the combined effect of moisture content and test temperature can be obtained from the data in tables 3.1-VII(c) and 3.1-VIII. These two tables are for Douglas fir/epoxy specimens with no joints in the laminations. One set of data was run at an average laminate moisture content of a little less than 5 percent and a test temperature of 71 °F, and the other set at a moisture content of approximately 10 percent and a test temperature of 90 °F. The lower-temperature, lower-moisture-content tests showed a mean uncorrected failure stress approximately 3.5 percent higher than that for the higher-temperature, higher-moisture-content tests. Reference 3 indicates that, on the basis of temperature effect alone, there should be approximately a 5 percent strength difference. Reference 3 also indicates that the correction for moisture content would be much higher than the temperature correction. If the mean failure stresses corrected to 6 percent laminate moisture content (K = 1.21) from tables 3.1-VII(c) and 3.1-VIII are compared, it is obvious that the data presented are opposite to the trend expected from reference 3. The

TABLE 3.1-IX.—SUMMARY OF STATIC TENSION STRENGTHS FROM TABLES 3.1-VII AND 3.1-VIII

Veneer grade	Joints in laminations	Mean corrected failure stress, psi	Standard deviation, σ, psi	Minimum corrected failure stress, psi	Mean corrected failure stress minus 2 σ, psi	Mean corrected failure stress minus 3 σ, psi
A +	None	10 452	1784	8040	688[a]	5100
A +	Butt	10 961	1826	8316	7309	5483
A	None	10 787	1021	8879	8745	7724
A	Butt	9 198	1020	7498	7158	6138
A	None	[a]11 493	[a]1898	[a]7875	[a]7697	[a]5799
C	None	9 667	811	7691	8045	7234
C	Butt	7 973	816	6748	6341	5525

[a]Specimens tested at approximately 10 percent laminate moisture content

corrected mean failure stress in table 3.1–VIII should be about 5 percent lower than the corrected mean failure stress in table 3.1–VII(c) if the data were consistent with the reference 3 corrections for both temperature and moisture content. Instead table 3.1–VIII shows a corrected mean failure stress 6.5 percent higher than that of table 3.1–VII(c)—a trend in the wrong direction. Another factor to consider, however, is the greater uncertainty of the data for the higher moisture content, as indicated by the larger standard deviation σ of the data. The mean corrected failure stress minus 1σ for the two tables results in stresses that approach the correct stress ratio based upon reference 3 considering both temperature and moisture content corrections. There is not an obvious justification for comparing the mean minus 1σ stresses except to point out that the greater uncertainties in the mean value of failure stress for the higher moisture content do make it difficult to draw definitive conclusions on the effect of moisture content on failure stress for Douglas fir/epoxy laminates. It can be concluded therefore that there is neither sufficient quantity nor quality of data to provide definitive conclusions on how temperature or moisture content affects the strength of Douglas fir/epoxy laminates.

3.1.2 Perpendicular to grain.—Static tension tests were conducted perpendicular to the grain in both the radial and tangential directions on veneer grade A and in the radial direction on veneer grade C. Limited tests were also conducted in the tangential direction with glass fiber fabric augmentation between laminations.

Radial direction tests were performed on the specimen configuration shown in figure 2.2–5. Tangential direction tests without fiberglass reinforcement were performed on the specimen configuration shown in figure 2.2–6. Tangential direction tests with fiberglass reinforcement were done on a specimen similar to that shown in figure 2.2–6 except that the specimen was 50 in. long and 1.48 in. thick and composed of 13 laminations with 10-oz/yd^2 glass fiber fabric (Burlington Style 7500 or Burlington Style 7781) placed in the glue line between laminations. The fibers in the glass fabric were oriented at 45° to the wood grain direction.

3.1.2.1 Specimens without glass fiber fabric augmentation: Test data are shown in tables 3.1–X to 3.1–XII. Static tension data with loading perpendicular to the grain showed low strength and erratic results. With loading in the radial direction the weakest veneer determined the strength of the specimen. With loading in the tangential direction lathe cracks in the veneers resulting from the peeling operation may have reduced strength.

Comparing tables 3.1–X(a) and (b) shows a significant reduction in tension strength perpendicular to the grain in the radial direction as test temperature increased. The moisture content of the test specimens and the test environment relative humidity were also higher for the higher test temperature. Although all data were corrected to 6 percent laminate moisture content, the validity of this correction is highly uncertain, as previously discussed.

Comparing table 3.1–XI with table 3.1–X shows that using a higher grade veneer (grade A instead of grade C) more than doubled the tension strength perpendicular to the grain in the radial direction. The greater number of imperfections inherent in the lower grade significantly affected the strength in the direction perpendicular to the grain.

Large reductions in strength perpendicular to the grain (in both the tangential and radial directions) relative to the strength parallel to the grain can be seen by comparing the mean values in tables 3.1–X, 3.1–XI, and 3.1–XII with the values shown in table 3.1–IX. For grade C veneer the tension strength perpendicular to the grain (radial direction) was only 1/45 of the strength parallel to the grain. For grade A veneer the tension strength perpendicular to the grain (radial direction) was 1/22 of the strength parallel to the grain, and the tension strength perpendicular to the grain (tangential direction) was 1/40 of the strength parallel to the grain. These comparisons emphasize the care required in orienting load with grain direction and the need to eliminate cross-grain areas when selecting veneers for applications requiring high strength.

3.1.2.2 Specimens with glass fiber fabric augmentation: Tests were conducted in tension perpendicular to the grain in the tangential direction with both Burlington Style 7500 and Burlington Style 7781 glass fiber fabric augmentation on grade A Douglas fir veneers with epoxy glue. The following results were obtained:

Glass type	Failure load, lb	Failure stress, psi
7781	8 500	2872
7781	9 700	2939
7781	10 000	3378
Mean		3063
7500	9 000	3040

Failures in these specimens were significantly different from those in specimens without augmentation. Rather than failing in a localized area, the failure was spread over a large portion of each specimen.

The glass fiber fabric augmentation markedly increased the strength of the Douglas fir/epoxy laminates by a factor of approximately 11, as seen by comparing the values above with the mean value in table 3.1–II. Although the tests listed were limited, the type of glass fiber fabric used in the reinforcement had no significant effect.

3.1.3 Closing remarks on static tension strength.—Data from reference 1, and from unpublished preliminary reports that form the basis of reference 1, have been presented in this section. Some of the more significant conclusions that can be drawn from these data are as follows:

1. Although a significant number of laminated Douglas fir/epoxy tension specimens were tested in a variety of sizes, configurations, and moisture contents, the data contain too much scatter to conclude definitively whether the moisture-

TABLE 3.1-X.—STATIC TENSION STRENGTH PERPENDICULAR (RADIAL) TO GRAIN—VENEER GRADE C

[Laminated Douglas fir/epoxy specimens 1.5 in. thick with 15 laminations, 2 in. wide, and 2 in. long. No joints in veneers. Data corrected to 6 percent laminate moisture content ($K = 1.13$).]

(a) Test temperature, 71 °F

Stress area, in.^{2}	Laminate moisture content, percent	Failure load, lb	Failure stress, psi	Corrected failure stress, psi
3.93	4.7	329	84	83
3.98	4.5	952	239	235
3.93	4.4	1199	305	299
3.97	4.4	652	164	161
3.91	5.1	918	235	232
4.01	4.9	774	193	190
3.98	4.4	495	124	122
3.97	4.3	874	220	215
4.02	4.6	1002	249	245
3.97	4.7	1121	282	277
3.97	4.3	1303	328	321
3.98	5.3	725	182	180
4.06	4.8	971	239	235
4.02	4.6	740	184	181
3.99	4.7	614	154	152
3.98	4.0	658	165	161
4.02	4.6	1108	276	271
3.97	4.5	1425	359	352
4.00	4.5	648	162	159
3.97	4.3	686	173	169
3.95	4.0	233	59	58
3.94	4.2	1028	261	255
4.03	4.6	1344	333	327
4.00	4.2	1037	259	253
3.92	4.2	770	196	192
		Mean	217	213
		Standard deviation, σ	75	72

(b) Test temperature, 90 °F; relative humidity, 90 percent

Stress area, in.^{2}	Laminate moisture content, percent	Failure load, lb	Failure stress, psi	Corrected failure stress, psi
4.03	11.5	218	54	58
4.08	10.9	694	170	181
4.04	6.1	992	246	[a]246
4.09	10.7	662	162	172
4.01	6.7	472	118	[a]119
4.12	10.7	1006	244	259
4.07	9.7	456	112	117
4.05	10.9	336	83	88
4.07	11.0	366	90	96
4.01	7.8	784	196	[a]200
4.07	6.8	892	219	[a]221
4.10	11.2	590	144	154
4.15	10.7	588	142	151
4.06	10.1	478	118	124
4.09	6.3	373	91	[a]91
4.03	10.9	686	170	181
4.08	10.4	640	157	166
4.06	11.0	758	187	199
4.05	11.0	662	163	173
4.03	11.1	290	72	77
4.01	11.1	574	143	152
4.01	11.0	604	151	161
4.07	6.1	1196	294	[a]294
4.06	6.2	780	192	[a]192
4.01	10.5	738	184	195
		Mean	156	163
		Standard deviation, σ	58	57

[a]Failure stress of metal block/specimen glue line. The laminate strength is therefore greater. These stresses were included in mean and standard deviation.

content corrections presented for unlaminated-wood specimens in reference 3 are applicable to laminated-wood structures. For lack of a better approach, tension data in this report were corrected to a nominal value of 6 percent laminate moisture content by using the equations of reference 3 and $K = 1.21$.

2. Taking mean values of replicate tension tests of specimens with volumes varying between 132 to 32 832 in.^{3} and correcting the data for moisture content as previously described appeared to show a correlation of decreasing strength with increasing volume. Several models for predicting strength for volumes larger than the test specimen volumes were investigated. The most reasonable model, developed in chapter III, involved curve fitting mean values of experimental static strength for a range of specimen volumes to obtain a curve with an equation in the form

$$S = AV^{-B} + C \tag{16}$$

where

S mean failure stress

V volume

A,B,C empirical constants

In a similar manner the standard deviations σ for a range of specimen volumes were curve fit to obtain a curve with the equation in the form

$$\sigma = DV^{-B} \tag{17}$$

which has another empirical constant, D.

For the specimens investigated, letting the large-volume failure stress be equal to the constant C resulted in a predicted large-volume failure stress equal to $S - N\sigma$, where S is the curve-fit experimental failure stress and $N = 2.837$, which for a normal distribution would result in 99.5 percent of all data points having values larger than C.

TABLE 3.1-XI.—STATIC TENSION STRENGTH PERPENDICULAR (RADIAL) TO GRAIN—VENEER GRADE A

[Laminated Douglas fir/epoxy specimens 1.5 in. thick with 15 laminations, 2 in. wide, and 2 in. long. No joints in veneers. Test temperature, 77 °F. Data corrected to 6 percent laminate moisture content (K = 1.13).]

Stress area, in.^{2}	Laminate moisture content, percent	Failure load, lb	Failure stress, psi	Corrected failure stress, psi
4.04	5.2	1345	333	330
4.04	4.4	2203	545	534
4.00	4.7	1317	329	324
4.04	4.5	2417	598	587
4.02	4.8	1322	329	324
4.05	4.6	2265	559	549
4.05	4.2	2396	592	579
4.04	4.4	2035	504	494
4.02	4.6	1795	447	439
4.02	5.1	1465	364	360
4.04	4.6	1866	462	454
4.01	5.1	1873	467	462
4.02	4.2	2228	554	542
4.04	4.5	1615	400	393
4.05	4.3	2173	537	526
4.01	4.8	1727	431	425
4.04	4.3	2719	673	659
4.05	4.1	2402	593	579
4.03	4.5	2289	568	[a]558
4.00	4.9	2217	554	546
		Mean	492	483
		Standard deviation, σ	102	96

[a]Failure stress of metal block/specimen glue line. The laminate strength is therefore greater. These stresses were included in mean and standard deviation.

TABLE 3.1-XII.—STATIC TENSION STRENGTH PERPENDICULAR (TANGENTIAL) TO GRAIN—VENEER GRADE A

[Laminated Douglas fir/epoxy specimens 1.5 in. thick with 15 laminations, 2 in. wide, and 24 in. long. No joints in veneers. Test temperature, 77 °F. Data corrected to 6 percent laminate moisture content (K = 1.13).]

Stress area, in.^{2}	Laminate moisture content, percent	Failure load, lb	Failure stress, psi	Corrected failure stress, psi
3.10	5.7	920	297	296
3.10	5.6	740	239	238
3.11	6.0	920	296	296
3.04	5.2	940	303	300
3.05	5.2	780	256	253
3.06	4.9	800	261	257
3.03	5.3	700	231	229
3.07	5.2	940	306	303
3.08	5.1	680	221	219
3.05	5.0	960	315	311
3.06	4.8	1040	340	335
3.03	4.9	760	251	248
3.04	5.0	1280	421	416
↓	5.2	1160	382	378
↓	5.2	560	184	182
↓	5.1	840	276	273
3.03	4.9	740	244	241
3.04	4.7	580	191	188
3.05	5.0	720	236	233
3.05	4.7	620	203	200
		Mean	273	270
		Standard deviation, σ	69	59

3. Large laminated structures will require joints in the laminations both parallel and perpendicular to the applied load. Those lamination joints oriented perpendicular to the load will most affect the structural strength. Two configurations of these joints perpendicular to the load were investigated. Tests were made with adjacent laminations (in a longitudinal direction) (1) butted up to each other to form a squared-off butt joint (often with a gap between adjacent laminations) or (2) scarfed in length typically 12 times the lamination thickness to aid in transferring load between the two laminations. The scarf joints were staggered in adjacent laminations (in a thickness direction) by a distance of 3 or 6 in. One spacing had no significant advantage over the other, but the tension strength with load parallel to the grain was consistently, but marginally, higher for the scarf-jointed specimens than for the butt-jointed specimens on the basis of mean values of replicate tests. Data scatter, however, was much greater than the differences in mean strength for the two types of joints. It appears doubtful if the cost and complexity of providing scarf joints in the laminations is warranted for laminated Douglas fir/epoxy structures governed entirely by a static tension load.

4. A measure of the quality, and therefore strength, of a veneer can be inferred from its sonic transit time. Sonic transit time in a material is related to its modulus of elasticity. An ultrasonic grader was used for all veneers to grade grain quality. Grades of A+, A, and C were assigned on the basis of sonic transit times and visual grading of veneers. Defects in the veneers increased the transit time, as measured by the ultrasonic grader, and decreased the average modulus of elasticity. For tension testing with the load parallel to the grain specimens made of grade A+ or grade A veneers had only a negligible strength difference, but specimens made of grade C veneers were measureably weaker. With the load perpendicular to the grain the veneer grade effect was quite significant. Specimens made from grade A veneers had twice the strength of specimens made from grade C veneers.

5. In general, reduced specimen temperature, below about 400 °F, increased wood strength as determined from data in

the literature. Only limited data were available from tests at different temperatures for laminated Douglas fir/epoxy specimens. The data on the temperature effect for laminated specimens in static tension were inconclusive.

6. Grain orientation relative to load is important in wood. Tests on laminated Douglas fir/epoxy specimens showed the failure stress with load perpendicular to the grain to be from 1/22 to 1/40 of the failure stress with load parallel to the grain.

3.2 Static Compression Strength

3.2.1 Parallel to grain.—Compression strength tests were conducted on laminated Douglas fir/epoxy specimens shown in figure 2.2-7, and on cylinders 2.25 or 3 in. in diameter by 8 in. long. Tests were conducted on veneer grades A+, A, and C. Most tests were for a laminate moisture content of approximately 4 percent, but some tests involved specimens with laminate moisture contents ranging from 4 to 10 percent. In addition, in one series of tests all of the specimens contained about 10 percent moisture content. Tests were also conducted over a range of temperatures from 30 to 120 °F. The effects of scarf joints with a taper ratio of 12:1 and butt joints in the laminates were also investigated. The joints were spaced 3 in. apart in adjacent laminations. Load rate was 0.01 in./min and failure stress was based upon maximum crushing load.

3.2.1.1 Effect of temperature on compression strength: Data on the compression strength parallel to the grain of veneer grade A laminated Douglas fir/epoxy specimens are shown in tables 3.2-I(a), 3.2-I(c), and 3.2-II for test temperatures of 30, 69, and 120 °F. Tests were conducted on specimens with no joints in the laminations and on specimens having butt joints spaced 3 in. apart in adjacent laminations. Figure 3.2-1 is a summary plot of these data. Also shown in the figure are trend lines passing through the points at 69 °F. These trend lines are based on curve bands from figure 4-10 of reference 3 for clear wood specimens in compression parallel to the grain. The same trend is also applicable to clear wood specimens in tension parallel to the grain. Figure 3.2-1 shows a larger effect of temperature than indicated in reference 3. In each case (with or without butt joints in the laminations) the increase in the mean corrected failure stress predicted by reference 3 was only 60 percent of that found in the experimental data reported herein. The effect of temperature can be quite significant. For the two types of specimens shown in the figure the strength increased on the order of 350 psi per 10 deg F reduction in test temperature, which corresponds to approximately 4 percent strength increase per 10 deg F reduction in test temperature.

Keep in mind while evaluating the effect of temperature on compression strength that moisture content also affects strength and that variations in the moisture content of the test specimens can influence the temperature effect trends. The laminate moisture content of most of the specimens tested was in the range 3 to 4.5 percent. These data points were corrected to a 6 percent laminate moisture content in evaluating the temperature effects. The validity of this correction is open to doubt as previously discussed, but since the test specimens were grouped within a fairly narrow moisture content range, it is not thought that moisture content significantly affected the trends of strength reduction with temperature increase.

The effect of butt joints in the compression specimen laminations reduced the compression strength by 4 to 10 percent depending on the temperature level, but the strength trend with temperature was approximately the same for both types of specimens.

3.2.1.2 Effect of moisture content on compression strength: Tables 3.2-I(a) and (b) present data from two groups of tests of 20 grade A veneer specimens, one at an average laminate moisture content of approximately 4 percent and one at 10 percent. Note that the mean uncorrected failure stress decreased substantially (about 29 percent) as the moisture content increased from 4 to 10 percent with a concurrent increase in test temperature from 69 to 90 °F. This was, of course, an expected trend. Data from reference 3 show an expected 5.5 percent strength loss when the test temperature is increased from 69 to 90 °F, and the experimental data in figure 3.2-1 indicate about a 7.5 percent strength loss. Increased moisture content should further reduce strength.

Data from reference 3 for defect-free unlaminated Douglas fir in compression parallel to the grain indicate a value of $K = 1.92$ in equation (7) of chapter III for correcting test data to a laminate moisture content of 6 percent. Tables 3.2-I(a) and (b) show that $K = 1.92$ overcorrected the data. It was found empirically that $K = 1.51$ provided approximately the proper correction factor for the 40 test points in the two tables for static compression parallel to the grain. With this correction the mean corrected stress for a test temperature of 90 °F was slightly more than 7.5 percent lower than that for a test temperature of 69 °F. This is about right after accounting for the temperature effect as demonstrated in figure 3.2-1.

Recall that similar effects of moisture content were not found for static tension strength parallel to the grain. Tables 3.1-VII(c) and 3.1-VIII show essentially no effect of moisture content on the tension strength of laminated Douglas fir/epoxy specimens. The lower-temperature, lower-moisture-content specimens had a mean uncorrected strength about 3.5 percent higher than did the higher-temperature, higher-moisture-content specimens. This 3.5 percent strength difference is even slightly less than the value normally attributed to temperature effect, leaving no accountable difference for moisture content.

The conclusion one can draw from these results is that the data in this report show that Douglas fir/epoxy laminates in compression parallel to the grain show moisture effects on strength somewhat consistent with those for defect-free unlaminated Douglas fir but that the value of K required to correct for moisture is smaller than that indicated in reference 3. This effect of strength reduction for increased moisture content was not demonstrated for Douglas fir/epoxy laminates in tension parallel to the grain.

It appears to be unwarranted to conclude on the basis of 40

TABLE 3.2-I.—STATIC COMPRESSION STRENGTH PARALLEL TO GRAIN—RECTANGULAR SPECIMENS

[Laminated Douglas fir/epoxy specimens 1.5 in. thick with 15 laminations, 2 in. wide, and 6.5 in. long. Data corrected to 6 percent laminate moisture content.]

(a) Veneer grade, A; laminations contained butt joints spaced 3 in. apart in adjacent laminations; test temperature, 69 °F

Stress area, in.²	Laminate moisture content, percent	Failure load, lb	Failure stress, psi	Corrected failure stress, psi	
				$K = 1.92$	$K = 1.51$
3.02	3.8	30 350	10 050	8686	9 165
3.08	4.2	28 420	9 227	8189	8 557
3.06	3.7	30 070	9 827	8437	8 924
3.06	4.1	28 740	9 392	8280	8 673
3.08	4.1	28 720	9 325	8221	8 612
3.02	4.5	28 130	9 315	8433	8 748
3.03	4.5	27 050	8 927	8082	8 383
3.03	4.2	28 100	9 274	8231	8 600
3.01	4.3	27 130	9 013	8052	8 393
3.08	4.3	27 870	9 049	8084	8 427
3.04	4.2	28 860	9 493	8425	8 803
3.11	4.0	30 670	9 862	8637	9 069
3.04	3.7	34 370	11 306	9707	10 267
3.05	3.0	32 440	10 636	8717	9 380
3.03	3.2	31 620	10 436	8667	9 281
3.04	2.8	31 130	10 240	8282	8 955
3.10	4.0	27 450	8 855	7755	8 143
3.12	4.2	24 440	7 833	6952	7 264
3.09	4.1	28 730	9 298	8197	8 587
3.06	4.3	25 920	8 471	7568	7 889
		Mean	9491	8280	8706
		Standard deviation, σ	787	521	595

(b) Veneer grade, A; laminations contained butt joints spaced 3 in. apart in adjacent laminations; test temperature, 90 °F; relative humidity, 90 percent

3.09	10.0	19 800	6 408	8355	7577
3.11	10.0	20 450	6 576	8574	7776
3.11	10.1	20 800	6 688	8778	7942
3.10	10.3	21 000	6 774	9010	8111
3.08	9.7	21 000	6 818	8714	7961
3.09	9.9	22 200	7 184	9305	8459
3.11	10.2	21 500	6 913	9134	8243
3.12	9.4	21 800	6 987	8754	8057
3.08	10.1	20 750	6 737	8842	8000
3.07	9.8	21 400	6 971	8969	8174
3.08	9.8	20 300	6 591	8480	7729
3.08	9.8	21 050	6 834	8793	8014
3.09	9.9	20 800	6 731	8718	7926
3.07	10.2	21 050	6 857	9060	8176
3.06	10.5	20 700	6 765	9118	8169
3.07	10.3	19 500	6 352	8448	7606
3.06	10.4	20 400	6 667	8926	8017
3.07	10.1	21 200	6 906	9064	8200
3.07	9.8	21 250	6 922	8906	8117
3.06	10.4	20 750	6 781	9079	8154
		Mean	6773	8851	8020
		Standard deviation, σ	196	247	214

(c) Veneer grade, A; no joints in veneer; test temperature, 69 °F

Stress area, in.²	Laminate moisture content, percent	Failure load, lb	Failure stress, psi	Corrected failure stress ($K = 1.92$), psi
3.05	4.4	32 270	10 580	9515
3.07	4.5	31 710	10 329	9351
3.05	4.4	29 280	9 600	8634
	5.5	29 510	9 675	9360
	5.4	29 010	9 511	9140
↓	4.6	28 640	9 390	8557
3.03	4.6	29 460	9 723	8861
3.00	4.9	26 770	8 923	8295
3.03	4.4	28 630	9 449	8498
3.07	4.3	31 800	10 358	9254
3.06	4.3	31 020	10 137	9056
3.04	4.4	31 730	10 438	9387
3.03	4.4	33 290	10 987	9881
3.04	4.2	31 800	10 461	9284
3.04	4.1	32 380	10 651	9390
2.97	4.2	31 170	10 495	9314
2.98	4.3	33 040	11 087	9905
3.03	4.0	32 830	10 835	9489
3.06	3.5	34 710	11 343	9610
3.06	3.5	32 830	10 729	9090
		Mean	10 235	9194
		Standard deviation, σ	656	427

(d) Veneer grade, A+; no joints in veneer; test temperature, 71 °F

3.07	3.2	35 860	11 681	9 701
3.07	3.8	34 720	11 309	9 774
3.10	3.3	34 690	11 190	9 356
3.06	3.5	33 320	10 889	9 225
3.07	3.4	33 800	11 010	9 266
3.07	2.9	34 720	11 309	9 207
3.05	3.0	35 960	11 790	9 663
3.09	3.6	34 650	11 214	9 564
3.11	3.2	36 080	11 601	9 635
3.03	4.0	34 700	11 452	10 030
3.04	4.0	31 890	10 490	9 187
3.03	4.0	33 420	11 030	9 660
3.07	3.4	35 730	11 638	9 795
3.06	3.4	35 430	11 578	9 744
3.07	3.4	35 340	11 511	9 688
3.05	3.2	35 520	11 646	9 672
3.07	3.4	34 130	11 117	9 356
3.07	3.4	34 040	11 088	9 332
3.07	3.4	32 540	10 599	8 920
3.09	3.2	35 710	11 557	9 598
		Mean	11 285	9519
		Standard deviation, σ	362	265

TABLE 3.2-II.—EFFECTS OF TEST TEMPERATURE AND BUTT JOINTS ON STATIC COMPRESSION STRENGTH PARALLEL TO GRAIN

[Laminated Douglas fir/epoxy specimens 1.5 in. thick with 15 laminations, 2 in. wide, and 6.5 in. long. Veneer grade, A. Data corrected to 6 percent laminate moisture content ($K = 1.92$).]

(a) No joints in veneer; test temperature, 30 °F

Stress area, in.^{2}	Laminate moisture content, percent	Failure load, lb	Failure stress, psi	Corrected failure stress, psi
3.05	3.8	33 060	10 839	9 368
3.04	4.1	36 150	11 891	10 483
3.04	4.2	36 030	11 852	10 518
3.03	4.3	35 800	11 815	10 555
3.04	3.8	38 700	12 730	11 002
3.04	3.9	37 850	12 451	10 832
2.97	3.6	39 210	13 202	11 259
3.00	3.7	38 350	12 850	11 032
3.02	3.2	39 900	13 212	10 973
3.01	3.9	39 460	13 110	11 406
		Mean	12 395	10 743
		Standard deviation, σ	779	544

(b) Laminations contained butt joints spaced 3 in. apart in adjacent laminations; test temperature, 30 °F

3.06	3.8	31 960	10 444	9 026
3.04	4.1	36 610	12 043	10 617
3.04	3.9	31 840	10 474	9 112
3.05	3.9	36 160	11 856	10 315
3.02	3.8	35 540	11 768	10 170
3.04	3.7	34 790	11 444	9 825
3.01	3.8	38 570	12 814	11 074
3.01	3.5	37 490	12 455	10 552
3.04	2.9	35 920	11 816	9 620
3.04	2.8	36 990	12 168	9 841
		Mean	11 728	10 015
		Standard deviation, σ	769	625

(c) No joints in veneer; test temperature, 120 °F

Stress area, in.^{2}	Laminate moisture content, percent	Failure load, lb	Failure stress, psi	Corrected failure stress, psi
3.02	3.8	22 360	7404	6399
3.03	3.7	25 910	8551	7341
3.03	3.6	26 350	8696	7416
3.04	3.2	24 210	7964	6614
3.06	3.9	26 500	8660	7534
3.04	3.8	27 210	8951	7736
3.00	4.1	26 140	8713	7682
3.02	3.9	27 710	9176	7983
3.03	2.9	27 210	8980	7311
3.04	3.1	27 500	9046	7463
		Mean	8614	7348
		Standard deviation, σ	541	465

(d) Laminations contained butt joints spaced 3 in. apart in adjacent laminations; test temperature, 120 °F

3.03	3.7	20 540	6779	5820
3.04	3.4	24 100	7928	6672
3.06	3.7	25 800	8431	7238
3.06	3.7	24 500	8007	6874
3.05	3.4	24 940	8177	6882
3.04	3.2	28 050	9227	7663
3.03	3.4	28 190	9304	7830
3.00	3.2	26 390	8797	7306
3.06	2.9	26 680	8719	7099
3.05	3.0	27 210	8921	7312
		Mean	8429	7070
		Standard deviation, σ	751	535

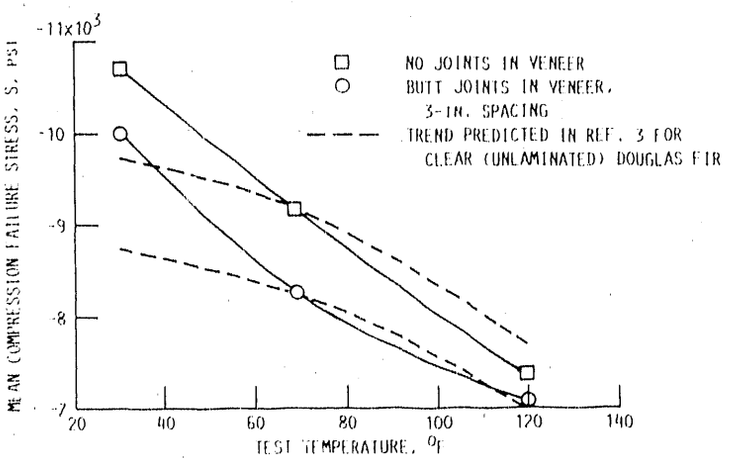

Figure 3.2-1.—Effect of test temperature on compression failure stress parallel to grain of laminated Douglas fir/epoxy test specimens. Each data point is mean of 10 specimens corrected to 6 percent laminate moisture content ($K = 1.92$).

TABLE 3.2–III.—EFFECTS OF VENEER GRADE AND JOINT TYPE ON STATIC COMPRESSION STRENGTH PARALLEL TO GRAIN—CYLINDRICAL SPECIMENS

[Laminated Douglas fir/epoxy specimens. Test temperature, 70 °F. Data corrected to 6 percent laminate moisture content ($K = 1.92$).]

(a) Veneer grade A+ and A specimens: 2.25-in.-diameter by 8-in.-long cylinder with three transverse 12:1-slope scarf joints in center veneers spaced 3 in. apart in adjacent laminations

Laminate moisture content, percent	Failure stress, psi	Corrected failure stress, psi
6.5	10 651	11 010
4.5	11 783	10 667
6.4	10 324	10 602
4.5	11 670	10 565
6.3	10 689	10 904
5.0	11 783	11 027
8.9	7 779	9 429
4.0	11 020	9 651
Mean	10 712	10 482
Standard deviation, σ	1228	571

(b) Veneer grade A+ and A specimens: 2.25-in.-diameter by 8-in.-long cylinder with three transverse butt joints in center veneers spaced 3 in. apart in adjacent laminations

7.0	10 438	11 154
4.6	11 519	10 498
9.0	7 719	9 418
3.7	10 920	9 375
5.3	10 168	9 707
5.1	10 224	9 632
5.7	9 608	9 419
5.8	9 960	9 829
5.9	[a]10 332	10 264
6.0	[a]9 574	9 574
8.3	8 317	9 688
8.6	8 170	9 708
10.1	8 421	11 053
8.5	8 371	9 881
9.2	7 895	9 762
8.5	8 070	9 525
8.5	8 070	9 525
8.8	8 095	9 747
6.3	8 525	8 696
8.7	9 102	10 887
8.3	9 296	10 828
8.0	9 273	10 588
8.9	9 198	11 149
8.1	8 747	10 054
10.2	[a]8 413	11 116
Mean	9137	10 043
Standard deviation, σ	1020	665

[a]Dogbone-shaped specimen (fig. 2.2–14).

(c) Veneer grade A+ and A specimens: 3-in.-diameter by 8-in.-long cylinder with three transverse butt joints in center veneers spaced 3 in. apart in adjacent laminations

Laminate moisture content, percent	Failure stress, psi	Corrected failure stress, psi
5.3	10 186	9724
5.1	10 224	9632
5.7	9 608	9419
5.8	9 960	9829
Mean	9995	9651
Standard deviation, σ	245	151

(d) Veneer grade C specimens: 2.25-in.-diameter by 8-in.-long cylinder with three transverse butt joints in center veneers spaced 3 in. apart in adjacent laminations

7.6	7791	8 663
10.0	7975	10 398
8.3	8239	9 597
8.1	8210	9 437
9.4	8500	10 650
9.3	8624	10 734
7.1	9352	10 060
7.2	9426	10 207
6.9	8513	9 037
6.7	9257	9 697
6.5	9057	9 362
6.2	9089	9 210
6.2	9239	9 362
Mean	8713	9724
Standard deviation, σ	534	614

TABLE 3.2-IV.--SUMMARY OF STATIC COMPRESSION STRENGTHS FROM TABLES 3.2-I AND 3.2-III

Veneer grade	Joints in laminations	Specimen cross section, in.	Specimen length, in.	Mean corrected failure stress, psi	Standard deviation, σ, psi	Table
A+	Butt	1.5 by 2	6.5	8 974	500	3.2-I(e)
A+	None			9 519	265	3.2-I(d)
A	Butt			8 280	521	3.2-I(a)
A	None			9 194	427	3.2-I(c)
C	Butt			8 573	484	3.2-I(g)
C	None			8 889	423	3.2-I(f)
A	None			9 638	515	3.2-I(h)[a]
A+ and A	Scarf	2.25 diam	8.0	10 482	571	3.2-III(a)
A+ and A	Butt	2.25 diam		10 043	665	3.2-III(b)
A+ and A	Butt	3.0 diam		9 651	151	3.2-III(c)
C	Butt	2.23 diam		9 724	614	3.2-III(d)

[a]Delamination film

control specimen tests were run that did not have the unidirectional fibers between the Douglas fir laminations. Tests were conducted at nominal test temperatures of 75, 120, and −40 °F. The low-temperature test specimens warmed as much as 24 deg F during testing.

The compression strengthening effect of the graphite fibers was impressive at all three test temperatures. The standard deviations of the test points for these compression tests were relatively high in relation to other testing, but the data scatter did not hide the strengthening effect. At room temperature and at approximately −40 °F ORCOWEB augmentation increased the mean failure stress by about 35 percent. Note, however, that the strength increase from adding ORCOWEB at −40 °F was a conservative value, since three of the five specimens did not fail because the load required for failure was greater than the capacity of the test machine.

Only two data points were taken with FIBERITE augmentation. The data showed a mean strengthening effect of 56 percent at room temperature. At a test temperature of nominally 120 °F strength was increased almost 25 percent by adding ORCOWEB fibers.

3.2.1.6 Strengthening effect of glass fiber fabric between laminations: As part of an investigation on the use of finger joints to join large sections of a laminated-wood structure, static compression tests were conducted on specimens 2 by 2 by 8 in. fabricated with and without Burlington Style 7500 glass fiber fabric between laminations. The results of these tests are listed in table 3.2-VII. Adding glass fiber fabric between laminations increased the compression strength by 24 percent, less than the 35 and 56 percent increases shown for the ORCOWEB and FIBERITE graphite fibers previously discussed.

3.2.1.7 Effect of circular cutouts on compression strength: Static compression tests were conducted on unaugmented specimens of the configuration shown in figure 2.2-9. For comparison, tests were conducted on control specimens without the hole but with approximately the same cross-sectional area. These specimens were the same thickness as the specimen in figure 2.2-9 but were 2.8 in. wide by 6 in. long. Some tests were on specimens containing a ply of 10-oz glass fiber fabric between Douglas fir laminations for strength augmentation. The fibers of the glass fabric were oriented 45° to the wood grain. Other tests were conducted with a glass fiber/epoxy ring 0.12 in. thick around the inside diameter of the circular cutout for reinforcement. The results of these tests are presented in table 3.2-VIII.

Tables 3.2-VIII(a) and (b) are for specimens without glass fiber fabric augmentation between the wood laminations. In table 3.2-VIII(a) the mean corrected failure stress for specimens without cutouts was higher than the results of most static compression tests previously reported herein. Summary table 3.2-IV shows only one other compression strength as high. Comparing the mean corrected stress for a specimen containing a 2-in.-diameter cutout (table 3.2-VIII(b)) but without any reinforcement of the hole shows a strength reduction of 6.5 percent due to the stress concentration of the hole. Placing a glass fiber/epoxy reinforcing ring around the inside of the hole removed this stress concentration effect and provided slightly over a 2 percent increase in strength relative to a specimen without the cutout.

Tables 3.2-VIII(c) and (d) show a similar comparison where strength was augmented by placing 10-oz glass fiber fabric between the Douglas fir laminations. Comparing the strengths listed in tables 3.2-VIII(c) and (d) with those in tables

TABLE 3.2 V.—EFFECT OF LAMINATE SCARF JOINT CONFIGURATION ON STATIC COMPRESSION STRENGTH PARALLEL TO GRAIN

[Laminated Douglas fir/epoxy specimens 2 in. thick with 20 laminations, 2 in. wide, and 12 in. long. Veneer grades, A+ and A; Test temperature, 65 to 70 °F. Data corrected to 6 percent laminate moisture content ($K = 1.92$).]

(a) Control specimens without joints

Laminate moisture content, percent	Failure stress, psi	Corrected failure stress, psi
6.4	9120	9365
6.2	8940	9059
6.2	8910	9029
5.9	8930	8871
5.9	7720	7669
6.0	8810	8810
6.0	9140	9140
6.0	9680	9680
6.1	9260	9322
↓	9270	9332
	9450	9513
	9290	9352
	9430	9493
	9350	9412
	9300	9362
	9000	9060
Mean	9100	9154
Standard deviation, σ	422	448

(b) Specimens with three 4:1-slope scarf joints in center three laminations spaced 3 in. apart; no overlap or gaps in joints

6.1	8880	8939
↓	9000	9060
	9030	9090
	9200	9261
Mean	9027	9088
Standard deviation, σ	114	115

(c) Specimens with three 10:1-slope scarf joints in center three laminations spaced 3 in. apart; no overlap or gaps in joints

Laminate moisture content, percent	Failure stress, psi	Corrected failure stress, psi
6.0	9320	9320
6.0	9040	9040
6.1	9140	9201
6.0	9450	9450
Mean	9237	9253
Standard deviation, σ	158	151

(d) Specimens with three 16:1-slope scarf joints in center three laminations spaced 3 in. apart; no overlap or gaps in joints

6.1	9240	9302
6.1	9020	9080
6.1	9200	9261
6.0	9470	9470
Mean	9232	9278
Standard deviation, σ	160	139

(e) Specimens with three 10:1-slope scarf joints in center three laminations spaced 3 in. apart; 25 percent overlap in joints

6.2	8540	8654
6.3	9150	9334
6.2	9270	9394
6.2	9240	9364
Mean	9050	9186
Standard deviation, σ	298	308

(f) Specimens with three 10:1-slope scarf joints in center three laminations spaced 3 in. apart; 50 percent overlap in joints

Laminate moisture content, percent	Failure stress, psi	Corrected failure stress, psi
6.0	8990	8990
6.0	8980	8980
5.9	9200	9139
6.0	9150	9150
↓	9430	9430
	9200	9200
	9220	9220
	9170	9170
Mean	9168	9160
Standard deviation, σ	133	132

(g) Specimens with three 10:1-slope scarf joints in center three laminations spaced 3 in. apart; 25 percent gap in joints

5.9	9300	9239
↓	9180	9119
	9310	9249
	9260	9199
5.7	9240	9058
5.4	8970	8620
5.7	9340	9156
6.0	9080	9080
Mean	9210	9090
Standard deviation, σ	110	189

(h) Specimens with three 10:1-slope scarf joints in center three laminations spaced 3 in. apart; 50 percent gap in joints

5.9	9210	9149
↓	8970	8911
	8980	8921
	9050	8990
Mean	9053	8993
Standard deviation, σ	96	95

TABLE 3.2 VI.—EFFECTS OF GRAPHITE FIBER FABRIC AUGMENTATION AND TEST TEMPERATURE ON STATIC COMPRESSION STRENGTH PARALLEL TO GRAIN

[Laminated Douglas fir/epoxy specimens 2 in. thick with 19 Douglas fir laminations and 18 graphite fiber plies, 2 in. wide, and 8 in. long. Veneer grade, C. Data not corrected for moisture content. Estimated laminate moisture content, 4.5 to 6 percent.

(a) Test temperature, 75 °F

Control specimens without augmentation	Specimens with graphite fiber augmentation[a]
Failure stress, psi	
10 310	14 870
10 500	14 260
540	14 470
10 160	13 950
10 210	13 040
100	11 830
9 040	12 420
8 740	11 910
8 960	12 670
9 180	12 390
9 850	
340	[b]13 181
9 150	[c]1058
9 000	
10 730	[d]16 320
10 720	[d]13 990
10 510	
[b]9708	[b]15 155
[c]675	[c]1165

(b) Test temperature, 120 °F

8 650	10 520
8 600	10 990
8 750	10 760
9 140	11 800
8 690	12 510
8 620	9 270
7 540	8 280
7 810	9 270
7 800	9 330
7 900	
7 640	[b]10 303
[b]8285	[c]1292
[c]525	

(c) Test temperature, −40 to −16 °F

12 990	[e]16 940
12 580	[e]16 950
13 210	[e]17 030
11 770	15 600
11 050	15 030
11 420	
11 120	[b,f]16 310
[b]12 020	[c]833
[c]832	

[a]Graphite fiber was ORIENTED unless otherwise identified.
[b]Mean.
[c]Standard deviation, σ.
[d]OMITTED.
[e]Specimen did not fail; exceeded limit of test machine.
[f]Values too low because failure stress of three specimens were not reached.

TABLE 3.2 VII.—EFFECT OF GLASS FIBER FABRIC AUGMENTATION ON STATIC COMPRESSION STRENGTH PARALLEL TO GRAIN

[Laminated Douglas fir/epoxy specimens 2 by 2 by 8 in. Laminated wood same as used in finger joint tests. Veneer grade, A-1; test temperature, ~68 °F. Data corrected to 6 percent laminate moisture content.]

(a) No augmentation between wood plies

Laminate moisture content, percent	Failure stress, psi	Corrected failure stress, psi	
		$K = 1.92$	$K = 1.50$
5.0	8 898	8327	8 539
5.2	8 914	8453	8 625
5.5	9 432	9124	9 240
5.8	9 671	9544	9 592
5.0	10 473	9801	10 050
5.0	10 061	9416	9 655
Mean	9575	9111	9284
Standard deviation, σ	573	548	549

(b) Burlington glass fiber fabric 7500 augmentation between wood plies.

6.0	11 540	11 540	11 540
5.8	11 775	11 620	11 678
5.6	11 562	11 259	11 373
5.6	11 417	11 118	11 230
6.0	11 883	11 883	11 883
5.9	11 525	11 449	11 478
Mean	11 617	11 478	11 530
Standard deviation, σ	160	247	210

3.2–VIII(a) and (b) shows that glass fiber fabric augmentation between the laminations did not increase failure stress for the control specimens and only marginally increased it for specimens with circular cutouts. The larger cross-sectional area resulting from the glass fiber fabric augmentation reduced failure stress for the control specimens (but somewhat increased the total load-carrying ability). Comparing tables 3.2–VIII(c) and (d) shows somewhat higher failure stress for hole reinforcement when the glass fiber fabric augmentation was used between laminations than when it was not used. Introducing the hole did not reduce failure stress. The glass fiber/epoxy ring increased the strength of specimens without glass fiber fabric augmentation between laminations by 9 percent and that of specimens with the glass fiber reinforcement between laminations by 7.5 percent.

It can be concluded that reinforcing laminated Douglas fir/epoxy laminates with a glass fiber/epoxy ring inside a relatively small diameter cutout can effectively remove the stress concentration effect.

3.2.2 Perpendicular to grain.—Compression tests were conducted perpendicular to the grain in the tangential direction

TABLE 3.2-VIII.—EFFECT OF CIRCULAR CUTOUTS WITH AND WITHOUT AUGMENTATION ON STATIC COMPRESSION STRENGTH PARALLEL TO GRAIN

[Laminated Douglas fir/epoxy specimens. Veneer grades, A+ and A; test temperature, 70 °F. Data corrected to 6 percent laminate moisture content (K = 1.92).]

(a) Control specimens 1.5 in. thick with 15 laminations, 2.8 in. wide, and 6 in. long (in direction of compressive load); no fiber glass augmentation between Douglas-fir laminations

Laminate moisture content, percent	Failure stress, psi	Corrected failure stress, psi	Stress ratio	Hole reinforcement
5.2	10 872	10 310	------	----------
↓	10 918	10 354	------	----------
	11 213	10 634	------	----------
	10 946	10 381	------	----------
Mean		10 420	------	----------
Standard deviation, σ		126	------	----------

(b) Specimens containing circular cutout 2 in. in diameter in specimen center; specimens 1.5 in. thick, 6 in. wide, and 12 in. long (in direction of compressive load); no fiber glass augmentation between Douglas fir laminations

5.2	[a]10 275	[a]9 744	[b]0.935	None
5.2	[a]11 226	[a]10 646	[b]1.022	Fiber glass/epoxy circular sleeve 0.12 in. thick

(c) Control specimens 1.66 in. thick with 15 Douglas fir laminations and 14 fiber glass augmentation plies, 2.8 in. wide, and 6 in. long (in direction of compressive load)

4.6	11 136	10 149	------	----------
↓	10 999	10 024	------	----------
	11 348	10 342	------	----------
	10 703	9 754	------	----------
Mean	11 046	10 067	------	----------
Standard deviation, σ	234	213	------	----------

(d) Specimens containing circular cutout 2 in. in diameter in specimen center; specimens 1.66 in. thick, 6 in. wide, and 12 inches long (in direction of compressive load); fiber glass augmentation ply between Douglas fir laminations

4.6	[a]11 145	[a]10 157	[b]1.009	None
4.6	[a]11 970	[a]10 903	[b]1.083	Fiber glass/epoxy circular sleeve 0.12 in. thick

[a]Stress based on net cross-sectional area including fiber glass/epoxy sleeve, where used.
[b]Ratio of failure stress to mean corrected failure stress of control specimens without cutout

on the Douglas fir/epoxy specimens shown in figure 2.2–8. These specimens were 1.5 in. thick with 15 laminations and 2 in. wide in the load direction. The specimens were 6 in. long, but the load was applied on a platen covering only 2 in. of the 6-in. length. The loaded area was thus approximately 3 $in.^2$. Failure was considered to occur when the specimen was compressed 0.1 in. in the loaded area (5 percent of the specimen thickness in the load direction).

Because the load was not applied to the entire face of the 6-in. specimens but only to the 2-in. platen, the measured failure stresses may be artificially high. The peripheral areas of wood fiber not under compression may lend support to the wood fibers within the boundaries of the platen. Limited testing was therefore conducted on specimens similar to those of figure 2.2–8 except that the specimen length was only 2 in. rather than 6 in. and the platen size was increased to 6 in. to ensure equal loading over the face of the 2-in.-long specimens. Tests in both the tangential and radial directions were conducted on these specimens.

The compression strength data in the tangential direction are shown in table 3.2–IX for a range of laminate moisture contents from near 5 percent to over 10 percent. Both types of specimens (6 in. long and 2 in. long) were tested.

3.2.2.1 Effect of moisture content on compression strength: In a manner similar to that employed in subsection 3.2.1.2 an empirical determination was made of the value of K in equation (7) of chapter III that would correct failure stress for moisture content. As tables 3.2–IX(a) and (b) show, if K was set at 1.50, the corrected failure stress for a test temperature of 90 °F and an average laminate moisture content of about 10 percent was about 96 percent of the corrected failure stress at 71 °F. This 4 percent difference is the amount of temperature correction obtained from reference 3. This value of K for compression perpendicular to the grain was close to the value of 1.51 that was found to provide a moisture-content correction for compression parallel to the grain as observed in tables 3.2–I(a) and (b). For both cases (compression parallel and perpendicular to the grain) K = 1.92 overcorrected for moisture content.

3.2.2.2 Compression strength level in tangential and radial directions: Comparing corrected compression strengths (K = 1.92) for veneer grade C with no joints shows that the strength parallel to the grain (table 3.2–I(f)) is over three times that perpendicular to the grain in the tangential direction for 6-in.-long specimens (table 3.2–IX(a)). Remember, however, that the failure modes were different for the two cases. The strength parallel to the grain was based upon the crushing load to failure, whereas the strength perpendicular to the grain was based on a 5 percent deformation of the specimen.

By comparing the data in table 3.2–IX(c), where the entire specimen face was covered by the testing machine platen, with the data in table 3.2–IX(a), where only one-third of the specimen face was covered by the platen, it is obvious that there was a reinforcing effect from the portion of the specimen not under pressure from the platen. The 2-in.-long specimens had only 71 to 77 percent of the measured corrected strength of the 6-in.-long specimens depending on the value of K used for correcting for moisture content. On the order of 3 percent of this difference can probably be attributed to the higher test temperature of the 2-in.-long specimens. The proportional limit

TABLE 3.2 IX.—STATIC COMPRESSION STRENGTH PERPENDICULAR (TANGENTIAL) TO GRAIN

[Laminated Douglas fir/epoxy specimens 1.5 in. thick with 15 laminations, 2 in. wide, and 6 in. long, load direction parallel to laminations and perpendicular to grain with 2-in.-wide platen. No joints in veneer. Data corrected to 6 percent laminate moisture content.]

(a) Veneer grade, C; test temperature, 71 °F

Stress area, in.^{2}	Laminate moisture content, percent	Failure load, lb	Failure stress, psi	Corrected failure stress, psi	
				$K = 1.92$	$K = 1.50$
2.96	5.3	8 490	2868	2738	2786
2.93	4.8	8 690	2966	2739	2823
2.95	4.7	10 180	3451	3166	3271
2.97	5.9	9 180	3091	3071	3078
2.97	4.4	9 180	3091	2780	2894
2.95	4.3	9 290	3149	2813	2936
2.98	4.4	8 220	2758	2480	2582
2.99	4.1	9 110	3047	2686	2817
3.00	4.8	8 600	2867	2648	2729
2.97	4.7	9 070	3054	2802	2895
2.98	4.6	8 980	3013	2746	2844
2.97	5.2	8 280	2788	2644	2698
2.97	4.8	9 040	3044	2811	2897
2.94	4.6	9 450	3214	2929	3034
2.95	4.5	8 140	2759	2498	2594
2.95	4.2	8 800	2983	2647	2770
2.97	4.5	8 810	2966	2685	2788
2.98	4.7	9 200	3087	2832	2926
2.99	4.7	9 200	3077	2823	2916
2.99	4.7	8 900	2977	2731	2822
	Mean		3013	2763	2855
	Standard deviation, σ		163	159	155

(b) Veneer grade, C; test temperature, 90 °F; relative humidity, 90 percent

Stress area, in.^{2}	Laminate moisture content, percent	Failure load, lb	Failure stress, psi	Corrected failure stress, psi	
				$K = 1.92$	$K = 1.50$
2.98	10.7	6 040	2027	2768	2460
2.98	10.2	6 900	2317	3061	2755
2.99	10.4	6 810	2278	3050	2731
2.97	10.4	6 520	2192	2935	2628
3.00	10.6	6 910	2305	3127	2786
2.99	10.5	7 120	2378	3205	2863
3.02	10.8	6 760	2241	3081	2731
3.03	10.6	6 410	2118	2874	2560
3.01	10.8	7 000	2322	3192	2830
3.02	10.7	7 020	2325	3175	2822
2.98	10.4	7 040	2359	3158	2828
3.00	10.7	7 290	2432	3322	2952
3.00	10.7	7 330	2442	3335	2964
2.97	10.1	6 560	2206	2895	2612
2.96	10.2	6 920	2335	3085	2766
2.97	10.4	6 830	2297	3075	2754
3.00	10.1	6 560	2190	2874	2593
3.01	10.6	6 930	2304	3126	2785
3.01	10.6	6 960	2309	3133	2791
3.02	10.5	6 270	2073	2794	2496
	Mean		2273	3063	2736
	Standard deviation, σ		110	156	135

(c) Veneer grade, C; test temperature, 81 °F

Laminate moisture content, percent	Failure stress, psi	Corrected failure stress, psi		Proportional limit, psi	Inelastic threshold, psi	Modulus of elasticity, psi
		$K = 1.92$	$K = 1.50$			
7.7	1993	2231	2138	1000	.....	.....
7.7	2020	2261	2167	1100	.....	.....
7.4	1993	2187	2111	1067	.....	.....
7.4	1930	2118	2045	1067	.....	.....
8.5	1847	2180	2048	1100	682	143 000
8.0	1890	2158	2052	1100	726	142 000
8.3	1910	2225	2100	1133	678	140 000
8.4	1800	2111	1987	1067	728	139 000
8.1	1710	1966	1865	1000	.....	.....
8.3	1750	2038	1924	1033	.....	.....
7.9	1813	2057	1961	1067	.....	.....
8.2	1770	2048	1938	1033	.....	.....
Mean	1869	2132	2028	1064	.....	.....
Standard deviation, σ	99	87	90	40	.....	.....

was found to be approximately 57 percent of the uncorrected stress required to obtain a 5 percent deformation of the specimen height.

Tests were also conducted to determine if damage can occur to laminated-wood specimens, even in a short time, by multiple applications of load at a level well below the proportional limit. These data are shown as the "inelastic threshold" in table 3.2-IX(c). These values were obtained by observing a decrease of 0.00025 in. in stroke over a period of 5 min while maintaining a constant cyclic compression load at sinusoidal peaks at a rate of 3 Hz. Table 3.2-IX(c) shows the inelastic threshold to be on the order of 60 to 68 percent of the proportional limit.

The modulus of elasticity values shown in table 3.2-IX(c) are approximately 7 percent of the moduli of the veneers parallel to the grain (about 2 million for grade C Douglas fir). Reference 3 (table 4-1) indicates that this value for clear Douglas fir, not laminated, would be 5 percent. The higher moduli of the laminated Douglas fir/epoxy specimens may result from the added rigidity of the epoxy glue.

Table 3.2-X provides data on the same type of specimen as table 3.2-IX(c) except that the compression loading perpendicular to the grain was in the radial direction. In other words the compression load was applied perpendicular to the laminations. The table shows that the compression stress required to obtain a 5 percent compression deformation was only about one-half of that required in the tangential direction. The proportional limit of 62 percent of the uncorrected failure stress was somewhat higher than the proportional limit in the tangential direction. The inelastic threshold varied from 59 to 78 percent of the proportional limit compared with 60 to 68 percent for the tangential direction specimens. The moduli of elasticity in the radial direction varied from 5.35 to 6.15 percent of the grade C veneer moduli parallel to the grain. Table 4-1 of reference 3 shows a value of 6.8 percent. The investigators in these tests surmised that possible lathe checks from the veneer peeling process may have contributed to the lower moduli.

3.2.3 Closing remarks on static compression strength.— Some conclusions that can be drawn from the data on static compression strength are as follows:

1. For laminated Douglas fir/epoxy specimens in compression parallel to the grain the effect of test temperature on strength was higher than predicted for clear Douglas fir without laminations in reference 3. For temperatures between 30 and 120 °F there was approximately a 4 percent increase in strength for each 10 degrees reduction in temperature.

2. Contrary to the static tension strength tests, where a definable effect of moisture content on specimen strength could not be found, it was possible to determine this effect for Douglas fir/epoxy specimens in compression both parallel and perpendicular to the grain. Data from reference 3 for clear (unlaminated) Douglas fir overcorrected the moisture content effects. The factor K in equation (7) of chapter III, equal to 1.51 for compression parallel to the grain and 1.50 for compression perpendicular to the grain in the tangential direction, appeared to provide failure stress corrections for laminate moisture contents of 4 and 10 percent for the limited data available.

3. Veneer grade generally correlated with compression strength parallel to the grain. The correlation was good without butt joints in the laminations and marginal with butt joints.

4. Butt joints in laminations perpendicular to the grain were found to weaken specimens tested in compression parallel to

TABLE 3.2-X.—STATIC COMPRESSION STRENGTH PERPENDICULAR (RADIAL) TO GRAIN

[Laminated Douglas fir/epoxy specimens 1.5 in. thick with 15 laminations, 2 in. wide, and 2 in. long. No joints in veneer; veneer grade, C; test temperature, 79 °F. Data corrected to 6 percent laminate moisture content.]

Laminate moisture content, percent	Failure stress, psi	Corrected failure stress, psi		Proportional limit, psi	Inelastic threshold, psi	Modulus of elasticity, psi
		K = 1.92	K = 1.50			
8.4	867	1017	957	538	425	122 000
8.5	845	997	937	538	350	123 000
8.1	848	975	925	550	325	107 000
8.5	868	1025	962	575	375	115 000
8.4	868	1018	958	575	...	...
8.3	850	990	935	575	...	...
8.5	860	1015	953	575	...	...
8.3	845	984	929	500	...	...
8.2	860	995	942	525	...	...
8.1	870	1000	949	475	...	...
8.3	860	1002	946	500	...	...
Mean	858	1002	945	539		
Standard deviation, σ	9	15	12	34		

the grain by 3.5 to 11 percent. However, scarf joints had no measurable effect on compression strength even when there was a gap or overlap in the adjoining scarf-jointed veneers.

5. The compression strength parallel to the grain for laminated Douglas fir/epoxy specimens was higher than reference 3 indicates for clear (unlaminated) Douglas fir. It is believed that the epoxy glue had a strengthening effect on the laminated specimens.

6. The use of unidirectional graphite fibers between laminations in Douglas fir/epoxy specimens was found to increase compression strength parallel to the grain approximately 35 to 56 percent, depending on the type of fiber material relative to specimens without the graphite fibers. The use of glass fiber fabric increased strength 24 percent.

7. A conventional ASTM test specimen for compression perpendicular to the grain in the tangential direction, in which the platen of the test machine covered only about one-third of the specimen face, resulted in stresses for 5 percent specimen deformation being higher than those for shorter specimens in which the platen covered the entire specimen face. These shorter specimens had test stresses on the order of 71 to 77 percent of those for the longer specimens.

8. Specimens in compression parallel to the grain were found to be three times as strong as those in compression perpendicular to the grain in the tangential direction. Remember, however, that the criterion for failure was different for the two types of compression. For failure in compression parallel to the grain the maximum crushing load at failure was measured; the failure stress for compression perpendicular to the grain was taken as the stress when the specimen had compressed 5 percent

9. The ratio of proportional limit to failure stress for compression perpendicular to the grain was found to be 57 percent in the tangential direction and 62 percent in the radial direction.

10. Damage can occur to wood specimens at compression stresses considerably less than the elastic limit in a low number of cycles. The stress at this initial damage level was defined at the inelastic threshold, whose values were obtained by observing a decrease of 0.00025 in. in stroke for a 2-in.-thick specimen over a period of 5 min while maintaining a constant recurring compression load at sinusoidal peaks at a rate of 3 Hz. The inelastic threshold for compression perpendicular to the grain was found to be on the order of 60 to 68 percent of the proportional limit in the tangential direction and 59 to 78 percent of the proportional limit in the radial direction.

11. The compression strength perpendicular to the grain for Douglas fir/epoxy was found to be only one-half as strong in the radial direction as in the tangential direction. The modulus of elasticity was higher than expected, based on reference 3 information, in the tangential direction and lower than expected in the radial direction. It is believed that the epoxy provided strength and rigidity in the tangential direction. In the radial direction possible lathe checks during the veneer peeling operation may have lowered the modulus.

3.3 Block Shear Strength

3.3.1 Effect of moisture content on shear strength parallel to grain and laminations.—According to data from reference 3, $K = 1.26$ should be used in equation (7) of chapter III to correct failure strength values to 6 percent laminate moisture content in Douglas fir shear specimens. Tables 3.3–I(a) and (b) show block shear failure data (parallel to the grain and the laminations) for veneer grade C Douglas fir/epoxy specimens of the type shown in figure 2.2–11 for two levels of laminate moisture content (approx. 3.5 and 11.5 percent). These tests were also conducted at two test temperatures—an estimated 70 °F (test temperature was not listed in the data report, but most testing was done in the range 68 to 71 °F) and 90 °F, respectively.Reference 3 indicates that this 20 deg F increase in temperature would decrease strength about 5 percent. Comparing the mean corrected failure stresses for $K = 1.26$ in tables 3.3–I(a) and (b) shows the correction to overcompensate for moisture content. In a manner similar to that described in section 3.2.1.2 for Douglas fir/epoxy specimens in static compression, an empirical value of K was determined that provided a mean corrected shear failure stress at test conditions of 70 °F and 3.5 percent laminate moisture content that was 5 percent higher (temperature effect) than the mean corrected shear failure stress at test conditions of 90 °F and 11.5 percent laminate moisture content. The value of K required to obtain this correction was 1.07 for the 25 test points at each moisture content. As stated previously, it was not feasible to draw a definite conclusion on the proper value of K from these few data points. All tables for shear strengths of Douglas fir/epoxy specimens therefore include two columns of corrected failure stresses based on K values of 1.26 and 1.07, as well as a column for the uncorrected shear failure stresses.

3.3.2 Effect of glue spread rate.—Tests were conducted to determine the block shear strength parallel to the laminations for WEST SYSTEM 105 epoxy resin and 206 hardener applied by Gougeon Brothers, Inc., Bay City, Michigan. Application rates were 45, 50, 55, 60, and 65 pounds per thousand square feet of double glue line, abbreviated lb/MDGL, to specimens of the type shown in figure 2.2–11. (Note that a double glue line merges into a single glue line in the finished laminate.) These specimens were machined from a laminate made of 15 veneers. For this configuration the initial shearing load was applied to the center of the specimen's center lamination. Data for the five glue spread rates are listed in tables 3.3–I(a) and (c) to (k). The mean corrected failure stresses and the mean percent of wood failure along the failure surface are plotted in figure 3.3–1.

Figure 3.3–1 shows a definite peaking of the shear failure strength at glue spread rates near 60 lb/MDGL particularly for veneer grade A+ and to a less pronounced degree for veneer grade C. The scatterbands in the figure show a similar peaking. In general the shear failure stress was higher for the grade A+ veneers than for the grade C veneers, but for a nonobvious

TABLE 3.3-I.—EFFECTS OF VENEER GRADE AND GLUE SPREAD RATE ON BLOCK SHEAR STRENGTH PARALLEL TO GRAIN AND LAMINATIONS

[Laminated Douglas fir/epoxy specimens. No joints in veneer. Data corrected to 6 percent laminate moisture content. See fig. 2.2-10 for geometry.]

(a) Veneer grade, C; glue spread rate, 60 lb/MDGL; estimated test temperature, 70 °F

Stress area, in.²	Laminate moisture content, percent	Failure load, lb	Failure stress, psi	Corrected failure stress, psi		Wood failure, percent
				K = 1.26	K = 1.07	
2.98	4.2	4706	1579	1514	1560	100
2.96	4.0	3842	1298	1238	1280	100
2.95	3.8	4892	1658	1574	1633	100
2.96	3.5	4962	1676	1580	1647	100
2.95	4.1	5434	1842	1762	1818	80
2.98	3.5	4452	1494	1409	1469	100
2.97	3.4	3284	1106	1040	1086	50
2.93	3.1	4703	1605	1499	1573	95
2.94	3.2	4948	1683	1576	1651	100
2.91	3.9	4868	1673	1592	1649	100
2.93	3.6	4594	1568	1482	1542	100
2.95	3.4	4399	1491	1403	1465	100
2.96	2.6	3916	1323	1221	1292	40
2.98	3.0	5632	1890	1761	1851	100
2.95	3.6	4975	1686	1594	1658	95
3.02	3.2	5540	1834	1717	1799	100
2.98	2.7	4277	1435	1328	1403	100
2.99	3.6	4587	1534	1450	1509	75
2.91	3.7	4883	1678	1590	1652	100
2.99	3.8	5408	1809	1718	1782	95
2.96	3.9	5254	1775	1690	1750	100
2.96	3.8	3811	1288	1223	1269	70
2.92	4.0	5038	1725	1646	1701	85
2.94	3.9	4878	1659	1579	1635	95
2.97	4.1	4649	1565	1497	1545	95
		Mean	1595	1507	1569	91
		Standard deviation, σ	189	181	186	16

(b) Veneer grade, C; glue spread rate, 60 lb/MDGL; estimated test temperature, 90 °F; relative humidity, 90 percent

3.04	11.9	3840	1263	1451	1315	90
3.03	11.6	4180	1380	1574	1434	100
3.05	11.5	4770	1564	1780	1624	80
3.07	11.8	4400	1433	1642	1491	80
3.03	11.4	3930	1297	1472	1346	95
3.08	11.4	4580	1487	1688	1543	100
3.05	11.6	4400	1443	1646	1500	95
3.05	11.2	4780	1567	1771	1624	100
3.07	11.4	4580	1492	1694	1548	100
3.05	11.4	4790	1570	1782	1629	95
3.03	11.6	4890	1614	1841	1677	85
3.03	11.6	4170	1376	1570	1430	90
3.05	11.1	4880	1600	1804	1657	100
3.07	11.2	4540	1479	1671	1533	85
3.07	11.3	4190	1365	1546	1416	80
3.05	11.6	4230	1387	1582	1441	75
3.04	12.1	4470	1470	1697	1533	50
3.05	11.5	3780	1239	1410	1287	85
3.04	11.4	4370	1438	1633	1492	100
3.03	11.4	4120	1360	1544	1411	90
3.03	11.6	4090	1350	1540	1403	95
3.05	11.6	4200	1377	1571	1431	90
3.04	11.7	4320	1444	1651	1502	90
3.05	11.8	4360	1430	1639	1488	85
3.04	11.8	4490	1477	1693	1537	95
		Mean	1436	1636	1492	89
		Standard deviation, σ	98	109	101	

(c) Veneer grade, A+; glue spread rate, 65 lb/MDGL; estimated test temperature, 70 °F

Stress area, in.²	Laminate moisture content, percent	Failure load, lb	Failure stress, psi	Corrected failure stress, psi		Wood failure, percent
				K = 1.27	K = 1.07	
2.99	3.3	5759	1926	1808	1891	100
3.01	3.6	5750	1910	1805	1879	100
3.05	3.1	5270	1728	1614	1694	85
3.03	3.1	4889	1614	1508	1582	95
3.02	3.2	5880	1947	1823	1910	100
3.04	2.8	4808	1582	1467	1548	100
2.99	2.8	5611	1877	1741	1836	95
3.06	2.6	5698	1892	1747	1848	100
3.03	3.1	3574	1180	1102	1157	100
3.06	3.4	5587	1826	1718	1794	90
3.02	3.0	5308	1758	1638	1722	95
3.09	2.6	5715	1850	1708	1807	90
3.03	2.8	5675	1873	1737	1832	90
3.01	3.0	5695	1892	1763	1853	90
3.02	2.0	5665	1876	1708	1825	95
2.99	3.4	5226	1748	1644	1717	95
3.05	2.8	5306	1740	1614	1702	90
3.05	2.6	4160	1364	1259	1332	100
3.05	2.8	5244	1719	1594	1682	95
3.03	2.9	4587	1514	1408	1482	100
3.01	3.5	4728	1571	1481	1544	95
3.02	3.3	4437	1469	1379	1442	100
3.04	3.1	4951	1629	1522	1597	100
3.04	3.5	4062	1336	1260	1313	100
3.01	3.5	4954	1646	1552	1618	95
		Mean	1699	1584	1664	96
		Standard deviation, σ	202	187	197	4

(d) Veneer grade, A+; glue spread rate, 60 lb/MDGL; estimated test temperature, 70 °F

3.07	3.4	4850	1580	1486	1552	40
3.04	3.1	6016	1979	1849	1940	95
3.06	3.2	4917	1607	1505	1576	80
2.97	3.2	5756	1938	1815	1901	80
3.07	3.4	5801	1891	1779	1857	85
3.03	2.6	6016	1985	1833	1939	15
3.06	2.5	5170	1690	1557	1650	75
3.02	2.2	5053	1673	1530	1630	85
2.98	2.8	4691	1574	1460	1540	75
3.10	3.2	5972	1926	1803	1889	65
3.04	2.8	5940	1954	1812	1911	85
3.01	2.6	5728	1903	1757	1859	90
3.02	2.1	5550	1838	1677	1789	85
2.97	2.5	5704	1921	1769	1875	90
3.06	2.5	5290	1729	1593	1688	95
3.03	2.6	5654	1866	1723	1823	90
3.02	2.1	5432	1799	1641	1751	75
2.96	2.0	4520	1527	1390	1486	85
3.09	2.5	5592	1810	1667	1767	90
3.11	2.7	6022	1936	1792	1893	90
3.01	3 1/8	5504	1829	1709	1793	80
2.99	2.7	5184	1734	1605	1695	65
3.05	2.6	5888	1930	1782	1885	85
3.02	3.2	5670	1877	1757	1841	90
3.02	3.3	6380	2113	1983	2074	95
		Mean	1824	1691	1784	79
		Standard deviation, σ	147	141	145	18

TABLE 3.3-L.—Continued.

(e) Veneer grade, A+; glue spread rate, 55 lb/MDGL; estimated test temperature, 70 °F

Stress area, in.²	Laminate moisture content, percent	Failure load, lb	Failure stress, psi	Corrected failure stress, psi		Wood failure, percent
				$K = 1.26$	$K = 1.07$	
3.02	3.8	4840	1603	1522	1579	95
3.05	3.6	5189	1701	1608	1673	90
3.04	3.2	5400	1776	1663	1742	75
3.01	3.3	4569	1518	1425	1490	90
3.04	3.3	5619	1848	1734	1814	95
3.02	3.2	5268	1744	1633	1711	↓
3.06	2.4	5263	1720	1580	1678	↓
3.06	2.7	5965	1949	1804	1905	↓
2.99	2.3	5533	1851	1697	1804	↓
3.02	2.7	5056	1674	1549	1636	90
3.06	2.9	4024	1315	1223	1287	95
3.07	2.3	4466	1455	1334	1418	100
3.05	2.7	4782	1568	1451	1533	↓
3.07	2.5	5270	1717	1581	1676	↓
3.05	3.1	4395	1441	1346	1413	↓
3.01	2.7	5505	1829	1693	1788	95
3.04	2.7	3527	1160	1073	1134	100
2.98	2.1	3890	1305	1191	1270	95
2.98	2.3	5465	1834	1681	1788	95
3.00	3.3	5207	1736	1629	1704	100
3.06	3.3	4824	1576	1479	1547	95
3.05	3.1	5380	1764	1648	1729	↓
3.00	3.0	5751	1917	1787	1878	↓
2.99	3.3	5458	1825	1713	1791	↓
3.00	3.1	4946	1649	1540	1616	100
		Mean	1659	1543	1624	95
		Standard deviation, σ	198	186	194	5

(f) Veneer grade, A+; glue spread rate, 50 lb/MDGL; estimated test temperature, 70 °F

3.07	3.8	4922	1603	1522	1579	100
3.06	3.4	4862	1589	1495	1561	70
3.07	2.9	4271	1391	1293	1362	95
3.04	2.8	4110	1352	1254	1323	70
3.05	3.5	3967	1301	1227	1279	95
3.03	3.2	4942	1631	1527	1600	↓
3.04	2.5	5039	1658	1527	1619	↓
3.04	2.7	4765	1567	1450	1532	↓
3.06	2.7	4420	1444	1336	1412	90
3.01	3.3	4452	1479	1388	1452	95
3.07	3.1	5110	1664	1554	1631	95
3.04	2.4	4244	1396	1283	1362	95
3.06	2.5	4286	1401	1290	1368	100
3.06	3.1	2900	948	886	929	60
3.07	3.4	5285	1721	1619	1690	90
3.05	2.9	4638	1521	1414	1489	95
3.07	3.3	5460	1779	1670	1746	100
3.08	2.5	4586	1489	1371	1454	95
3.06	2.9	4839	1581	1470	1548	95
3.06	3.3	4941	1615	1516	1585	100
3.05	3.0	4883	1601	1492	1568	100
3.05	3.3	4324	1418	1331	1392	50
3.04	3.4	4830	1589	1495	1561	85
3.03	3.6	4533	1496	1414	1472	80
3.04	3.4	4694	1544	1453	1517	90
		Mean	1511	1411	1481	89
		Standard deviation, σ	163	155	161	13

(g) Veneer grade, A+; glue spread rate, 45 lb/MDGL; estimated test temperature, 70 °F

Stress area, in.²	Laminate moisture content, percent	Failure load, lb	Failure stress, psi	Corrected failure stress, psi		Wood failure, percent
				$K = 1.26$	$K = 1.07$	
3.09	3.9	2731	884	841	871	20
3.02	3.8	2382	789	749	777	20
2.99	3.3	2852	954	895	936	20
3.04	3.6	2094	689	651	678	25
3.04	3.4	3650	1201	1130	1180	100
3.05	3.4	2116	694	653	682	10
3.03	3.4	2605	860	809	845	20
3.06	3.2	4464	1459	1366	1431	90
3.06	4.0	4078	1333	1272	1315	70
3.02	3.4	3333	1104	1039	1084	10
3.05	3.5	2962	971	916	954	10
3.04	3.0	3134	1031	961	1010	50
3.03	3.2	2235	738	691	724	25
3.01	4.2	3086	1025	983	112	10
2.98	3.7	3516	1180	1118	1161	20
3.05	3.6	3334	1093	1033	1075	10
3.06	2.7	3634	1188	1099	1161	10
3.02	3.4	3080	1020	960	1002	85
3.06	3.3	3529	1153	1082	1132	10
3.06	3.1	3557	1162	1085	1139	100
3.07	3.5	2702	880	830	865	10
3.02	3.1	3576	1184	1106	1161	10
3.08	3.5	3734	1212	1143	1191	100
3.07	3.7	3507	1142	1082	1124	10
3.07	3.7	4454	1451	1375	1428	10
		Mean	1056	995	1038	34
		Standard deviation, σ	208	196	204	34

(h) Veneer grade, C; glue spread rate, 65 lb/MDGL; estimated test temperature, 70 °F

3.08	4.1	4146	1346	1287	1329	90
3.02	3.7	4627	1532	1451	1508	95
3.05	3.4	4740	1554	1462	1526	100
3.07	3.2	4626	1507	1411	1478	90
3.05	3.8	4967	1629	1547	1605	100
3.05	3.6	4912	1610	1522	1584	95
3.03	3.1	3190	1053	984	1032	40
3.06	3.8	4627	1512	1436	1489	95
3.07	3.2	4593	1496	1401	1467	90
3.07	3.7	5002	1629	1543	1603	90
3.06	3.8	3447	1126	1069	1109	95
3.06	3.0	4321	1412	1316	1383	90
3.04	2.8	4751	1563	1450	1529	95
3.06	3.3	4550	1487	1396	1460	95
3.04	3.4	5046	1660	1562	1631	100
3.07	3.1	3319	1081	1010	1060	40
3.09	3.5	5072	1641	1547	1613	95
3.02	3.0	4867	1612	1502	1579	100
3.04	3.4	5043	1659	1561	1630	90
3.06	3.3	4919	1608	1509	1578	80
3.04	3.4	4738	1559	1467	1531	95
3.05	3.6	4506	1477	1396	1453	70
3.04	3.8	4889	1608	1527	1584	95
3.04	3.3	4115	1354	1271	1329	40
3.05	3.4	4919	1613	1517	1584	85
		Mean	1493	1406	1467	86
		Standard deviation, σ	173	163	170	19

TABLE 3.3-1.—Concluded.

(i) Veneer grade, C; glue spread rate, 55 lb/MDGL; estimated test temperature, 70 °F

Stress area, in.^{2}	Laminate moisture content, percent	Failure load, lb	Failure stress, psi	Corrected failure stress, psi		Wood failure, percent
				K = 1.26	K = 1.07	
2.97	4.1	2589	872	834	861	95
2.98	3.9	2646	888	845	875	100
2.94	4.0	4882	1661	1585	1638	100
2.97	4.0	4212	1418	1353	1399	95
2.97	4.1	4841	1630	1559	1609	100
3.00	3.4	5189	1730	1627	1699	100
2.97	3.5	4635	1561	1472	1534	100
2.99	3.7	3991	1335	1265	1314	80
2.98	3.5	3640	1221	1151	1200	100
2.98	3.3	4916	1650	1549	1620	95
2.98	3.7	4822	1618	1533	1593	95
2.95	3.5	4367	1480	1396	1455	95
2.97	3.1	3444	1160	1084	1137	40
2.98	3.2	4537	1522	1425	1493	95
2.98	3.3	3422	1148	1077	1127	25
3.01	3.7	4937	1640	1554	1614	100
2.99	3.1	4072	1362	1272	1335	80
2.96	3.1	3713	1254	1171	1229	40
3.01	3.3	5025	1669	1566	1638	95
2.93	3.7	3434	1172	1110	1154	70
2.95	3.9	4152	1407	1339	1387	90
2.96	3.5	4163	1406	1326	1382	85
2.97	3.6	3814	1284	1214	1263	40
2.97	3.9	4309	1451	1381	1430	90
2.95	4.1	4761	1614	1544	1593	95
		Mean	1406	1329	1383	84
		Standard deviation, σ	233	221	229	23

(j) Veneer grade, C; glue spread rate, 50 lb/MDGL; estimated test temperature, 70 °F

2.90	4.4	4063	1401	1349	1386	100
2.96	4.3	4859	1642	1578	1623	95
2.97	4.1	4856	1635	1564	1614	100
2.92	4.3	4946	1694	1628	1674	85
2.96	4.3	4727	1597	1534	1578	100
2.96	4.5	4959	1675	1617	1658	100
2.90	4.0	4102	1414	1349	1395	95
2.90	3.9	4527	1561	1486	1539	100
2.91	3.9	4774	1641	1562	1617	100
2.98	4.3	3086	1030	990	1018	15
2.98	3.9	3201	1074	1022	1059	40
3.00	4.0	4422	1474	1406	1454	95
2.97	3.7	4717	1588	1504	1563	100
2.97	3.7	4614	1563	1481	1538	100
2.99	4.1	4751	1589	1520	1568	100
2.97	4.1	2200	741	709	731	40
3.00	3.9	4579	1526	1453	1504	100
2.97	4.0	4330	1458	1391	1438	↓
3.00	4.1	4012	1337	1279	1320	
3.01	4.1	4645	1543	1476	1523	
3.00	4.1	4722	1574	1505	1554	85
2.98	3.8	3853	1293	1228	1274	100
2.98	4.4	3872	1299	1251	1285	50
2.96	4.3	4216	1424	1368	1407	95
2.96	4.2	4240	1432	1373	1414	90
		Mean	1448	1385	1429	87
		Standard deviation, σ	221	211	218	23

(k) Veneer grade, C; glue spread rate, 45 lb/MDGL; estimated test temperature, 70 °F

Stress area, in.^{2}	Laminate moisture content, percent	Failure load, lb	Failure stress, psi	Corrected failure stress, psi		Wood failure, percent
				K = 1.26	K = 1.07	
3.00	4.5	1648	561	542	555	15
3.09	4.6	4000	1294	1252	1282	90
3.07	4.9	2611	850	828	844	50
3.09	4.3	3109	1006	967	994	95
3.08	4.3	3027	983	945	972	90
3.06	4.1	4195	1371	1311	1353	95
3.08	3.7	3438	1116	1057	1098	90
3.06	3.8	2467	806	765	794	70
3.04	3.6	3328	1095	1035	1077	95
3.06	3.9	2493	815	776	803	25
3.12	4.0	3284	1053	1005	1039	60
3.06	3.6	2792	912	862	897	50
3.08	3.5	4385	1424	1343	1400	100
3.09	4.3	3117	1009	969	997	95
3.09	4.0	3262	1056	1008	1042	95
3.08	3.8	3777	1226	1164	1208	100
3.10	4.0	4333	1398	1334	1379	80
3.09	4.0	4280	1385	1321	1366	95
3.06	3.3	4292	1403	1317	1377	75
3.06	3.8	4235	1384	1314	1363	75
3.07	4.0	4630	1508	1439	1487	60
3.07	3.8	3706	1207	1146	1189	25
3.07	3.8	3732	1216	1155	1198	40
3.06	3.8	4310	1408	1337	1387	60
3.11	4.1	4669	1501	1435	1482	100
		Mean	1159	1105	1143	73
		Standard deviation, σ	247	233	243	26

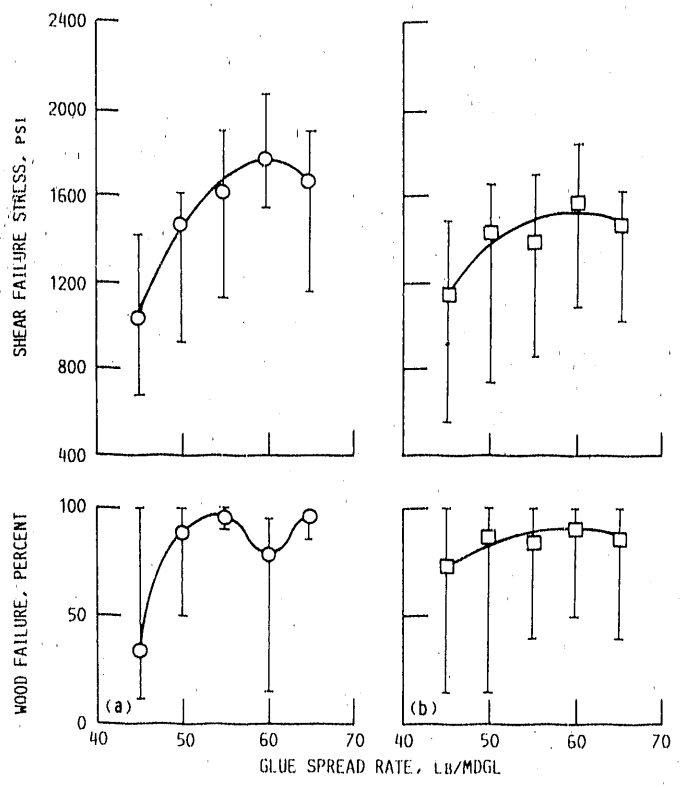

(a) Veneer grade, A+.
(b) Veneer grade, C.

Figure 3.3-1.—Effect of glue spread rate on shear strength and percent of failure in wood surface for laminated Douglas fir/epoxy specimens. Shear parallel to grain and laminations. Strength corrected to 6 percent laminate moisture content (K = 1.07).

reason the mean shear failure stress at a glue spread rate of 45 lb/MDGL was higher for grade C than for grade A+.

Figure 3.3-1 also shows the percent of wood failure in the failure surfaces of the sheared specimens. There are some unexplained anomalies in the amount of wood failure. Each group of 25 specimens had at least some, and often many, specimens in which the failure in the wood was 100 percent except for the grade A+ veneer at the strongest glue spread rate of 60 lb/MDGL. In addition, the scatterband was quite large, whereas the scatterbands for 55 and 65 lb/MDGL were small. Further, the shear failure stress and percent of wood failure values in the tables show a weak correlation between percent of fracture in the wood and strength.

As a result of these studies on optimum glue spread rate, all other Douglas fir/epoxy data in this report are for a glue spread rate of 60 lb/MDGL.

3.3.3 Effect of veneer grade parallel to grain and laminations.—Figure 3.3-1, as well as tables 3.3-I(a) and (c) to (k), shows the mean corrected shear strength values for veneer grades A+ and C. These results are consistent with previously discussed results for static tension and static compression with grade A+ veneer and show a strength advantage of approximately 14 percent over grade C veneer at a glue spread rate of 60 lb/MDGL. The strength advantage of grade A+ is consistent for all spread rates except 45 lb/MDGL. The effect at 45 lb/MDGL is unexplained.

3.3.4 Block shear strength perpendicular to laminations and parallel to grain.—The test specimen for block shear strength perpendicular to the laminations and parallel to the grain is shown in figure 2.2-11. Test results for 25 of these specimens are shown in table 3.3-II for veneer grade C and a glue spread rate of 60 lb/MDGL. The effect of lamination orientation on the shear strength can be obtained by comparing the data in tables 3.3-II and 3.3-I(a). The corrected shear failure strength was 27 to 28 percent higher (depending upon which value of K was considered) for shear perpendicular to the laminations than for shear parallel to the laminations. Observe also that the failure was 100 percent in the wood for shear aligned with the glue line perpendicular to the laminations. This means that there was no interlaminar failure. For shear parallel to the laminations, where the initial shearing load was maximum at the middle of the center wood lamination, the average failure in the wood was 91 percent.

TABLE 3.3-II.—BLOCK SHEAR STRENGTH PERPENDICULAR TO LAMINATIONS AND PARALLEL TO GRAIN

[Laminated Douglas fir/epoxy specimens. No joints in veneer. Veneer grade, C; glue spread rate, 60 lb/MDGL; test temperature, 76 °F. Data corrected to 6 percent laminate moisture content. See fig. 2.2-10 for geometry.]

Stress area, in.^{2}	Laminate moisture content, percent	Failure load, lb	Failure stress, psi	Corrected failure stress, psi		Wood failure percent,
				K = 1.26	K = 1.07	
2.27	4.9	4870	2145	2090	2129	100
2.30	4.9	4668	2030	1978	2015	
2.27	4.6	4760	2097	2029	2077	
2.25	4.2	4865	2162	2072	2135	
2.28	4.7	4869	2136	2072	2117	
2.30	3.6	4998	2173	2054	2137	
2.24	3.7	4373	1952	1849	1921	
2.29	4.6	4818	2104	2036	2084	
2.26	4.3	4907	2171	2086	2146	
2.27	3.2	5390	2374	2223	2329	
2.27	4.2	4758	2096	2009	2070	
2.25	4.3	4564	2028	1949	2004	
2.26	4.1	4501	1992	1905	1966	
2.30	3.5	4658	2025	1909	1990	
2.27	3.4	3973	1750	1646	1719	
2.25	3.5	4559	2026	1910	1991	
2.26	3.1	4418	1955	1826	1916	
2.25	4.7	4743	2108	2045	2089	
2.27	4.6	4323	1904	1842	1886	
2.25	4.1	4091	1818	1739	1794	
2.24	4.8	3171	1416	1377	1404	
2.24	4.6	4589	2049	1983	2029	
2.23	5.0	3874	1737	1697	1725	
2.29	4.6	4444	1941	1878	1922	
2.24	4.1	5079	2267	2168	2238	
		Mean	2018	1935	1993	100
		Standard deviation, σ	189	179	186	0

3.3.5 Closing remarks on block shear strength.—Some conclusions that can be drawn from the data on block shear strength are as follows:

1. From limited testing on the effect of moisture content on block shear strength parallel to the laminations for Douglas fir/epoxy, it appears that $K = 1.07$ in equation (7) of chapter III provides a better correlation of the data than the value of 1.26 that can be obtained from data in reference 3 for clear (unlaminated) Douglas fir.

2. Tests conducted with epoxy glue at spread rates from 45 to 65 pounds per thousand square feet of double glue line (abbreviated lb/MDGL) for block shear of laminated Douglas fir specimens with the shear load parallel to the laminations showed a peaking in strength at 60 lb/MDGL for both veneer grades A+ and C. On the basis of these data all other test results in this report are for spread rates of 60 lb/MDGL.

3. Block shear strength parallel to the grain and the laminations was about 14 percent higher for veneer grade A+ than for veneer grade C. This effect was consistent at all glue spread rates except 45 lb/MDGL and is consistent with results for static tension and static compression.

4. Block shear strength was found to be 27 to 28 percent higher when the shear load was miximum on a glue plane perpendicular to the laminations than when the load was parallel to the laminations.

3.4 Bending Strength

3.4.1 Effect of moisture content on bending strength.—A series of tests were conducted on specimens of the configuration shown in figure 2.2-12. The tests to evaluate the effect of moisture content on strength utilized bending with vertical laminations for veneer grade A. The data obtained for moisture content evaluation were for two groups of samples averaging about 4.5 and 10 percent laminate moisture content, respectively. The data are tabulated in tables 3.4-I(a) and (b). Using a K of 1.25 (based on data from ref. 3) in equation (7) of chapter III to correct test data to a 6 percent laminate moisture content resulted in an overcorrection. Using the same approach as discussed previously for static compression and block shear to correct for both temperature and moisture content resulted in an empirical determination of $K = 1.05$ to correct bending stress data for moisture content.

It is not clear how modulus of elasticity (derived from flexural stiffness) is affected by temperature. If, however, increasing temperature approximately 20 deg F were to reduce the modulus on the order of 5 percent, as it is expected to do on strength, the higher-moisture-content, higher-temperature data will not correct to a 6 percent laminate moisture content value that is consistent with the corrected lower-temperature, lower-moisture-content data for any value of K. If temperature does not affect modulus of elasticity, a value of $K = 1.05$, the same as for bending strength, does a reasonable job of correcting the data. A value of $K = 1.06$ is better. Although not shown in tables 3.4-I(a) and (b), the corrected values of modulus are 1.96 million for both sets of data for $K = 1.06$.

Remember that the empirical value of K to correct the block shear data was 1.07. Values of K of 1.50 and 1.51 were found to best correct the data for static compression. Available data for static tension were not sufficient to determine an empirical value of K for tension. The empirical values that have been determined for laminated-wood products have all been lower values than one would obtain from reference 3 for clear (unlaminated) wood. It would therefore appear that the epoxy glue lessened the effects of strength reduction with increased moisture content. This is a reasonable conclusion, since the epoxy absorbs little water and therefore its strength is essentially unaffected by moisture.

3.4.2 Effect of veneer grade on bending strength.—Tables 3.4-I(a), (c), and (d) tabulate results of bending strength and modulus with vertical laminations at a test temperature of nearly 70 °F for veneer grades A+, A, and C. The data were not entirely consistent. The specimens made from veneer grade A+ did have the highest bending strength and the highest modulus, but the lowest strength and modulus were obtained in the specimens made from veneer grade A. The veneer grade A specimens were about 1 percent weaker than veneer grade C specimens and about 14 percent weaker than veneer grade A+ specimens. The modulus of the veneer grade A specimens was about 7 percent less than for veneer grade C and about 9 percent less than for veneer grade A+. These inconsistencies in modulus and strength may be explained by the greater data scatter for the veneer grade A material as indicated by values of σ being about 10 percent higher for strength and about 40 percent higher for modulus for the veneer grade A specimens than for the veneer grade C specimens. The samples were cut from large sheets of the laminate, and inconsistencies in the sheet may result from areas of cross grain in the veneers; some of the veneer grade A specimens may have contained such areas. Remember also that grade C can be superior to grade A in ultrasonic testing as discussed in subsection 1.2.2.

3.4.3 Effect of lamination orientation relative to bending load.—Table 3.4-I(e) tabulates bending strength and modulus data for bending with horizontal laminations (fig. 2.2-12) for veneer grade A samples. Comparing tables 3.4-I(a) and (e) shows the horizontal laminations to be about 4 percent stronger and 0.5 percent higher in modulus than the vertical laminations. This effect is believed to result from the outer 0.1 in. of the horizontal laminated beam being of wood, which is stronger and stiffer than the epoxy. In bending, the outer fibers most affect strength and stiffness. For the vertical laminated beam, on the other hand, the outer fibers are a combination of wood and the weaker epoxy.

TABLE 3.4-I.—EFFECTS OF VENEER GRADE AND LAMINATION ORIENTATION ON BENDING STRENGTH AND MODULUS

[Laminated Douglas fir/epoxy specimens with butt joints spaced 3 in. apart in adjacent laminations. Data corrected to 6 percent laminate moisture content.]

(a) Veneer grade, A; vertical laminations; test temperature, 71 °F

Stress area		Laminate moisture content, percent	Failure load, lb	Failure stress, psi	Corrected failure stress, psi		Modulus, E, psi	Corrected modulus, E, psi	
Width, in.	Depth, in.				$K = 1.25$	$K = 1.05$		$K = 1.25$	$K = 1.05$
1.512	2.019	4.9	1079	12 605	12 294	12 536	1.91×10^6	1.86×10^6	1.90×10^6
1.512	2.016	4.9	1143	13 392	13 062	13 319	1.92	1.87	1.91
1.521	2.017	4.7	1067	12 415	12 054	12 335	1.93	1.87	1.92
1.524	2.012	5.0	1050	12 254	11 979	12 193	1.92	1.88	1.91
1.515	2.008	5.5	954	11 245	11 118	11 217	1.73	1.71	1.73
1.519	2.027	5.3	963	11 109	10 934	11 071	1.88	1.85	1.87
1.515	2.024	5.2	1069	12 402	12 179	12 353	1.90	1.87	1.89
1.498	2.020	5.5	973	11 461	11 332	11 433	1.84	1.82	1.84
1.503	2.025	4.4	1029	12 021	11 593	11 926	1.91	1.84	1.89
1.523	2.023	4.7	1098	12 684	12 315	12 602	1.90	1.84	1.89
1.515	2.028	4.5	1102	12 734	12 308	12 640	2.01	1.94	2.00
1.509	2.027	4.7	1105	12 832	12 459	12 750	2.05	1.99	2.04
1.510	2.003	4.5	1190	14 143	13 670	14 038	2.07	2.00	2.05
1.512	2.020	4.1	1050	12 254	11 737	12 139	2.12	2.03	2.10
1.490	2.025	4.6	1009	11 890	11 518	11 878	1.93	1.87	1.92
1.496	2.022	4.5	1265	14 891	14 393	14 781	2.27	2.19	2.25
1.496	2.019	4.4	1193	14 085	13 583	13 974	2.35	2.27	2.33
1.506	2.000	4.4	908	10 853	10 466	10 767	1.98	1.91	1.96
1.524	2.010	3.6	981	11 472	10 864	11 336	1.93	1.83	1.91
1.517	2.010	3.1	989	11 619	10 879	11 453	1.89	1.77	1.86
			Mean	12 418	12 037	12 334	1.97×10^6	1.91×10^6	1.96×10^6
			Standard deviation, σ	1041	1009	1032	0.14×10^6	0.13×10^6	0.14×10^6

(b) Veneer grade, A; vertical laminations; test temperature, 90 °F; relative humidity, 90 percent

1.540	2.020	10.1	954	10 931	11 997	11 156	1.79×10^6	1.96×10^6	1.83×10^6
1.542	2.013	10.0	986	11 362	12 441	11 590	1.90	2.08	1.94
1.540	2.010	9.8	1005	11 630	12 677	11 851	1.91	2.08	1.95
1.538	2.007	9.5	991	11 517	12 469	11 719	1.92	2.08	1.95
1.535	2.024	9.9	924	10 580	11 559	10 787	1.85	2.02	1.89
1.534	2.026	9.6	965	11 035	11 974	11 234	1.89	2.05	1.92
1.525	2.024	9.8	972	11 202	12 211	11 415	1.93	2.10	1.97
1.520	2.018	9.8	981	11 411	12 438	11 628	1.84	2.01	1.88
1.515	2.007	10.3	963	11 362	12 526	11 607	1.77	1.95	1.81
1.529	2.014	9.4	1038	12 050	13 016	12 255	1.91	2.06	1.94
1.531	2.021	9.8	1062	12 228	13 329	12 461	1.93	2.10	1.97
1.528	2.014	9.9	1003	11 652	12 730	11 880	1.91	2.09	1.95
1.519	2.024	10.0	1041	12 045	13 189	12 286	1.94	2.12	1.98
1.531	2.029	10.3	1068	12 200	13 450	12 463	1.94	2.14	1.98
1.528	2.031	10.2	1049	11 983	13 181	12 235	1.96	2.16	2.00
1.520	2.024	10.2	1044	12 072	13 279	12 326	2.04	2.24	2.08
1.520	2.016	11.0	999	11 643	13 042	11 935	2.01	2.25	2.06
1.520	2.030	10.0	1011	11 621	12 725	11 854	1.87	2.05	1.91
1.527	2.024	10.1	884	10 175	11 167	10 384	1.84	2.02	1.88
1.533	2.031	9.3	991	11 284	12 161	11 470	1.88	2.03	1.91
			Mean	11 499	12 578	11 727	1.90×10^6	2.08×10^6	1.94×10^6
			Standard deviation, σ	528	596	541	0.06×10^6	0.08×10^6	0.06×10^6

TABLE 3.4-I.—Continued.

(c) Veneer grade, A+; vertical laminations; test temperature, 72 °F

Stress area		Laminate moisture content, percent	Failure load, lb	Failure stress, psi	Corrected failure stress, psi		Modulus, E, psi	Corrected modulus, E, psi	
Width, in.	Depth, in.				$K = 1.25$	$K = 1.05$		$K = 1.25$	$K = 1.05$
1.530	2.014	3.6	1304	15 129	14 327	14 950	2.21×10^6	2.09×10^6	2.18×10^6
1.534	2.019	3.6	1222	14 070	13 324	13 904	2.19	2.07	2.16
1.533	2.017	3.4	1279	14 766	13 920	14 577	2.20	2.07	2.17
1.529	2.020	3.3	1265	14 599	13 732	14 405	2.36	2.22	2.33
1.523	2.027	3.7	1303	14 992	14 230	14 822	2.28	2.16	2.25
1.519	2.033	4.0	1198	13 739	130	13 603	2.23	2.13	2.21
1.515	2.018	4.1	1313	15 323	1 677	15 179	2.10	2.01	2.08
1.520	2.025	3.5	1285	14 8[illegible]	14 026	14 661	2.16	2.04	2.13
1.521	2.023	3.6	1329	15 372	14 557	15 190	2.23	2.11	2.20
1.519	2.027	3.7	1257	14 501	13 764	14 337	2.18	2.07	2.16
1.515	2.028	3.7	1361	15 727	14 927	15 549	2.25	2.14	2.22
1.510	2.032	3.9	1324	15 290	14 579	15 132	2.18	2.08	2.16
1.495	2.025	4.7	1222	14 352	13 935	14 260	2.23	2.17	2.22
1.520	2.015	3.6	1289	15 038	14 241	14 860	2.16	2.05	2.13
1.522	2.000	3.5	1273	15 055	14 225	14 869	2.37	2.24	2.34
1.520	2.000	3.6	1111	13 157	12 460	13 001	2.21	2.09	2.18
1.518	2.019	3.6	1337	15 557	14 733	15 373	2.18	2.06	2.15
1.517	2.014	3.6	1204	14 088	13 341	13 921	2.14	2.03	2.11
1.513	2.010	3.7	1170	13 781	13 080	13 625	2.42	2.30	2.39
1.510	2.019	4.2	1312	15 347	14 733	15 211	2.04	1.96	2.02
			Mean	14 736	13 997	14 571	2.22×10^6	2.10×10^6	2.19×10^6
			Standard deviation, σ	671	646	664	0.09×10^6	0.08×10^6	0.09×10^6

(d) Veneer grade, C; vertical laminations; test temperature, 69 °F

1.500	2.020	5.8	1040	12 234	12 179	12 222	1.93×10^6	1.92×10^6	1.93×10^6
1.506	2.030	4.9	1076	12 483	12 175	12 415	2.04	1 99	2.03
1.507	2.027	4.4	972	11 303	10 900	11 214	2.17	2.09	2.15
1 499	2.020	4.9	1092	12 854	12 537	12 784	2.08	2.03	2.07
1.496	2.026	5.4	989	11 596	11 439	11 562	1.99	1.96	1.98
1.490	2.019	5.9	979	11 605	11 579	11 599	2.05	2.05	2.05
1.504	2.003	4.8	1222	14 581	14 189	14 494	2.39	2.33	2.38
1.508	2.006	4.4	1139	13 514	13 032	13 407	2.24	2.16	2.22
1.512	2.008	4.2	1142	13 487	12 947	13 367	2.10	2.02	2.08
1.516	2.013	4.2	943	11 052	10 610	10 954	2.20	2.11	2.18
1.519	2.013	4.3	1068	12 493	12 020	12 388	2.02	1.94	2.00
1.518	2.011	4.2	1121	13 147	12 621	13 030	2.17	2.08	2.15
1.522	2.031	4.9	1028	11 789	11 498	11 725	2.08	2.03	2.07
1.532	2.032	4.5	1111	12 646	12 223	12 552	2.03	1.96	2.01
1.528	2.034	4.0	952	10 843	10 362	10 736	2.06	1.97	2.04
1.523	2.030	4.1	1110	12 734	12 197	12 615	2.14	2.05	2.12
1.529	2.030	4.4	1203	13 747	13 257	13 638	2.10	2.03	2.08
1.527	2.027	4.7	1139	13 071	12 691	12 987	2.14	2.08	2.13
1.528	2.021	4.8	1149	13 256	12 900	13 177	2.19	2.13	2.18
1.525	2.025	5.3	1144	13 172	12 965	13 126	2.09	2.06	2.08
			Mean	12 580	12 216	12 500	2.11×10^6	2.05×10^6	2.10×10^6
			Standard deviation, σ	954	922	945	0.10×10^6	0.09×10^6	0.10×10^6

TABLE 3.4-1.—Concluded.

(e) Veneer grade, A; horizontal laminations; test temperature, 70°F

Stress area		Laminate moisture content, percent	Failure load, lb	Failure stress, psi	Corrected failure stress, psi		Modulus, E, psi	Corrected modulus, E, psi	
Width, in.	Depth, in.				$K = 1.25$	$K = 1.05$		$K = 1.25$	$K = 1.05$
2.013	1.517	4.7	1199	13 976	13 570	13 886	2.04×10^6	1.98×10^6	2.03×10^6
2.017	1.523	4.9	1186	13 689	13 352	13 615	1.88	1.83	1.87
2.017	1.535	4.6	1065	12 133	11 754	12 049	1.84	1.78	1.83
2.015	1.522	4.6	1010	11 685	11 320	11 604	1.83	1.77	1.82
2.030	1.519	5.1	1037	11 955	11 713	11 902	1.82	1.78	1.81
2.029	1.521	4.8	1059	12 183	11 856	12 111	1.94	1.89	1.93
2.023	1.505	5.1	1050	12 374	12 124	12 319	1.94	1.90	1.93
2.023	1.485	5.3	1070	12 952	12 748	12 907	2.02	1.99	2.01
2.005	1.510	4.4	1143	13 501	13 020	13 394	2.08	2.01	2.06
1.999	1.521	4.4	1202	14 035	13 535	13 924	2.04	1.97	2.02
2.030	1.511	4.6	1151	13 410	12 991	13 317	2.05	1.99	2.04
2.015	1.512	4.6	1171	13 727	13 298	13 632	1.99	1.93	1.98
2.008	1.520	3.9	1011	11 768	11 221	11 646	1.97	1.88	1.95
2.018	1.510	4.2	1002	11 759	11 289	11 654	2.00	1.92	1.98
2.015	1.482	4.5	1013	12 360	11 947	12 268	2.11	2.04	2.09
2.015	1.490	4.4	1136	13 713	13 224	13 605	2.23	2.15	2.21
2.020	1.490	4.0	1106	13 318	12 727	13 187	2.01	1.92	1.99
2.006	1.522	3.5	1353	15 723	14 856	15 529	1.96	1.85	1.94
2.004	1.532	3.0	1226	14 076	13 150	13 868	2.15	2.01	2.12
2.010	1.515	3.4	1063	12 442	11 729	12 283	2.02	1.90	1.99
			Mean	13 039	12 571	12 935	2.00×10^6	1.92×10^6	1.98×10^6
			Standard deviation, σ	1025	941	1004	0.10×10^6	0.09×10^6	0.10×10^6

4.0 Fatigue Strength of Laminated Composite Specimens

Data are available for tension-tension fatigue, compression-compression fatigue, and reverse axial tension-compression fatigue. Among the variables investigated were constants to use in the moisture correction equations and the effects of veneer grade, the type of joints used in the laminates, the stress range used in fatigue testing, the test section volume, augmentation by use of graphite fibers between wood plies, and stress concentrations from cutouts in the specimens. All data presented are for Douglas fir/epoxy specimens made of 0.1-in.-thick veneers with the load applied parallel to the grain. The glue spread rate was 60 pounds per thousand square feet of double glue line.

Most of the tables and figures presenting fatigue data for laminated composite specimens in this report also show a failure stress that was obtained from static tension or compression tests. These tests were conducted with 5-min ramps. The ramp time was converted to estimated equivalent cycles to failure on the basis of the number of cycles that would accumulate in 5 min of fatigue testing. Thus 5 min is equivalent to 1200 cycles at a cycle rate of 4 cycles/sec, 2400 cycles at 8 cycles/sec, etc. It was found to be beneficial, in most cases, to use the static test data converted to equivalent cycles for calculating the regression curves. These static points improved the consistency of regression line slopes for various test conditions.

The static data used were from two sources. In some cases control specimens were static tested by using specimens from the same billets and the same configuration as the fatigue specimens. In other cases similar specimen data were used from other investigations. The source of the static data is listed on each of the tables. In all cases the static strength was the mean of replicate tests, but in calculating the regression lines the static strength was considered as a single test point in order to not unduly weight the low-cycle end of the regression line. In some cases as many as 20 replicate tests were used in calculating the mean value of the static test point.

During some of the fatigue testing the tests were terminated prior to specimen failure. In these cases the regression line was first calculated while neglecting these unfailed specimens. If, however, the data point for the unfailed specimen was found to lie on or above the regression line, the regression line was recalculated to include the unfailed specimen, and the equation for this recalculated line is the one given on the plots. From the location relative to the regression line of the unfailed specimen points (indicated by arrows extending from the plotted point), it can be seen whether the point was included

in calculating the regression line. The number of "cycles to failure" for the unfailed specimen was taken as the number of cycles accumulated when the test was terminated. No attempt was made to hypothesize the remaining life in the specimen.

4.1 Tension-Tension Fatigue Strength

4.1.1 Effect of moisture content on tension-tension fatigue strength.—The approach for applying a moisture correction to strength is presented in reference 3 for static tension, compression, shear, and modulus of elasticity. No information is presented on correcting for fatigue. In the fatigue data presented in this report it seemed logical to use the moisture corrections developed for static strength to determine if they would be appropriate for fatigue strength. Data are presented in table 4.1-I and figure 4.1-1 for tension-tension fatigue over a modest range of laminate moisture contents from 4.6 to 7 percent for dogbone specimens as shown in figure 2.2-13. The center three laminations of these specimens contained scarf joints with a slope of 12:1. The joints were displaced by 3 in. in adjacent laminations. The fatigue tests were conducted for a stress ratio R (ratio of minimum stress to maximum stress) of 0.1.

In figure 4.1-1(a) the uncorrected data are shown on a log-log plot. Each data point is labeled with the laminate moisture content as tested. The correlation coefficient r (see chapter III) of the least-squares regression line, neglecting the point labeled with the arrow, where the test was terminated by premature failure resulting from accidental damage to the specimen, is shown to be −0.9891.

Figure 4.1-1(b) shows the data corrected for moisture content by using equation (7) of chapter III and $K = 1.21$ for static tension. In this case the correlation coefficient has improved to −0.9930. Calculations were made for other values of K, but none improved the correlation coefficient. The range of laminate moisture contents was so small for these tests that the value of K did not have a marked effect on moisture content correction, but it appears that the value of K from reference 3 for clear Douglas fir in static tension was probably appropriate for Douglas fir/epoxy laminates in tension-tension fatigue.

TABLE 4.1-I.—TENSION-TENSION FATIGUE STRENGTH PARALLEL TO GRAIN FOR DOGBONE SPECIMENS

[Laminated Douglas fir/epoxy dogbone specimens with 2.25-in.-diameter by 8-in.-long test section and 57-in. overall length. Three 12:1-slope scarf joints in veneers in center of specimens staggered 3 in. apart in adjacent laminations. Stress ratio, R, 0.1; test temperature, 70 °F; cycle rate, 4 Hz. Data corrected to 6 percent laminate moisture content. See fig. 2.2-13 for geometry.]

Laminate moisture content, percent	Minimum stress, psi	Maximum stress, psi	Cycles to failure	Corrected failure stress ($K = 1.21$), psi
6.5	900	9000	178 500	9 088
6.3	850	8500	597 900	8 550
4.6	850	8500	[a]305 320	8 272
4.7	800	8000	1 930 730	7 801
7.0	700	7000	7 550 000	7 137
4.6–9.0			[b]1 200	11 418

[a]Premature failure due to accidental damage to specimen.
[b]Static test of six control specimens—estimated equivalent cycles

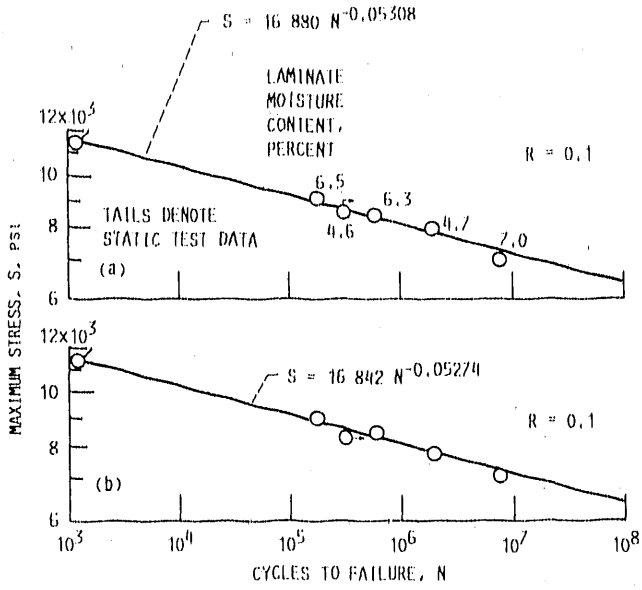

(a) Data not corrected for moisture content. Correlation coefficient, r, −0.9891.

(b) Data corrected to 6 percent laminate moisture content ($K = 1.21$). Correlation coefficient, r, −0.9930.

Figure 4.1-1.—Moisture correction for tension-tension fatigue ($R = 0.1$) parallel to grain for laminated Douglas fir/epoxy specimens. Dogbone specimens with 2.25 in. diameter test section (see fig. 2.2-13) and 12:1 scarf joints staggered 3 in. apart in center three laminations. Veneer grade, A+; test temperature, 70 °F.

4.1.2 Effect of veneer grade on tension-tension fatigue strength.—Tension-tension fatigue tests were conducted on dogbone specimens made of both veneer grades A+ and A, and the results are presented in table 4.1-II and figure 4.1-2. The specimens in these tests had butt joints in the center three laminations, with the joints displaced by 3 in. in adjacent laminations. Figure 4.1-2(a) shows the butt joint data for $R = 0.1$ and the regression line for scarf joints from figure 4.1-1(b). All data points are for grade A+ veneers in the specimens. Figure 4.1-2(b) shows similar butt joint data for grade A veneers in the specimens and compares them with the data for grade A+ from figure 4.1-2(a). The data in figure 4.1-2(b) show a somewhat higher fatigue strength for grade A specimens than for grade A+ specimens, contrary to what one would expect. Even though the regression lines show a separation of approximately 600 psi in fatigue strength, if one were to superimpose the data points from figures 4.1-2(a) and (b), all of the data for grade A would fall within the scatterband for grade A+. It is likely then that veneer grade may not significantly affect tension-tension fatigue strength.

TABLE 4.1-II.—EFFECTS OF BUTT JOINTS, VENEER GRADE, AND STRESS RATIO ON TENSION-TENSION FATIGUE STRENGTH PARALLEL TO GRAIN FOR DOGBONE SPECIMENS

[Laminated Douglas fir/epoxy dogbone specimens with 2.25-in.-diameter test section. Butt joints staggered 3 in. apart in center three laminations. Test temperature, 70 °F. Data corrected to 6 percent laminate moisture content (K = 1.21). See fig. 2.2-13 for geometry.]

(a) Veneer grade, A+; stress ratio, R, 0.1

Cycle rate, Hz	Laminate moisture content, percent	Minimum stress, psi	Maximum stress, psi	Cycles to failure	Corrected failure stress (K = 1.21), psi
4	5.8	850	8500	21 450	8 467
↓	5.6	850	8500	111 910	8 434
	5.7	800	8000	429 570	7 954
	5.6	750	7500	922 390	7 442
4.5	6.0	750	7500	138 960	7 500
4.5	6.1	750	7500	1 148 940	7 515
4	[a]6.7	580	5800	845 800	5 879
	6.5	710	7089	206 500	7 167
	5.6	473	4732	6 718 300	4 695
	5.2	620	6200	2 450 000	6 105
	4.4	600	6000	1 470 500	5 817
	5.5	779	7789	59 400	7 714
↓	4.4	519	5192	[b]10 000 000	5 033
				[c]1 200	11 487

(b) Veneer grade, A; stress ratio, R, 0.1

4	6.5	642	6419	493 000	6 482
4	9.2	778	7780	210 600	8 278
4	7.6	712	7120	1 285 300	7 344
1.5	8.6	850	8500	97 300	8 939
3	9.4	850	8500	67 500	9 079
				[c]1 200	12 099

(c) Veneer grade, A; stress ratio, R, 0.4

4	6.4	2864	7160	316 900	7 216
4	6.4	2869	7166	14 200	7 222
				[c]1 200	12 099

[a]Estimated from error in moisture content measurement
[b]Specimen did not fail
[c]Static test - estimated equivalent cycles (table 3.1-I)

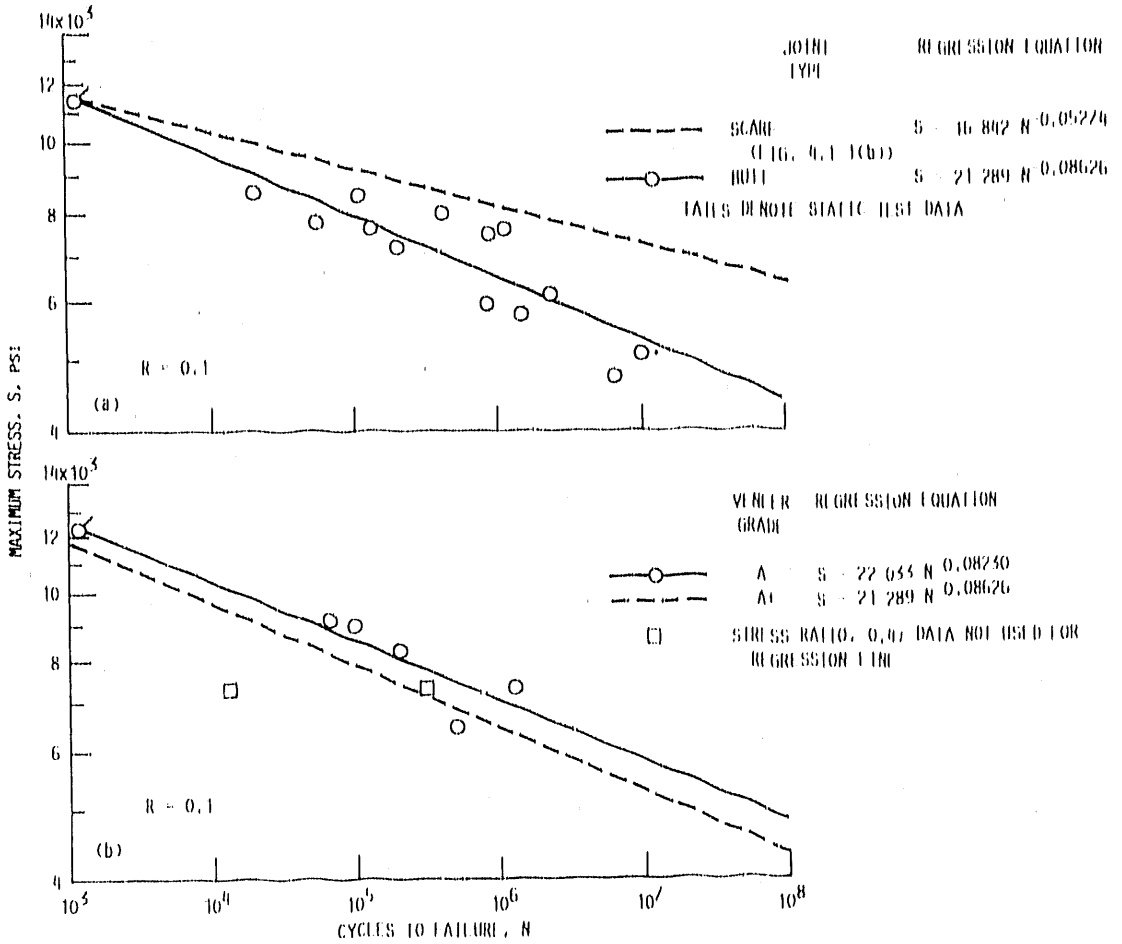

(a) Grade A+ veneer, with comparison of scarf and butt joints.
(b) Butt joints, with comparison of grade A+ and A veneers.

Figure 4.1-2.—Effect of veneer grade on tension-tension fatigue ($R = 0.1$) parallel to grain for grades A+ and A laminated Douglas fir/epoxy specimens. Dogbone specimens with 2.25-in. diameter test section (see fig. 2.2-13) and butt joints staggered 3 in. apart in center three laminations. Data corrected to 6 percent laminate moisture content ($K = 1.21$). Test temperature, 70 °F.

4.1.3 Effect of laminate joint configuration on tension-tension fatigue strength.—Figure 4.1-2(a) shows tension-tension fatigue strength regression lines for both butt joints and 12:1-slope scarf joints for dogbone specimens. The figure shows that the scarf-jointed specimens are from 16 to 36 percent stronger than the butt-jointed specimens at 10^5 to 10^7 cycles to failure. The butt joints create more of a discontinuity, and thus a site for initiation of a fatigue failure, than the scarf joints do. Well-fitted scarf joints are more likely to provide load transfer through the glue line.

4.1.4 Effect of tension-tension fatigue stress ratio on failure strength.—Only very limited data were available, and they are shown in figure 4.1-2(b). Most data were obtained at a stress ratio R of 0.1. Two points for $R = 0.4$ are shown in figure 4.1-2(b) for specimens made of grade A veneer. The two points show markedly different reductions in tension-tension fatigue strength than the data obtained at $R = 0.1$. It is therefore difficult to draw conclusions on the magnitude of these fatigue strength differences.

4.1.5 Effect of specimen size on tension-tension fatigue strength.—Table 4.1-III and figure 4.1-3 show tension-tension fatigue data for large specimens 2 in. thick (composed of 20 grade A+ laminations) by 8 in. wide and 360 in. long. The volume in the test section part of the specimens was 4992 in.^{3} The specimens had 12:1 slope scarf joints at 8-ft intervals in each lamination. The joints in adjacent laminations were offset by 3 in. For comparison purposes the regression line for grade A+ dogbone specimens (test section volume of 31.8 in.^{3}) with scarf joints in the center three laminations is also shown. The small specimens were from 54 to 64 percent stronger than the large specimens at 10^5 to 10^7 cycles to failure. The large specimens had many more sites for possible initiation of fatigue failure than the smaller specimens, from the standpoints of both the number of scarf joints and possible defects in the laminations.

4.1.6 Closing remarks on tension-tension fatigue strength.—The tension-tension fatigue strength data available were relatively limited, but from these data it appears that the effects

TABLE 4.1-III.—TENSION-TENSION FATIGUE STRENGTH PARALLEL TO GRAIN FOR LARGE-VOLUME SPECIMENS

[Laminated Douglas fir/epoxy specimens 2 in. thick (20 laminations) by 8 in. wide by 360 in. long (4992-in.^{3} test volume). 12:1-Slope scarf joints staggered 3 in. apart in all adjacent laminations (spaced 8 ft in each lamination). Stress ratio, R, 0.1; test temperature, 70 °F. Data corrected to 6 percent laminate moisture content (K = 1.21).]

Laminate moisture content, percent	Minimum stress, psi	Maximum stress, psi	Cycles to failure	Corrected failure stress, psi
5.0	650	6500	20 421	6375
5.0	700	7000	49 686	6866
5.2	650	6500	5 626	6400
5.2	580	5800	164 458	5711
5.0	520	5200	1 366 128	5100
			[a]300	9497

[a]Static test—estimated equivalent cycles (table 3.1-III) for volume of 3768 in.^{3}

of the moisture content of the laminated fatigue specimens can be corrected in the same manner as for static tension specimens. On the basis of this limited number of tests, veneer grade did not appear to significantly affect tension-tension fatigue for specimens made of grade A+ and grade A veneers. As one would expect, scarf joints in the laminations resulted in better tension-tension fatigue strength than butt joints in the laminations, and large specimens failed at lower stress, fewer cycles, or both than small specimens. Figure 13 of chapter III illustrates all these effects.

4.2 Compression-Compression Fatigue Strength

4.2.1 Effect of moisture content on compression-compression fatigue strength.—Compression-compression fatigue data (R = 10) were available for tests conducted with laminate moisture contents ranging from 4.5 to 8.1. The tests were conducted on cylindrical specimens 2.25 in. in diameter and 8 in. long. The test specimens are shown in figure 2.2-15. The center three laminations of the specimens contained 12:1-slope scarf joints. The joints were staggered 3 in. apart in adjacent laminations. The specimens were made from grade A+ Douglas fir veneers. Data are shown in table 4.2-I and figure 4.2-1. The uncorrected data are shown in figure 4.2-1(a), and the data corrected to 6 percent laminate moisture content by using K = 1.92 in equation (7) of chapter III are shown in figure 4.2-1(b). This value of K is the same as that used for static compression in reference 3. This moisture content correction improved the correlation coefficient r from −0.8254 for no moisture correction to −0.8975 for correction to 6 percent laminate moisture content (K = 1.92). It therefore appears that the method used for correcting static compression data for moisture content works well for compression-compression fatigue. In fact the correction is superior to that found for static compression of laminated specimens (see subsection 3.2.1.2).

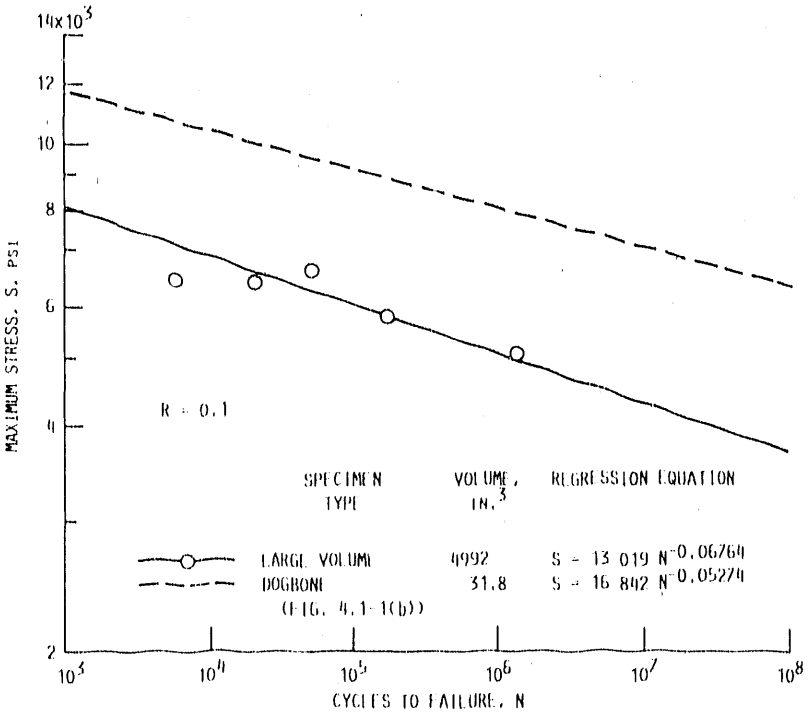

Figure 4.1-3.—Effect of tension-tension fatigue (R = 0.1) parallel to grain for large-volume laminated Douglas fir/epoxy specimens. Specimens 2 in. thick (20 laminations) by 8 in. wide by 360 in. long (4992-in.^{3} test volume) with 12:1 slope scarf joints staggered 3 in. apart in all adjacent laminations. Joints spaced 8 ft apart in each lamination. Data corrected to 6 percent laminate moisture content (K = 1.21). Veneer grade, A+; test temperature, 70 °F. Static test data at 9497 psi and 300 equivalent cycles not shown.

S = -8656 N -0.03869
0.03869

YES 1.5 HY 6 H
IN.

SPECIM
SIZE

CUTOUT ?

REGRESSION LINE

AUGMENTATION?	RE-INFORCEMENT?	
NO	NO	○
YES	NO	◇
NO	YES	▽
YES	YES	□

TABLE 4.2-I.--COMPRESSION-COMPRESSION FATIGUE STRENGTH PARALLEL TO GRAIN FOR CYLINDRICAL SPECIMENS

[Laminated Douglas fir/epoxy cylindrical specimens 2.25 in. in diameter by 8 in. long. Three 12:1-slope scarf joints in veneers in center of specimens staggered 3 in. apart in adjacent laminations. Veneer grade, A+; stress ratio, R, 10; test temperature, 70 °F. Data corrected to 6 percent laminate moisture content (K = 1.92).]

Cycle rate, Hz	Laminate moisture content, percent	Minimum stress, psi	Maximum stress, psi	Cycles to failure	Corrected failure stress, psi
8	5.0	−950	−9500	50 640	−8890
8	8.1	−750	−7500	71 860	−8621
10	6.8	−780	−7800	325 010	−8225
8	4.6	−870	−8700	316 740	−7929
10	6.7	−750	−7500	1 333 400	−7856
8	4.5	−850	−8500	1 655 890	−7695
[a]10	6.2	−700	−7000	18 571 520	−7094
8	7.3	−650	−6500	17 509 310	−7085
10	5.7	−750	−7500	[b]260 100	−7352
10	5.3	−800	−8000	[b]48 030	−7637
10	5.4	−850	−8500	[b]22 970	−8169
---	4.0–8.9	-----	-----	[c]3 000	−9906

[a]Test conducted at two laboratories. Tests started at 10 Hz and completed at 9 Hz.
[b]Specimens contained imperfect scarf joints. One joint overlapped 0.5 in., middle joint overlapped 0.25 in., and other joint underlapped 0.25 in.
[c]Static test of eight control specimens—estimated equivalent cycles.

4.2.2 Effect of veneer grade on compression-compression fatigue strength.—Compression-compression fatigue tests were conducted on specimens made from both grade A+ and grade A veneers with butt joints in the center three laminations staggered 3 in. apart in adjacent laminations. The specimens were 2.25 in. in diameter and 8 in. long. The data are shown in table 4.2–II and figure 4.2–2 for R of 2.5 and 10. Although the data for grade A veneers were quite limited, it would appear that veneer grade does not significantly affect compression-compression fatigue strength for either value of R, since the data for both veneer grades fell within the same scatterband. These results are similar to those obtained for tension-tension fatigue.

4.2.3 Effect of laminate joint configuration on compression-compression fatigue strength.—A number of joint configurations were tested in compression-compression fatigue. These configurations included both butt and scarf joints with scarf slopes varying from 4:1 to 16:1. In addition, scarf joints were tested that were imperfect, having either overlaps or gaps in the layup of the scarfed laminates. All tests were for grade A+ Douglas fir/epoxy with the grain parallel to the load direction. Tests were conducted on both cylindrical and square-cross-section specimens. All of the laminate joints tested were in the center three laminations with the joints staggered 3 in. apart in adjacent laminations. The tests were conducted at a stress ratio R of 10.

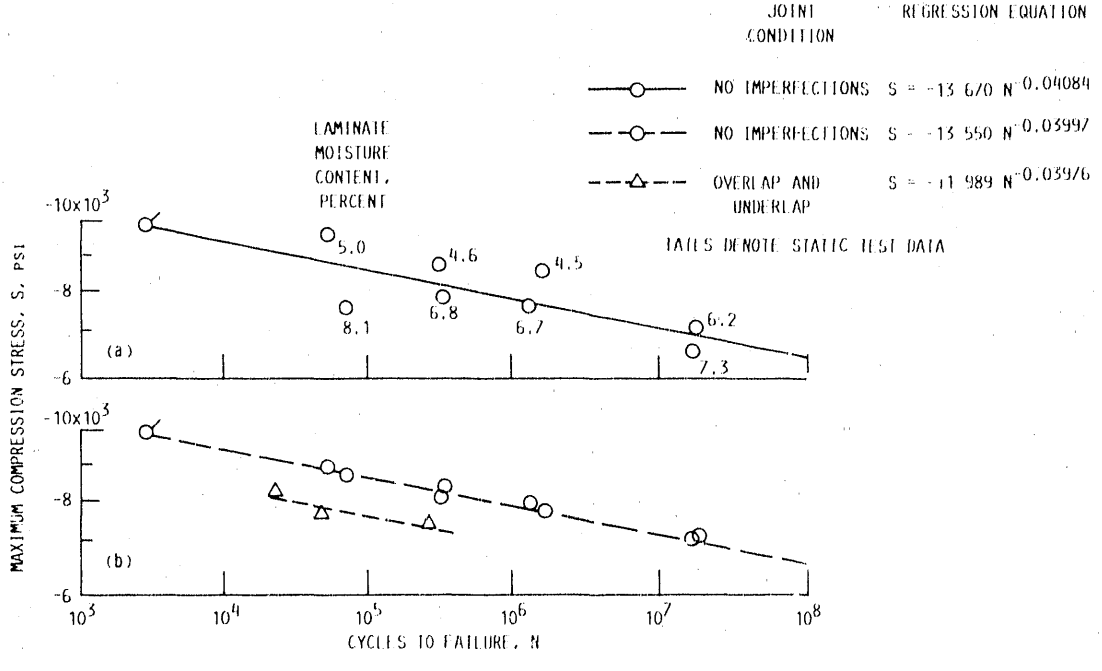

(a) Data not corrected for moisture content.
(b) Data corrected to 6 percent laminate moisture content (K = 1.92).

Figure 4.2-1.—Moisture correction for compression-compression fatigue (R = 10) parallel to grain for laminated Douglas fir/epoxy specimens. Cylindrical specimens 2.25 in. in diameter by 8 in. long with 12:1 slope scarf joints staggered 3 in. apart in center three laminations. Veneer grade, A+; test temperature, 70 °F.

TABLE 4.2-II.—EFFECTS OF VENEER GRADE AND STRESS RATIO ON COMPRESSION-COMPRESSION FATIGUE STRENGTH PARALLEL TO GRAIN

[Laminated Douglas fir/epoxy cylindrical specimens 2.25 in. in diameter and 8 in. long. Butt joints staggered 3 in. apart in center three laminations. Test temperature, 70 °F. Data corrected to 6 percent laminate moisture content ($K = 1.92$).]

(a) Veneer grade, A+

Stress ratio, R	Laminate moisture content, percent	Minimum stress, psi	Maximum stress, psi	Cycles to failure	Corrected failure stress, psi
10	5.6	−900	−9000	14 910	−8 764
	5.5	−850	−8500	13 850	−8 223
	5.5	−850	−8500	20 930	−8 223
	5.3	−800	−8000	153 030	−7 637
	5.3	−750	−7500	82 720	−7 160
	5.2	−750	−7500	518 430	−7 113
	[a]5.4	−750	−7500	549 720	−7 208
	4.5	−750	−7500	2 351 000	−6 790
	5.6	−650	−6500	303 000	−6 330
	6.1	−529	−5285	10 593 000	−5 320
	6.0	−593	−5930	4 674 600	−5 930
	5.5	−547	−5474	3 031 200	−5 296
↓	[a]5.6	−540	−5400	[b]12 675 200	−5 258
2.5	6.2	−2569	−6423	8 751 600	−6 509
2.5	6.3	−2760	−6900	4 019 400	−7 039
				[c]1 200	−10 043

(b) Veneer grade, A

10	6.6	−584	−5840	304 000	−6 077
10	6.8	−565	−5650	1 360 000	−5 958
10	6.3	−667	−6666	1 370 000	−6 800
2.5	6.3	−2967	−7417	61 200	−7 566
2.5	6.1	−2967	−7417	1 120 000	−7 466
2.5	5.4	−2920	−7300	4 229 051	−7 015
				[c]1 200	−9 724

[a]Estimated.
[b]Specimen did not fail.
[c]Static tests—estimated equivalent cycles (table 3.2-IV).

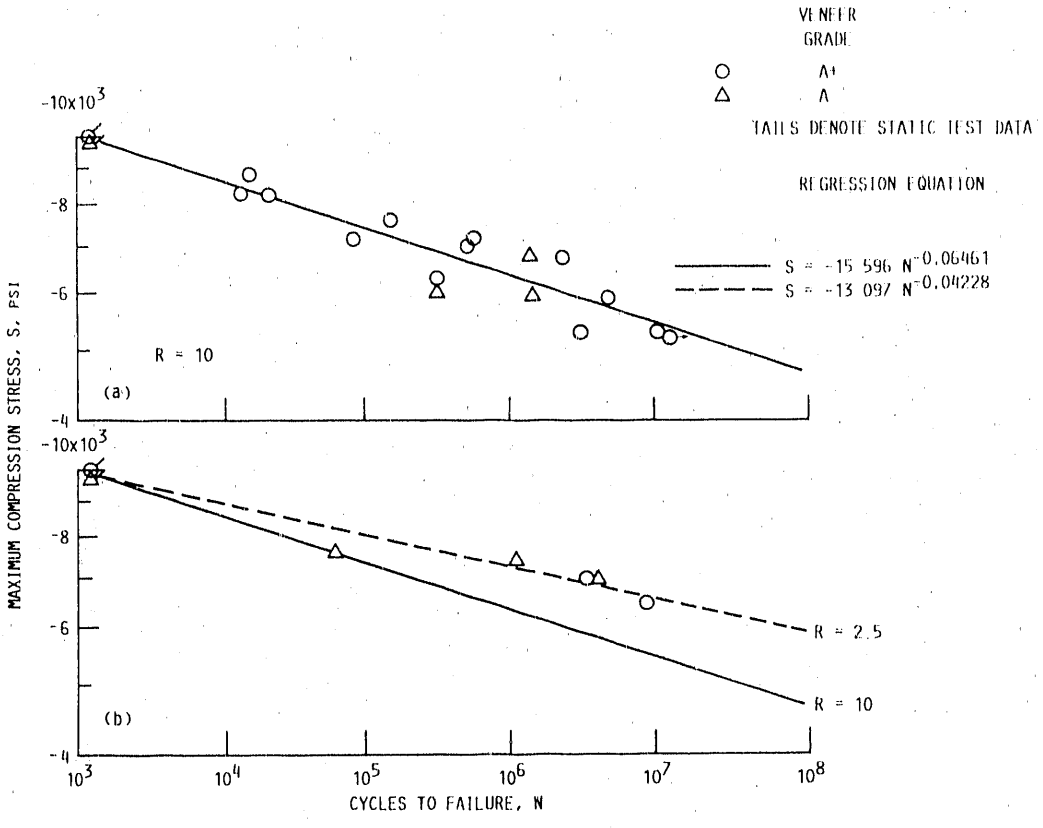

(a) $R = 10$.
(b) $R = 2.5$ with comparison to $R = 10$.

Figure 4.2-2.—Effect of veneer grade and fatigue stress ratio R on compression-compression fatigue parallel to grain for laminated Douglas fir/epoxy specimens. Cylindrical specimens 2.25 in. in diameter by 8 in. long with butt joints staggered 3 in. apart in center three laminations. Data corrected to 6 percent laminate moisture content ($K = 1.92$). Veneer grades, A and A+; test temperature, 70 °F.

Table 4.2-III and figure 4.2-3(b) show butt joint data for cylindrical specimens 8 in. long with diameters of 2.25 and 3 in. The small difference in specimen diameter did not significantly affect compression-compression fatigue strength. Equations of the regression lines for each type of specimen are shown in figure 4.2-3(b). Also shown in the figure is the regression line for 12:1-slope scarf-jointed specimens from figure 4.2-1(b). The 2.25-in.-diameter scarf-jointed specimens were 11 to 19 percent stronger in compression-compression fatigue than the 2.25-in.-diameter butt-jointed specimens at 10^5 to 10^7 cycles to failure.

Table 4.2-IV and figure 4.2-4 compare the compression-compression fatigue strengths of specimens having scarf joints with scarf slopes of 4:1, 10:1, and 16:1 and specimens having no joints in the laminations. The tests were conducted on specimens that were 2 by 2 by 12 in. The scarf joints were in the center three laminations and were staggered 3 in. apart in adjacent laminations.

For all three scarf joint configurations some tests were terminated prior to specimen failure, and in all three cases the regression lines would have had a smaller negative slope if the tests had been continued to failure. As a result, when regression lines were calculated, these unfailed specimen data points were taken into consideration. Although not completely valid, these regression lines were considered to be more representative than if the unfailed points had been neglected. In the comparisons that follow, the regression lines that included the unfailed specimen data were used. Figures 4.2-4(a) to (d) show the data points used for calculating each regression line. The summary effect of the regression lines from these four figures is shown in figure 4.2-4(g). The data are consistent, showing steadily decreasing fatigue strength as the slope becomes steeper (as indicated by the smaller ratio; i.e., 4:1 being smaller than 16:1). Specimens with scarf joints having shallower slopes permitted increased load transfer through the sloping glue line at the joint and were thus stronger in fatigue. As the slope became steeper, the joint began to more nearly take on the character of a butt joint.

Tables 4.2-I and 4.2-IV and figures 4.2-1(b) and 4.2-4(e), (f), and (h) show the results of imperfect scarf joints on specimen strength. Figure 4.2-1(b) shows that relatively large mismatches in the scarf joint weakened the specimens on the order of 12 percent. These imperfect scarf joints had the joint in the middle lamination overlapped by 0.25 in., the joint in

TABLE 4.2-III.—EFFECTS OF STRESS RATIO AND JOINT TYPE ON COMPRESSION-COMPRESSION FATIGUE STRENGTH PARALLEL TO GRAIN

[Laminated Douglas fir/epoxy cylindrical specimens. All joints staggered 3 in. apart in center three laminations. Test temperature, 70 °F. Data corrected to 6 percent laminate moisture content (K = 1.92).]

(a) 12:1-Slope scarf joints in laminations; stress ratio, R, 2.5; specimens 2.25 in. in diameter by 8 in. long

Cycle rate, Hz	Laminate moisture content, percent	Minimum stress, psi	Maximum stress, psi	Cycles to failure	Corrected failure stress, psi
10	6.6	−3600	−9 000	89 500	−9 365
10	6.5	−3600	−9 000	1 036 100	−9 304
8	4.3	−4000	−10 000	328 920	−8 934
10	6.5	−3400	−8 500	10 795 730	−8 787
				[a]3 000	−10 482

(b) Butt joints in laminations; stress ratio, R, 10; specimens 2.25 in. in diameter by 8 in. long

10	6.7	−780	−7 800	44 990	−8 171
8	4.6	−820	−8 200	61 200	−7 473
10	6.3	−700	−7 000	1 024 650	−7 141
8	4.6	−750	−7 500	792 690	−6 835
10	6.5	−800	−8 000	13 410	−8 270
10	5.8	−800	−8 000	34 040	−7 895
				[a]3 000	−10 043

(c) Butt joints in laminations, stress ratio, R, 10; specimens 3 in. in diameter by 8 in. long

8	5.6	−900	−9 000	14 910	−8 764
10	5.5	−850	−8 500	13 850	−8 223
	5.5	−850	−8 500	20 930	−8 223
	5.3	−800	−8 000	153 030	−7 637
	5.3	−750	−7 500	82 720	−7 160
	5.2	−750	−7 500	518 430	−7 113
	[b]5.4	−750	−7 500	549 720	−7 207
	4.5	−750	−7 500	2 351 000	−6 790
				[a]3 000	−9 651

[a]Static tests—estimated equivalent cycles (table 3.2-IV).
[b]Estimated because of error in moisture content measurement.

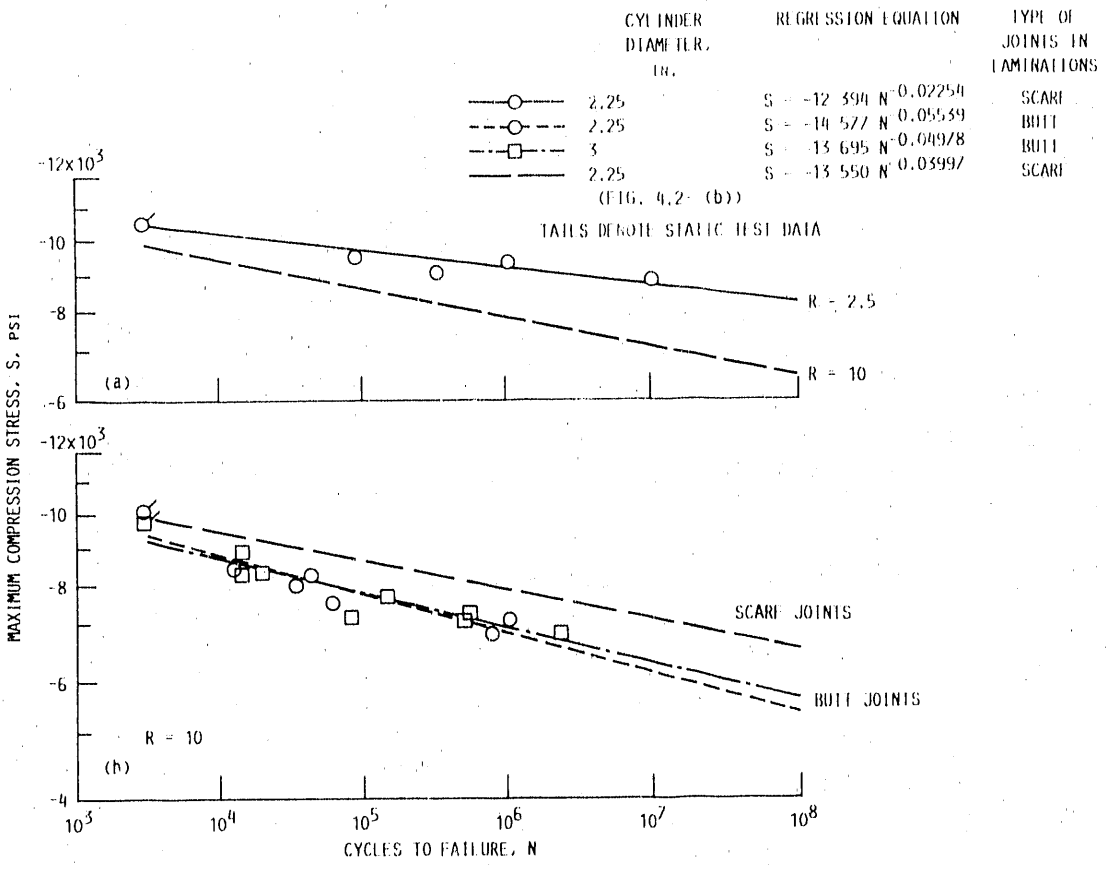

(a) 12:1 Slope scarf joints in laminations, $R = 2.5$ compared with $R = 10$.
(b) Butt joints in laminations compared with scarf joints, $R = 10$.

Figure 4.2-3.—Effect of stress ratio R and joint type on compression-compression fatigue parallel to grain for laminated Douglas fir/epoxy specimens. Cylindrical specimens 2.25 or 3 in. in diameter by 8 in. long with joints staggered 3 in. apart in center three laminations. Data corrected to 6 percent laminate moisture content ($K = 1.92$). Veneer grade, A+; test temperature, 70 °F. (r denotes correlation coefficient.)

the lamination on one side of the middle lamination overlapped by 0.5 in., and the joint in the lamination on the other side of the middle lamination underlapped by 0.25 in.

Figures 4.2-4(e), (f), and (h) show much smaller effects of overlap and gaps in the scarf joints. The gaps and overlaps are of the same magnitude as those for the specimens whose fatigue strength was shown in figure 4.2-1(b), except that each specimen whose fatigue strength is shown in figure 4.2-4 had only one type of imperfection rather than the three different types of imperfections built into each specimen in figure 4.2-1(b). Figure 4.2-4(h) shows that the specimens with overlaps, the specimens with gaps in the joints, and the specimens with no imperfections all had fatigue strength regression lines that differed by no more than 3 percent. Although there is some conflict between the data in figures 4.2-1(b) and 4.2-4(h), it appears that some misalignment in scarf joints may not seriously affect compression-compression fatigue strength.

4.2.4 Effect of compression-compression fatigue stress ratio on failure strength.—Tables 4.2-II and 4.2-III and figures 4.2-2(b) and 4.2-3(a) show compression-compression fatigue strength for $R = 2.5$ and $R = 10$ for butt joints and scarf joints in the center three laminations of cylindrical specimens 2.25 in. in diameter and 8 in. long. For both types of joints in the laminations the lower R value resulted in a shallower negative slope for the regression line and higher compression-compression fatigue strength.

4.2.5 Effect of graphite fibers between laminations on compression-compression fatigue strength.—Tests were conducted to determine the strengthening effect of unidirectional graphite fibers laid up between the 0.1-in.-thick Douglas fir plies of the laminated specimen. The veneer grade for all tests was grade A, and the compression-compression fatigue tests were conducted at $R = 10$. The graphite fiber cloth used was ORCOWEB graphite 4.75 oz/yd^2 and 0.010 in. thick. The speci-

TABLE 4.2-IV.—EFFECT OF SCARF JOINT CONFIGURATION ON COMPRESSION-COMPRESSION FATIGUE STRENGTH PARALLEL TO GRAIN

[Laminated Douglas fir/epoxy square-cross-section specimens 2 in. by 2 in. by 12 in. long. Scarf joints staggered 3 in. apart in center three laminations. Stress ratio, R, 10; veneer grade, A+; test temperature, 70 °F; cycle rate, 4 Hz. Data corrected to 6 percent laminate moisture content (K = 1.92).]

Scarf configuration	Laminate moisture content, percent	Minimum stress, psi	Maximum stress, psi	Cycles to failure	Corrected failure stress, psi
No joints	[a]6.1	−830	−8300	7 650	−8355
	6.4	−830	−8300	10 120	−8523
	6.2	−790	−7900	14 180	−8006
	6.1	−710	−7100	65 530	−7147
	[a]6.1	−740	−7400	69 700	−7449
	[a]6.1	−740	−7400	547 030	−7449
	[a]6.0	−600	−6000	[b]2 835 500	−6000
				[c]1 200	−9154
4:1 Slope	6.3	−830	−8300	1 530	−8467
	6.2	−740	−7400	10 930	−7499
	[a]6.1	−610	−6100	47 550	−6141
	5.9	−590	−5900	128 270	−5861
	[a]6.1	−560	−5600	[b]1 569 500	−5637
	[a]6.1	−540	−5400	[b]2 907 540	−5436
				[c]1 200	−9088
10:1 Slope	6.1	−790	−7900	11 870	−7953
	6.1	−790	−7900	13 810	−7953
	6.0	−710	−7100	35 850	−7100
	[a]6.0	−670	−6700	64 840	−6700
	5.8	−630	−6300	525 900	−6217
	[a]6.0	−650	−6500	[b]1 019 500	−6500
				[c]1 200	−9253
16:1 Slope	6.3	−790	−7900	10 030	−8059
	5.8	−790	−7900	16 980	−7796
	6.1	−720	−7200	73 260	−7248
	[a]6.1	−720	−7200	114 930	−7248
	[a]6.1	−650	−6500	938 460	−6543
	[a]6.1	−650	−6500	[b]2 337 140	−6543
				[c]1 200	−9278
10:1 Slope and 25-percent overlap	6.0	−690	−6900	55 400	−6900
	[a]6.2	−630	−6300	261 190	−6384
				[d]1 200	−9186
10:1 Slope and 50-percent overlap	6.1	−760	−7600	18 630	−7651
	[a]6.0	−770	−7700	19 510	−7700
	5.9	−710	−7100	61 370	−7053
	[a]6.0	−690	−6900	65 860	−6900
	[a]6.0	−710	−7100	499 420	−7100
	[a]6.0	−640	−6400	529 890	−6400
				[d]1 200	−9160
10:1 Slope and 25-percent gap	5.9	−690	−6900	59 530	−6854
	[a]5.9	−620	−6200	[b]1 260 000	−6159
				[d]1 200	−9090
10:1 Slope and 50-percent gap	6.0	−770	−7700	5 430	−7700
	5.8	−740	−7400	21 520	−7303
	[a]5.9	−690	−6900	45 630	−6854
	[a]5.9	−640	−6400	115 790	−6358
	5.9	−680	−6800	156 640	−6755
	5.6	−630	−6300	976 100	−6135
				[d]1 200	−8993

[a]Estimated laminate moisture content.
[b]Specimen did not fail.
[c]Static tests—estimated equivalent cycles (table 3.2-V).
[d]Static tests—no overlap or gap—estimated equivalent cycles (table 3.2-V).

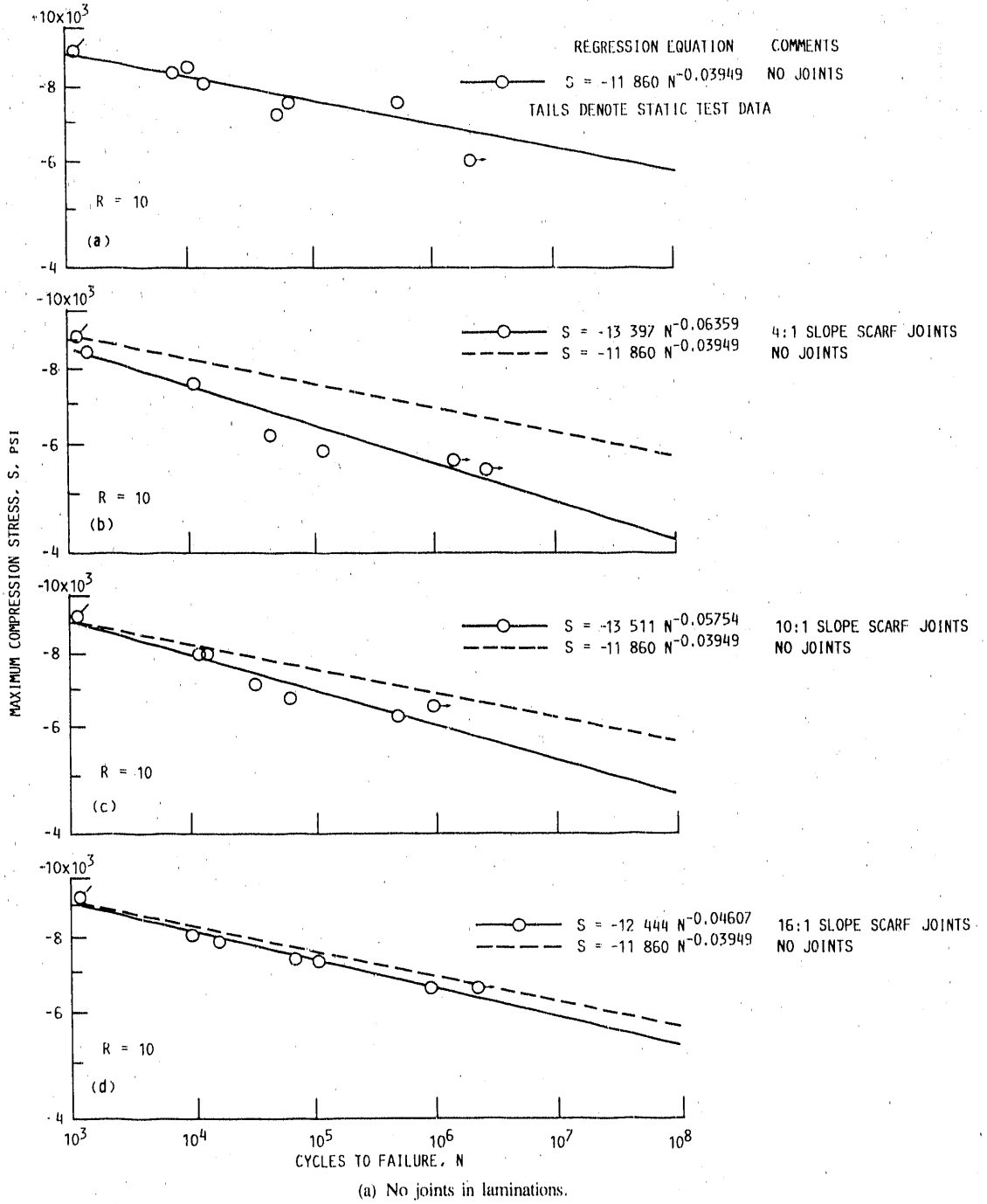

(a) No joints in laminations.
(b) 4:1-Slope scarf joints.
(c) 10:1-Slope scarf joints.
(d) 16:1-Slope scarf joints.

Figure 4.2-4.—Effect of scarf slope and imperfections in lamination joints for compression-compression fatigue (R = 10) parallel to grain in laminated Douglas fir/epoxy specimens. Square-cross-section specimens 2 in. by 2 in. by 12 in. long with scarf joints staggered 3 in. apart in center three laminations. Data corrected to 6 percent laminate moisture content (K = 1.92). Veneer grade, A+; test temperature, 70 °F.

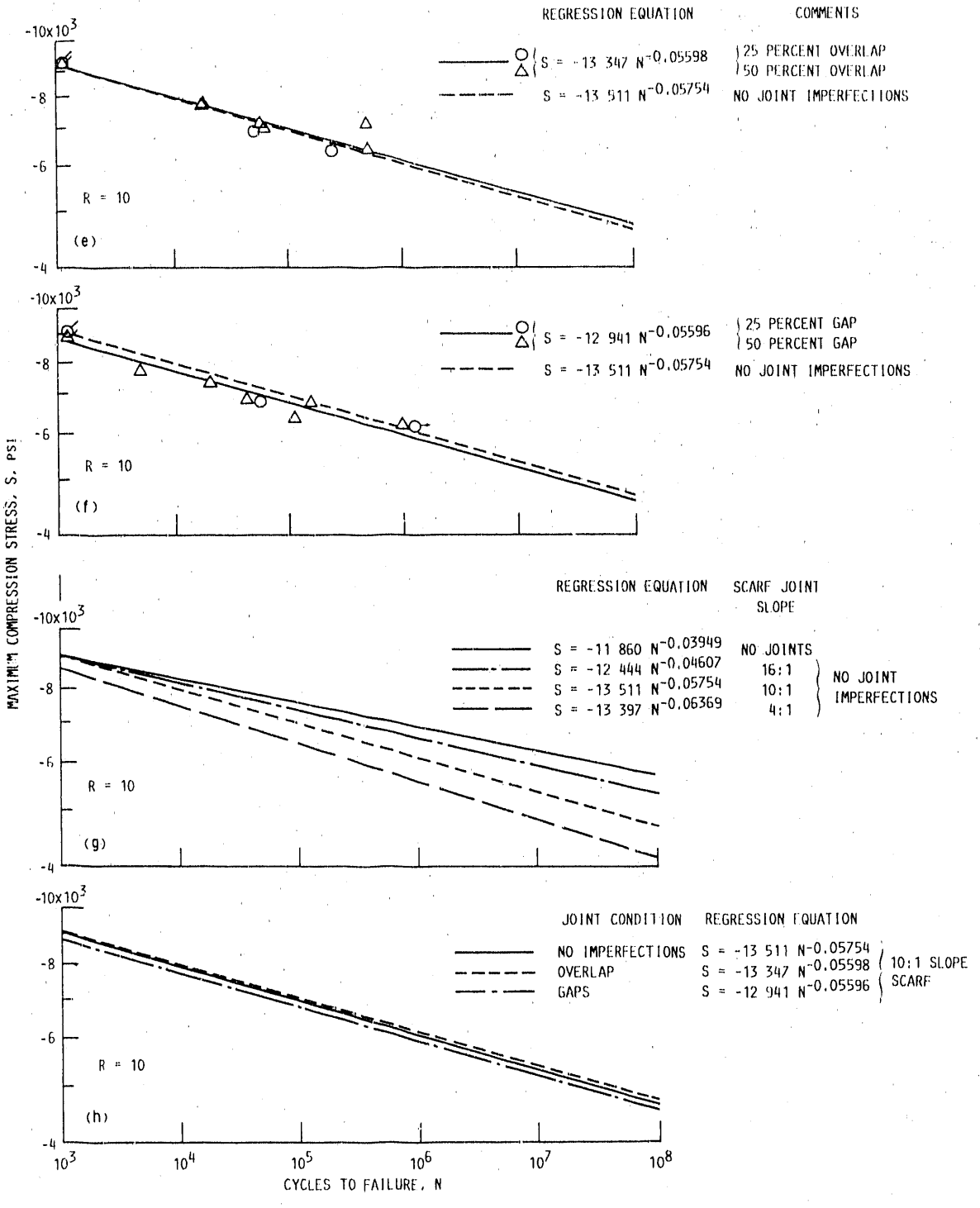

(e) 10:1-Slope scarf joints. Scarfs had overlaps of 25 or 50 percent in joints.
(f) 10:1-Slope scarf joints. Scarfs had gaps of 25 or 50 percent in joints.
(g) Summary of scarf slope effects.
(h) Summary of effects of imperfections in 10:1-slope scarf joints.

Figure 4.2-4.—Concluded.

men size was 1.86 by 1.86 by 7.44 in. There were no joints in the laminates. Tests were conducted at temperatures from −40 to 120 °F. Data are shown in table 4.2–V and figure 4.2–5.

Figure 4.2–5(a) shows the compression-compression fatigue data for Douglas fir/epoxy laminates at a test temperature of 75 °F without any graphite fiber augmentation. The regression line has a smaller slope than similar data from figure 4.2–4(a), indicating less sensitivity to the number of cycles over the range tested. The test specimens for figure 4.2–4(a) were 2 by 2 by 12 in. and hence had an aspect ratio of 6 as compared with the aspect ratio of 4 for the 1.86- by 1.86- by 7.44-in. specimens in figure 4.2–5(a). The fatigue strength values shown in both figures at 10 million cycles are consistent with those shown in figure 10 of chapter III, which presents a model of the effect of specimen aspect ratio on compression-compression fatigue strength.

The effect of test temperature on specimens without graphite fiber augmentation can be seen in figure 4.2–5(b). Although regression lines are shown for each test temperature, the data appear to be inconsistent, and it is suggested that the regression lines not be used for design purposes, particularly those from the low-temperature tests that have an unbelievable positive slope. The tests at 120 °F appear to show a high negative regression line slope that results in a large temperature effect on high-cycle fatigue strength.

Figure 4.2–5(c) illustrates the strengthening effect of the graphite fibers between the wood plies. The slope of the regression line at a test temperature of 75 °F was flat. The augmented specimens were on the order or 35 to 48 percent stronger than the unaugmented specimens over the range of cycles to failure investigated. Test data at 120 °F and for the low temperatures of −20 to −40 °F were sparse and erratic but indicated the trend of higher fatigue strength with lower temperature.

Tests were also conducted on the effects of partial augmentation with graphite fibers. In this case the graphite fibers were placed between the center 12 wood plies only. In addition the length of fiber augmentation varied. Between the center laminations the fibers extended for a distance of 6 in. from one end of the specimen. In adjacent laminations the fiber augmentation lengths were 5, 4, 3, 2, and 1 in., beginning at the end of the specimen. This arrangement resulted in a greater length of augmentation in the middle of the specimen and less toward one end. On the other end there was no augmentation. The results of these tests are shown in figure 4.2–5(d). The effect from this partial augmentation was small—on the order of 5 percent over the entire range of cycles to failure investigated. These data show that if it is necessary to provide fiber augmentation in some portions of a structure and not in others, step tapering of the augmentation can be used to terminate the augmentation without significantly affecting the strength of the downstream unaugmented structure.

4.2.6 Effects of specimen configuration and laminate joints on compression-compression fatigue strength.—Figure 4.2–6 is a compilation of regression lines from figures 4.2–1, 4.2–3, 4.2–4, and 4.2–5. Probably the most obvious feature of the plot is the regression line for 1.86- by 1.86- by 7.44-in. specimens, which shows a flatter slope and higher strength at high cycles to failure than the regression lines for all other configurations. The explanation for this flatter slope is not completely clear, but it is probably a combination of aspect ratio and absence of laminate joints in the specimens. Fatigue strength lines shown in the figure for the two types of specimens without joints tended to have flatter slopes than those for the specimens with joints in the laminations. At 10 million cycles the fatigue strengths in figure 4.2–6 for all types of specimens are consistent with the model of the effects of laminate joint and specimen aspect ratio illustrated in figure 10 of chapter III. Higher specimen aspect ratios, steeper slopes, or both in the laminate joints resulted in lower compression-compression fatigue strength.

4.2.7 Effect of stress concentrations from circular cutouts on compression-compression fatigue strength.—Rectangular test specimens were used for these tests. The specimens were 1.5 in. thick (15 laminations of grade A+ Douglas fir/epoxy), 6 in. wide, and 12 in. long as shown in figure 2.2–9. Compression-compression fatigue tests were conducted with a stress ratio R of 10. A 2-in.-diameter circular cutout was placed in the specimens. Tests were made without any augmentation of the laminate or reinforcement in the hole. Other tests were made in which 10-oz/yd^2 Burlington Style 7550 glass fiber fabric was placed between the wood plies with the glass fibers oriented at 45° to the wood grain direction. In addition, the hole in some specimens was reinforced by placing a ring of glass fabric/epoxy inside the hole. The 0.12-in.-thick ring reduced the hole diameter to 1.75 in. Hereinafter the glass fabric between plies will be called augmentation, and the glass fabric/epoxy ring in the hole will be called reinforcement.

The results of tests are presented in table 4.2–VI and figure 4.2–7. Figure 4.2–7(a) shows the compression-compression fatigue strength of the specimens with the cutout but without augmentation or reinforcement. Also shown is the regression line from figure 4.2–4(a) for 2- by 2- by 12-in. specimens of grade A+ veneers without a cutout. The stress concentration of the cutout reduced the compression-compression fatigue strength approximately 38 percent. The fatigue strength reduction from cutouts was much higher than the static compression strength reduction discussed in subsection 3.2.1.7.

Note the large reduction in actual fatigue in relation to the data point based upon static testing. The difference in compression strength was approximately 3200 psi. Such differences were not found for specimens that did not contain cutouts.

Figure 4.2–7(b) shows the effect of augmentation, reinforcement, or both. Augmentation alone or reinforcement alone only minimally improved the strength of the specimens with the cutouts. However, combining augmentation with reinforcement resulted in about a 20-percent improvement in the compression-compression fatigue strength, but only about half of the strength lost by installing the cutout was regained.

TABLE 4.2–V.—EFFECT OF GRAPHITE FIBER FABRIC AUGMENTATION ON COMPRESSION-COMPRESSION FATIGUE STRENGTH PARALLEL TO GRAIN

[Laminate: Douglas fir/epoxy specimens. Data not corrected for moisture content. Laminate moisture content in range 4 to 7 percent (not measured).]

(a) No graphite fiber fabric augmentation. Specimens 1.86 in. by 1.86 in. by 7.44 in. long.

Test temperature, °F	Cycle rate, Hz	Minimum stress, psi	Maximum stress, psi	Cycles to failure
75	10	−860	−8 600	31 970
	10	−791	−7 910	11 960
	10	−814	−8 140	15 328
	8	−838	−8 380	281 400
		−766	−7 660	307 900
		−802	−8 020	[a]3 632 400
		−694	−6 940	[a]5 185 700
		0	−9 708	[b]2 400
120	8	−785	−7 850	4 307
		−764	−7 640	10 233
		−758	−7 580	5 578
		−672	−6 720	15 499
		0	−8 285	[b]2 400
−40 to −20	8	−1069	−10 690	24 100
−40 to −20	8	−1027	−10 270	300
−40 to −20	8	−1065	−10 650	900
		0	−12 020	[b]2 400

(b) Graphite fiber fabric augmentation between wood plies. Specimens 1.86 in. by 1.86 in. by 7.44 in. long.

Test temperature, °F	Cycle rate, Hz	Minimum stress, psi	Maximum stress, psi	Cycles to failure
75	10	−1224	−12 240	13 658
	10	−1072	−10 720	9 961
	10	−1216	−12 160	15 946
	8	−1186	−11 860	1 316 600
		−1213	−12 130	4 209 500
		−1032	−10 320	37 800
		−1033	−10 330	1 534 300
		−1230	−12 300	64 200
		−1150	−11 500	[a]4 269 000
		0	−13 181	[b]2 400
120	8	998	−9 980	7 856
120	8	763	−7 630	3 444
		0	−10 303	[b]2 400
−40 to −20	8	−1464	−14 640	[a]10 000
−40 to −20	8	−1464	−14 640	5 900
		0	−16 310	[b]2 400

(c) Partial graphite fiber fabric augmentation between 12 plies over a portion of specimen length. Graphite fiber fabric lengths varied from 1 to 6 in. from one end of specimen in a stepped configuration. Specimens 2 in. by 2 in. by 8 in. long.

Test temperature, °F	Cycle rate, Hz	Minimum stress, psi	Maximum stress, psi	Cycles to failure
75	8	−797	−7 970	29 800
		−797	−7 970	21 592
		−769	−7 690	53 900
		−769	−7 690	74 500
		−751	−7 510	91 500
		−725	−7 250	82 000
		−700	−7 000	274 100
		−650	−6 500	10 105 500
		−830	−8 300	989 400
		−778	−7 780	5 592 100
		−768	−7 680	6 087 700
		−830	−8 300	1 119 200
		−820	−8 200	3 442 800

[a]Specimen did not fail

[b]Static tests—estimated equivalent cycles (table 3.2–IV)

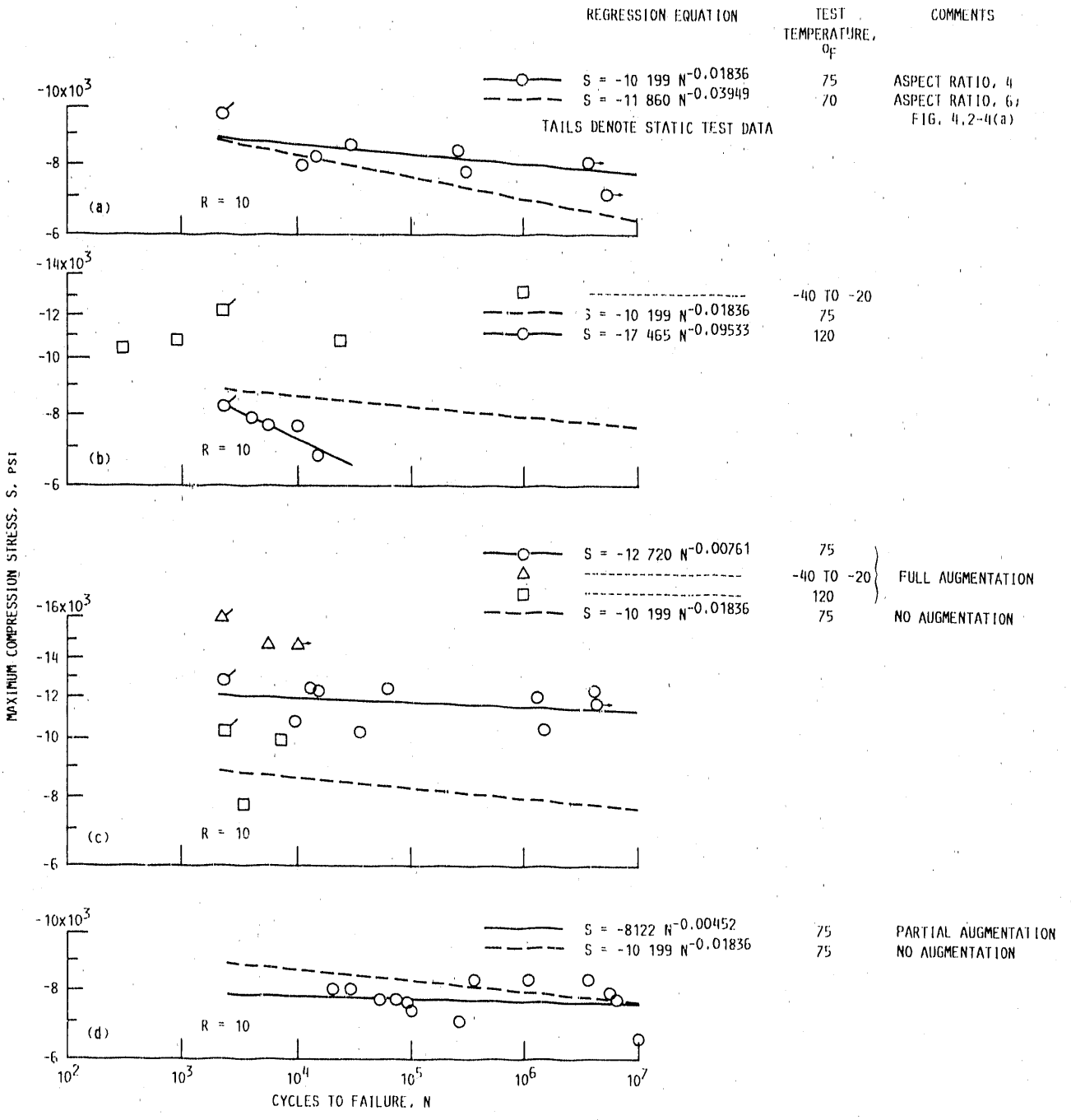

(a) No graphite fiber augmentation. Test temperature, 75 °F.

(b) No graphite fiber augmentation. Range of test temperatures.

(c) Graphite fiber augmentation between wood plies. Test temperature, −40 to 120 °F.

(d) Partial graphite fiber augmentation between 12 plies over a portion of specimen length. Graphite fiber lengths varied from 1 to 6 in. from one end of specimen in a stepped configuration. Test temperature, 75 °F.

Figure 4.2-5.—Effect of graphite fiber augmentation between laminations on compression-compression fatigue ($R = 10$) parallel to grain for laminated Douglas fir/epoxy specimens. Square-cross-section specimens 1.86 in. by 1.86 in. by 7.44 in. long without joints in the laminations. Data not corrected for moisture content; laminate moisture content, 4 to 7 percent. Veneer grade, A.

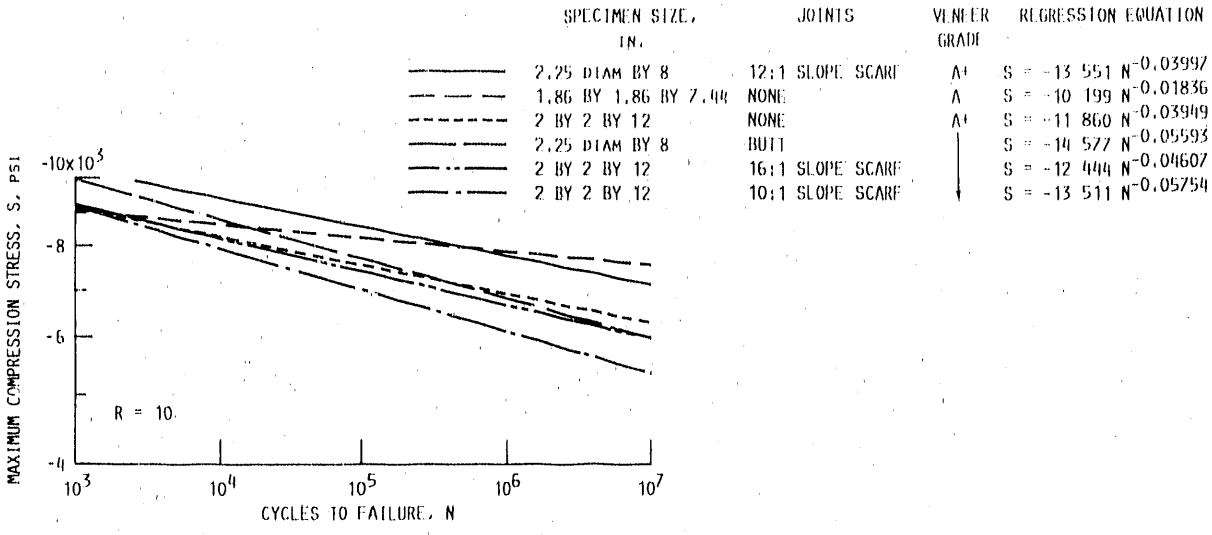

Figure 4.2-6.—Comparison of compression-compression fatigue (R = 10) regression curves for variations in specimen and laminate joint configurations. Regression curves from figures 4.2-1, 4.2-3, 4.2-4, and 4.2-5. All data corrected to 6 percent laminate moisture content (K = 1.92). Test temperature, 70 °F.

TABLE 4.2-VI.—EFFECT OF 2-in.-DIAMETER CIRCULAR CUTOUT ON COMPRESSION-COMPRESSION FATIGUE STRENGTH PARALLEL TO GRAIN

[Laminated Douglas fir/epoxy rectangular bar 1 5 in. by 6 in. by 12 in. long. Veneer grade, A+; test temperature, 70 °F; cycle rate, 8 Hz. Data corrected to 6 percent laminate moisture content (K = 1.92).]

(a) No glass fiber fabric augmentation or reinforcement sleeve

Laminate moisture content, percent	Minimum stress, psi	Maximum stress, psi	Cycles to failure	Corrected failure stress, psi
5.2	−621	−6211	13 530	−5 890
5.2	−684	−6835	2 390	−6 482
5.2	−546	−5462	644 700	−5 180
---	-----	------	[a]2 400	−9 744

(b) Glass fiber fabric augmentation, but no reinforcement sleeve

4.6	−632	−6325	20 660	−5 764
4.6	−578	−5778	293 600	−5 266
---	-----	------	[a]2 400	−10 157

(c) Glass fiber/epoxy reinforcement sleeve, but no glass fiber fabric augmentation

5.2	−649	−6488	25 170	−6 153
5.2	−732	−7317	3 400	−6 939
5.2	−590	−5897	170 000	−5 592
---	-----	------	[a]2 400	−10 646

(d) Glass fiber fabric augmentation and glass fiber/epoxy reinforcement sleeve

4.6	−713	−7130	186 950	−6 498
4.6	−703	−7029	622 640	−6 406
---	-----	------	[a]2 400	−10 903

[a]Static test; estimated equivalent cycles (table 4.2-VIII).

4.2.8 Closing remarks on compression-compression fatigue strength.—The following significant results were obtained from the tests of Douglas fir/epoxy specimens in compression-compression fatigue:

1. Correcting compression-compression fatigue strength data for laminate moisture content by the same method used for static compression of clear wood specimens provided an excellent correlation for the range of moisture contents investigated.

2. Tests made on specimens of grade A+ and A veneers with butt joints in the laminations showed no significant effect of veneer grade on compression-compression fatigue strength.

3. Specimens containing 12:1-slope scarf joints in the center three laminations had compression-compression fatigue strengths 11 to 19 percent higher than similar specimens containing butt joints in the laminations.

4. Scarf joints in laminates were investigated over a range of slopes from 4:1 to 16:1. The shallower slopes were consistently stronger than the steeper slopes. As the slopes became steeper, the specimens started approaching the strength characteristics of specimens containing butt joints.

5. Imperfect scarf joints in which the joints overlapped or had gaps were weaker than more perfectly aligned scarfed laminates, with compression-compression fatigue strength losses ranging from less than 3 percent to as much as 12 percent depending upon the combination of imperfections in the joints.

6. Compression-compression fatigue tests at a stress ratio R of 2.5 resulted in regression lines having a shallower slope and greater strength at high cycles to failure than did tests at R = 10.

7. Unidirectional graphite fibers placed between the wood plies had a significant effect on compression-compression fatigue strength. Strength increases up to 48 percent over those of unaugmented specimens were measured.

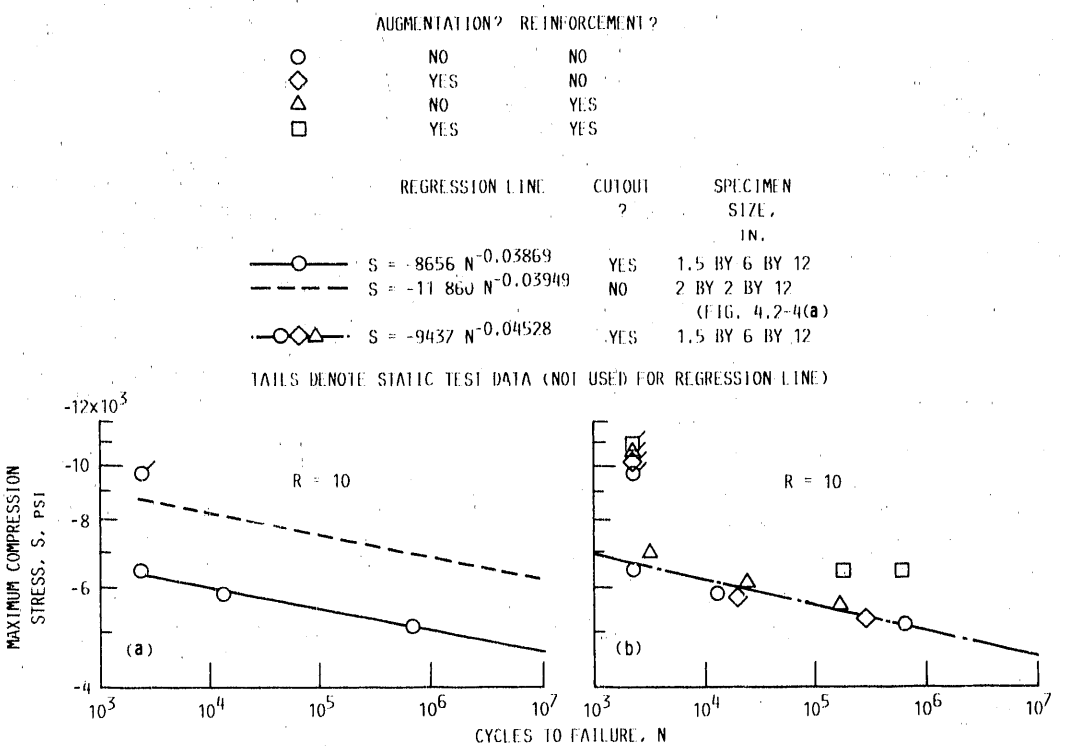

(a) No glass fiber fabric augmentation nor reinforcement sleeve.
(b) Effect of glass fiber fabric augmentation between laminations, glass fiber/epoxy reinforcement sleeve in cutout, or both.

Figure 4.2-7.—Effect of 2-in.-diameter circular cutout on compression-compression fatigue (R = 10) parallel to grain for laminated Douglas fir/epoxy specimens. Rectangular-cross-section specimens 1.5 in. by 6 in. by 12 in. long. Data corrected to 6 percent laminate moisture content (K = 1.92). Veneer grade, A+; test temperature, 70 °F.

8. A 2-in.-diameter circular cutout in a specimen 6 in. wide reduced the compression-compression fatigue stress approximately 38 percent. Approximately half of that strength reduction could be regained by augmenting the laminate with glass fiber cloth between the wood plies and placing a glass fiber/epoxy ring 0.12 in. thick inside the cutout.

4.3 Reverse Axial Tension-Compression Fatigue

4.3.1 Effect of moisture content on reverse axial tension-compression fatigue strength.—Reverse axial tension-compression fatigue does not have a direct counterpart in static testing. Therefore it cannot be expected that the same constant K in equation (7) of chapter III that was used for static testing will be applicable for this type of fatigue. The value of K to use was therefore obtained by a trial-and-error process to determine a K value that would result in a high correlation coefficient r for the data. Data corrected to 6 percent laminate moisture content by using several values of K are presented in table 4.3-I and figure 4.3-1. Figure 4.3-1(a) shows a plot of uncorrected data for laminate moisture contents from 4.3 to 9.7 percent. The tests were conducted on dogbone specimens with a 2.25-in.-diameter test section and an overall length of 57 in. as illustrated in figure 2.2-13. The specimens were fabricated from grade A+ laminates with 12:1 slope scarf joints in the center three laminates staggered 3 in. apart in adjacent laminations. The stress ratio R for the tests was -1 with the magnitudes of the stresses in compression and tension being equal. All tests were conducted at 70 °F.

The plotted data points, with the indicated moisture contents, in figure 4.3-1(a) show considerable scatter in the data, with moisture contents of less than 6 percent generally lying above the regression line and moisture contents greater than 6 percent generally lying below the regression line. The correlation coefficient was only -0.6831. Figure 4.3-1(b) shows correlation lines of data corrected to 6 percent moisture content by using values of K that corresponded to those used for static tension (1.21) and static compression (1.92). The corresponding correlation coefficients for these two cases were -0.7960 and -0.8304, respectively, an indication of improved correlation of the data relative to the case where the data were not corrected for moisture content. Averaging the K values for tension and compression yielded a value of 1.57. It is interesting to note (and most likely a coincidence) that no other value of K (to three significant figures) resulted in a higher correlation coefficient, -0.8715, for the data presented in table 4.3-I.

For the data evaluated in this investigation the regression line was not significantly affected by the value of K used for

TABLE 4.3-I.—EFFECT OF MOISTURE-CONTENT CORRECTION ON REVERSE AXIAL TENSION-COMPRESSION FATIGUE STRENGTH PARALLEL TO GRAIN

[Laminated Douglas fir/epoxy dogbone specimens with 2.25-in.-diameter test section by 57-in. overall length. 12:1-Slope scarf joints staggered 3 in. apart in center three laminations. Stress ratio, R, −1; test temperature, 70 °F.]

(a) Correctly aligned scarf joints

Cycle rate, Hz	Laminate moisture content, percent	Maximum tension stress, psi	Maximum compression stress, psi	Cycles to failure	Corrected failure stress, psi		
					K = 1.21	K = 1.92	K = 1.57
2.2	4.7	6500	−6500	17 710	6338	5963	6134
3.0	6.6	5500	−5500	32 400	5564	5723	5649
	9.6	4500	−4500	34 360	4825	5714	5283
	8.8	4500	−4500	1 323 640	4751	5418	5098
	6.7	5000	−5000	643 400	5068	5238	5158
	4.8	5500	−5500	486 250	5374	5079	5214
	4.3	5200	−5200	699 500	5031	4646	4821
	4.5	5000	−5000	355 450	4857	4527	4677
	6.2	4000	−4000	10 169 100	4016	4053	4036
	9.7	3750	−3750	[a]2 592 180	4029	4793	4422
	8.8	3500	−3500	[b]10 260 000	3695	4214	3695

(b) Three scarf joints in each specimen containing (1) 0.5-in. overlap, (2) 0.25-in. overlap, and (3) 0.25-in. underlap. Stresses corrected for K = 1.57 only

3.0	4.5	4000	−4000	770 030	-----	-----	3741
3.0	5.3	5000	−5000	29 890	-----	-----	4846
2.5	5.7	6000	−5000	8 900	-----	-----	5920

[a]Premature failure outside of test section
[b]Specimen did not fail.

correlating the data. The reason for the small differences for different values of K is that the experimental data were obtained for laminate moisture contents scattered on either side of the value of 6 percent to which the data were corrected. For extrapolation of the data to values significantly different from 6 percent the proper value of K is more important. From the data available the value of K to use for reverse axial tension-compression fatigue was 1.57. Imperfections in scarf joints can cause large reductions in tension-compression fatigue strength, as indicated by the data in table 4.3-I(b).

4.3.2 Effect of laminate joint configuration on reverse axial tension-compression fatigue strength.—Tests were conducted on dogbone specimens of grade A+ Douglas fir/epoxy. The specimens were 2.25 in. in diameter by 8 in. long at the test section with an overall length of 57 in., and the center three laminations contained either 12:1-slope scarf joints or butt joints. The joints were staggered 3 in. apart in adjacent laminations. The tests were conducted at $R = -1$. The data corrected to 6 percent laminate moisture content for butt-jointed specimens are shown in table 4.3-II and figure 4.3-2(a) along with the regression line for scarf-jointed specimens from figure 4.3-1(d). The slope of the regression line was steeper for the butt-jointed specimens, and they were weaker than the scarf-jointed specimens at high cycles to failure. The trend shown for reverse axial tension-compression fatigue, in which the regression lines for butt and scarf joints cross, is probably unrealistic. More low-cycle data would be required to better establish the regression line slopes, particularly for the specimens with scarf joints.

4.3.3 Effect of specimen size on reverse axial tension-compression fatigue strength.—Tests were conducted on specimens that were 3 by 8 by 360 in. (7488-in.^{3} test section volume) as well as on dogbone specimens with 31.8-in.^{3} test section volume. All specimens were grade A+ Douglas fir/epoxy with 12:1-slope scarf joints in the laminations. The dogbone specimens had joints in only the center three laminations; the large specimens had joints in each lamination at 8-ft intervals. The joints in adjacent laminations were displaced by 3 in. Figure 4.3-2(b) shows regression lines for small and large specimens. The fatigue strength of the small specimens was on the order of 1.5 times that of the large specimens. This trend was similar to that found for tension-tension fatigue in figure 4.1-3. The large specimens tested in tension-tension fatigue were smaller (4992-in.^{3} test section volume) than the specimens tested in reverse axial tension-compression fatigue. Data were not available to determine any differences in fatigue strength for specimens varying between 4992- and 7488-in.^{3} test section volume.

4.3.4 Effect of veneer grade on reverse axial tension-compression fatigue strength.—Table 4.3-II and figure 4.3-2(c) show data for two veneer grades, A+ and A, for dogbone

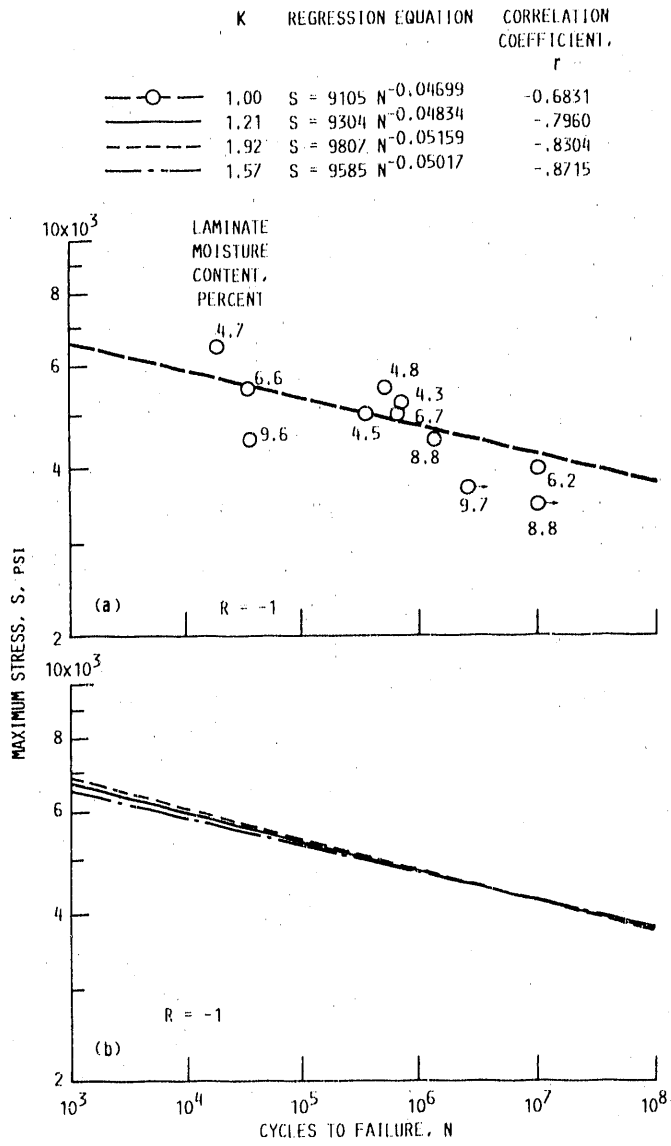

(a) Data not corrected for moisture content.

(b) Comparison of least-squares lines for various moisture-content corrections (K = 1.21 – Value for tension; K = 1.92 – Value for compression; K = 1.57 – Average for tension and compression).

Figure 4.3-1.—Moisture correction for reverse axial tension-compression fatigue (R = –1) parallel to grain in laminated Douglas fir/epoxy specimens. Dogbone specimens with 2.25 in. diameter test section (fig. 2.2-13) and 12:1 slope scarf joints staggered 3 in. apart in center three laminations. Veneer grade, A+; test temperature, 70 °F.

TABLE 4.3-II.—EFFECTS OF SPECIMEN SIZE AND JOINT TYPE ON REVERSE AXIAL TENSION-COMPRESSION FATIGUE STRENGTH PARALLEL TO GRAIN

[Laminated Douglas fir/epoxy specimens. Stress ratio, R, −1; test temperature, 70 °F. Data corrected to 6 percent laminate moisture content ($K' = 1.55$).]

(a) Butt joints in veneer grade A+ dogbone specimens with 2.25-in.-diameter test section (31.8-in.^{3} test section volume)

Cycle rate, Hz	Laminate moisture content, percent	Minimum stress, psi	Maximum stress, psi	Cycles to failure	Corrected failure stress, psi
2.2	5.2	7500	−7500	2 360	7237
↓	6.4	7000	−7000	3 060	7126
↓	6.2	6000	−6000	2 450	6054
↓	5.3	5000	−5000	227 650	4846
↓	5.7	4500	−4500	138 710	4440
↓	5.6	4500	−4500	551 940	4421
2.5	6.3	4000	−4000	632 420	4054
3.0	5.5	3400	−3400	8 262 200	3325
↓	6.3	3500	−3500	5 926 310	3547
↓	5.1	3200	−3200	23 672 280	3074
↓	5.7	3500	−3500	4 079 940	3454
↓	5.9	4000	−4000	895 000	3982
↓	4.9	4000	−4000	728 800	3809

(b) Scarf joints in very large grade A+ specimens with 3- by 8- by 360-in. test section (7488-in.^{3} test section volume)

(a)	6.3	3750	−3750	40 654	3800
↓	[b]6.2	3122	−3122	[c]1 300 000	3150
↓	6.4	3500	−3500	303 068	3308
↓	6.1	3000	−3000	1 050 000	3013

(c) Butt joints in veneer grade A dogbone specimens with 2.25-in.-diameter test section (31.8-in.^{3} test section volume)

3.0	6.9	3320	−3320	698 500	3456
↓	5.4	3500	−3500	4 764 600	3408
↓	6.0	4700	−4700	204 600	4700
↓	6.1	3700	−3700	2 635 700	3717
2.7	5.5	4500	−4500	175 030	4401
3.0	5.5	4000	−4000	479 280	3912
2.5	5.7	5000	−5000	44 620	4934
3.0	5.5	3700	−3700	2 138 300	3619
3.0	6.0	4700	−4700	150 700	4700

[a]Not specified
[b]Estimated
[c]Specimen did not fail.

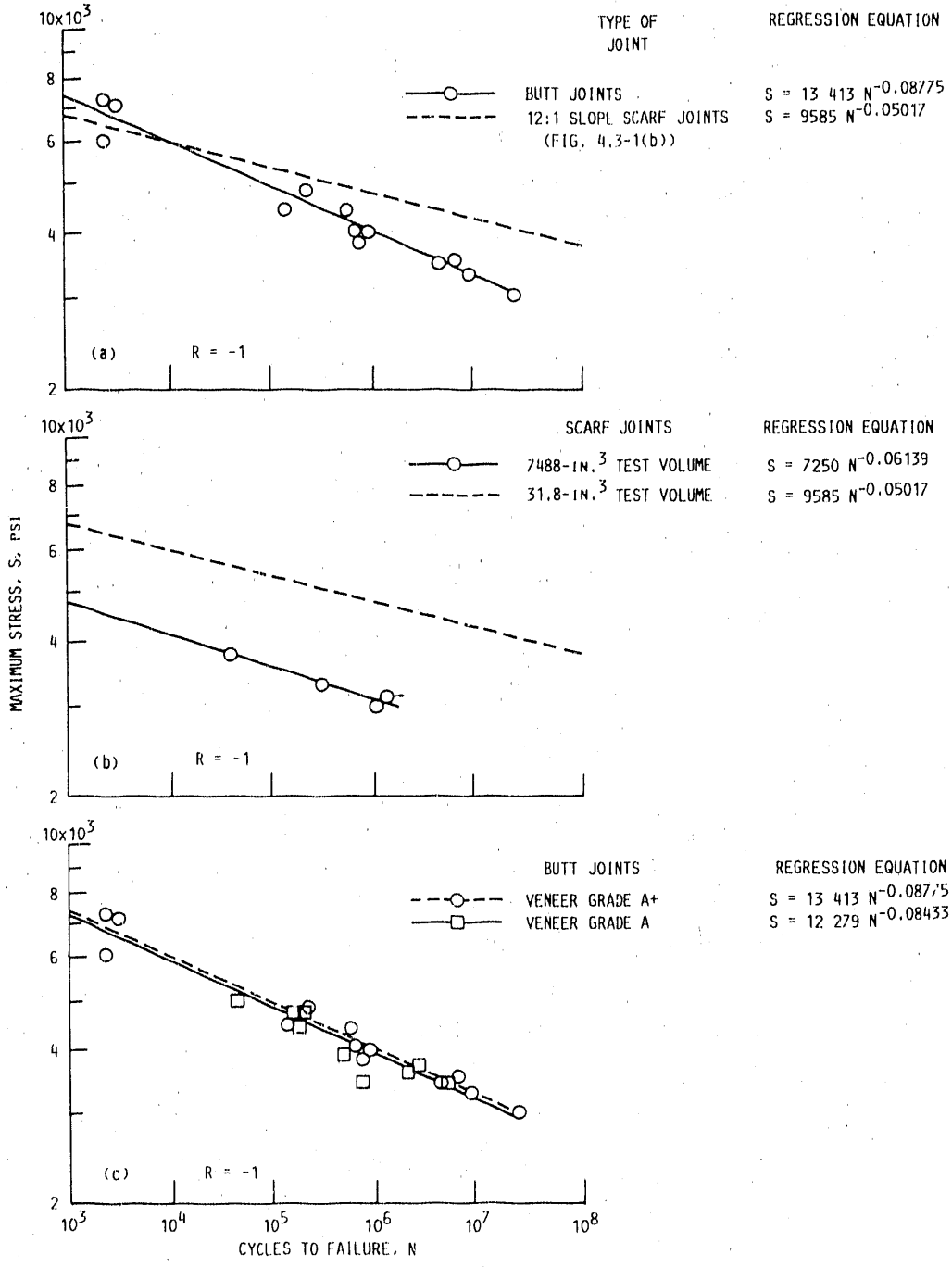

(a) Butt joints in dogbone specimens with 2.25-in.-diameter test section (fig. 2.2-13). Test section volume, 31.8 in.^{3}; veneer grade, A+.
(b) Scarf joints in large, rectangular-cross-section specimens 3 in. by 8 in. by 360 in. long. Test section volume, 7488 in.^{3}; veneer grade, A+.
(c) Effect of veneer grade for butt-jointed specimens in dogbone configuration.

Figure 4.3-2.—Effect of specimen size and joint type in laminations on reverse axial tension-compression fatigue ($R = -1$) parallel to grain for laminated Douglas fir/epoxy specimens. Data corrected to 6 percent laminate moisture content ($K = 1.57$). Test temperature, 70 °F.

specimens with butt joints in the center three laminations. The effect of veneer grade was small. These results are consistent with those found for tension-tension fatigue (fig. 4.1-2(b)) and for compression-compression fatigue (fig. 4.2-2(a)).

4.3.5 Closing remarks on reverse axial tension-compression fatigue.—In general the results of tests in reverse axial tension-compression fatigue exhibited trends similar to those for tension-tension fatigue and compression-compression fatigue. The constant K used in calculating the effect of moisture content on reverse axial tension-compression fatigue was found to be exactly the average of the constants used for tension-tension and compression-compression fatigue when the experimental data were correlated to obtain a maximum correlation coefficient r. Scarf joints in the laminations were found to have higher fatigue strength than butt joints, similar to the results for tension-tension or compression-compression fatigue. The fatigue strength of large specimens was found to be reduced relative to small specimens by about the same proportion for tension-tension fatigue and reverse axial tension-compression fatigue. Similar data were not available for compression-compression fatigue. Tests of grades A+ and A veneers for all three types of fatigue showed only small differences in fatigue strength as a result of veneer grade.

5.0 Damping Characteristics of Laminated Composite Specimens

A limited number of tests were conducted by F.K. Bechtel and J.R. Allen of Metriguard, Inc., Pullman, Washington, to determine the damping ratio of four laminated Douglas fir/epoxy specimens that were 1.5 in. thick (15 laminations) by 2 in. wide and ranged in length from 166 to 235.6 in. Tests were conducted on apparatus illustrated in figure 2.4-1 and test equipment listed in table 2.4-I. Tests were conducted on the bare specimens as illustrated in the figure and also with an 8-lb weight in the center of the span. Damping ratio ζ was determined by two methods: The vibration signal was processed by the E-Computer listed in table 2.4-I to determine material weight, density, modulus of elasticity, and number of vibration cycles N required for the vibration amplitude to decay from a threshold value to $1/e$ (e is base of natural logarithms) of the threshold value. The damping ratio was then calculated from the equation

$$\zeta = \frac{1}{\left| 1 + (2\pi N)^2 \right|^{1/2}}$$

The second method was similar except that the vibration signal stored in the oscilloscope was recorded and measurements were made to determine a value of R' by scaling the recorded waveform, where R' is the maximum minus minimum (peak to peak) amplitude of one vibration cycle divided by the maximum minus minimum amplitude N cycles later. Although N is an arbitrary number of cycles, measurement error is better averaged by choosing a large value of N. Then

$$\zeta = \frac{1}{\left[1 + \left(\frac{2\pi N}{\ln R'} \right)^2 \right]^{1/2}}$$

Values of the damping ratio ζ and the modulus of elasticity E are listed in table 5.0-I along with the dimensions, weight, and density of the test specimens. The data without mass loading on the specimen are plotted in figure 5.0-1. Note that there were four test pieces labeled P1, P2, P3, and P4. Tests were also made on the four faces F1, F2, F3, and F4 as labeled in figure 2.4-7.

The results in table 5.0-I and figure 5.0-1 show all of the damping ratios to be in the range 0.00215 to 0.00300, with

TABLE 5.0-I.—DAMPING RATIO FOR DOUGLAS FIR/EPOXY SPECIMENS CONTAINING 15 LAMINATIONS

(a) Test pieces

Piece	Length, in.	Thickness, in.	Width, in.	Weight, lb	Density, lb/ft^3
P1	178.5	1.51	2.03	13.2	42.2
P2	166.0	1.49	2.01	10.7	37.6
P3	223.6	1.53	2.02	15.7	39.6
P4	235.6	1.50	2.02	15.3	37.4

(b) Test results with no concentrated mass on test piece

Piece and test face	E-Computer measurements			From amplitude envelope		
	Modulus of elasticity, E	Number of cycles, N	Damping ratio, ζ	Number of cycles, N	Amplitude ratio, R'	Damping ratio, ζ
P1F1	2.71×10^6	56	0.00284	93	5.757	0.00300
P1F2	2.60	65	.00245	122	7.497	.00263
P1F3	2.71	56	.00284	---	-----	-------
P1F4	2.60	64	.00249	---	-----	-------
P2F1	2.33	66	.00241	103	5.450	.00262
P2F2	2.31	68	.00234	139	8.247	.00242
P2F3	2.33	66	.00241	---	-----	-------
P2F4	2.30	69	.00231	---	-----	-------
P3F1	2.48	64	.00249	57	2.435	.00248
P3F2	2.51	72	.00221	77	3.032	.00229
P4F1	2.38	60	.00265	52	2.443	.00273
P4F2	2.30	66	.00241	69	2.988	.00252

(c) Test results with 8-lbm load in center of span

P3F1	--------	70	0.00227	40	1.829	0.00240
P3F2	--------	74	.00215	54	2.174	.00229
P4F1	--------	64	.00249	---	-----	-------
P4F2	--------	68	.00234	47	2.070	.00246
P4F2	--------	---	-------	47	2.077	.00248

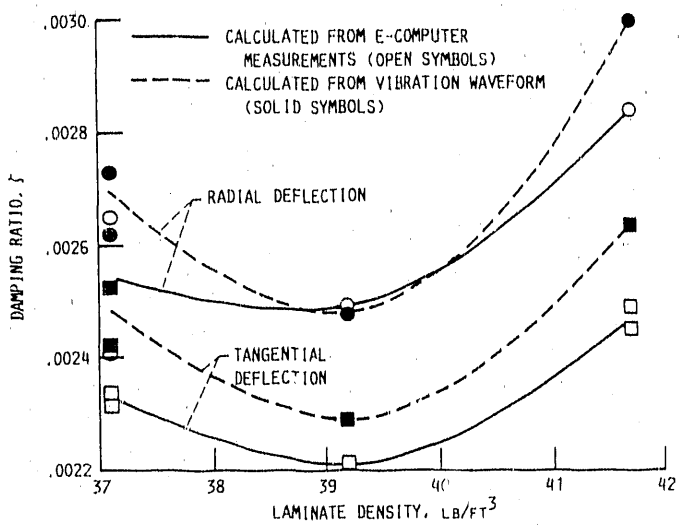

Figure 5.0-1.—Damping ratio for laminated Douglas fir/epoxy specimens 1.5 in. by 2 in. in cross section (15 laminations) and from 166 to 235.6 in. long.

most lying between 0.00220 and 0.00260. There appears to be some trend in ζ with density. When the specimens were deflected perpendicular to the laminations (radially), the damping ratio was somewhat higher than when the specimens were deflected parallel to the laminations (tangentially). Decreasing modulus of elasticity appeared to correlate closely with the decreasing density of the test pieces.

6.0 Strength of Bonded Structural Joints

Large structures made of laminated wood may be too large to be fabricated and vacuum bagged in a single assembly. As a result it may be necessary to fabricate a number of subassemblies and then join these subassemblies together. Three types of joints for joining these subassemblies are considered in this section of the report:

(1) Finger joints made up of a line of glued intermeshing "V" cuts in the joint area of the two subassemblies. The finger joints carry load parallel to the grain of the laminations.

(2) Longitudinal bonded joints, which may be either butt joints or joints with a wedge insert. These joints carry load perpendicular to the grain of the laminations.

(3) Stud joints, used primarily to connect the wood structure to a metal structure. Metal studs are embedded and bonded to the laminated structure.

6.1 Finger Joints in Static Tension

Finger joints are illustrated in figures 2.3-1 and 2.3-2. A variety of configurations of these joints were tested in static tension. Proprietary epoxy adhesives thickened with asbestos fibers were used for bonding the joints by Gougeon Brothers, Inc.

6.1.1 Effect of finger joint configuration.—Three variables in the configuration were investigated (fig. 2.3-2): (1) slope of the fingers, (2) length of the fingers, and (3) gap in the bond line of the fingers. Most of the tests were conducted on rectangular-cross-section specimens 1.5 by 2.25 (or 2.31) by 92 in. as shown in figure 2.3-3, but a few tests were conducted on dogbone specimens with a 2.25-in.-diameter test section and an overall length of 57 in. as shown in figure 2.3-8. Further details of the machined fingers are shown in figures 2.3-4 to 2.3-6. All specimens were grade A+ Douglas fir/epoxy. Results of control tests in static tension for specimens without joints are shown in table 6.1-I(a). There is no ready explanation why the four data points at the bottom of the table

TABLE 6.1-I.—STATIC TENSION STRENGTH PARALLEL TO GRAIN FOR GRADE A+ DOUGLAS FIR/EPOXY SPECIMENS WITHOUT FINGER JOINTS AS CONTROL SPECIMENS

[1.5- by 2.25- (or 2.31) by 92-in. specimens. No augmentation; type of failure, splintering tension; test temperature, 68 °F. Data corrected to 6 percent laminate moisture content (K = 1.21).]

(a) Unaged

Stress area, in.^{2}	Laminate moisture content, percent	Failure load, lb	Failure stress, psi	Corrected failure stress, psi
3.47	6.6	42 500	12 248	12 391
3.63	6.5	38 720	10 667	10 771
3.44	6.3	40 760	11 849	11 918
3.45	6.4	42 960	12 452	12 549
3.44	6.7	39 840	11 581	11 739
3.48	6.0	36 100	10 374	10 374
3.25	6.0	37 520	11 545	11 545
3.27	6.2	38 600	11 804	11 850
		Mean	11 565	11 642
		Standard deviation, σ	672	697
3.52	4.3	49 520	[a]14 068	[a]13 612
3.53	4.5	50 880	[a]14 414	[a]14 001
3.53	4.4	45 860	[a]12 992	[a]12 595
3.45	4.4	49 360	[a]14 307	[a]13 870

(b) Aged 8 months before testing

3.51	5.1	36 900	10 513	10 331
3.51	4.7	41 320	11 772	11 479
3.51	5.4	26 820	7 641	7 553
3.52	4.7	39 700	11 278	10 997
3.32	5.2	30 660	9 235	9 093
3.45	4.7	34 021	9 861	9 616
		Mean	10 050	9 845
		Standard deviation, σ	1366	1298

[a]From separate portions of the investigation. Stresses not included in mean or σ.

have an average failure stress approximately 16 percent higher than the top six data points. It is believed, however, that the top points (with a mean corrected stress of 11 642 psi) are from specimens more representative of the laminates used for finger-jointed specimens and should be used as the basis for comparing the effect of weakening due to the addition of finger joints.

Table 6.1–II compares joint strength for specimens having fingers 6 in. long and finger slopes varying from 1:6 to 1:14. Table 6.1–III shows strength for fingers 3 in. long and a finger slope of 1:8. Table 6.1–IV(a) shows data for dogbone specimens with fingers 10 in. long, a finger slope of 1:10, and bond line gaps between the fingers of 0.015 and 0.062 in. Figure 2.3–9 illustrates the gaps. The mean failure stresses from tables 6.1–I to 6.1–IV are plotted in figure 6.1–1.

The figure shows that for specimens with fingers 6 in. long, tension strength increased significantly as the finger slope was increased from 1:6 to 1:10, with only slight improvement as the slope was further increased to 1:14. The static strength for a slope of 1:10 was about 94 percent of the strength without finger joints.

Only limited data were available on the effect of finger length. Data for 3-in.-long fingers were only available for a finger slope of 1:8. There was little difference in strength for 3- and 6-in.-long fingers. Data for 10-in.-long fingers were only available for a finger slope of 1:10, and the data showed a somewhat inconsistent trend. Two 10-in.-long finger specimens of rectangular cross section (from table 6.1–VI) showed a slight strength reduction relative to 6-in.-long finger specimens at a slope of 1:10, but two other 10-in.-long finger

TABLE 6.1–II.—EFFECT OF FINGER SLOPE ON STATIC TENSION STRENGTH PARALLEL TO GRAIN—6-in. FINGERS

[Laminated Douglas fir/epoxy specimens 1.5 in. thick (15 laminations), 2.25 (or 2.31) in. wide, and 92 in. long. Bond gap, 0.015 in.; test temperature, ~68 °F. Data corrected to 6 percent laminate moisture content ($K = 1.21$).]

(a) Slope of fingers, 1:6

Stress area, in.^{2}	Laminate moisture content, percent	Failure load, lb	Failure stress, psi	Corrected failure stress, psi	Type of failure[a]
3.48	6.4	25 060	7 201	7 257	1
3.49	6.6	35 980	10 309	10 430	
3.50	6.6	34 260	9 789	9 904	
3.44	6.1	30 920	8 988	9 005	
3.44	6.6	31 400	9 128	9 235	
3.42	6.5	31 440	9 193	9 283	
3.49	6.8	23 760	6 808	6 914	
3.45	6.3	27 660	8 017	8 064	
3.45	6.5	30 320	8 788	8 874	
3.49	6.4	29 760	8 527	8 593	
		Mean	8675	8756	
		Standard deviation, σ	1030	1042	

(b) Slope of fingers, 1:8

3.26	6.2	29 360	9 006	9 041	1
3.25	6.3	24 920	7 668	7 713	2
3.24	6.2	37 560	11 593	11 638	2
3.29	6.3	43 600	10 517	10 578	2
3.27	6.0	33 420	10 220	10 220	1
3.25	6.5	36 700	11 292	11 402	1
3.20	6.4	40 700	12 719	12 818	2
3.21	6.3	30 800	9 595	9 651	2
3.20	6.2	37 940	11 856	11 902	1
3.23	6.3	32 720	10 130	10 189	2
		Mean	10 460	10 515	
		Standard deviation, σ	1409	1423	

(c) Slope of fingers, 1:10

Stress area, in.^{2}	Laminate moisture content, percent	Failure load, lb	Failure stress, psi	Corrected failure stress, psi	Type of failure[a]
3.49	6.3	35 400	10 143	10 202	2
3.47	6.4	37 320	10 755	10 839	
3.46	6.6	44 280	12 798	12 948	
3.47	6.5	40 800	11 758	11 873	
3.47	6.7	31 300	9 020	9 143	1
3.44	6.1	39 100	11 366	11 388	1
3.48	6.3	37 140	10 672	10 734	3
3.46	6.3	34 060	9 844	9 901	1
3.44	6.5	42 140	12 250	12 369	1
3.49	6.1	34 960	10 017	10 036	3
		Mean	10 862	10 943	
		Standard deviation, σ	1115	1134	

(d) Slope of fingers, 1:14

3.43	6.3	39 240	11 440	11 507	1
3.47	6.3	37 520	10 813	10 876	3
3.50	6.6	30 840	8 811	8 914	2
3.54	6.2	41 460	11 712	11 758	1
3.47	6.3	36 900	10 634	10 696	1
3.46	6.1	45 080	13 209	13 235	1
3.43	6.3	39 360	11 475	11 542	2
3.46	6.2	36 060	10 133	10 172	1
3.50	6.1	40 580	11 594	11 617	1
3.49	6.4	35 540	10 183	10 262	3
		Mean	11 000	11 058	
		Standard deviation, σ	1120	1103	

[a]Type of failure: 1 – failure in joint
2 – failure from joint to some point outside of joint
3 – failure outside of joint

TABLE 6.1-III.—STATIC TENSION STRENGTH PARALLEL TO GRAIN—3-in. FINGERS WITH SLOPE OF 1:8

[Laminated Douglas fir/epoxy specimens 1.5 in. thick (15 laminations), 2.25 (or 2.31) in. wide, and 92 in. long. Bond gap, 0.015 in.; test temperature, ~68 °F. Data corrected to 6 percent laminate moisture content (K = 1.21).]

Stress area, in.^{2}	Laminate moisture content, percent	Failure load, lb	Failure stress, psi	Corrected failure stress, psi	Type of failure[a]
3.26	6.2	34 600	10 613	10 654	3
3.25	6.4	36 840	11 335	11 423	1
3.28	6.3	36 600	11 159	11 224	↓
3.26	6.2	38 020	11 663	11 708	↓
3.29	6.2	36 340	11 046	11 089	↓
3.27	6.2	30 900	9 450	9 487	2
3.21	6.3	29 420	9 165	9 218	2
3.23	6.0	33 180	10 272	10 272	1
3.19	6.1	35 340	11 078	11 100	1
3.25	6.4	33 820	10 406	10 487	1
		Mean	10 619	10 666	---
		Standard deviation, σ	770	775	---

[a]Type of failure: 1 = failure in joint
2 = failure from joint to some point outside of joint
3 = failure outside of joint

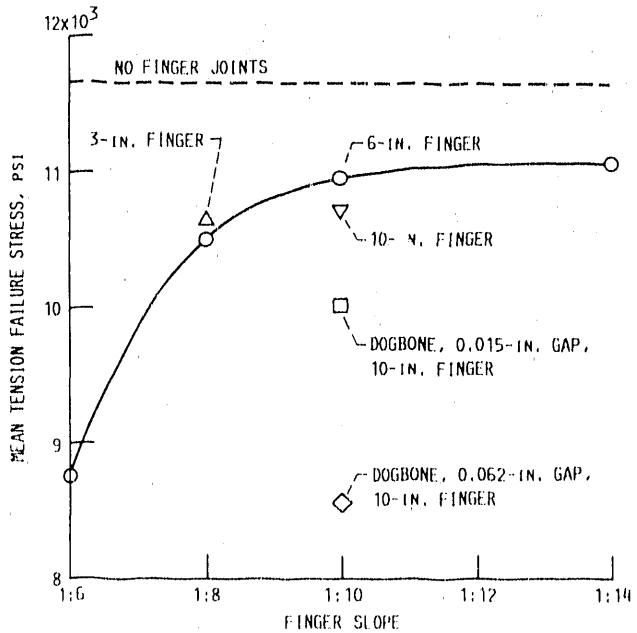

Figure 6.1-1.—Effect of finger joint configuration on static tensile strength parallel to grain for laminated Douglas fir/epoxy specimens. Unless specified otherwise, finger length was 6 in., bond line gap was 0.015 in., and specimens were 1.5 in. (15 laminations) by 2.25 or 2.31 in. by 92 in. Failure stresses corrected to 6 percent laminate moisture content (K = 1.21). Veneer grade, A+; test temperature, ~68 °F.

TABLE 6.1-IV.—STATIC TENSION AND TENSION-TENSION FATIGUE STRENGTH PARALLEL TO GRAIN—10-in. FINGERS WITH SLOPE OF 1:10

[Laminated Douglas fir/epoxy dogbone specimens 2.25 in. in diameter and 57 in. long. Veneer grade, A+; test temperature, ~68 °F. Data corrected to 6 percent laminate moisture content (K = 1.21).]

(a) Static tension tests

Stress area, in.^{2}	Laminate moisture content, percent	Failure load, lb	Failure stress, psi	Corrected failure stress, psi	Bond gap, in.
4.02	5.07	34 160	8 510	8 358	0.062
3.98	4.00	39 500	9 930	9 553	.015
4.02	4.61	36 240	9 020	8 780	.062
3.98	4.47	42 920	10 780	10 465	.015

(b) Tension-tension fatigue tests; stress ratio, R, 0.1

Bond gap, in.	Laminate moisture content, percent	Minimum stress, psi	Maximum stress, psi	Cycles to failure	Corrected failure stress, psi
0.062	4.02	400	4000	2 715 700	3849
.015	4.28	450	4500	4 134 300	4352
.015	4.95	425	4250	4 822 500	4164
.062	5.11	450	4500	202 000	4423
.015	4.95	450	4500	5 143 600	4409
↓	4.87	425	4250	13 830 800	4158
↓	4.70	425	4250	23 319 500	4144
↓	5.13	550	5500	344 800	5408
↓	4.65	550	5500	442 700	5358
↓	4.61	700	7000	31 700	6814
↓	4.54	650	6500	32 600	6319
↓	6.50	700	7000	[a]3 900	7068
↓	6.00	550	5500	[a]207 770	5500
↓	6.15	600	6000	[b]227 800	6017
↓	6.05	750	7500	[b]8 830	7507
↓	6.30	512	5125	[b]493 110	5155

[a]Tests by different investigators.
[b]Specimens augmented with Burlington style 7500 glass fiber fabric between plies.

specimens of a dogbone configuration showed corrected strengths that were significantly lower (by about 9 percent) than those for the shorter finger lengths in rectangular-cross-section specimens. Note that the tip width of the 10-in.-long fingers was approximately 2.5 times that of the shorter fingers, as shown in figure 2.3–6. This extra width was due to manufacturing requirements for the deeper cut of the 10-in.-long fingers. This wider tip resulted in a butt joint or gap, reduced the load-carrying area, and thus explains the lower strength of the 10-in.-long fingers. However, t tests for the 3-, 6-, and 10-in.-finger-length specimens with 0.015-in. bond gap and matched finger slopes yielded values of t from 0.25 to 1.04. Therefore there is a high probability that the mean tension strengths of a large population of 3-, 6-, and 10-in.-long finger specimens are the same.

Comparing 10-in.-long fingers having a finger slope of 1:10 with two different finger bond line gaps in dogbone specimens showed that the 0.062-in.-gap specimens were only 86 percent as strong as the 0.015-in.-gap specimens. There were valid reasons for this strength reduction. The gap was increased from 0.015 to 0.062 in. by moving the two halves of the finger joint specimens apart approximately ½ in. The effect was twofold: it reduced the bonded finger length by 5 percent, and it also further increased the effective tip width and thus further decreased the load-carrying capability. Another variable was the adhesive. Different adhesives were used for the two gaps. The amount of asbestos fiber was increased almost 200 percent for bonding with the wide gaps.

6.1.2 Effect of aging cut joints prior to bonding.—In manufacturing subassemblies some time may elapse before it is possible to bond two or more subassemblies together. Therefore tests were conducted in which the finger joints were machined and then aged for 8 months before bonding to determine if the joint surfaces might deteriorate and affect bond strength. Table 6.1-I compares the strengths of specimens without joints where tension tests were conducted on some of the specimens a short time after fabrication and on other specimens 8 months after fabrication. Aging significantly reduced strength. The aged specimens were only 85 percent as strong as the unaged specimens, and the specimen data were more erratic. The standard deviation for the aged specimens was almost twice that for the unaged specimens. None of the aged specimens had a strength as high as the mean of the unaged specimens.

Table 6.1-V shows the strength of finger-jointed specimens with finger lengths of 6 and 10 in. and finger slopes of 1:10. The finger joints were machined and then aged 8 months before they were glued. Comparing the mean strength values from tables 6.1-II(c) and 6.1-V(a) for 6-in.-long fingers showed the aged specimens to have 86 percent of the corrected strength of the unaged specimens with improved standard deviation σ and the aged finger-jointed specimens to have 96 percent of the strength of aged specimens without finger joints (table 6.1-I(b)). The strength reduction resulting from aging was somewhat higher for specimens without finger joints than for specimens with finger joints (table 6.1-I). It appears that a delay between the time when the finger joints are machined and the time when they are bonded will probably result in a significant reduction in bonded joint strength. From t tests of the data there is less than 1 chance in 50 that the aged specimens, with or without finger joints, will have as high mean strength as the unaged specimens.

Table 6.1-V shows 10-in.-long aged finger joints to be only 92 percent as strong as 6-in.-long aged finger joints. This is consistent with the strength reduction between some of the 6- and 10-in. finger lengths in figure 6.1-1.

6.1.3 Effect of fiber augmentation between wood laminations.—Table 6.1-VI shows tension strengths of specimens containing 10-in.-long finger joints with a finger slope of 1:10 in which either 10-oz/yd^2 Burlington Style 7500 glass fiber fabric or Burlington Style 5285 Kevlar fiber fabric was installed between the wood plies (fig. 2.3-7). Also shown in the table are strengths of finger-jointed control specimens made from the same billet but from a portion of the billet that did not include fiber fabric. The billet was laid up so that part was without fiber fabric in order to get a consistent comparison of specimens with and without the fiber augmentation. The mean corrected failure stresses show that the glass fiber augmentation increased strength 19 percent relative to the specimen without augmentation. With Kevlar fiber augmentation the strength increase was 33 percent.

TABLE 6.1-V.—STATIC TENSION STRENGTH PARALLEL TO GRAIN FOR SPECIMENS WITH FINGER JOINTS AGED 8 MONTHS BEFORE BONDING

[Laminated Douglas fir/epoxy specimens 1.5 in. thick (15 laminations), 2.25 (or 2.31) in. wide, and 92 in. long. Finger slope, 1:10; bond gap, 0.015 in.; test temperature, ~68 °F. Data corrected to 6 percent laminate moisture content (K = 1.21).]

(a) Finger length, 6 in.

Stress area, in.^{2}	Laminate moisture content, percent	Failure load, lb	Failure stress, psi	Corrected failure stress, psi	Type of failure[a]
3.47	4.3	29 260	8 432	8 159	1
3.54	4.5	32 800	9 266	9 001	
3.51	4.3	31 100	8 860	8 573	
3.41	4.6	33 800	9 912	9 647	
3.52	4.5	33 820	9 608	9 333	2
3.55	4.7	38 620	10 879	10 608	1
3.48	4.7	36 460	10 477	10 216	1
3.36	4.3	30 320	9 024	8 732	2
3.46	4.3	34 880	10 081	9 754	2
3.50	5.1	36 660	10 474	10 293	1
		Mean	9791	9432	------
		Standard deviation, σ	758	770	------

(b) Finger length, 10 in.

3.48	4.6	29 660	8 523	8 295	1
3.47	4.3	30 440	8 772	8 488	
3.48	4.6	28 580	8 213	7 993	
3.50	4.9	29 120	8 320	8 145	
3.53	4.6	27 460	7 779	7 571	
3.51	4.3	32 240	9 185	8 887	
3.42	4.6	27 540	8 053	7 837	
3.31	4.5	31 760	9 595	9 320	
3.32	4.6	35 200	10 602	10 318	2
3.42	4.4	35 060	10 251	9 938	1
		Mean	8929	8679	------
		Standard deviation, σ	907	872	------

[a]Type of failure: 1 = failure in joint
2 = failure from joint to some point outside of joint
3 = failure outside of joint

TABLE 6.1-VI.—EFFECT OF GLASS FIBER FABRIC AUGMENTATION ON STATIC TENSION STRENGTH PARALLEL TO GRAIN—FINGER-JOINTED SPECIMENS

[Laminated Douglas fir/epoxy specimens 1.5 in. thick (15 laminations), 2.25 (or 2.31) in. wide, and 92 in. long. Failure in joint; finger slope, 1:10; finger length, 10 in.; bond gap, 0.015 in.; test temperature, ~68 °F. Data corrected to 6 percent laminate moisture content ($K = 1.21$).]

(a) Augmented with Burlington style 7500 glass fiber fabric

Stress area, $in.^2$	Laminate moisture content, percent	Failure load, lb	Failure stress, psi	Corrected failure stress, psi
3.90	3.0	48 860	12 528	11 820
3.92	2.9	55 240	14 092	13 270
3.95	2.6	54 840	13 884	12 999
3.86	3.0	52 020	13 477	12 716
3.94	2.9	54 660	13 873	13 064
3.93	3.2	55 220	14 051	13 309
		Mean	13 651	12 863
		Standard deviation, σ	540	505
3.51	3.7	39 660	[a]11 299	[a]10 806

(b) Augmented with Burlington style 5285 Kevlar fiber fabric

3.83	3.5	58 160	15 185	14 467
3.88	3.4	56 920	14 670	13 949
3.92	3.8	57 600	14 694	14 081
3.92	3.6	57 000	14 541	13 880
3.88	3.5	60 580	15 613	14 875
3.85	3.8	54 540	14 166	13 575
		Mean	14 812	14 138
		Standard deviation, σ	466	423
3.55	4.1	39 180	[a]11 037	[a]10 638

[a]Control specimens without fiber fabric augmentation; not included in mean or σ.

6.1.4 Closing remarks on finger joints in static tension.— The strength of finger-jointed specimens significantly improved as the finger slopes were increased from 1:6 to 1:10, but only marginal improvement occurred with a further increase in slope to 1:14. Finger-jointed specimens with 6 in.-long fingers and a finger slope of 1:10 were about 94 percent as strong as specimens without joints.

Some of the experimental static tension data show approximately the same strength for 3-, 6-, and 10-in.-long fingers, but the data for the 3- and 10-in.-long fingers were extremely limited. Conversely, part of the tests showed a strength reduction on the order of 9 percent for 10-in.-long fingers. This effect was most likely due to greater total fingertip thickness, which resulted in a larger tip butt joint area for the 10-in.-long fingers than for the 6-in.-long fingers.

The bond gap in the finger joints can appreciably affect joint strength. Gaps of 0.062 in. resulted in tension strengths only 86 percent of those for 0.015-in. gaps. At least a portion of this strength reduction resulted from the manner in which the bond gap was increased, which reduced the length of the bond on each of the fingers.

Aging had a deleterious effect on specimens with and without finger joints. Strength reductions of approximately 78 to 86 percent were found after aging for 8 months.

Static tension strength could be appreciably increased by placing a glass fiber fabric or a Kevlar fiber fabric between the wood plies. The strength was increased by 19 percent by augmentation with glass fiber and by 33 percent with Kevlar fiber.

6.2 Finger Joints in Tension-Tension Fatigue

Tests were conducted in tension-tension fatigue at a stress ratio R of 0.1 on dogbone specimens shown in figure 2.3-8 with finger joints 10 in. long and a finger slope of 1:10. The specimens were made of grade A+ Douglas fir/epoxy. All tests were conducted at approximately 68 °F, and the data were corrected to 6 percent laminate moisture content. Most of the tests were conducted with a 0.015-in. bond gap in the finger joints, but a few tests were conducted with a bond gap of 0.062 in. The adhesive used for the gap in the finger joints was a proprietary epoxy adhesive thickened with asbestos fibers. The adhesive used for the wider gap had almost 200 percent more asbestos fibers in it than that for the narrower gap. The adhesive was developed and applied by Gougeon Brothers, Inc. Limited testing was also conducted on specimens in which Burlington Style 7500 glass fiber fabric was applied between the wood plies to augment the specimen strength around the joint.

The results of the tension-tension fatigue tests are presented in table 6.1-IV(b) and figure 6.2-1. Also shown in figure 6.2-1 is the regression line for grade A+ Douglas fir/epoxy tension-tension fatigue specimens without finger joints. The specimens did, however, have scarf joints in the laminates. The regression line was obtained from figure 4.1-1(b). The data in figure 6.2-1 show a tension-tension fatigue joint efficiency of approximately 61 percent at 10^6 cycles for the specimens with a bond gap of 0.015 in. and without glass fiber augmentation. When the bond gap was increased to 0.062 in., the tension-tension fatigue strength of the finger-jointed specimens was decreased another 18 percent relative to the narrower gap, resulting in a fatigue joint efficiency of approximately 50 percent. Some of this strength loss with the wider gaps was the result of shortened bonding length because of the manner in which the gap was increased.

The augmentation obtained by adding glass fiber between the wood plies improved the tension-tension fatigue strength

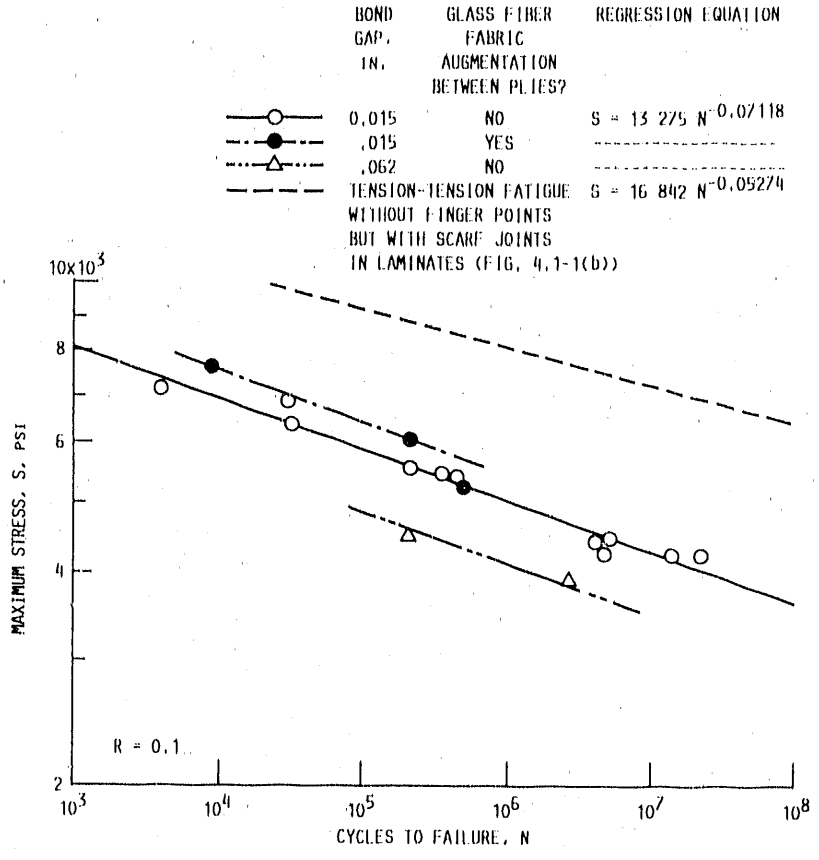

Figure 6.2-1.—Effect of finger joints on tension-tension fatigue (R = 0.1) parallel to grain for laminated Douglas fir/epoxy specimens. Finger joints, 10 in. long; finger slope, 1:10. Dogbone specimens 2.25 in. in diameter at test section and 57 in. long. Data corrected to 6 percent laminate moisture content (K = 1.21). Veneer grade, A+; temperature, −68 °F.

approximately 9 percent, if one neglects the one specimen whose fatigue strength fell on the regression line for specimens without the glass fiber fabric augmentation. Note that the lines in figure 6.2-1 for glass fiber fabric augmentation and for a bond gap of 0.062 in. are not true regression lines. Instead they are lines of best fit while having a slope the same as that for the specimens with a bond gap of 0.015 in. and no augmentation.

It can be concluded from these results that the need to use finger joints to attach subassemblies in large structures results in a significant tension-tension fatigue strength penalty that can be improved only marginally by glass fiber fabric augmentation. It is beneficial to use narrow gaps in finger joints, but this requires close machining tolerances.

6.3 Longitudinal Joints in Static Bending

Large structures will require the joining of subassemblies in directions both parallel and transverse to the applied load direction. Tests were therefore conducted on longitudinal joints parallel to the primary load. Such joints are illustrated in figure 16 of chapter III. Loads on such joints are primarily from bending in the longitudinal direction, which results in a shear load in the specimen or structure. Two types of longitudinal joints were investigated: butt joints and wedge joints as illustrated in figure 16 of chapter III with additional details shown in figures 2.3-10 and 2.3-11. Wedge joints are easier to manufacture than butt joints because the tapered wedge can more readily accommodate misalignments and provide better control of the bond thickness and because the bonding adhesive is more easily introduced into the wide, tapered opening. The epoxy adhesive used in the joints was a Gougeon Brothers, Inc., proprietary adhesive that had asbestos added for thickening. This thicker adhesive facilitated maintaining a fill in the relatively wide bonding gaps that can be expected in joining subassemblies.

The equations for calculating bending and shear stresses for three-point bending of specimens containing the two types of joints are given in figure 2.3-13.

6.3.1 Longitudinal butt-jointed specimens.—This type of specimen is illustrated in figure 2.3-10. Static bending data are presented in table 6.3-I. Tests were conducted at test temperatures from −40 to 100 °F with specimens expected to have essentially defect-free joints and with specimens having joints that had simulated defects built into them by means of nylon inserted in the glue line of the joint in the form of strips, small squares, or small balls.

The maximum shear stress data in table 6.3-I were corrected to 6 percent laminate moisture content. The table shows data corrected with two different K's in equation (7) of chapter III.

TABLE 6.3-I.—STATIC SHEAR STRENGTH WITH THREE-POINT BENDING FOR LONGITUDINAL BUTT-JOINTED SPECIMENS

[Laminated Douglas fir/epoxy specimens 3 in. deep (with nominal 1-in.-wide joint at mid-depth), 4 in. wide (40 laminations perpendicular to joint), and 30 in. long. Epoxy/asbestos adhesive joint. Veneer grade, A. Data corrected to 6 percent laminate moisture content.]

(a) Specimen temperature, 70 °F; no defects in joint

Joint dimensions		Laminate moisture content, percent	Failure load, lb	Maximum bending stress, psi	Maximum shear stress, psi	Corrected maximum shear stress, psi		Type of failure
Width, in.	Thickness, in.					$K = 1.26$	$K = 1.07$	
0.95	0.059	[a]6.0	5469	5469	1439	1439	1439	Wood
[a]1.00	.042		5174	5174	1293	1293	1293	(b)
.98	.047		4500	4500	1148	1148	1148	Wood
.85	.055		4484	4484	1319	1319	1319	Wood
.95	.065		6406	6406	1686	1686	1686	Wood
[a]1.00	.052	↓	6530	6530	1632	1632	1632	(b)
				Mean	1420	1420	1420	-----
				Standard deviation, σ	190	190	190	-----

(b) Specimen temperature, 100 °F; no defects in joint

1.03	0.042	[a]6.0	5469	5469	1327	1327	1327	Wood
1.00	.048		5078	5078	1269	1269	1269	Bond
.95	.038		5781	5781	1521	1521	1521	Wood
.95	.042		5937	5937	1562	1562	1562	Wood
1.03	.045	↓	6250	6250	1517	1517	1517	Wood
				Mean	1439	1439	1439	-----
				Standard deviation, σ	118	118	118	-----

(c) Specimen temperature, 100 °F after conditioning at 160 °F; no defects in joint

0.97	0.050	6.1	6797	6797	1752	1756	1753	Wood
.94	.043	6.1	6718	6718	1787	1791	1788	↓
.97	.043	6.1	6375	6375	1643	1647	1644	
.98	.032	5.8	6797	6797	1734	1726	1732	
				Mean	1729	1730	1729	-----
				Standard deviation, σ	53	53	53	-----

(d) Specimen temperature, −40 °F; no defects in joint

0.97	0.052	5.6	6748	6748	1739	1723	1734	Wood
.94	.057	6.0	6248	6248	1662	1662	1662	↓
.97	.040	5.8	6795	6795	1751	1743	1749	
.94	.038	5.8	6719	6719	1787	1779	1785	
				Mean	1735	1727	1732	-----
				Standard deviation, σ	46	42	45	-----

(e) Specimen temperature, 70 °F; 0.75-in.-wide nylon strip 0.062 in. thick across joint

0.97	0.060	5.8	6172	6172	1590	1583	1588	Wood
[a]1.00	.055	[a]6.0	6797	6797	1699	1699	1699	(b)
1.06	.058	5.9	6875	6875	1621	1617	1620	Wood
.84	.060	5.6	7344	7344	2186	2166	2180	Wood
1.09	.062	5.8	7500	7500	1720	1712	1718	Wood
				Mean	1763	1755	1761	-----
				Standard deviation, σ	217	211	215	-----

TABLE 6.3-I.—Concluded.

(f) Specimen temperature, 70 °F; four 0.44-in. nylon squares 0.062 in. thick along joint length

Joint dimensions		Laminate moisture content, percent	Failure load, lb	Maximum bending stress, psi	Maximum shear stress, psi	Corrected maximum shear stress, psi		Type of failure
Width, in.	Thickness, in.					$K = 1.26$	$K = 1.07$	
1.06	0.060	6.0	7295	7295	1720	1720	1720	Wood
1.09	.057	6.2	6139	6139	1408	1415	1410	↓
1.06	.062	5.5	7341	7341	1731	1711	1725	
.95	.063	5.8	6560	6560	1726	1718	1724	
1.15	.062	6.1	7497	7497	1630	1634	1631	↓
				Mean	1643	1640	1642	------
				Standard deviation, σ	123	117	121	------

(g) Specimen temperature, 70 °F; 370 nylon balls 0.062 in. in diameter along joint length

1.09	0.035	5.9	7732	7732	1773	1769	1772	Wood
1.09	.032	6.0	6717	6717	1540	1540	1540	↓
.97	.053	[a]6.0	6404	6404	1650	1650	1650	
.97	.030	5.8	7981	7981	2057	2047	2054	
.97	.037	5.9	7919	7919	2041	2036	2040	↓
				Mean	1812	1808	1811	------
				Standard deviation, σ	207	204	206	------

[a]Estimated.
[b]Not applicable.

The K value of 1.26 can be obtained from reference 3; the value of 1.07 was found in subsection 3.3.1 to provide a better correlation for block shear. The data for these bending tests were obtained for laminate moisture contents not far from 6 percent. As a result the value of K used in correcting the data had only a minimal effect.

The corrected ($K = 1.26$) mean and σ values from table 6.3-I can be summarized as follows:

Test temperature, °F	Simulated joint defects	Corrected mean maximum stress	Standard deviation, σ, psi	Table
70	None	1420	190	6.3-I(a)
100	↓	1439	118	6.3-I(b)
[a]100		1730	53	6.3-I(c)
−40	↓	1727	42	6.3-I(d)
70	Nylon strip	1755	211	6.3-I(e)
70	Nylon squares	1640	117	6.3-I(f)
70	Nylon balls	1808	204	6.3-I(g)

[a]Specimens preconditioned at 160 °F.

The mean maximum shear stresses shown in this table are somewhat inconsistent. The specimens without simulated defects at 70 and 100 °F had the lowest mean failure stresses, even lower than the specimens with simulated defects. Post-test examination of the specimens revealed areas of poor bonding in the joints, which undoubtedly contributed to the lower failure stresses, but it made comparison of the strength of specimens with and without simulated defects inconclusive. The relatively high strength of the specimens tested at 100 °F after preconditioning at 160 °F was attributed to possible enhanced curing of the epoxy asbestos adhesive. No deleterious effects of low-temperature static testing at −40 °F were observed. Surprisingly, the highest strengths were found with specimens containing the simulated defects. But the four 0.44-by 0.44-in. nylon squares in each joint apparently reduced corrected shear strength approximately 7 to 10 percent below that for the other two types of simulated defects.

The t tests (subsection 2.6.2) were conducted on the data from table 6.3-I. The tests revealed that at the 95 percent confidence level all of the specimen failure stresses, except for those at 70 and 100 °F without defects, were of the same population. Therefore drawing conclusions as to the relative strengths of the remaining specimens at various temperatures and with and without defects appeared to be meaningless.

Block shear test results for specimens with laminations perpendicular to the joint are shown in table 3.3-II. The mean corrected shear strength was 1935 psi, 7 percent higher than any of the mean strengths listed in the preceding table for bending tests but less than the σ value of data from table 3.3-II. The t tests of the data showed that at the 95 percent confidence level the data from table 3.3-II and the data for simulated defects of nylon strips and nylon balls from table 6.3-I were from the same population. The t test rejected the hypothesis that the other data samples in table 6.3-I were from the same

population as those in table 3.3–II (block shear with laminations perpendicular to the joint). Therefore those indicated strength differences can be considered as real.

6.3.2 Longitudinal wedge-jointed specimens.—This type of specimen is illustrated in figure 2.3–11. Only limited bending tests were conducted. The results are summarized in table 6.3–II for three wedge configurations: (1) wedge centered to provide 0.12-in.-thick bonds on both sides of the wedge, (2) wedge shifted to provide a 0.25-in.-thick bond on one side and minimum thickness on the other side, and (3) wedge centered to provide 0.12-in.-thick bonds on both sides and four 0.44-in. nylon squares 0.062 in. thick embedded in both bond lines. The results shown in the table indicate a weakening from shifting the wedge but no weakening from the simulated defects. In fact, the specimens with the simulated defects showed the highest strength. At 95 percent confidence level the *t* test confirmed that there was indeed a difference in strength (specimens from different populations) between the wedge that was shifted and the wedge with simulated defects. The *t* test indicated, however, that the shifted wedge and the wedge with the simulated defects could be from the same population as the centered wedge. As a result there is not high confidence that table 6.3–II shows significant strength trends. It does appear, however, that the wedge-jointed specimens (table 6.3–II) were weaker than the butt-jointed specimens (table 6.3–I).

6.4 Longitudinal Joints in Shear Fatigue

Fatigue tests were conducted at a stress ratio R of 0.1 on butt-jointed specimens with and without nylon square simulated defects and on wedge-jointed specimens with the wedge centered, shifted, and centered with nylon square simulated defects. The results are shown in table 6.4–I and figure 6.4–1.

An attempt was made to determine if $K = 1.26$ should be used to correct the data to 6 percent laminate moisture content. Since most of the data were obtained at laminate moisture contents near 6 percent, the corrections were small and the value of K used did not have a significant effect. Correlation coefficients (see eq. (10) in chapter III) were calculated for a range of K values from 1.07 to 3.0. The correlation coefficient r varied less than ± 1 percent over the entire range. Since the effect was too small for empirically determining the best value of K, the wood handbook (ref. 3) value of K (1.26) was used for the fatigue data.

TABLE 6.3–II.—STATIC SHEAR STRENGTH WITH THREE-POINT BENDING FOR LONGITUDINAL WEDGE-JOINTED SPECIMENS

[Laminated Douglas fir/epoxy specimens having "I" cross section 3 in. high (with wedge joint in middle 1-in. section), 4 in. wide, and 30 in. long. Epoxy asbestos adhesive joint 1 in. wide; veneer grade, A; specimen temperature, 70 °F. Data corrected to 6 percent laminate moisture content.]

(a) Wedge centered with 0.12-in. bond thicknesses on both sides of wedge

Laminate moisture content, percent	Failure load, lb	Maximum bending stress, psi	Maximum shear stress, psi	Corrected maximum shear stress, psi		Type of failure
				$K = 1.26$	$K = 1.07$	
5.6	6543	6732	1544	1530	1540	Wood
5.8	6144	6320	1450	1443	1448	[a]Wood
		Mean	1497	1486	1494	----

(b) Wedge shifted to provide 0.25-in. bond thickness on one side and minimum bond thickness on other side

6.0	5905	6076	1394	1394	1394	[a]Wood
6.4	5666	5830	1337	1350	1341	Wood
		Mean	1366	1372	1368	----

(c) Wedge centered with 0.12-in. bond thicknesses on both sides of wedge but with four 0.44-in. nylon squares 0.062 in. thick in both bond lines

5.7	6623	6815	1563	1552	1560	[a]Wood
6.2	6863	7062	1620	1628	1622	[a]Wood
		Mean	1592	1590	1591	----

[a]Failed outside of joint area

TABLE 6.4-1.—SHEAR FATIGUE STRENGTH WITH THREE-POINT BENDING FOR LONGITUDINAL-JOINTED SPECIMENS

[Laminated Douglas fir/epoxy specimens. Epoxy asbestos adhesive joints 1 in. wide. Stress ratio, R, 0.1; test temperature, 70 °F; cycle rate, 5 Hz. Data corrected to 6 percent laminate moisture content (K = 1.26).]

(a) Butt-jointed specimens (fig. 2.3-11) without defects

Joint thickness, in.	Laminate moisture content, percent	Minimum shear stress, psi	Maximum shear stress, psi	Cycles to failure	Corrected maximum shear stress, psi	Type of failure
0.045	6.3	125	1250	134 613	1259	(a)
.050	6.3	119	1190	302 960	1198	(a)
.056	6.1	109	1092	191 482	1095	Bond
.054	6.0	99	990	513 255	990	Bond
(a)	[b]5.5	92	921	301 843	910	(a)
.064	5.5	87	866	8 564 236	856	Bond
.060	5.7	98	980	160 000	973	Wood
.045	5.7	89	893	173 192	887	Wood
.062	[b]5.5	88	875	2 126 614	865	(a)
.062	[b]5.5	78	776	10 000 000	767	↓
.055	5.3	89	893	8 514 000	878	↓
.060	5.5	95	947	5 725 800	936	↓
.056	4.7	94	937	2 827 800	909	↓
.065	5.0	97	971	3 655 000	948	↓
.060	6.1	158	1581	28 000	1585	Wood
.030	6.2	153	1530	800	1537	↓
.062	6.3	111	1107	693 000	1115	↓
.060	6.9	114	1136	63 000	1160	↓
-----	---	---	-----	[c]1 500	1420	↓

(b) Butt-jointed specimens (fig. 2.3-11) with simulated defects in joint of four nylon squares 0.062 in. thick by 0.44 in. by 0.44 in.

0.075	6.9	110	1103	65 700	1127	Wood
.070	6.8	99	990	586 312	1009	↓
.070	7.0	99	990	279 900	1014	↓
.070	6.8	95	947	1 301 400	995	↓
.063	6.8	95	947	405 500	995	↓
.076	7.1	87	866	3 104 800	889	↓
-----	---	---	-----	[d]1 500	1642	↓

(c) Wedge-jointed specimens (fig. 2.3-12) with wedge centered and no defects in joints

0.012	6.0	100	1003	32 400	1003	Wood
↓	6.1	88	885	3 321 000	887	↓
↓	6.4	77	767	150 300	774	↓
↓	6.1	77	767	1 370 000	769	↓
↓	6.8	83	826	1 434 600	842	[e]Wood
↓	6.3	88	885	68 400	891	Wood
-----	-----	-----	-----	[f]1 500	1494	-----

[a]Not applicable.
[b]Estimated.
[c]Static test—estimated equivalent cycles (table 6.3 I(a)).
[d]Static test—estimated equivalent cycles (table 6.3 I(f)).
[e]Failed outside of joint area.

TABLE 6.4-I—Concluded.

(d) Wedge-jointed specimens (fig. 2.3-12) with wedge shifted and no defects in joints

Joint thickness, in.	Laminate moisture content, percent	Minimum shear stress, psi	Maximum shear stress, psi	Cycles to failure	Corrected maximum shear stress, psi	Type of failure
[g]0.025	6.0	100	1003	65 000	1003	[e]Wood
	6.0	100	1003	7 000	1003	Wood
	6.3	88	885	27 814	891	Wood
	6.2	88	885	17 100	889	[e]Bond
	6.8	77	767	596 700	782	[e]Wood
-----	---	---	----	[h]1 500	1368	

(e) Wedge-jointed specimens with wedge centered and simulated defects of four nylon squares 0.062 in. thick by 0.44 in. by 0.44 in. in each side of wedge joint

0.012	6.2	88	885	77 400	889	Wood
	6.2	83	826	1 314 000	830	[e]Bond
	6.1	88	885	3 884 400	887	Wood
	6.1	94	944	579 600	946	
	6.1	94	944	83 700	946	
	6.3	88	885	1 666 800	891	
-----	---	---	----	[i]1 500	1591	

[e]Failed outside of joint area.
[f]Static test—estimated equivalent cycles (table 6.3-II(a)).
[g]Maximum bond thickness on one side of wedge. Bond thickness on other side of wedge was minimal.
[h]Static test—estimated equivalent cycles (table 6.3-II(b)).
[i]Static test—estimated equivalent cycles (table 6.3-II(c)).

The effect of simulated defects on butt-jointed specimens is shown in figure 6.4-1(a). The simulated defects were four nylon squares placed in the joint of the specimen. The nylon squares were 0.062 in. thick by 0.44 in. by 0.44 in. The regression lines for specimens with and without simulated defects built into the butt joints were quite close together. The separation of the lines was considerably less than the scatter in the data. The lines crossed at about 100 000 cycles, which is not realistic. Note that static test data were included in the regression line calculation in the manner described in subsection 4.0. Regression lines were calculated with and without these static data points. The static data had a small effect on the slope and crossing point of the lines and did not alter the conclusions to be drawn from the data, namely that the three-point-bending fatigue tests did not show a significant weakening effect from simulated defects in the butt joints of the specimens.

Shear fatigue data, obtained by three-point bending, for wedge-jointed specimens are shown in figure 6.4-1(b). For the wedge-jointed specimens a large discrepancy in strength occurred between the static test data and the fatigue data that was not readily explainable. Therefore it did not appear prudent to include the static data when calculating the regression lines. An effect similar to that for butt-jointed specimens was evident; the regression lines all, unrealistically, crossed each other. Again the scatter in the data was larger than the differences in the regression lines for the range of cycles to failure for which data were obtained. Since there was some question as to the validity of the regression lines for each of the three types of wedge-jointed specimens, the following regression equation, which included all of the wedge-jointed specimen data, was calculated:

$$S = 1160N^{-0.02182} \tag{23}$$

This equation is probably a more realistic representation of the wedge-jointed fatigue data than the individual lines shown in figure 6.4-1(b). This single regression line is shown in figure 6.4-1(c) along with the regression line for the butt-jointed specimens without defects from figure 6.4-1(a). The higher slope of the butt-jointed specimen line indicates a greater sensitivity to cyclic stresses than is indicated for the wedge-jointed specimens. The butt joints therefore appeared to be stronger in low-cycle fatigue than the wedge joints, but became weaker at high cycles. However, this conclusion may be questionable because it can be seen from figures 6.4-1(a) and (b) that the static strengths of both types of specimens were approximately equal. Therefore additional data are probably required before definite conclusions can be drawn on the relative superiority of butt-jointed or wedge-jointed longitudinal joints.

It can be concluded from the results of static bending and bending fatigue tests on longitudinal joints that simulated defects had no definitive effects on joint strength for either butt-jointed or wedge-jointed specimens. The static strengths

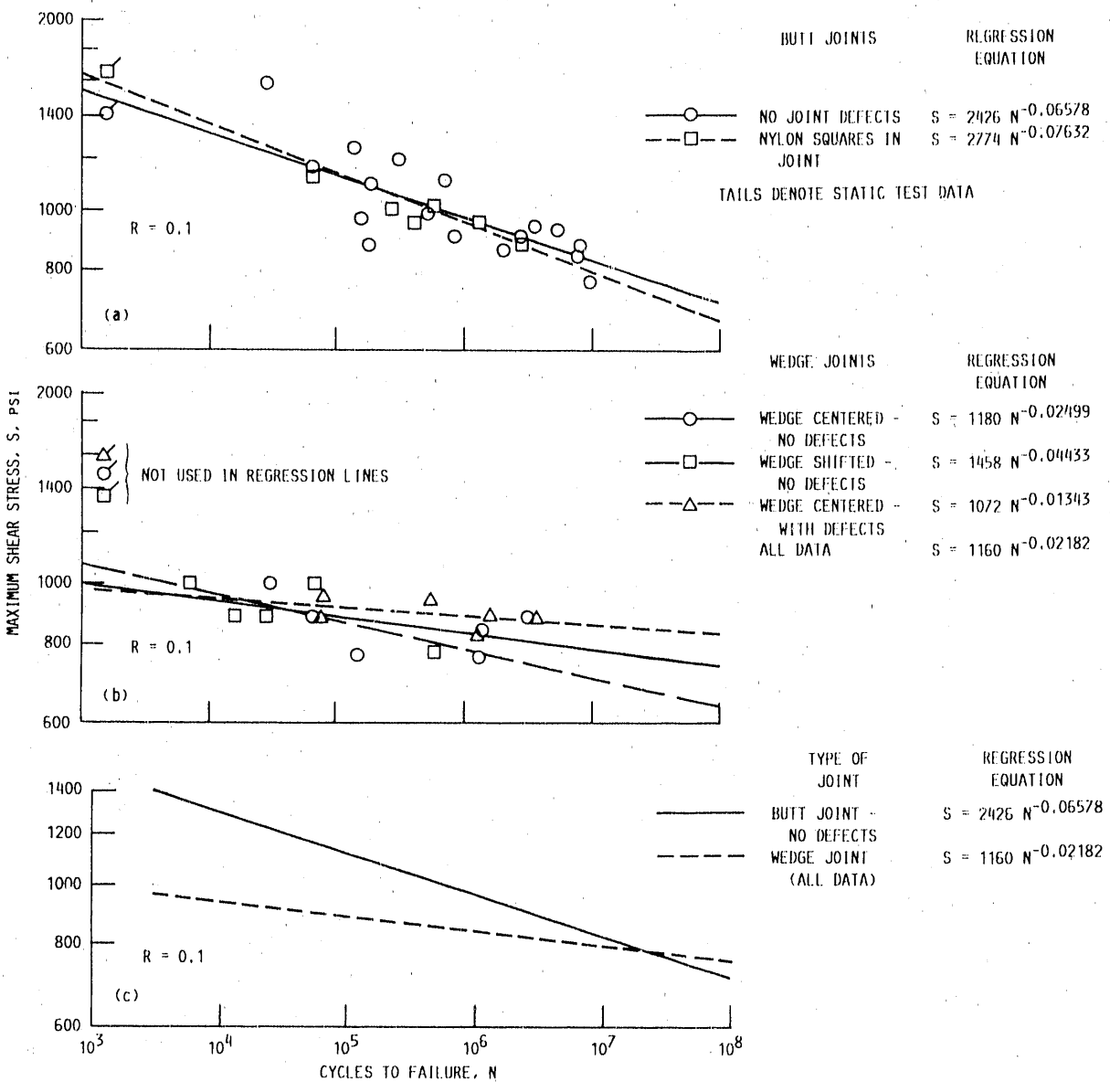

(a) Butt-jointed specimens.
(b) Wedge-jointed specimens.
(c) Fatigue comparison of mean of all wedge joint data with butt joint data.

Figure 6.4-1.—Three-point-bending fatigue tests (R = 0.1) on longitudinal joints with and without simulated joint defects for laminated Douglas fir/epoxy specimens. Simulated defects were four nylon squares 0.062 in. thick by 0.44 in. by 0.44 in. Epoxy asbestos adhesive in joints 1 in. wide. Data corrected to 6 percent laminate moisture content (K = 1.26). Veneer grade, A; test temperature, 70 °F.

of the butt-jointed and wedge-jointed specimens were of similar magnitude. When fatigue strength was considered, there were still some questions as to whether butt or wedge joints are superior.

7.0 Strength of Metal Stud Structural Joints

For some laminated-wood structures such as wind turbines blades it is necessary to attach wooden components to metal structures. One method of fabricating such a joint is to embed metal studs into the wooden structure and bond the studs to the wood with an epoxy resin thickened with carbon or asbestos fibers. Threads or convolutions on the metal studs aid in this bonding. A typical configuration of a metal stud embedded in a test specimen is shown in figure 2.3-13. Data are available for a variety of stud configurations. Reported herein is a summary of the failure loads at both static and fatigue conditions for the strongest specimen designs investigated up to the present. These data were obtained from reference 9.

7.1 Screening Tests

Five "advanced" and three reference specimen designs were considered. These designs are shown in figure 7.1-1. The significant differences between the designs are listed in table 7.1-I. The four thread configurations on the portion of the studs that were embedded in the laminated wood are shown in figure 7.1-2. Note that the threads on the studs are not screw threads. Instead they are convolutions with zero helix angle.

Tension-tension fatigue data for $R = 0.14$ are listed in table 7.1-II and figure 7.1-3. The data presented for all of the fatigue strengths are based on the failure load rather than the stress. For studs the maximum fatigue load that the stud can take is more meaningful than a stud stress. These data can be used to determine the number of studs required to support a given structural load. Figure 7.1-3 shows a regression line based upon all of the data. This line has no significance except to help illustrate the variations in the fatigue strength of each type of specimen design. Specimen designs 3, 4, and 5 are superior to the others. Configuration 3 was made of titanium; all the rest were of 4140 steel. The lower modulus of elasticity of titanium tended to make the stud's strain characteristics more compatible with those of the wood. Specimen designs 4 and 5, made of 4140 steel, were tip drilled to a greater depth to provide a longer thin wall. Again this was an attempt to increase the stud strain (by increasing stress through the thinner walls) in order to improve strain compatibility with the laminated Douglas fir/epoxy structure. The tapers on the studs of specimen designs 4 and 5 were nonlinear; therefore the wall thickness was also varied nonlinearly in an attempt to improve strain compatibility. All other studs were tapered linearly. As a result of the screening tests shown in figure 7.1-3, more extensive testing was conducted on specimen designs 4 and 5. Funding limitations precluded additional testing on design 3 (made of titanium).

TABLE 7.1-I.—SPECIMEN DESIGNS USED IN SCREENING TESTS

Specimen design	Shoulder	Tip drill		Taper	Embedded length, in.	Thread	Material
		Diameter, in.	Length, in.				
1	Yes	0.438	8.0	Linear	18.0	Zuteck	4140
2	Yes	.625	8.0	Linear			4140
3	No		8.0	Linear			Titanium
[a]4			15.0	Nonlinear			4140
4a			15.0	Nonlinear		Modified Zuteck	
[a]5			15.0	Nonlinear		Zuteck	
[b]6	Yes	Not drilled		Linear		Zuteck	
[b]7	Yes	Not drilled		Linear	11.25	Shallow Acme	
[b]8	Yes	Not drilled		Linear	15.0	Deep Acme	

[a]Stud designs 4 and 5 differed only in the amount of nonlinear taper in the stud wall. Design 4 had greater nonlinearity. There was also a difference in the test specimens, the difference being in the wooden block in which the studs were embedded. The block for design 5 had carbon fiber augmentation between the veneers to stiffen the block and improve strain compatibility.

[b]Reference design.

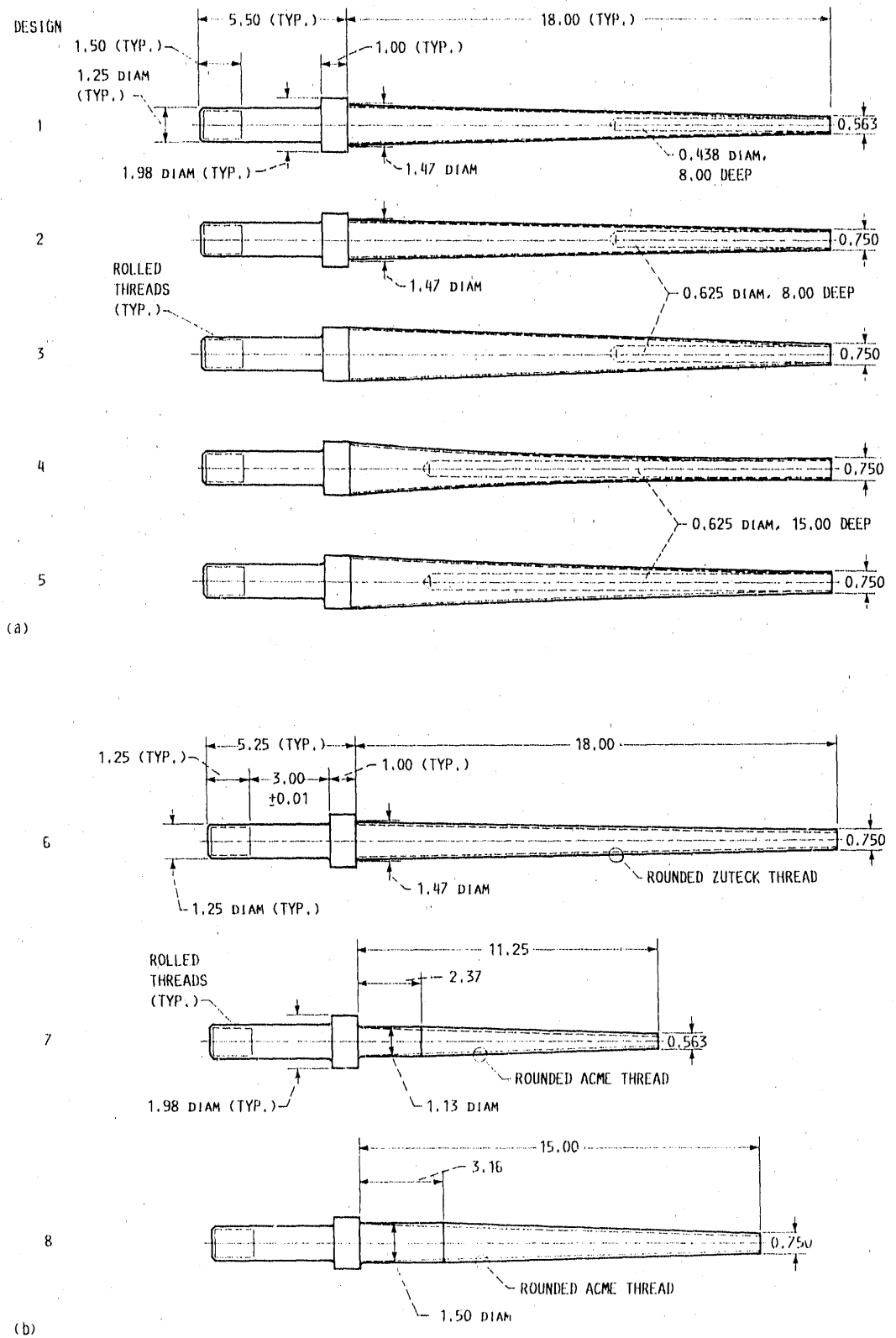

(a) Advanced specimen designs.
(b) Reference specimen designs.

Figure 7.1-1.—Metal stud designs investigated. (Dimensions are in inches.)

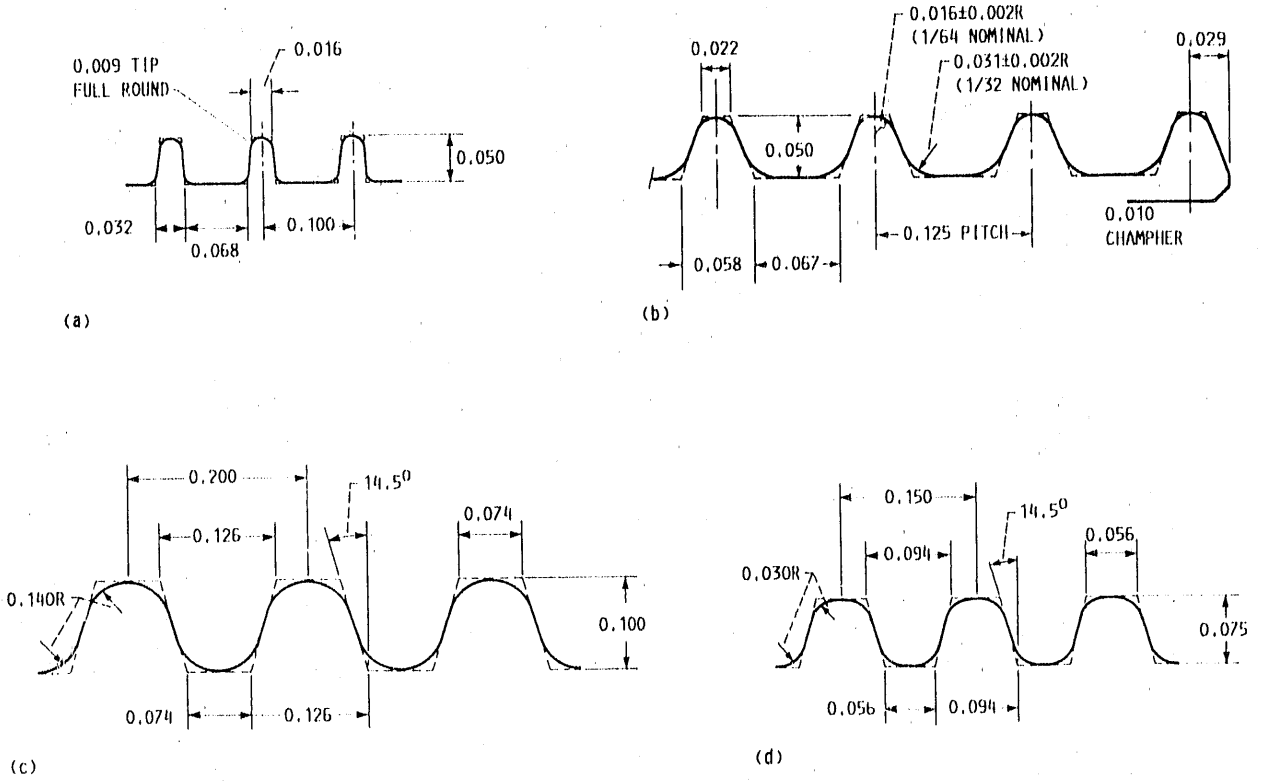

(a) Standard Zuteck thread.
(b) Modified Mark II Zuteck thread.
(c) Deep Acme thread.
(d) Shallow Acme thread.

Figure 7.1-2.—Threads used on portion of metal studs embedded in laminated wood. All threads are ring shape (helix angle, 0°). (Dimensions are in inches.)

TABLE 7.1-II.—TENSION-TENSION FATIGUE SCREENING TESTS OF METAL STUDS

[Eight bonded 18-in.-long stud configurations embedded in 3- by 3-in. laminated Douglas fir/epoxy specimens and bonded with asbestos-thickened epoxy adhesive. Studs, 4140 steel unless noted differently; stress ratio, R, 0.14.]

Specimen design	Minimum load, lb	Maximum load, lb	Cycles to failure
[a]1	4900	35 000	16 704
1	4620	33 000	494 058
[b]2	4520	33 000	666 000
2	4520	33 000	929 382
[c]3	6300	45 000	160 380
[c]3	6300	45 000	122 364
4	5600	40 000	171 190
4	5600	40 000	124 608
4	4480	32 000	2 228 652
5	6300	45 000	404 766
5	6300	45 000	438 660
[d]6	4900	35 000	91 512
7	2800	20 000	663 130
7	2800	20 000	283 392
8	5600	40 000	74 073
8	4900	35 000	217 729

[a]Same specimen completed 1 037 952 cycles at 30 000 lb without failure.
[b]Grip failed.
[c]Titanium stud.
[d]Same specimen completed 1 651 644 cycles at 25 000 to 32 500 lb without failure.

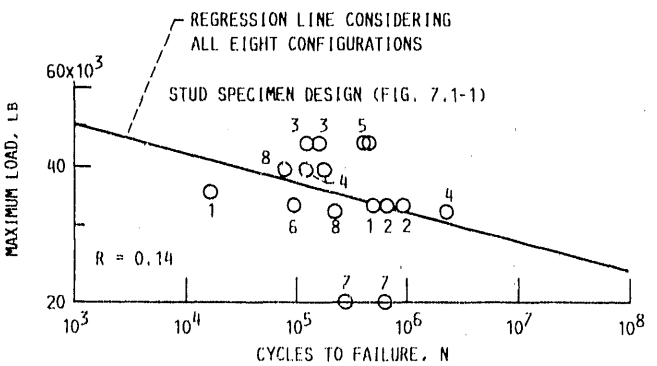

Figure 7.1-3.—Tension-tension fatigue strength screening tests (R = 0.14) of eight configurations of metal studs embedded in laminated Douglas fir/epoxy specimens and bonded with asbestos-thickened epoxy adhesive. Room temperature tests. (Numbers adjacent to symbols denote stud specimen design (fig. 7.1-1).

7.2 Steel Stud Fatigue Tests

Fatigue tests were conducted on designs 4, 4a, and 5. Tension-tension, compression-compression, and simulated reverse axial tension-compression tests were conducted. Tests were conducted at room temperature and at 100 and 120 °F. Tests were also conducted with both asbestos and carbon-filled epoxy resins used for bonding the studs to the laminated wood. All designs were not tested at all conditions. The fatigue data are tabulated in tables 7.2-I to 7.2-III and plotted in figures 7.2-1 to 7.2-3.

7.2.1 Fatigue strength at room temperature.—Figures 7.2-1 and 7.2-2 show the results of tension-tension, compression-compression, and simulated reverse axial tension-compression fatigue tests on specimen designs 4, 4a, and 5. See figure 7.1-1 and table 7.1-I for the specimen design details. As previously noted, the metal studs in designs 4 and 5 were similar. The differences were in the amount of nonlinear taper in the stud wall and the stiffness of the wooden block part of the specimen. Carbon fibers were placed between the veneers to increase stiffness and improve the strain compatibility between the wood and the metal studs in design 5.

Figure 7.2-1(a) shows the tension-tension fatigue strength of specimen design 4. In a manner similar to other fatigue tests previously discussed, if a specimen did not fail before the test was terminated, the specimen data were used to calculate the regression line if the point fell above the regression line but not if it fell below the regression line. The unfailed specimen data points are marked with a horizontal arrow. In most cases testing was terminated because of grip failure, but in one case the stud threads failed. The reasons for the test termination are listed in the tables.

Two thread configurations on the portion of the studs embedded in the wood were tested (see fig. 7.1-2 for details of the standard Zuteck thread and the modified Mark II Zuteck thread). The specimens tested to failure showed little or no difference in fatigue strength, as measured by load on the stud, of the specimens with the two threads. The modified thread lends itself to easier and cheaper manufacturing.

For design 4 at 1 million cycles the carbon-filled adhesive (or resin) resulted in a fatigue failure load L approximately 37 percent higher than for asbestos-filled adhesive. The difference was somewhat higher at a greater number of cycles. A similar trend was observed for design 5 except that the carbon-filled adhesive exhibited only a 19 percent increase in failure load relative to the asbestos-filled adhesive. With carbon-filled adhesive in both designs 4 and 5, design 5 was about 16 percent stronger than design 4 at 1 million cycles. The improved strain compatibility obtained by adding the carbon fibers between the wood laminations was therefore shown to be beneficial.

Figure 7.2-2(a) shows simulated reverse axial tension-compression fatigue strength for designs 4 and 5. Because of the clevis design in the test specimen (fig. 2.3-13) conventional

TABLE 7.2-I.—FATIGUE TESTS OF SPECIMEN METAL STUD DESIGN 4

[Nonlinear tapered 4140 steel studs 18 in. long embedded in 3- by 3-in. laminated Douglas fir/epoxy specimens and bonded with asbestos- or carbon-fiber-filled epoxy resin. (Carbon-filled resin unless noted.)]

(a) Tension-tension fatigue

Cycle rate, Hz	Stress ratio, R	Minimum load, lb	Maximum load, lb	Cycles to failure
3.5	0.14	5 600	40 000	[a]171 000
3.0	0.14	5 600	40 000	[a]125 000
3.5	0.14	4 480	32 000	[a]2 229 000
4.0	0.10	6 500	65 000	[b]17 000
↓	↓	4 800	48 000	433 000
		3 500	35 000	[b]8 412 000
		5 500	55 000	261 000
		6 000	60 000	30 000
		4 500	45 000	1 791 000
		4 800	48 000	371 000
		6 500	65 000	[b]6 800
---	---	-------	97 300	[c]1
---	---	-------	104 000	[c]1
---	---	-------	100 100	[c]1

(b) Tension-tension fatigue; modified stud thread (see fig. 7.1-2)

4.0	0.10	5 300	53 000	103 000
5.0	↓	4 800	48 000	[b]105 000
4.5		6 000	60 000	[b]22 700
5.0		5 300	53 000	[b]21 200
5.5		4 800	48 000	[b]1 536 000
5.2		5 000	50 000	327 000

(c) Block loading tension-compression fatigue; tension cycles listed in "cycles to failure"; tests run in blocks of tension-tension cycles and blocks of compression-compression cycles at $R = 0.10$ and $R = 10$

4.5	−1.0	−45 000	45 000	[d]811 000
4.1	−1.0	−50 000	50 000	[e]176 000
4.0	−1.0	−65 000	65 000	[f]14 200

(d) Compression fatigue

4.0	10.0	−5 500	−55 000	243 000
4.0	↓	−7 000	−70 000	36 000
4.1		−5 000	−50 000	10 127 000
4.0		−6 000	−60 000	167 000

[a]Asbestos filler
[b]Grip failed
[c]Ultimate load test
[d]1 210 000 Compression cycles
[e]671 000 Compression cycles
[f]12 000 Compression cycles

TABLE 7.2-II.—FATIGUE TESTS OF SPECIMEN METAL STUD DESIGN 5

[Nonlinear tapered 4140 steel studs 18 in. long embedded in 3- by 3-in. laminated Douglas fir/epoxy block with carbon fiber augmentation between plies. Studs bonded with asbestos- or carbon-fiber-filled epoxy resin. (Carbon filled resin unless noted.)]

(a) Tension-tension fatigue

Cycle rate, Hz	Stress ratio, R	Minimum load, lb	Maximum load, lb	Cycles to failure
3.6–4.1	0.14	6 300	45 000	[a]405 000
3.6–3.8	.14	6 300	45 000	[a]439 000
4.0	.10	7 200	72 000	40 300
4.0	↓	5 000	50 000	[a]576 000
4.5		3 230	32 300	[a,b]1 244 000
4.5–5.0		4 800	48 000	[a]1 369 000
4.5		4 600	46 000	906 000
4.0		5 200	52 000	196 000
4.0		5 500	55 000	300 000
4.0		6 000	60 000	163 000
3.0		8 000	80 000	28 400
4.0		4 500	45 000	[c]2 513 000
4.2		6 300	63 000	219 000
4.0		6 500	65 000	117 000
3.4		7 000	70 000	[d]46 900
4.0		5 700	57 000	431 000
4.0	↓	5 000	50 000	3 657 000

(b) Block loading tension-compression fatigue; tension cycles listed in "cycles to failure"; tests run in blocks of tension-tension cycles and blocks of compression-compression cycles at $R = 0.10$ and $R = 10$

4.1	−1.0	−57 000	57 000	[e]170 000
4.0	−1.0	−60 000	60 000	[f]28 000
4.1	−1.0	−50 000	50 000	[g]1 475 000

(c) Compression-compression fatigue

4.0	10.0	−6 000	−60 000	1 416 000
4.5	10.0	−5 500	−55 000	4 241 000
4.0	10.0	−7 000	−70 000	114 000

[a]Asbestos filler
[b]No failure
[c]Stud threads failed
[d]Grip failed
[e]353 000 Compression cycles
[f]35 400 Compression cycles
[g]1 471 000 Compression cycles

reverse axial tension-compression tests were not feasible because clearances resulted in dynamic loading when changing from compression to tension. As a result simulated tests were conducted in which blocks of tension-tension fatigue cycles were run first and then blocks of compression-compression fatigue cycles. The same number of tension-tension and compression-compression fatigue cycles were not necessarily completed at specimen failure. The plots list the tension cycles.

The data in figure 7.2-2(a) show a crossover in the regression lines at about 25 000 cycles. The figure shows design 5 to be superior for cycles higher than 25 000. It is unlikely, however, that figure 7.2-2(a) is a true representation of the actual fatigue characteristics. Additional data would probably show a flatter slope for design 4 and the crossover would be eliminated. Although static test data were available for design 4 (table 7.2-I(a)), similar data were not available for

TABLE 7.2-III.—TENSION-TENSION FATIGUE OF METAL STUDS AT ELEVATED TEMPERATURES

[Nonlinear 4140 tapered steel studs 18 in. long embedded in 3- by 3-in. laminated Douglas fir/epoxy blocks. Studs bonded with carbon-fiber-filled epoxy resin. Stress ratio, R, 0.10 to 0.14.]

(a) Specimen design 4

Test temperature, °F	Maximum load, lb	Cycles to failure
120	60 000	264
120	50 000	125
100	50 000	1 332
100	35 000	8 763
100	[a]67 100	1

(b) Stud configuration 5.

Test temperature, °F	Maximum load, lb	Cycles to failure
120	60 000	604
120	50 000	1 603
100	50 000	2 437
100	35 000	50 044
100	[a]108 600	1

[a]Ultimate load test.

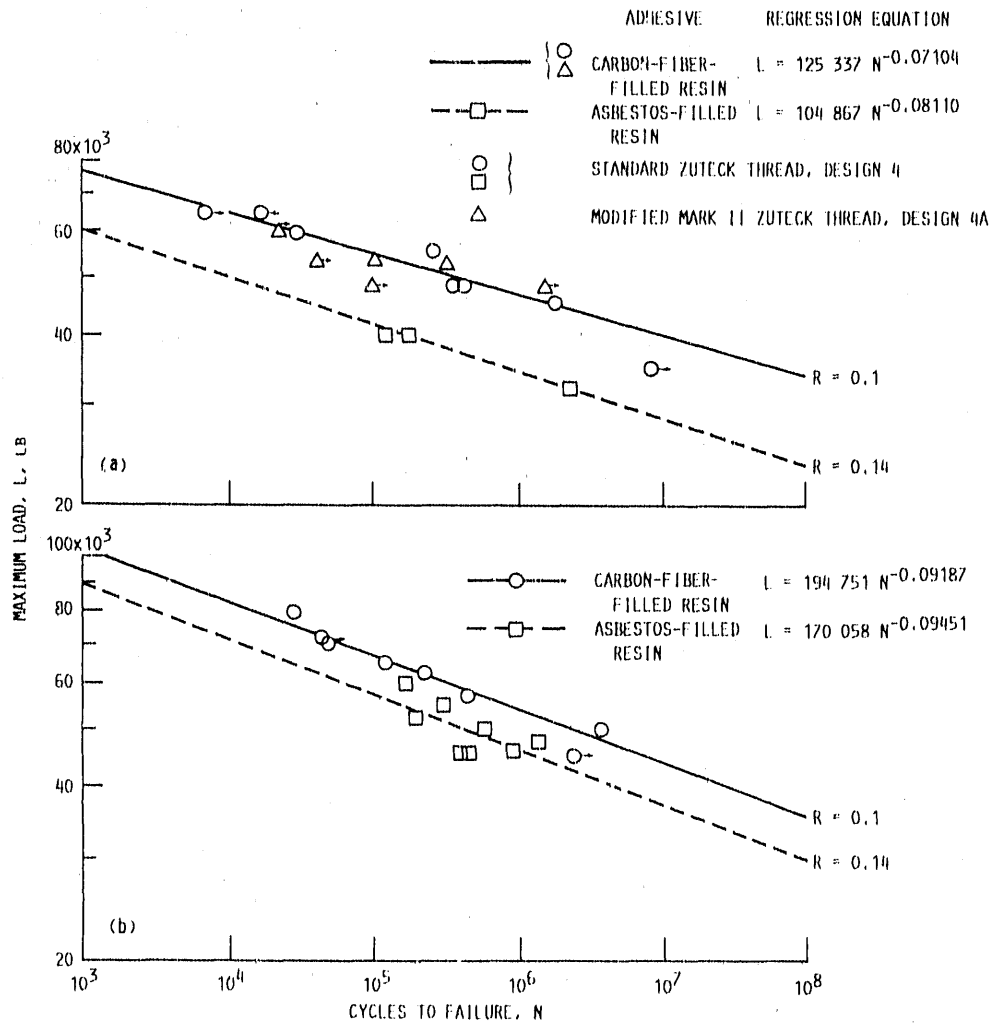

(a) Design 4 with two thread configurations (see fig. 7.1-2).

(b) Design 5 (same as design 4 except different taper and wood was augmented with carbon fibers between veneers to increase stiffness and thus improve strain compatibility with stud).

Figure 7.2-1.—Tension-tension fatigue strength tests (R = 0.1 and 0.14) of two metal stud designs embedded in laminated Douglas fir/epoxy specimens with carbon-fiber- and asbestos-thickened adhesive (resin) for bonding studs to wood. Room-temperature tests.

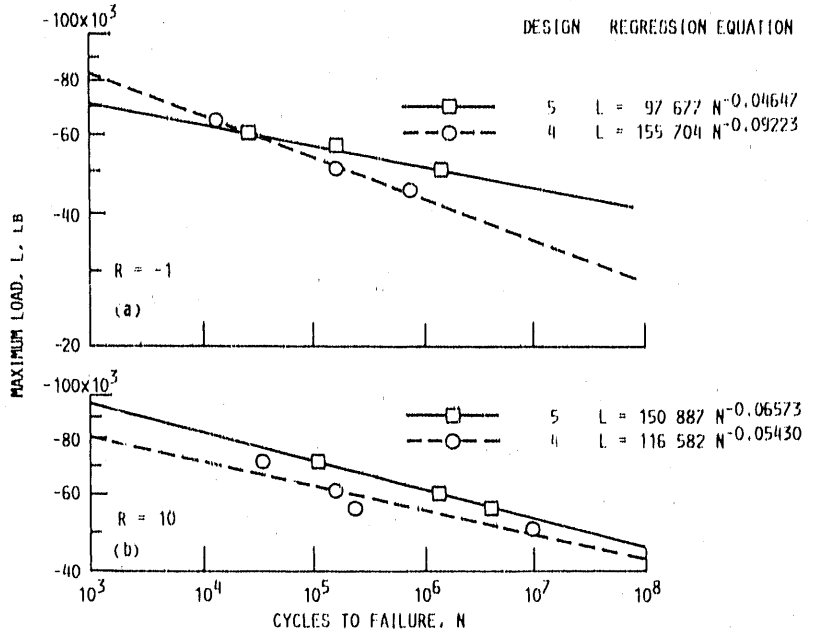

(a) Simulated reverse axial tension-compression fatigue. (Tension cycles listed.) Tests run in blocks of tension-tension (R = 0.1) and blocks of compression-compression (R = 10) cycles, at stress ratios R of 0.1 and 10.
(b) Compression-compression fatigue strength (R = 10).

Figure 7.2-2.—Compression-compression fatigue and simulated reverse axial tension-compression fatigue strength of two metal stud test specimen designs. Room-temperature tests. Studs bonded with carbon-fiber-filled epoxy resin.

design 5. Such data might have shown whether a crossover was realistic. Static data were not used in calculating any of the regression lines for metal stud fatigue test specimens. Use of such data would have increased regression line slope in nearly all cases and would have resulted in a much poorer fit of the fatigue data.

7.2.2 Fatigue strength at 100 to 120 °F.—Figure 7.2-3 shows the effect of modestly increasing the temperature level on the fatigue failure load for designs 4 and 5. Data for temperatures of both 100 and 120 °F were combined in calculating the regression lines. There appears to be little difference in fatigue strength between the 100 and 120 °F data, but there is a significant reduction in fatigue failure load relative to the strength at room temperature. The fatigue failure loads for temperatures of 100 to 120 °F were one-half or less of the room-temperature failure loads at 1 million cycles. Design 5 was still slightly stronger than design 4 at the higher test temperatures.

7.3 Conclusions Drawn From Fatigue Testing of Studs

Metal studs can be used to attach laminated-wood structures to metal structures. The studs can be embedded and bonded to the wood in such a manner that fatigue loads of 20 000 lb or more can be applied to each stud for 100 million cycles or less at room temperature. Increasing the temperature to 100 °F reduced these permissible loads by a factor of 2 or more. The data also show that the stud design should emphasize strain compatibility between the stud and the wooden structure. The specimens exhibiting the best fatigue life were those that improved compatibility through reduced stud modulus. These specimens had titanium studs, had thin stud walls achieved by counterdrilling and using a nonlinear wall thickness, or had stiffer wooden structures augmented with carbon fiber between the wood veneers.

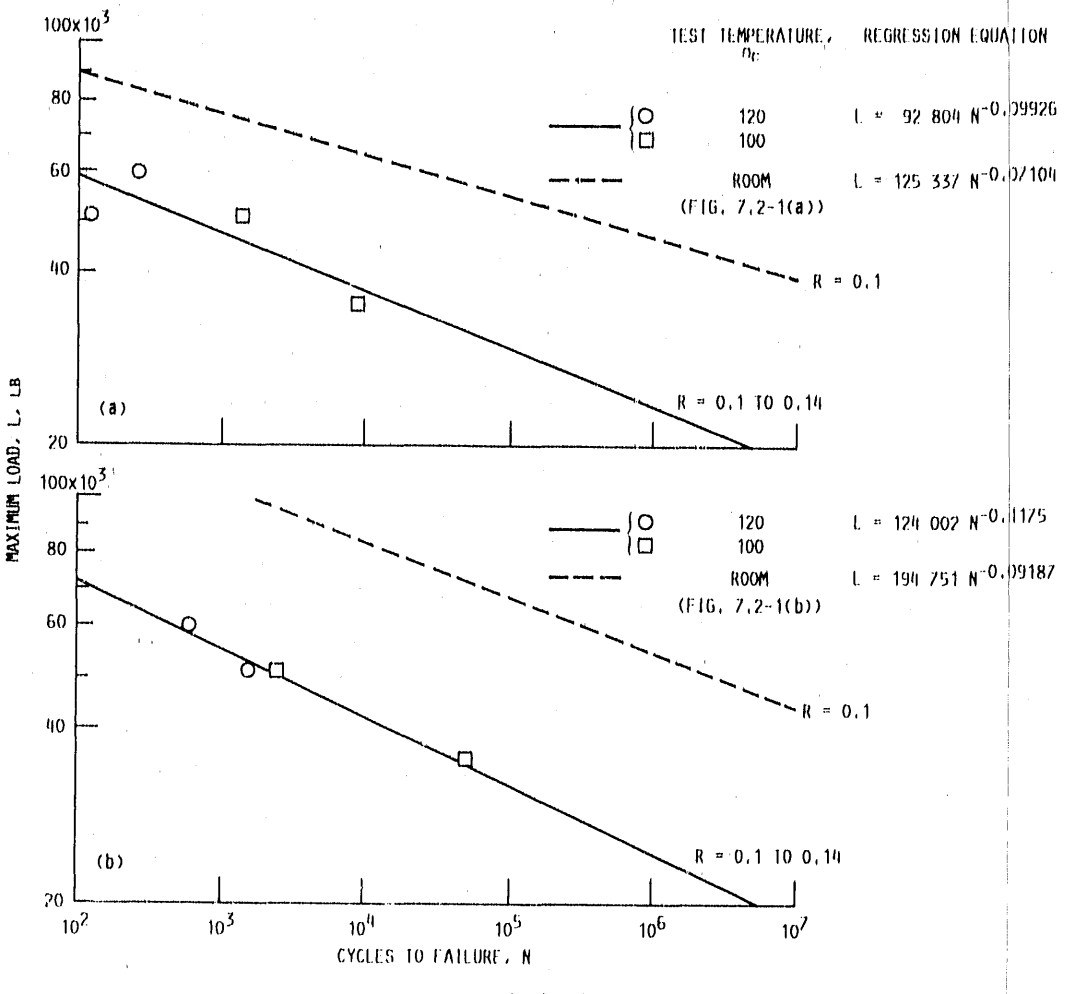

(a) Design 4.
(b) Design 5.

Figure 7.2-3.—Tension-tension fatigue strength at elevated temperature of two metal stud test specimen designs for stress ratios R of 0.10 to 0.14. Studs bonded with carbon-fiber-filled epoxy resin.

8.0 Concluding Remarks

This chapter has attempted to provide a collection of unpublished data available on laminated Douglas fir/epoxy material. The test results reported herein are the work of several organizations, which are listed in chapter I. The laminates were 0.1 in. thick and the grain of all laminates was oriented in the same direction. Several grades of Douglas fir were investigated. Epoxy glue applied at 60 pounds per thousand square feet of double glue line was used for nearly all of the data presented.

Most of the data presented have been corrected to 6 percent laminate moisture content by using an equation and constants that appear reasonable. Uncorrected data are also listed in tables throughout the chapter to permit reworking of the data.

The highlights of this chapter plus the development of mathematical models to represent strength data are presented in chapter III.

9.0 References

1. Mod-5A Wind Turbine Generator Program Design Report. Volume II - Conceptual and Preliminary Design. Books 1 and 2. NASA CR-174735-VOL2-BK1 and NASA CR-174735-VOL2-BK2, 1984.
2. Stroebel, T.; Dechow, C.; and Zuteck, M.: Design of Advanced Wood Composite Rotor and Development of Wood Composite Blade Technology. GBE-ER-11, Gougeon Brothers, Inc.; NASA Contract DEN3-260) NASA CR-174713, 1984.
3. Wood Handbook: Wood as an Engineering Material. Forest Service Agriculture Handbook No. 72, U.S. Forest Products Laboratory, 1974.
4. Jung, J.: Stress-Wave Grading Techniques on Veneer Sheets. Forest Products Laboratory, General Technical Report FPL-27, 1979.
5. Jung, J.: Properties of Parallel-Laminated Veneer From Stress-Wave-Tested Veneers. For. Prod. J., vol. 32, no. 7, July 1982, pp. 30-35.
6. 1985 Annual Book of ASTM Standards, Section 4, Volume 04.09, Wood.
   D 143-83 Standard Methods of Testing Small Clear Specimens of Timber
   D 198-84 Standard Methods of Static Tests of Timbers in Structural Sizes.
   D 1037-78 Standard Methods of Evaluating the Properties of Wood-Base Fiber and Particle Panel Materials
   D 2016-74 Standard Test Methods for Moisture Content of Wood
7. 1985 Annual Book of ASTM Standards, Section 15, Volume 15.06, Adhesives. D 905-49 Standard Test Method for Strength Properties of Adhesive Bonds in Shear by Compressive Loading.
8. Bohannan, B.: Effect of Size on Bending Strength of Wood Members. U.S. Forest Service Research Paper FPL-56, May 1966.
9. Faddoul, J.R.: Improved Stud Configurations for Attaching Laminated Wood Wind Turbine Blades. NASA TM-87109, 1985.

NASA
National Aeronautics and Space Administration

Report Documentation Page

1. Report No.	2. Government Accession No.	3. Recipient's Catalog No.
NASA RP-1236 DOE/NASA/20320-76		

4. Title and Subtitle	5. Report Date
Structural Properties of Laminated Douglas Fir/Epoxy Composite Material	
	6. Performing Organization Code May 1990
7. Author(s)	8. Performing Organization Report No.
David A. Spera, Jack B. Esgar, Meade Gougeon, and Michael D. Zuteck	E-4720
	10. Work Unit No. 776-33-41
9. Performing Organization Name and Address	11. Contract or Grant No.
National Aeronautics and Space Administration Lewis Research Center Cleveland, Ohio 44135-3191	
	13. Type of Report and Period Covered Reference Publication
12. Sponsoring Agency Name and Address	
National Aeronautics and Space Administration Washington, D.C. 20546-0001	14. Sponsoring Agency Code

15. Supplementary Notes

David A. Spera, NASA Lewis Research Center; Jack B. Esgar, Sverdrup Technology, Inc., NASA Lewis Research Center Group (NASA Contract NAS3-25266); Meade Gougeon and Michael D. Zuteck, Gougeon Brothers, Inc., Bay City, Michigan. Prepared under Interagency Agreement DE-AI01-76ET20320.

16. Abstract

This publication contains a compilation of static and fatigue strength data for laminated-wood material made from Douglas fir and epoxy. Results of tests conducted by several organizations are correlated to provide insight into the effects of variables such as moisture, size, lamina-to-lamina joint design, wood veneer grade, and the ratio of cyclic stress to steady stress during fatigue testing. These test data were originally obtained during development of wood rotor blades for large-scale wind turbines of the horizontal-axis (propeller) configuration. Most of the strength property data in this compilation are not found in the published literature. Test sections ranged from round cylinders 2.25 in. in diameter to rectangular slabs 6 in. by 24 in. in cross section and approximately 30 ft long. All specimens were made from Douglas fir veneers 0.10 in. thick, bonded together with the WEST epoxy system developed for fabrication and repair of wood boats. Loading was usually parallel to the grain. Size effects (reduction in strength with increase in test volume) are observed in some of the test data, and a simple mathematical model is presented that includes the probability of failure. General characteristics of the wood/epoxy laminate are discussed, including features that make it useful for a wide variety of applications.

17. Key Words (Suggested by Author(s))	18. Distribution Statement
Wood properties; Wood structures; Laminated wood; Douglas fir; Wood joints; Fatigue strength; Static strength; Wood composite; Test data; Size effect	Unclassified—Unlimited Subject Category 44 DOE Category UC-920

19. Security Classif. (of this report)	20. Security Classif. (of this page)	21. No of pages	22. Price*
Unclassified	Unclassified	140	A07

NASA FORM 1626 OCT 86

*For sale by the National Technical Information Service, Springfield, Virginia 22161

END

DATE FILMED

11 / 05 / 90